



Universitat Autònoma de Barcelona

**ADVERTIMENT.** L'accés als continguts d'aquesta tesi doctoral i la seva utilització ha de respectar els drets de la persona autora. Pot ser utilitzada per a consulta o estudi personal, així com en activitats o materials d'investigació i docència en els termes establerts a l'art. 32 del Text Refós de la Llei de Propietat Intel·lectual (RDL 1/1996). Per altres utilitzacions es requereix l'autorització prèvia i expressa de la persona autora. En qualsevol cas, en la utilització dels seus continguts caldrà indicar de forma clara el nom i cognoms de la persona autora i el títol de la tesi doctoral. No s'autoritza la seva reproducció o altres formes d'explotació efectuades amb finalitats de lucre ni la seva comunicació pública des d'un lloc aliè al servei TDX. Tampoc s'autoritza la presentació del seu contingut en una finestra o marc aliè a TDX (framing). Aquesta reserva de drets afecta tant als continguts de la tesi com als seus resums i índexs.

**ADVERTENCIA.** El acceso a los contenidos de esta tesis doctoral y su utilización debe respetar los derechos de la persona autora. Puede ser utilizada para consulta o estudio personal, así como en actividades o materiales de investigación y docencia en los términos establecidos en el art. 32 del Texto Refundido de la Ley de Propiedad Intelectual (RDL 1/1996). Para otros usos se requiere la autorización previa y expresa de la persona autora. En cualquier caso, en la utilización de sus contenidos se deberá indicar de forma clara el nombre y apellidos de la persona autora y el título de la tesis doctoral. No se autoriza su reproducción u otras formas de explotación efectuadas con fines lucrativos ni su comunicación pública desde un sitio ajeno al servicio TDR. Tampoco se autoriza la presentación de su contenido en una ventana o marco ajeno a TDR (framing). Esta reserva de derechos afecta tanto al contenido de la tesis como a sus resúmenes e índices.

**WARNING.** The access to the contents of this doctoral thesis and its use must respect the rights of the author. It can be used for reference or private study, as well as research and learning activities or materials in the terms established by the 32nd article of the Spanish Consolidated Copyright Act (RDL 1/1996). Express and previous authorization of the author is required for any other uses. In any case, when using its content, full name of the author and title of the thesis must be clearly indicated. Reproduction or other forms of for profit use or public communication from outside TDX service is not allowed. Presentation of its content in a window or frame external to TDX (framing) is not authorized either. These rights affect both the content of the thesis and its abstracts and indexes.



- Catalan Institute of Nanoscience and Nanotechnology (ICN2)
- Universitat Autònoma de Barcelona (UAB) Physics Department – Graduate School
- Secretaría Nacional de Educación Superior Ciencia Tecnología e Innovación (SENESCYT) – Gobierno del ECUADOR

## DOCTORAL THESIS

# VIRTUAL INSTRUMENTS FOR PHOTOVOLTAIC MEASUREMENTS

Defended by:

**FERNANDO ECHEVERRIA TROYA**

Thesis Director:

**Dr. MONICA LIRA CANTU**

Group Leader, Nanostructured Materials for Photovoltaic Energy – ICN2

Tutor:

**Dr. JORDI MOMPART PENINA**

Optics Group, Physics Department – Graduate School - UAB

*October 2017, Bellaterra*

*BARCELONA*

**Catalan Institute of Nanoscience and Nanotechnology (ICN2),  
CSIC and BIST, Campus UAB, Bellaterra, 08193 Barcelona**

**Universidad Autónoma de Barcelona  
Departamento de Física, Escuela de Doctorado, 08193 Barcelona**

**Secretaría Nacional de Educación Superior Ciencia Tecnología  
e Innovación (SENESCYT) – Gobierno del ECUADOR**

Memória presentada per aspirar al Grau de Doctor per Fernando Echeverría Troya:



Dra. Mónica Lira-Cantu

Group Leader

Nanostructured Materials for Photovoltaic Energy Group


Catalan Institute of Nanoscience and Nanotechnology (ICN2),

CSIC and the Barcelona Institut of Science and Technology (BIST)

Certifica que el treball descrit en aquesta tesis titulada:

**“Virtual Instruments for Photovoltaic Measurements”**

Presentada per Fernando Echeverría Troya per optar al grau de Doctor, ha estat realitzada sota la meva direcció.

  
Dra. Mónica Lira Cantú

Vist i plau del Tutor de tesis:

  
Dr. Jordi Mompert Penina

**To:** *Isabel, my wife*  
*Ariel, my son*  
*Dana and Anaí,*  
*my daughters.*









*...dig and search...*





## Acknowledgements

*I am very grateful with Dra. Mónica Lira, Thesis Director, for allowing me to be part of her Research Group, for her openness and patience. Without this opportunity, this work would not have been done.*

*In the Physics Department, Graduate School – UAB, I am grateful with Dr. Jordi Mompart Penina, my Tutor for his valuable guidance and concern in the progress of this project. Particularly, I am grateful with Dra. María Josefa Yzuel Giménez for her advice and motivation to persist in the present work..*

*This document is written in the frame of the Research Project for the development of a Solar Cell prototype.*

*As a Graduate Student in Physics at the Universidad Autónoma de Barcelona – UAB, the present work has been developed in the Catalán Institute of Nanoscience and Nanotechnology – CIN2, in the Laboratory for Nanostructured Materials for Photovoltaic Energy. Dra. Mónica Lira –Cantu is the Research Leader of this Group and Thesis Director for this Project. The Scholarship for this Research Programme has been granted by the Secretaría Nacional de Educación Superior Ciencia Tecnología e Innovación – SENESCYT from the Government of Ecuador.*

*I am grateful with all the persons that have contributed to convert this project in a reality. I cannot name all of them. However I would like to mention to Dr. Gustavo Ceballos Head of Support Laboratories for his good predisposition and openness to make possible these measurements and, particularly, I am grateful to Dr. Javier Saiz, we have worked together in the preliminary calibration and measurements for Irradiance, Spectral and Room Temperature were made in the ICN2 Laboratory for Common Services. To Dr. Jordi Prat for his help in the initial steps to use the*

*microcontroller. To Dr. Jordi Fraxedas and Dra. María José Esplandiú for their orientation in the proposition to develop a solar cell prototype.*

*In Sabadell, I would like to thank to Ulugbeck Mamadzjanov and Monserrat Sastre for their solidarity and preoccupation to solve the Android ↔ Windows data transfer transparency in the present work.*

*Also, allow me to manifest that I have felt an attitude of cordiality and good will in all those persons around me during this research work: Authorities, Research Group Leaders, Staff from Laboratories, Administrative Staff, other workers in the Institute; Graduate Students. In particular the members of the Laboratory of Nanostructures Materials for Photovoltaic Energy Group. I won't mention their names but I am grateful with all of them.*

*F.E.*

*ICN2 – UAB – Bellaterra*

*Barcelona*

*October 2017*

## **MOTIVATION**

There are several aspects that have motivated this work.

The first one is to learn, i.e. to experience with new things for one's knowledge.

Another not least important: To have trustable magnitudes of the physical parameters related with light.

It constitutes a challenge to have trustable values of these physical magnitudes employing very simple equipment and low cost "off the shelf" components.

The actual technological development has no precedent in History. Very advanced artefacts are nowadays of general use and low cost. Tiny electronic components have extraordinary characteristics useful for this purpose.

On the other hand to spread the knowledge towards young students interested in these matters is not affordable with commercial instruments.

It is so important to have a "comprehensive and hands on it" approach in this matters for young students since this is the background for research in new fields such as Nanoscience and Nanotechnology, Solar Cells development and a broad and diverse spectra of very many applications.

## **OBJECTIVE**

To play and experiment with Light. To imagine alternatives to measure Light Parameters with very simple equipment and low cost off the shelf components.

## **GENERAL CONTENTS**

**page**

<b>CHAPTER 1</b>	<b>LIGHT: PHYSICAL PRINCIPLES</b>	<b>1-1</b>
<b>CHAPTER 2</b>	<b>ESSENTIAL OPTICAL COMPONENTS AND FRONT END CIRCUITS</b>	<b>2-1</b>
<b>CHAPTER 3</b>	<b>DATA ACQUISITION AND CONTROL USING MICROCONTROLLERS</b>	<b>3-1</b>
<b>CHAPTER 4</b>	<b>MEASUREMENT AND EVALUATION USING PROGRAMMABLE – GRAPHIC EMULATORS</b>	<b>4-1</b>
<b>CHAPTER 5</b>	<b>METHODS AND MATERIALS</b>	<b>5-1</b>
<b>CONCLUSSIONS AND RECOMMENDATIONS</b>		<b>CR-1</b>
<b>ANNEXES TO ALL CHAPTERS</b>		<b>ANNX-1</b>

# **CONTENTS IN DETAIL**

## **CHAPTER 1**

<b>LIGHT: PHYSICAL PRINCIPLES</b>	<b>1-1</b>
OUTLINE OF THE CHAPTER	1-3
A. PRELIMINARY TOPICS	1-7
1. PRELIMINARY DEFINITIONS	1-7
2. ELECTROMAGNETIC SPECTRUM	1-9
3. PLANCK'S EQUATION	1-12
4. SUNLIGHT	1-19
B. LIGHT AS WAVE	1-24
1. THEORETICAL SUPPORT	1-24
2. LIGHT SOURCES	1-31
3. LINEAR ARRAY OF COHERENT SOURCES	1-33
C. PHOTONS	1-43
1. PHOTOELECTRIC EFFECT	1-43
2. SEMICONDUCTOR LIGHT DETECTORS	1-47
3. RESPONSIVITY	1-49
4. INCANDESCENT LIGHT SOURCES	1-55
5. CALIBRATION OF Si AND Ge PHOTODIODES USING A STANDARD TUNGSTEN FILAMENT LIGHT SOURCE	1-57
6. SPECTRAL RESPONSIVITY OF Si AND Ge PHOTODIODES	1-63
D. OBJECTIVES AND SCOPE OF THE PRESENT WORK	1-73
1. GENERAL OBJECTIVE	1-73
2. SPECIFIC OBJECTIVES	1-74
3. SCOPE OF THE WORK	1-76
Bibliography	1-77
Basic References	1-79



## CHAPTER 2

### OPTICAL AND ELECTRONICS

#### ESSENTIAL COMPONENTS .....2-1

OUTLINE OF THE CHAPTER	2-3
A. ESSENTIAL OPTICAL COMPONENTS .....	2-7
1. DESIGN PARAMETERS FOR A SPECTROMETER	2-8
2. "DARK ROOM"	2-10
3. OPTICAL SLITS	2-10
4. DIFFRACTION GRIDS	2-23
5. SIMPLE SPECTROMETER AND MONOCHROMATOR DESIGN PARAMETERS	2-40
6. SIMPLE SPECTROPHOTOMETER AND MONOCHROMATOR DESIGN	2-44
B. USEFUL ELECTRONIC COMPONENTS	2-46
1. PN JUNCTIONS AS TEMPERATURE SENSORS	2-46
2. FIELD EFFECT TRANSISTORS – FETs	2-47
3. OPERATIONAL AMPLIFIERS – OPAMPs	2-52
C. COMMON LIGHT SENSORS	2-55
1. LIGHT EMITTING DIODES – LEDs	2-55
2. SILICON PHOTODIODES	2-56
3. Si AND Ge SIGNAL DIODES	2-57
D. USEFUL ELECTRONIC STAGES FOR PHOTOVOLTAIC MEASUREMENTS	2-57
1. JFET CURRENT SOURCE	2-57
2. VOLTAGE FOLLOWER	2-58
3. INVERTER AND NON INVERTER OPAMPs AMPLIFIERS	2-58
4. PHOTOCURRENT TO VOLTAGE CONVERTER	2-59
E. FRONT END CIRCUITS	2-60
1. ENVIRONMENTAL THERMOMETER	2-60
2. SIMPLE SPECTROPHOTOMETER AND MONOCHROMATOR	2-60
3. PYROMETER (SPECTRAL TEMPERATURE METER)	2-61
4. PYRANOMETER (IRRADIANCE METER)	2-61
5. SOLAR CELL I – V CURVE GENERATOR	2-62
Bibliography	2-63
Basic References	2-64

## CHAPTER 3

### DATA ACQUISITION AND CONTROL USING MICROCONTROLLERS AND ANDROID DEVICES .....3-1

OUTLINE OF THE CHAPTER	3-3
A. PRELIMINARY TOPICS .....	3-7
1. MEASUREMENT	3-7
2. VIRTUAL INSTRUMENTATION	3-7
3. PHYSICAL PHENOMENA AND ANALOG FRONT END CIRCUITS	3-8
4. MICROCONTROLLERS	3-9
5. ANDROID DEVICES	3-9
6. ANDROID OPEN ACCESSORIES	3-10
7. PROGRAMMABLE AND GRAPHIC CALCULATOR EMULATORS	3-10
B. IOIO OTG CHARACTERIZATION AND INTERFACING	3-11
1. IOIO OTG: DESCRIPTION	3-11
2. IOIO OTG: CHARACTERIZATION	3-14
3. IOIO OTG: INTERFACING	3-16
C. ANDROID STUDIO AND IOIO OTG: PROGRAMMING ANDROID DEVICES AS MEASURING INSTRUMENTS	3-19
1. ANDROID STUDIO	3-19
2. INSIDE ANDROID STUDIO	3-20
3. DEVELOPING IOIO OTG APPLICATIONS FOR ANDROID DEVICES OR PC	3-25
4. IOIOLib ANDROID PACKAGE	3-36
5. REQUIRED COMMANDS FOR THE PRESENT APPLICATION	3-28
D. INTERFACING FRONT END CIRCUITS WITH THE MICROCONTROLLER	3-29
1. FRONT END CIRCUITS INPUTS AND OUTPUTS	3-29
2. SCHEMATIC DIAGRAMS	3-30
3. DATA STORAGE FOR EACH APPLICATION	3-32
E. ANDROID ↔ WINDOWS DATA TRANSFER TRANSPARENCY	3-33
Bibliography	3-34
Basic References	3-38

## **CHAPTER 4**

### **MEASUREMENT AND EVALUATION USING PROGRAMMABLE – GRAPHIC EMULATOR CALCULATORS ..... 4-1**

OUTLINE OF THE CHAPTER	4-3
A. HP 48 GX AND HP 50G AND THEIR EMULATORS	4-7
1. HP48 GX AND HP50G CALCULATORS	4-7
2. HP48 GX AND HP50G EMULATORS	4-10
3. HP48 GX AND HP50G EMULATORS FOR ANDROID DEVICES	4-10
B. COMMON TOPICS RELATED TO ALGORITHMS	4-13
1. A/D CONVERSION AND DC VOLTMETER	4-13
2. PHOTOCURRENT MEASUREMENTS	4-16
3. ENERGY OF A PHOTON FOR A MONOCHROMATIC SOURCE	4-17
4. LIGHT SENSORS ACTIVE AREA	4-17
5. LIGHT SPECTRUM PHOTOCURRENTS AND RESPONSIVITY	4-17
6. D/A CONVERSION AS A CONTROL TOOL	4-19
7. SENSORS AND FRONT END CIRCUITS CALIBRATION	4-19
<u>DESCRIPTION OF ALGOTRITHMS FOR VIRTUAL INSTRUMENTS</u>	4-19
C. ENVIRONMENTAL THERMOMETER	4-21
D. THERMAL RADIATION: SPECTRAL TEMPERATURE AND IRRADIANCE METERS	4-23
D.1. IRRADIANCE METER (PYRANOMENTER)	4-23
D.2. SPECTRAL TEMPERTATURE METER	4-29
E. SOLAR CELL I – V CURVE GENERATOR	4-58
F. SUMMARY OF VIRTUAL INSTRUMENTS MEASUREMENTS AND EVALUATION	4-70
Bibliography	4-72
Basic References	4-74

## **CHAPTER 5**

### **METHODS AND MATERIALS**

**5-1**

#### **OUTLINE OF THE CHAPTER**

5-3

##### **A. CALIBRATION PROCEDURES**

##### **AND EXPERIMENTAL RESULTS**

5-7

###### **1. ENVIRONMENTAL THERMOMETER**

5-7

###### **2. SPECTRAL TEMPERATURE METER**

5-10

###### **3. IRRADIANCE METER**

5-11

###### **4. LABORATORY MEASUREMENTS**

###### **OF THERMAL RADIATION**

5-13

###### **5. SOLAR I-V CURVE GENERATOR**

5-22

##### **B. MATERIALS USED IN THE PROJECT**

5-31

###### **1. ELECTRONIC COMPONENTS**

5-31

###### **2. MICROCONTROLLER BOARD**

5-32

###### **3. FREEWARE**

5-32

### **CONCLUSSION AND RECOMMENDATIONS**

**CR-1**

## **ANNEXES TO CHAPTERS**

## **ANNX-1**

### OUTLINE OF ANNEXES

#### **CHAPTER 1**

ANNEX 1: ARTICLE: SINGLE PHOTON: its size and internal electromagnetic fields Author: Fernando Echeverría T.	1-1
ANNEX 2: RESPONSIVITY FOR Si AND Ge PHOTODIODES	ANNX 2-1
ANNEX 3: RESPONSIVITY FOR Si AND Ge PHOTODIODES (Resol. 10[nm])	ANNX 3-1
ANNEX 4:	ANNX 4-1
a. STANDARD AND NORMALIZED TUNGSTEN FILAMENT LAMP SPECTRUM(Resol. 10 [nm])	
b. STANDARD AND NORMALIZED TUNGSTEN FILAMENT LAMP SPECTRUM (Spectral Range Bandwidth for Silicon	
c. STANDARD AND NORMALIZED TUNGSTEN FILAMENT LAMP SPECTRUM (Spectral Range Bandwidth for Germanium)	
ANNEX 5: PHOTODIODES TECHNICAL DATA	ANNX 5-1

#### **CHAPTER 2**

ANNEX 1: A DISGRESSION ON FOURIER TRANSFORMS	ANNX 1-1
--	----------

#### **CHAPTER 3**

ANNEX 1: DESCRIPTION OF ALGORITHM TO MEASURE A PHYSICAL MAGNITUDE	ANNX 1-1
ANNEX 2: ANDROID RELATED COMMAND SEQUENCES	ANNX 2-1
ANNEX 3: REQUIRED COMMANDS FOR THE PROJECT (CANONICAL FORM)	ANNX 3-1

#### **ANNEX F:**

#### **REFERENCE ON FIGURES INCLUDING THEIR ORIGIN**

REFERENCE ON FIGURES INCLUDING THEIR ORIGIN	ANNX F- 1
---	-----------



# **INDEX OF FIGURES**

**page**

## **CHAPTER 1**

### **LIGHT: PHYSICAL PRINCIPLES**

Fig A.1 Diffraction of light in a grating .....	1-8
Fig. A.2 Visible Spectrum .....	1-9
Fig. A.3 The Electromagnetic Spectrum.....	1-10
Fig. A.4 The Ultraviolet Range.....	1-11
Fig. A.5 The Infrared Range .....	1-11
Fig. A.6 The spectrum emitted by a hot filament depends of Temperature ....	1-12
Fig. A.7 The Planck's equation plotted for different temperatures .....	1-13
Fig. A.8 The energy levels of a harmonic oscillator .....	1-14
Fig. A.9 Ratio between a spherical surface and the surface subtended by a steradian .....	1-16
Fig. A.10 The function $F_0\lambda$ for $\lambda = \lambda_i$ .....	1-17
Fig. A.11 $F_0\lambda$ for: $T_1 = 5770$ [K], $T_2 = 3200$ [K] and $T_3 = 1200$ [K] .....	1-18
Fig. A.12 The Integral of $F_0\lambda$ for $T = 5770$ [K] .....	1-18
Fig.A.13 The Inverse Square Distance Law for Radiation .....	1-20
Fig. A.14 Solar Spectral Irradiance on Earth's outer atmosphere .....	1-21
Fig. A.15 Solar Irradiance on Earth's Surface at Sea Level. ....	1-22
Fig. A.16 High Resolution Solar Irradiance Spectral Bands photography .....	1-23
Fig. B.1 Traveling Waves .....	1-25
Fig. B.2 An EMG wave figure .....	1-26
Fig. B.3 Poynting Vector .....	1-26
Fig. B.4 Every volume element in space has an Energy density $u$ .....	1-27
Fig. B.5.....	1-28
(a) A plane wave front	
(b) A dipole antenna radiates spherical electromagnetic fields	
Fig. B.6 A harmonic plane electromagnetic wave .....	1-29
Fig. B.7 LEDs are examples of monochromatic light sources .....	1-31

Fig. B.8 Coherent and incoherent beams .....	1-32
Fig. B.9 Interpretation of a phasor .....	1-34
Fig. B.10 Intensity due to oscillation of two coherent sources in the far field ..	1-35
Fig. B.11 Two point sources radiating waves that are detected in the far field at $P$ .....	1-36
Fig. B.12 Array of $N$ coherent sources .....	1-37
Fig. B.13 The resultant amplitude of $n = 6$ equally spaced sources .....	1-38
Fig. B.14 The functions (a) $A_R / A$ and (b) $I / I_0$ for $n = 5$ .....	1-39
(a) The amplitude is proportional to $n$	
(b) The amplitude is proportional to $n^2$	
Fig. B.15 The function $\text{sinc}[\beta / 2]$ .....	1-40
Fig. B.16 The function $\text{sinc}^2 [\beta / 2]$ .....	1-41
Fig. B.17 Plot of $\tan(u) = u$ .....	1-42
Fig. C.1 Photodiode Idealized Spectral Response photodiode .....	1-48
Fig. C.2.....	1-48
(a) A Reverse Biased LED is a Light Detector	
(b) A Forward Biased LED is a Light Source.	
Fig. C.3 The Spectrum of a LED acting as a Light Source and as a Light Detector .....	1-49
Fig. C.4 Typical Responsivity for a Si photodiode.....	1-51
Fig. C.5 Typical Responsivity for a Ge Photodiode .....	1-52
Fig. C.6 Responsivity for Si, Ge and InSb on a common reference frame.....	1-52
Fig. C.7 Responsivity of a Blue Emitter Photodiode.....	1-53
Fig. C.8 Responsivity for germanium photodiode.....	1-54
Fig. C.9 Effect of temperature in germanium photodiode .....	1-54
Fig. C.10 Ge Photodiode Temperature Coefficient of Responsivity .....	1-55
Fig. C.11 Relative spectral radiant flux for tungsten filaments .....	1-56
Fig. C.12 Standard Lamp Spectral Distribution for $T = 2856$ [K].....	1-62



Fig. C.13 Spectral Responsivity for a Si Photodiode.....	1-63
Fig. C.14 Fragment of Spectrum that interacts with the Si Photodiode .....	1-64
Fig. C.15 Electric Current from a 1mm <sup>2</sup> Silicon Photodiode .....	1-68
Fig. C.17 Irradiance, Responsivity and Photocurrent for a 1 mm <sup>2</sup> Si photodiode .....	1-70
(a) Total Irradiance [mW/mm <sup>2</sup> ] vs $\lambda$ [m]	
(b) Responsivity [A/W] vs $\lambda$ [m]	
(c) Photocurrent [A] vs $\lambda$ [m]	
Fig. C.18 Irradiance, Responsivity and Photocurrent for a 1 mm <sup>2</sup> Ge photodiode .....	1-71
(a) Total Irradiance [mW/mm <sup>2</sup> ] vs $\lambda$ [m]	
(b) Responsivity [A/W] vs $\lambda$ [m]	
(c) Photocurrent [A] vs $\lambda$ [m]	

## CHAPTER 2

### OPTICAL AND ELECTRONICS

#### ESSENTIAL COMPONENTS

Fig A.1 An isolated environment to observe Light is “darkroom” .....	2-10
Fig. A.2 Image of a vertical narrow optical slit .....	2-11
Fig. A.3 Horizontal Light Pattern for a Narrow Vertical Slit .....	2-11
Fig. A.4 Horizontal Light Pattern for the whole Vertical Slit .....	2-12
Fig. A.5 Huygens – Fresnel Principle .....	2-12
Fig. A.6 Fraunhofer diffraction by a single slit .....	2-14
Fig. A.7 Phasor diagram for large number of coherent sources .....	2-14
Fig. A.8 The width of the diffraction peak varies inversely with the width of the slit. ....	2-18
Fig. A.9 Span displacement $\Delta y$ at distance X for the Observation Angle $\theta$ .....	2-21

Fig. A.10 Microphotography of a diffraction grid .....	2-23
Fig. A.11 Diffraction modes of Abeam through aslits.....	2-25
Fig. A.12 Geometry of Diffracted abeam crossing a grid.....	2-26
Fig. A.13 A beam reflected on a grid.....	2-28
Fig. A.14 A polychromatic beam is decomposed in its spectrum .....	2-28
Fig. A.15 The path difference for rays scattered from adjacent rulings of a grating .....	2-29
Fig. A.16 Illustration of the Rayleigh criterion.....	2-29
Fig. A.17 A linear array of an equal oscillators, driven with phases $\alpha_s = s.\alpha$ ...	2-26
Fig. A.18 Span of the angle of diffraction vs mode m for this example.....	2-32
Fig. A.19 Geometry of abeam diffracted from a grid .....	2-34
Fig. A.20 Geometries for Transmissive and Reflective Spectrophotometers....	2-39
Fig. A.21 Picture of the optical spectrometer prototype .....	2-44
Fig. A.22 Spectral Work Bench display for a user's spectra .....	2-45
Fig. B.1 Family of curves ID vs VDS for VGS constant for 2N5484 JFET. ...	2-48
Fig. B.2 FET transistor family of curves ID vs VDS for VGS constant.....	2-49
Fig. B.3 N-Ch JFET Field Effect Transistor .....	2-50
Fig. B.4 Circuit diagram to measure IDSS. ....	2-51
Fig. B.5 Alternative circuits to measure VP .....	2-52
Fig B.6 Symbol, physical image and pin distribution for an Op Amp .....	2-53
Fig. B.7 JFET input Op Amp schematic .....	2-54
Fig. B.8 Simplified diagram for a JFET input Op Amp .....	2-54
Fig. C.1.....	2-55
(a) A Reverse Biased LED is a Light Detector	
(b) A Forward Biased LED is a Light Source.	
Fig. C.2 Pictures of several photodiodes and its electronic symbol .....	2-56
Fig. C.3 Si or Ge signal diodes glass encapsulated can also be used as light sensors .....	2-57

Fig. D.1 Current sources with a n-JFET .....	2-58
Fig. D.2 Voltage Follower. ....	2-58
Fig. D.3 Amplifiers using Op Amps: .....	2-59
(a) Inverting and	
(b) Non Inverting	
Fig. D.4 Photocurrent to Voltage Converter using Op Amps.....	2-59
Fig. E.1 Thermometer front end circuit .....	2-60
Fig. E.2 Pyrometer Front End Circuit.....	2-61
Fig. E.3 Pyranometer Front End Circuit .....	2-61
Fig. E.4 Basic circuit diagram showing a solar cell connection with a JFET transistor .....	2-62

### **CHAPTER 3**

#### **DATA ACQUISITION AND CONTROL USING MICROCONTROLLERS AND ANDROID DEVICES**

Fig. B.1 Front and Back sides of the IOIO OTG card board .....	3-12
Fig. B.2.....	3-13
(a)Illustration of Analog to Digital Conversion	
(b)Schematic of A/D Conversion Circuit	
(c)Schematic of D/A Conversion Circuit	
Fig. B.3 IOIO OTG recognized by the PC when drivers are installed. ....	3-14
Fig. B.4 The most recent version to Upgrade IOIO OTG .....	3-15
Fig. B.5 Screenshot of the Command Line .....	3-15
Fig. B.6 Schematic diagram showing IOIO OTG card connected in host mode.....	3-17
Fig. B.7 Photography of IOIO OTG connected with USB OTG cable .....	3-18
Fig. B.8 IOIO OTG board (in Host Mode .....	3-18
Fig. C.1 Android Studio Logo .....	3-19

Fig. C.2 Android Studio and IOIO OTG Libraries plugin.....	3-24
Fig. C.3 IOIOLib API screenshot .....	3-28
Fig. D.1 Diagrams for Voltmeter, Thermometer, Spectral Temperature and Irradiance meters. ....	3-31
Fig. D.2 Schematic diagram for the Solar Cell I-V Curve Generator.....	3-32
Fig. E.1 Schematic to overlap Android and Windows Platforms .....	3-33

## CHAPTER 4

### MEASUREMENT AND EVALUATION USING PROGRAMMABLE GRAPHIC EMULATOR CALCULATORS

Fig. A.1 HP 48GX photography .....	4-8
Fig. A.2HP 48GX photography .....	4-9
Fig. A.3 Screenshot of Droid48 emulator.....	4-11
Fig. A.4 Screenshot of EMU50G for Windows.....	4-12
Fig B.1 Nyquist Sampling Criterion .....	4-14
Fig. B.2 Analog Input calibration .....	4-15
Fig. B.3.....	4-18
(a)Standard Lamp Spectral Distribution for $T = 2856$ [K]	
(b)Spectral Irradiance of a Xenon Lamp for Solar Simulator	
Fig. CR1 PLOTS2d and vmtr are a set of basic routines installed at HOME DIRECTORY .....	4-20
Fig.D.1 A planar Si photodiode. ....	4-24
Fig. D.2 Red LED Current vs $\lambda$ .....	4-32
Fig. D.3 Green LED Current vs $\lambda$ .....	4-33
Fig. D.4 Spectral photocurrents for LEDs. Green LED (left) Red LED (Right) .....	4-34
Fig. D.5 $F_0\lambda(3175, \lambda)$ .....	4-36

Fig. D.6 Sub-bands for Red LED and Green LED .....	4-37
Fig. D.7 Plots of Photocurrent, Irradiance and Abs. Responsivity vs $\lambda$ .....	4-50
Fig. D.8 Plots of Photocurrent, Irradiance and Abs. Responsivity vs $\lambda$ .....	4-52
Fig. D.9 Abs. Responsivity Red and Green LEDs.....	4-53
Fig. D.10 The function $F_0\lambda$ for $\lambda = \lambda_i$ is the marked area from $\lambda = 0$ to $\lambda = \lambda_i$	4-54
Fig. D.11 Two known spectral bands for a Planck's source.....	4-55
Fig. E.1 Photocurrent to Voltage Converter using Op Amps .....	4-59
Fig. E.2 Experimental Setup and Material.....	4-60
Fig. E.3 Basic circuit diagram showing .....	4-61
Fig. E.4 The equivalent circuit diagram for a solar cell and the resistances $R_S$ and $R_{SH}$ .....	4-68
Fig. E.5 The fill factor $FF$ for a solar cell and the related parameters .....	4-69
Fig. E.1 Suggests one possible approach to virtual instruments.....	4-71

## CHAPTER 5

### METHODS AND MATERIALS

Fig. A.1 Testing Virtual Pyrometer .....	5-11
Fig. A.2 Thermal Irradiance spectrum vs. wavelength .....	5-15
Fig. A.3 Spectral Irradiance of a Xenon Lamp for Solar Simulator .....	5.16
Fig. A.4 Thermal Irradiance vs. wavelength.....	5.17
Fig. A.5 Results after Calibration of VI prototype taking as Reference the Lab's Pyranometer.....	5.19
Fig. A.6 Results measured with VI prototype after being calibrated.....	5.20
Fig. A.7 Intercomparison for Cell VR-1	5.23
Fig. A.8 Intercomparison for Cell ALB-1	5.24
Fig. A.9 Intercomparison for Cell Si-e	5-25

Fig. A.10 Cell's short circuit current temporal response	5-27
Fig. A.11 Cell's open voltage temporal response	5.28
Fig. A.12 I-V Curves measured with intervals of 5 hours	5.29

# **INDEX OF TABLES**

**page**

## **CHAPTER 1**

### **LIGHT: PHYSICAL PRINCIPLES**

Table A.1: Wavelength bands corresponding to visible colours-----	1-9
Table B.1: Solid State Lasers and their Wavelengths .....	1-32
Table C.1: Energy Ranges in [eV] in the Region of Interest .....	1-46
Table C.2:Energy Gap [eV] for Si and Ge and the corresponding wavelengths .....	1-47
Table C.3: PHOTOCURRENT vs $\lambda$ FOR 1mm <sup>2</sup> ACTIVE AREA OF A Si PHOTODIODE.....	1-66

## **CHAPTER 2**

### **OPTICAL AND ELECTRONICS**

#### **ESSENTIAL COMPONENTS**

Table A.1: Ranges of Wavelengths for the Proposed Instruments .....	2-9
Table A.2: Slit Widths for three selected ranges of Wavelengths .....	2-22
Table A.3: Diffraction Grids for Optical Applications	2-24
Table A.4: Diffraction Grids for Optical Applications compared with $\lambda V$ and $\lambda R$ .....	2-24
Table A.5: Summary of parameters for the Visible Range Spectrometer (Transmissive Diffraction Grid); $400 < \lambda < 700$ [nm] .....	2-37
Table A.6: Summary of parameters for the Visible Range Spectrometer (Reflective Diffraction Grid) ; $400 < \lambda < 700$ [nm] .....	2-38
Table A.7: Summary of parameters for the Visible Range Spectrometer (Transmission Type) .....	2-41
Table A.8: Summary of parameters Near Infrared Range Spectrometer (Transmission Type) .....	2-42
Table A.9: Parameters for the UV Range Spectrometer (CD) REFLECTIVE.....	2-43

### CHAPTER 3

#### DATA ACQUISITION AND CONTROL USING MICROCONTROLLERS AND ANDROID DEVICES

TABLE D.1:

FRONT END CIRCUITS INPUTS, OUTPUTS AND REQUIRED

IOIO OTG COMMANDS ..... 3-29

**CHAPTER 4** ..... 4-28

#### MEASUREMENT AND EVALUATION USING PROGRAMMABLE GRAPHIC EMULATOR CALCULATORS

Table C.1 Junction Voltage for liquid nitrogen

Temperature and boiling water temperature. .... 4-22

Table D.1: Experimental Results for total Irradiance

using Si Photodiode TSP = 3175 [K] ..... 4-28

Table D.2: Monocromator selected parameters for measurements ..... 4-31

Table D.3: Red LED Current vs  $\lambda$  ..... 4-32

Table D.4: Green LED Current vs  $\lambda$  ..... 4-33

Table D.5: Bounded Wavelengths for Red and Green LEDs Spectra ..... 4-34

Table D.6: Irradiance for the measured Spectral Temperature TSP = 3175 [K]

for Irradiances of 1 [mW/mm<sup>2</sup>] and 0.229 [mW/mm<sup>2</sup>] ..... 4-37

Table D.7: Red LED Spectral Irradiance ISP vs  $\lambda$  and Total Irradiance ITOT ... 4-39

Table D.8:

Green LED Spectral Irradiance ISP vs  $\lambda$  and Total Irradiance ITOT ..... 4-40

Table D.9: Summary of Procedure for Red LED and Green LED ..... 4-44

Table D.10: Red LED Absolute Responsivity Calculation

Scale Intensity Factor = 19.3 Scaled Factor to 1 [mm<sup>2</sup>] = 2.356 ..... 4-46

Table D.11: Green LED Absolute Responsivity Calculation

\*Scale Intensity Factor 19.3 \*\*Scaled Factor to 1 [mm<sup>2</sup>] = 5.553 ..... 4-47



Table D.12:	
Red LED Photocurrent, Irradiance and Absolute Responsivity vs wavelength.....	4-49
Table D.13:	
Green LED Photocurrent, Irradiance and Absolute Responsivity vs wavelength .....	4-51
Table D.14: Virtual Pyrometer Parameters for LEDs .....	4-56

## **CHAPTER 5**

### **METHODS AND MATERIALS**

Table A..1: Useful temperature references for calibration .....	5-7
Table A..2: Junction Voltage for liquid nitrogen	
Temperature and boiling water temperature .....	5-9
Table A..3: Virtual Pyrometer Parameters for LEDs	5-10
Table A..4: Experimental Results for total Irradiance using Si Photodiode	
$T_{SP} = 3175$ [K]	5-12
Table B..1: Electronic components for the prototype.	5-31

---

*CHAPTER 1*

*LIGHT: PHYSICAL PRINCIPLES*

---



## OUTLINE OF THE CHAPTER

### A) PRELIMINARY TOPICS

1. PRELIMINARY DEFINITIONS
2. ELECTROMAGNETIC SPECTRUM
3. PLANCK'S EQUATION
4. SUNLIGHT

### B) LIGHT AS WAVE

1. THEORETICAL SUPPORT
2. LIGHT SOURCES
3. LINEAR ARRAY OF COHERENT SOURCES

### C) PHOTONS

1. PHOTOELECTRIC EFFECT
2. SEMICONDUCTOR LIGHT DETECTORS
3. RESPONSIVITY
4. INCANDESCENT LIGHT SOURCES
5. CALIBRATION OF Si AND Ge PHOTODIODES USING A STANDARD TUNGSTEN FILAMENT LIGHT SOURCE
6. SPECTRAL RESPONSIVITY OF Si AND Ge PHOTODIODES

### D) OBJECTIVES AND SCOPE OF THE PRESENT WORK

1. GENERAL OBJECTIVE
2. SPECIFIC OBJECTIVES
3. SCOPE OF THE WORK

## Bibliography

### Basic References

#### Annexes Chapter 1 (Shown at the end of this work)

ANNEX 1: ARTICLE: SINGLE PHOTON: its size and internal electromagnetic fields

Author: Fernando Echeverría T.

ANNEX 2: RESPONSIVITY FOR Si AND Ge PHOTODIODES

ANNEX 3: RESPONSIVITY FOR Si AND Ge PHOTODIODES (Resol. 10 [nm])

ANNEX 4:

- a) STANDARD AND NORMALIZED TUNGSTEN FILAMENT LAMP SPECTRUM (Resol. 10 [nm])
- b) STANDARD AND NORMALIZED TUNGSTEN FILAMENT LAMP SPECTRUM (Spectral Range Bandwidth for Silicon)
- c) STANDARD AND NORMALIZED TUNGSTEN FILAMENT LAMP SPECTRUM (Spectral Range Bandwidth for Germanium)

ANNEX 5: PHOTODIODES TECHNICAL DATA



## CHAPTER 1: LIGHT: PHYSICAL PRINCIPLES

This chapter describes the theoretical frame and support to this work.

It is divided in four sections.

### Section A:

Preliminary definitions, an introduction to electromagnetic spectrum and Planck's equation are exposed as the theoretical support to thermal radiation.

An important resource in this work is the normalized Planck's equation named  $F_0\lambda(T, \lambda)$ . This function is useful for calculations of Irradiance, Spectral Temperature and Absolute Responsivity as it is explained in this work.

Then, a brief description of sunlight as the primary source for photovoltaic energy follows.

### Section B:

Encompass the description of Electromagnetic Theory that conceptualises light as a wave. Starting from Maxwell's equations this idea is introduced. Light as a wave explains – among other phenomena – irradiance and interference. These concepts are essential to design optical slits, to use prisms or diffraction grids and to use these components to design simple instruments as a photometer or a monochromator in order to measure and apply the wave characteristics of light.

### Section C:

The description of light as photons starting from the basic equations from Quantum Mechanics is introduced. These concepts are essential to understand the use of LEDs as light sources or light detectors, to characterize responsivity in LEDs and photodiodes; to correlate irradiance, responsivity and photocurrent in measurements and experiments using semiconductor detectors as it is explained in the final section of this chapter.

Annex 1, Chapter 1 presents a research article that attempts conciliate the wave and photon description of light:

F. Echeverría, et al. *Single Photon: its size and internal electromagnetic fields* (in preparation), 2018.



## A. PRELIMINARY TOPICS

### 1. PRELIMINARY DEFINITIONS

Primary source of light for mankind is sunlight. Light is a narrow band of the Electromagnetic Field which is detected by our eyes producing the perception of colours. Most of the experience we have of what surround us is through the sense of vision i.e. through our interaction with light.

Light is composed of quantum wave-corpuscles called “photons” being the most energetic those with higher frequencies. Photons as elementary particles have a dual behaviour: as particles and as waves.

Every photon has energy, so light is an expression of energy. The SI unit for Energy is the Joule [J].

$$E_{PHOTON} = h.f \quad [J] \quad (A.1)$$

Where:

$h$  is the **Planck’s constant: 6.63E-34\_J\*s**

$f$  is frequency [Hz]

The connection between energy  $E_{PHOTON}$  and wavelength  $\lambda_{PHOTON}$  is easily obtained from

$$\lambda_{PHOTON} . f = c \quad [m/s] \quad (A.2)$$

Where:

**$c = 299.8E6\_m/s$**

Light and, in general, Electromagnetic Fields have a speed  $c = 299.8E6\_m/s$ . It is a universal physical constant.

#### **Definition of Wavelength**

For a monochromatic light – i.e. a single colour or single frequency electromagnetic wave - **wavelength  $\lambda$**  is the distance light travels in one complete cycle or period.

From Eq. (A.2):

$$\lambda_{PHOTON} = c / f = c.T \quad [m] \quad (A.3)$$



## Definition of Irradiance

If 1 square meter [ $1\text{ m}^2$ ] of a flat surface is perpendicularly crossed by a continuous flow of light during 1 second, then the energy in the flow through the surface during 1 second [ $1\text{ s}$ ] represents a power per unit surface. Since the unit of power is the Watt [ $1\text{ W}$ ]. The power content of light per square meter [ $1\text{ W/m}^2$ ] is named **Irradiance**.

## Spectrum

Light can be decomposed in its **spectrum** when crosses a glass prism or a grid (diffraction grid) as shown in Fig. A.1.

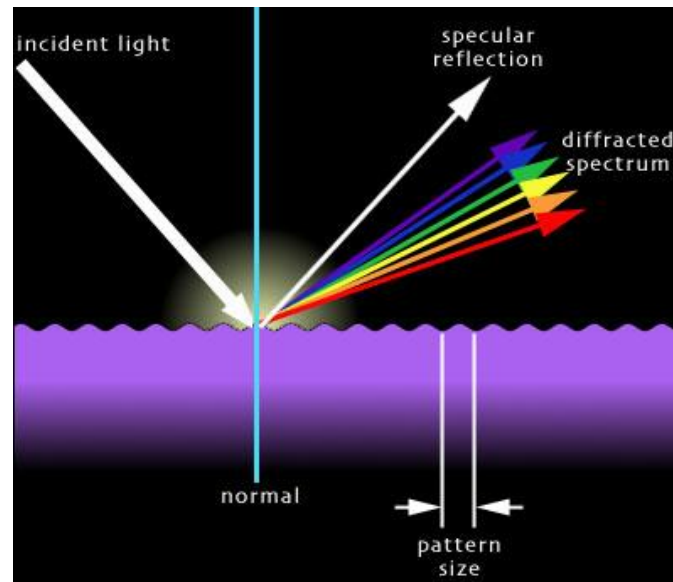


**Figure A.1:** *Diffraction of light in a reflective grating.*  
[Figure adapted from reference shown in ANNEX F]

It is very important to realise that the spectrum so obtained is a “wavelength ordered or is an increasing wavelength sequential distribution”. This means that there is a pattern sequence in wavelength (or energy) in the observed spectrum. Experimentally – as we will make it – it is observed that the red-band wavelengths are the longer or less energetic waves in the visible band (610 – 700 [nm]) and the shortest or more energetic visible band is Violet (below 450 [nm]) with the other colour bands in between as it is listed in Table A.1.

**Table A.1: Wavelength bands corresponding to visible colours**

---

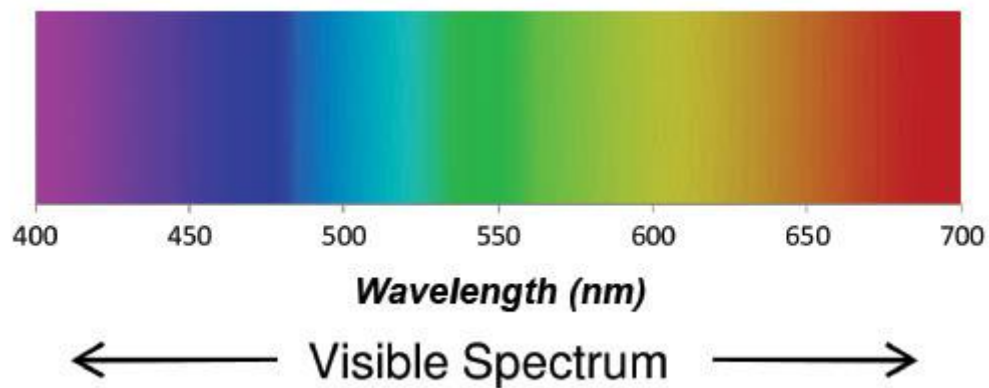
Violet	Below 450 nm
Blue	450 - 500 nm
Green	500 - 570 nm
Yellow	570 - 590 nm
Orange	590 - 610 nm
Red	610 - 700 nm

---

**Note:** 1 nanometre = 1 nm = 1E-9\_m = one thousand millionth of a meter  
= 1 millionth of a millimetre.

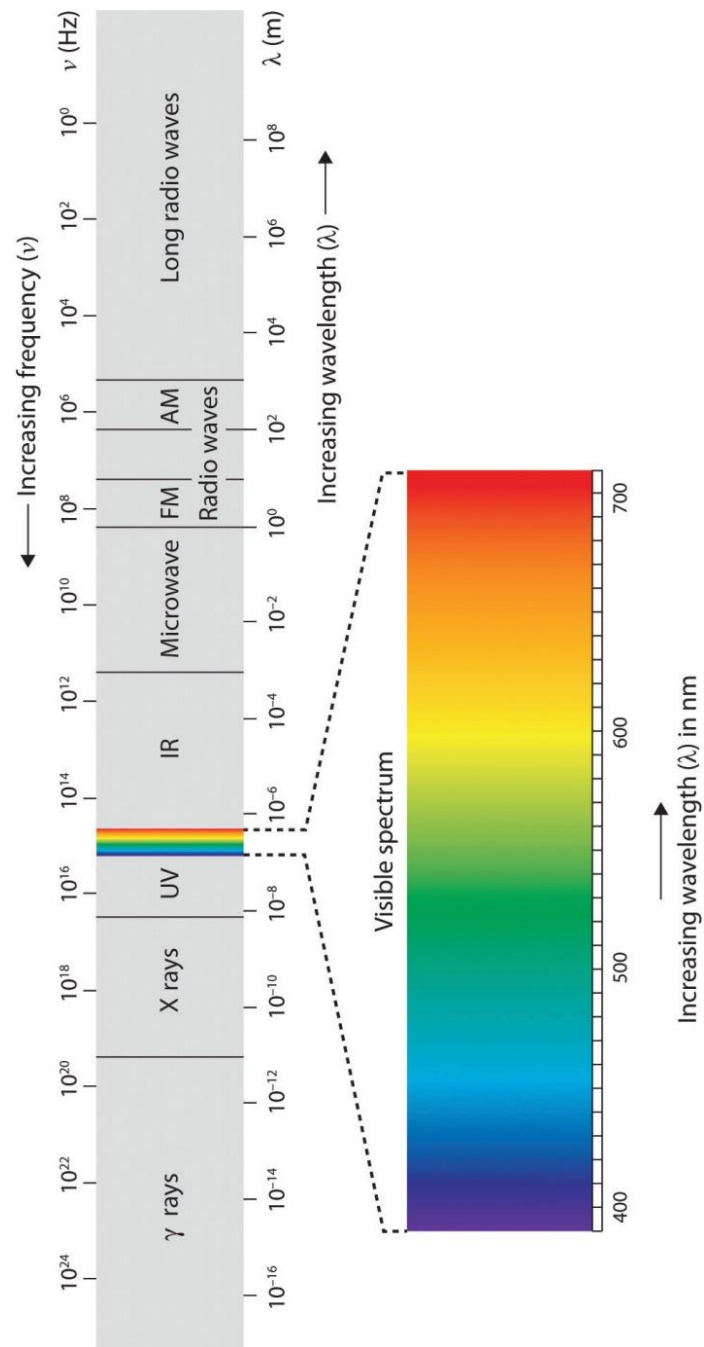
## 2 ELECTROMAGNETIC SPECTRUM

Fig. A.2 is a graphic of **Visible Spectrum** distribution.



**Figure A. 2:** *Visible spectrum band.*  
[Figure adapted from reference shown in ANNEX F]

Visible Spectrum does not cover the entire Electromagnetic Spectrum. On the contrary, the Visible Spectrum it is just a narrow band in Electromagnetic Spectrum as it is shown in Fig. A.3



**Figure A 3:** *Electromagnetic spectrum.*  
 [Figure adapted from reference shown in ANNEX F]

However in this work, we will deal only with the visible spectrum and their neighbour bands: near ultraviolet (UV) and near infrared bands (IR).

Fig. A.4 and Fig. A.5 show a classification for ultraviolet and infrared spectral ranges. These ranges are contiguous bands on both extremes of the visible range and partially are in the region of interest in this work.

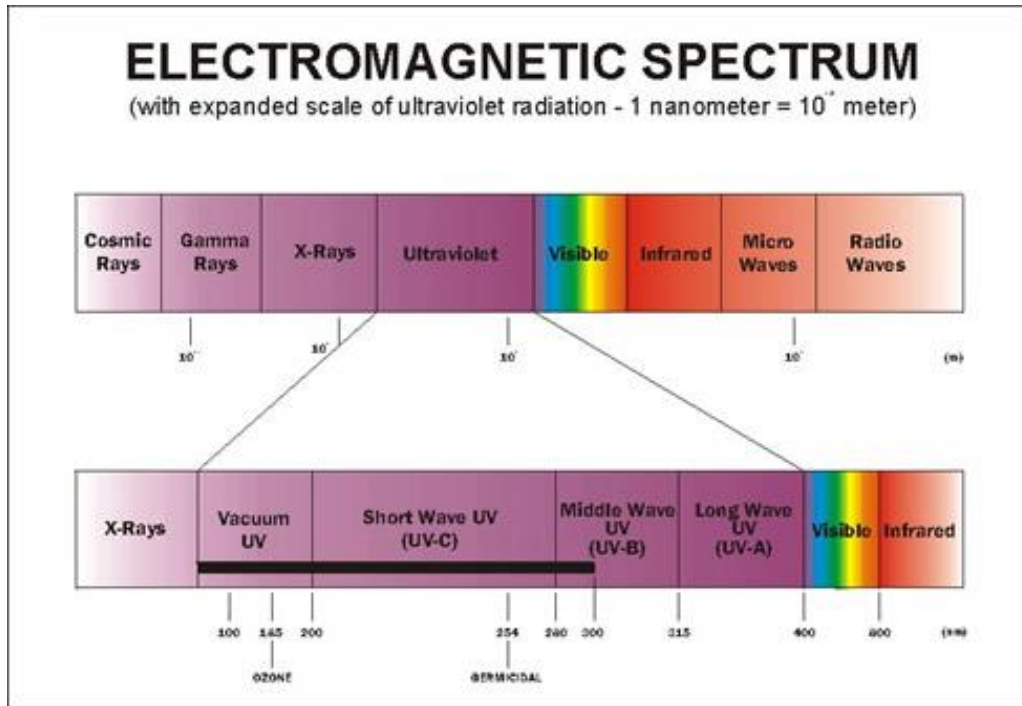


**Figure A. 4:** *Ultraviolet range.*  
 [Figure adapted from reference shown in ANNEX F]

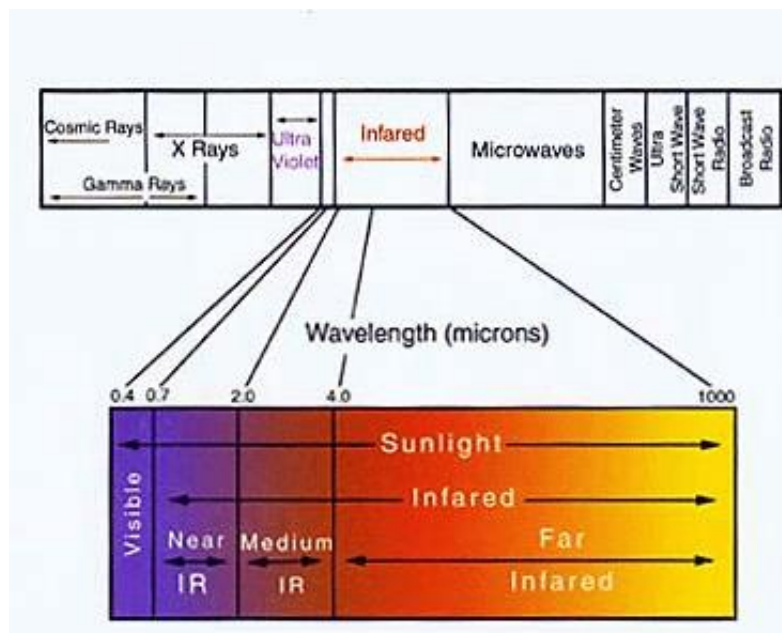


**Figure A. 5:** *Infrared range.*  
 [Figure adapted from reference shown in ANNEX F]

This is what concerns to **wavelength** of visible spectrum (or photon's energy through Eq. (A.1)).  
Next numeral exposes the topic of Irradiance in more detail.

### 3. PLANCK'S EQUATION

#### Irradiance

If **irradiance** is decomposed in a diagram of power per square meter per narrow bandwidths vs wavelength in the spectrum, then "**spectral irradiance distribution**" is obtained.

A very important thing one has to realise is that **spectral irradiance distribution depends on temperature of light source**, as it is illustrated in Fig. A.6

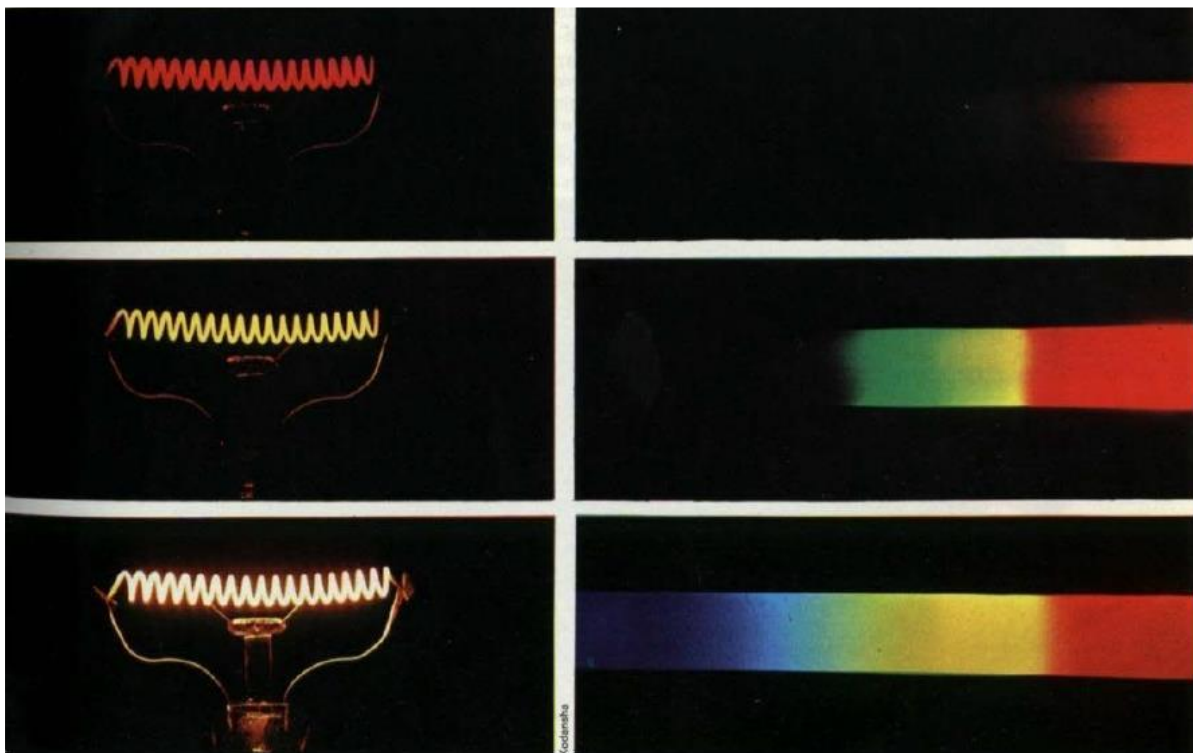


**Figure A. 6:** *Spectrum emitted by a hot filament depends on temperature.*  
[Figure adapted from reference shown in ANNEX F]

A common tungsten lamp filament is heated by an electric current circulating through it.

For low current – top pictures – filament is heated and temperature at filament is around ( $\approx 1000$  [K]). Only the red band of the spectrum is emitted (long red low energetic wavelengths).

If current is increased, the filament is at a higher temperature ( $\approx 2000$  [K] in as shown in central pictures); ( $\approx 3000$  [K] in bottom pictures), then filament is more brilliant and its spectrum is enriched with colours at shorter wavelengths.

The light power flowing per a unit surface perpendicular to the light propagation per narrow bandwidths is **spectral irradiance distribution**; its SI units are  $[W/m^2 m]$ . Last factor [m] corresponds to wavelength.

**Spectral irradiance distribution** plotted for different temperatures of radiant source is shown in Fig. A.7.

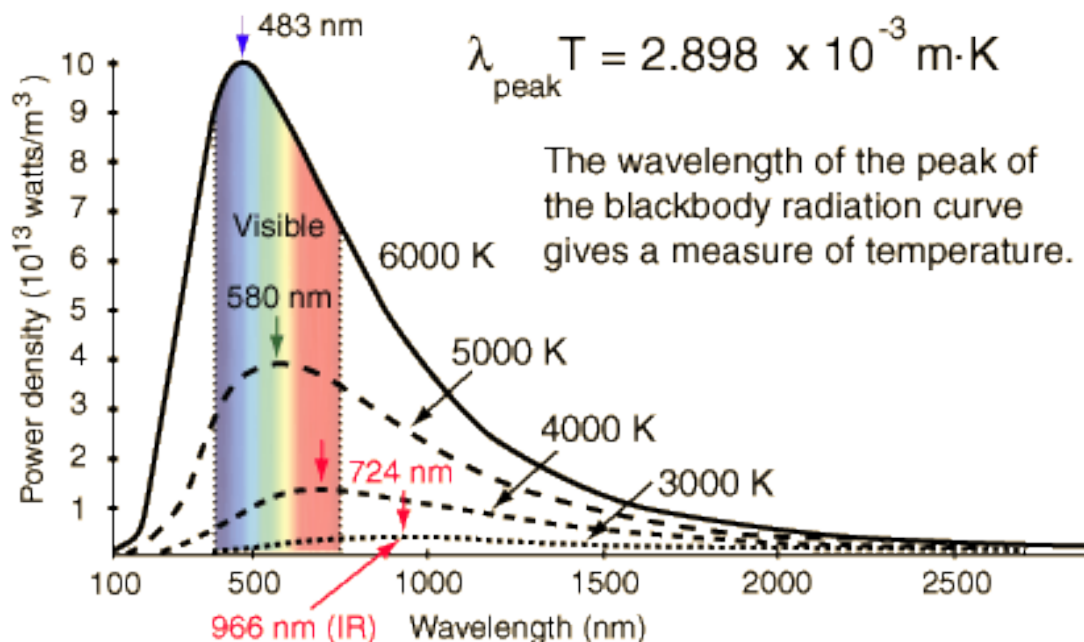


**Figure A.7:** Planck's equation plotted for different temperatures.  
[Figure adapted from reference shown in ANNEX F]

Equation that describes this experimental result is the very first correctly determined quantum mechanical formula. It was developed by Max Planck and it is known as **Planck's equation**.

Planck's equation starts considering that quantum systems behave as harmonic oscillators and these oscillators have permitted energy levels equally spaced at  $\hbar\omega_0$  energy steps apart, so the oscillator could take only these different energies as shown in Fig. A.8 [1]

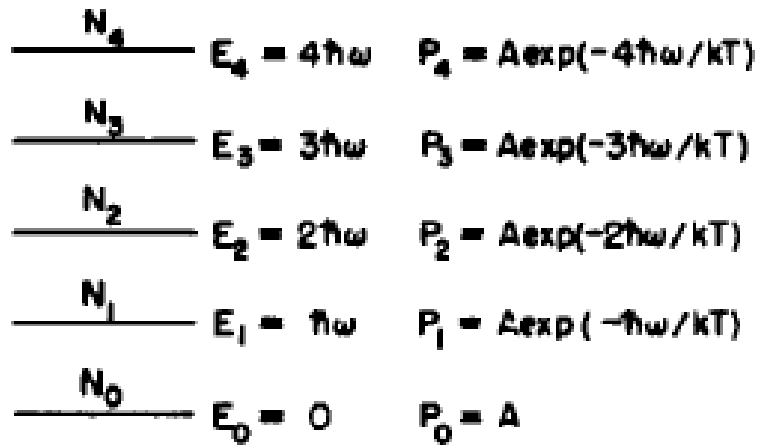


**Figure A.8:** Energy levels of a harmonic oscillator are equally spaced  $E_n = n\hbar\omega$  and the energy level transition probability  $P_n(E)$ .  
 [Figure adapted from reference shown in ANNEX F]

Planck demonstrated that the probability  $P(E)$  of occupying a level of energy  $E$  is

$$P(E) = \alpha e^{-\frac{\Delta E}{kT}} \quad \text{with} \quad E_n = n\hbar\omega \quad (\text{A.4})$$

This means that **the probability of occupying a level of Energy  $E$  decreases exponentially with the increment of the energy gap between the energy levels.**

Planck's equation is:

$$Id_\lambda = \frac{8\pi hc^2}{\lambda^5} \times \frac{1}{e^{\frac{hc}{\lambda kT}} - 1} \quad ; \quad \left[ \frac{W}{m^2 \times m} \right] \quad (\text{A.5})$$

Where:

- $Id_\lambda$  : Irradiance as a function of wavelength
- $h$  : Planck's constant : 6.6260755E-34\_J\*s
- $c$  : Speed of light : 299792458.\_m/s
- $\lambda$  : Wavelength [m]
- $k$  : Boltzmann's constant: 1.380658E-23\_J/K
- $T$  : Temperature [K]

Planck's equation is also expressed as a function of frequency  $\nu$  [Hz]:

$$I_{d\nu} = \frac{2h\nu^3}{c^2} \times \frac{1}{e^{\frac{h\nu}{k_B T}} - 1} \quad ; \quad \left[ \frac{W}{m^2 \times sr \times Hz} \right] \quad (A.6)$$

Where:

$$K_B = 1.380\,650\,5(24) \times 10^{-23} \text{ J}\cdot\text{K}^{-1} \quad \text{Boltzmann Constant}$$

### Stefan – Boltzmann law

Integrating the above equation over  $\nu$ , the power output given by the Stefan – Boltzmann law is obtained:

$$P = \sigma \times A \times T^4 \quad ; \quad [W] \quad (A.7)$$

Where:

$$\sigma = 5.670\,373\,(21) \times 10^{-8} \text{ W}\cdot\text{m}^{-2}\cdot\text{K}^{-4} \quad \text{Stefan – Boltzmann constant}$$

$$A = \text{radiating surface area [m}^2\text{]}$$

### Normalization of Planck's Distribution

In general, for a temperature  $T$ , the spectral irradiance in Eq. (A.5) expresses the power per unit area per wavelength and Eq. (A.7) is the total power per unit area for the total bandwidth.

Integral of Eq. (A.5) in an interval  $\lambda_1 \leq \lambda \leq \lambda_2$  is the power per unit area per bandwidth in the interval  $\lambda_1 \leq \lambda \leq \lambda_2$ . If this result is divided by Eq. (A.7) a dimensionless fraction is obtained and represents the fraction of total blackbody emissive power at temperature  $T$  in the wavelength interval.

Under these conditions it is said that the Planck's distribution is **normalized**.

$$L[\lambda_1; \lambda_2] = \frac{\int_{\lambda_1}^{\lambda_2} d\lambda \times \frac{8\pi^2}{\lambda^5} \times \frac{1}{e^{\frac{hc}{\lambda k T}} - 1}}{4 \times \sigma \times T^4} \quad [fraction] \quad (A.8)$$

Where:



$L[\lambda_1; \lambda_2]$  Is the fraction of total blackbody emissive power at temperature T in the wavelength interval  $[\lambda_1; \lambda_2]$ . It is a dimensionless fraction.

**Note:** Factor 4 in the denominator is due to the integral in the numerator is in units of  $[W / m^2]$  and in the denominator is in units of  $[W / \text{steradian}]$  [10]. For a given radius R, the ratio between the spherical surface and the area subtended by 1 steradian is 1/4 as it is illustrated in Fig. A.9

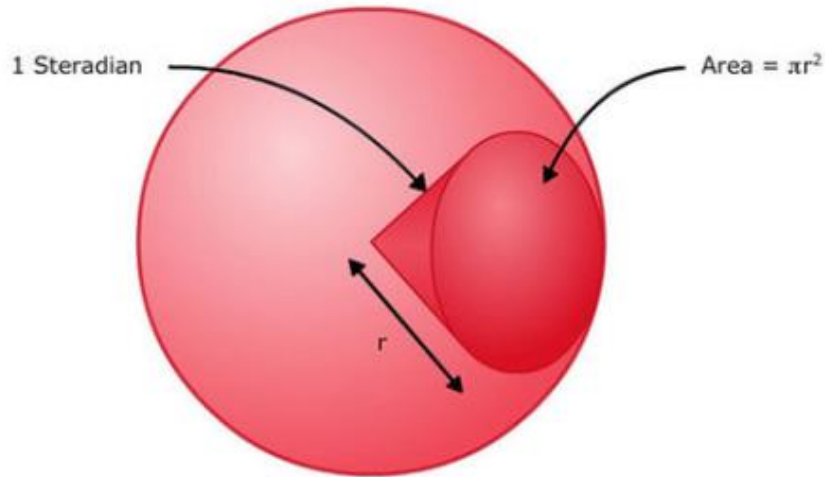


**Figure A.9:** Ratio between a spherical surface and the surface subtended by a steradian. [Figure adapted from reference shown in ANNEX F]

**The function  $F_{0\lambda}(T, \lambda)$**

Function  $F_{0\lambda}(T, \lambda)$  is Eq. (A.6) when  $\lambda_1 = 0$ .

$$F_{0\lambda}[T, \lambda] = \frac{\int_0^\lambda d\lambda \times \frac{8\pi^2}{\lambda^5} \times \frac{1}{e^{\frac{hc}{\lambda kT}} - 1}}{4 \times \sigma \times T^4} \quad [fraction] \quad (A.9)$$

It provides the black-body emissive power function: Returns the fraction of total black-body emissive power at temperature T between wavelengths 0 and lambda  $[\lambda]$ . For magnitudes in the SI system  $F_{0\lambda}$  returns a dimensionless fraction. [9]

In Fig. A.10, function  $F_{0\lambda}$  for a constant  $\lambda = \lambda_i$  is shown as the marked area from  $\lambda = 0$  to  $\lambda = \lambda_i$ .

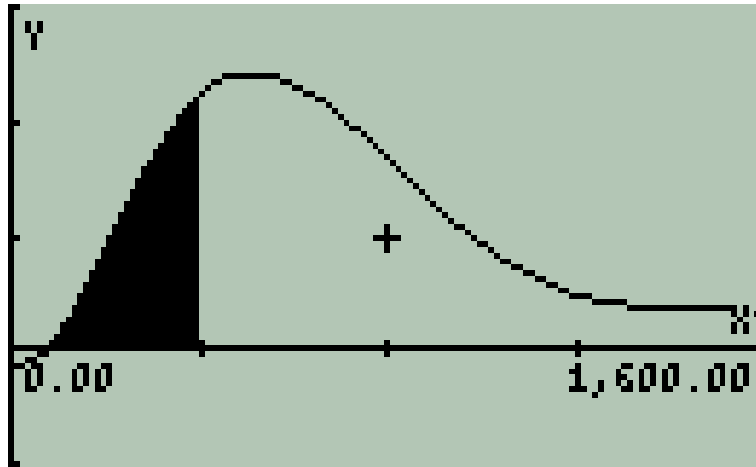


**Figure A.10:** Function  $F0\lambda$  for  $\lambda = \lambda_i$  is the marked area from  $\lambda = 0$  to  $\lambda = \lambda_i$  in the normalized Planck's Equation. Its maximum value when  $\lambda \rightarrow \infty$  is 1.

$$L[\lambda_1] = F0\lambda_1 \quad [fraction] \quad (A.10)$$

Function  $F0\lambda$  has been implemented to ease calculations. So, the fraction of total blackbody emissive power at temperature  $T$  in the wavelength  $[\lambda_1 ; \lambda_2]$  interval is just:

$$L[\lambda_1 ; \lambda_2] = F0\lambda_2 - F0\lambda_1 \quad [fraction] \quad (A.11)$$

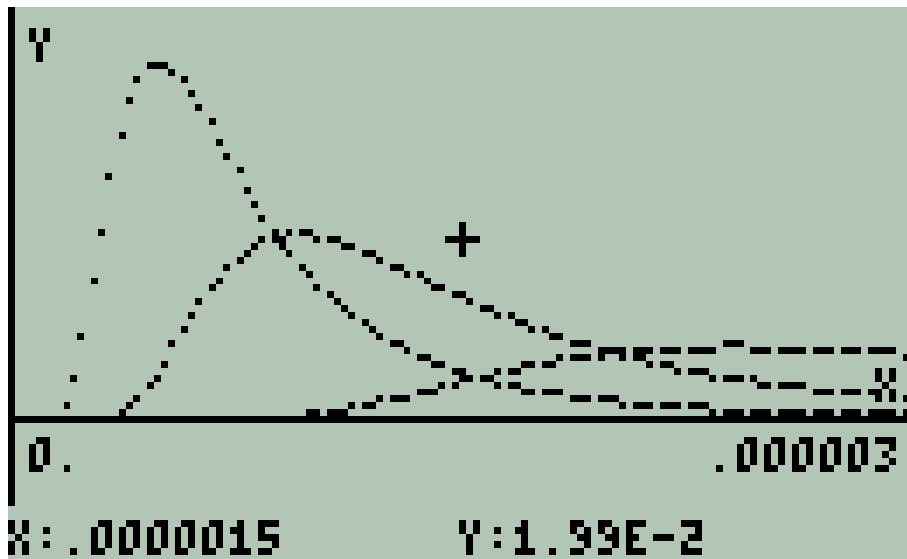
Certainly the normalized integral over the whole spectrum is 1:

$$L[\lambda_1 = 0; \lambda_2 = \infty] = 1 \quad [fraction] \quad (A.12)$$

Normalized function  $F0\lambda$  is also a function of temperature; i.e.:

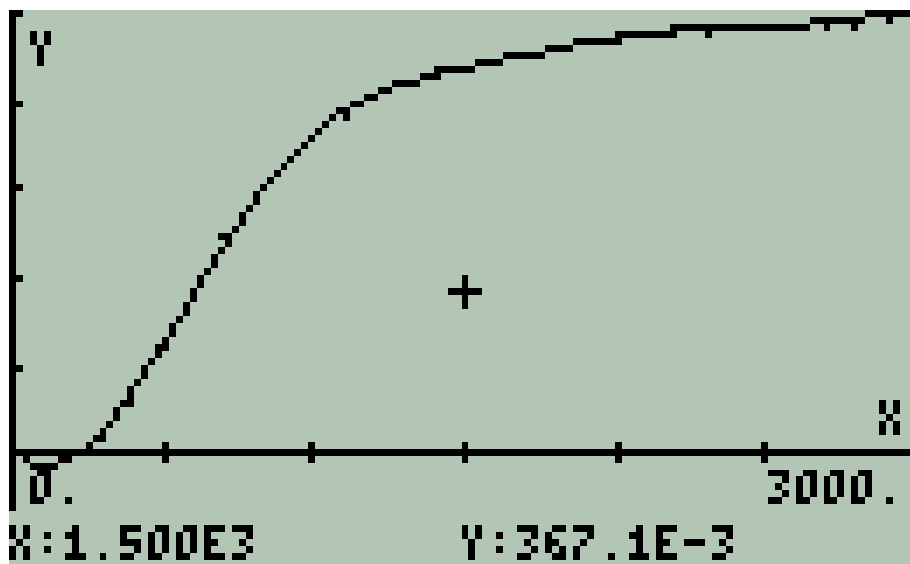
$$F0\lambda = F0\lambda(T, \lambda) \quad [fraction] \quad (A.13)$$

Fig. A.11 shows  $F0\lambda$  for three different temperatures  $T_1 = 5770$  [K] i.e: the sunlight spectral distribution,  $T_2 = 3200$  [K] the tungsten incandescent filament and  $T_3 = 1200$  [K] the steel melting point.



**Figure A.11:**  $F0\lambda$  for:  $T1 = 5770 [K]$ ,  $T2 = 3200 [K]$  and  $T3 = 1200 [K]$

Finally, Fig. A.12 is a plot of the integral of  $F0\lambda$  for  $T = 5770 [K]$ .



**Figure A.12:** *Integral of  $F0\lambda$  for  $T = 5770 [K]$ .*

Function  $F0\lambda$  is a useful algorithm for spectral measurements as it will be explained in Chapter 4.

#### 4. SUNLIGHT

Sun – in a similar manner than the heated tungsten filament – emits radiation (i.e.: sunlight or sun's radiation). Sun's irradiance spectrum has been experimentally measured out of the Earth's atmosphere. It is the yellow-coloured spectrum shown in next figure. This spectrum has been fitted with the Planck's Equation. In this way it has been found that this spectral temperature corresponds to 5777 [K].

Now, **Irradiance  $L$  is the integral of Spectral Irradiance in the whole spectrum.** This is the **Stefan – Boltzmann Law** [10].

$$L = \frac{2\pi^5 k^4}{15h^3 c^2} \times T^4 = \sigma \times T^4 \quad ; \quad \left[ \frac{W}{m^2} \right] \quad (A.14)$$

Where:

$$\sigma = \frac{2\pi^5 k^4}{15h^3 c^2} \quad (A.15)$$

$\sigma$  : Stefan – Boltzmann constant. : 5.67051E-8\_W/ (m<sup>2</sup>\*K<sup>4</sup>)

For  $T = 5770 [K]$ , the solar irradiance is:

$$L_{SOLAR\_SURFACE} = \sigma \times T^4 = 62.853E6 \quad ; \quad \left[ \frac{W}{m^2} \right] \quad (A.16)$$

This is solar irradiance obtained on the “sun's surface”.

Since irradiance on a surface perpendicular to the propagation of light is inversely proportional to the squared distance from the source as is shown in Fig. A.13.

$$\frac{I_{SOLAR\_SURFACE}}{R_{SUN}^2} = \frac{I_{EARTH\_SURFACE}}{R_{SUN\_EARTH\_DISTANCE}^2} \quad (A.17)$$

Where:

$$R_{SUN} = 6.55E8 \quad [m] \quad ; \quad R_{SUN\_EARTH} = 149.6E9 \quad [m]$$

See References [2] and [3]

Then, from (8) and (9):

$$L_{EARTH\_SURFACE} = \left( \frac{R_{SUN}}{R_{SUN\_EARTH}} \right)^2 \times L_{SOLAR\_SURFACE} \quad (A.18)$$

$$L_{EARTH\_SURFACE} = 1204.9 \left[ \frac{W}{m^2} \right] \quad (A.19.a)$$

Experimentally, the measured values for solar irradiance are:

$$L_{EARTH's\_UPPER\_ATMOSPHERE} = 1361 \left[ \frac{W}{m^2} \right] \quad (A.19.b)$$

$$L_{EARTH's\_SEA\_LEVEL\_ZENITH} = 1050 \left[ \frac{W}{m^2} \right] \quad (A.19.c)$$

For Laboratory experimentation 1 sun irradiance is typically defined as the nominal full sunlight intensity on a bright clear day on Earth, which measures 1000 W/m<sup>2</sup>.

$$L_{LABORATORY(1\_SUN)} = 1000 \left[ \frac{W}{m^2} \right] \quad (A.19.d)$$

See References [4], [5] and [6].

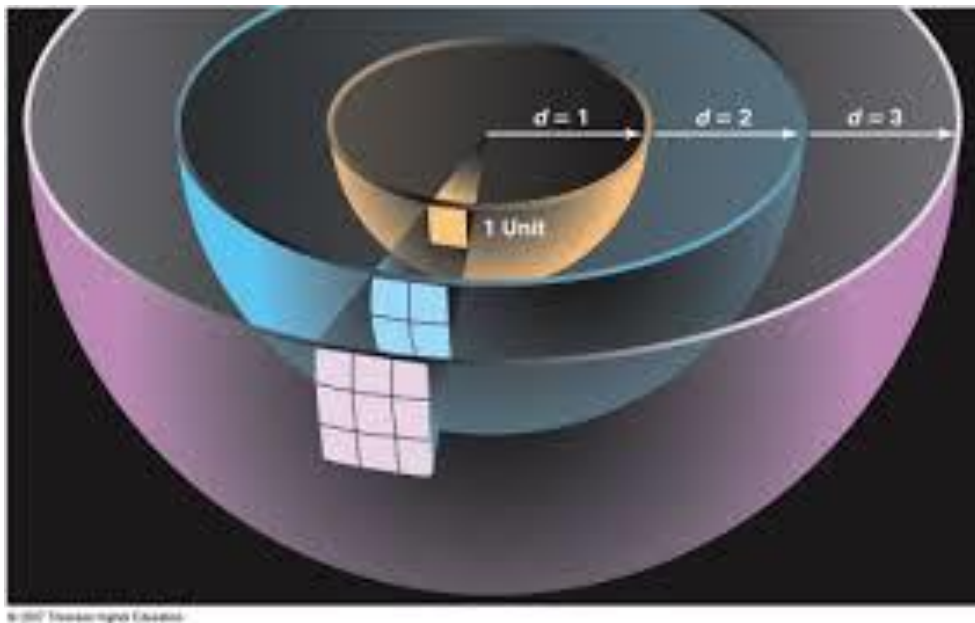


**Figure A.13:** *Inverse square distance law for radiation.*  
*[Figure adapted from reference shown in ANNEX F]*

### Reflection:

In vacuum, irradiance changes with distance as described by Eq (2); however spectral distribution is identical, what changes is the power per square meter – or power per steradian. In general, spectral distribution changes when light interacts with matter.

Total Irradiance from sunlight on Earth’s external atmosphere is 1367 [W/m<sup>2</sup>]. Fig. A.14 illustrates the experimental measurement fitting Planck’s equation for 5777 [K]

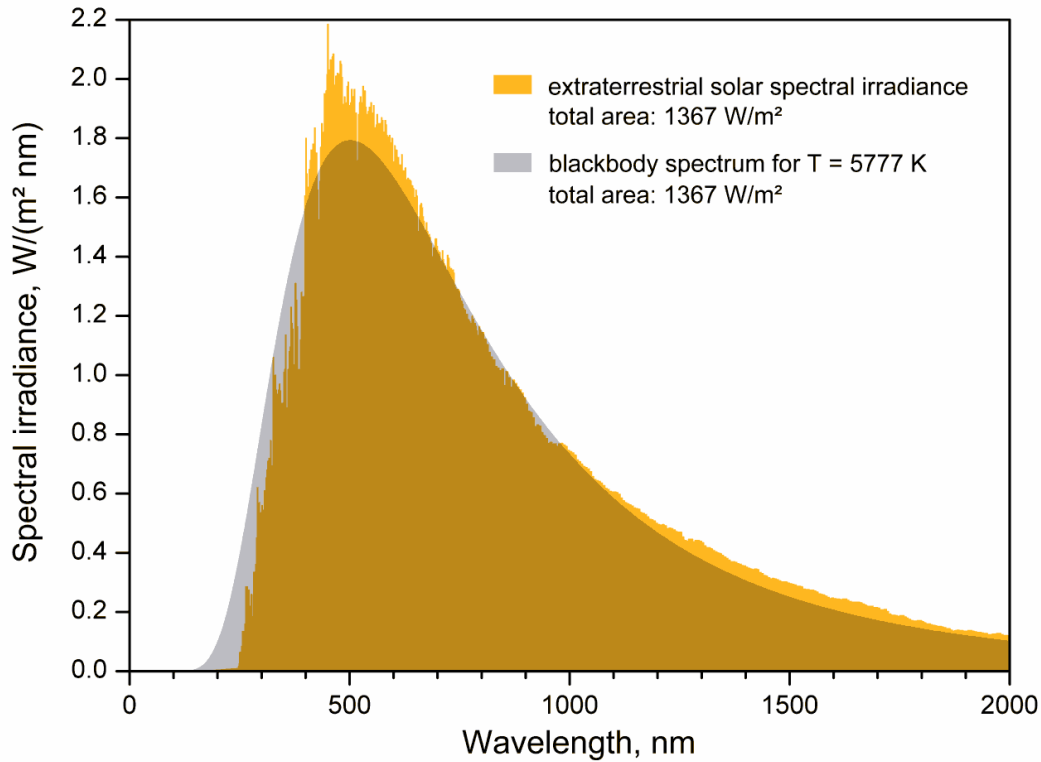


**Figure A.14:** Solar spectral irradiance on Earth’s outer atmosphere fits Planck’s Equation for a spectral temperature of 5777 [K].  
 [Figure adapted from reference shown in ANNEX F]

One should realise that the irradiance of 1367 [W/m<sup>2</sup>] corresponds to the surface of 1[m<sup>2</sup>] on Earth’s outer atmosphere perpendicular to the light propagation from Sun at the distance Sun – Earth, this distance is

$$R_{\text{SUN-EARTH}} = 149.6\text{E}9 \text{ [m]}$$

In fact, irradiance “on the Sun’s surface” is enormously bigger compared with irradiance measured on Earth’s stratosphere (around 62.853E6 [W/m<sup>2</sup>]) since

$$R_{\text{SUN}} = 6.55\text{E}8 \text{ [m]}$$

a distance magnitude 230 times smaller. Both magnitudes are related by the **inverse square distance law for radiation**. See Fig. 8.

It is important to realise that in vacuum (where propagation occurs almost without any interaction with atoms), the **spectral distribution is preserved** independently of the distance from the source; though **irradiance changes depending on distance between light source and point of measurement**.

However, when sunlight passes through Earth’s atmosphere, several spectral bands are absorbed, mainly due to the **Ozone – Oxygen cycle** in the UV region and **selective bands absorbed by O<sub>2</sub>, H<sub>2</sub>O and CO<sub>2</sub> molecules present in the Earth’s atmosphere**. See Fig. A.15

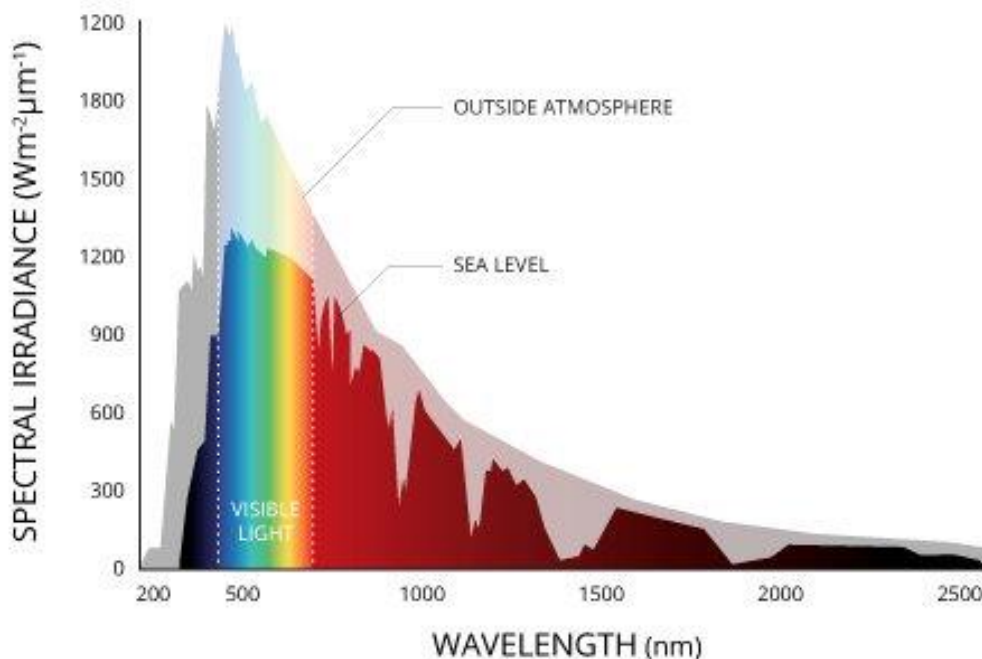


**Figure A.15:** *Solar irradiance on Earth’s outside atmosphere and on Earth’s surface at sea level Attenuation is observed mainly due to the **Ozone – Oxygen cycle** in the UV region and bands absorbed by O<sub>2</sub>, H<sub>2</sub>O and CO<sub>2</sub> molecules present in the Earth’s atmosphere. [Figure adapted from reference shown in ANNEX F]*

So, solar irradiance outside atmosphere is attenuated when crosses the atmosphere mainly due to the above mentioned causes. Actual radiation measured on Earth’s surface, at sea level, at the equator (Latitude 0° 0’ 0’’), at zenith in a clear day is about 1000 [W/m<sup>2</sup>]. [7]

For Laboratory experimentation 1 sun is typically defined as the nominal full sunlight intensity on a bright clear day on Earth, which measures 1000 W/m<sup>2</sup>. See Eq. (10).

If Sun’s spectrum is observed with a high resolution spectrometer it shows thousands of discontinuities that provide information about the transitions among levels in the electronic configurations of those chemical elements that are present in the solar corona. These discontinuities are known as **Fraunhofer’s spectral lines** and constitute a formidable evidence of the quantum behaviour of atomic transitions. A summary of these transitions are shown in a composed photography of spectral segments in an increasing wavelength array. See Fig. A.16. [8]

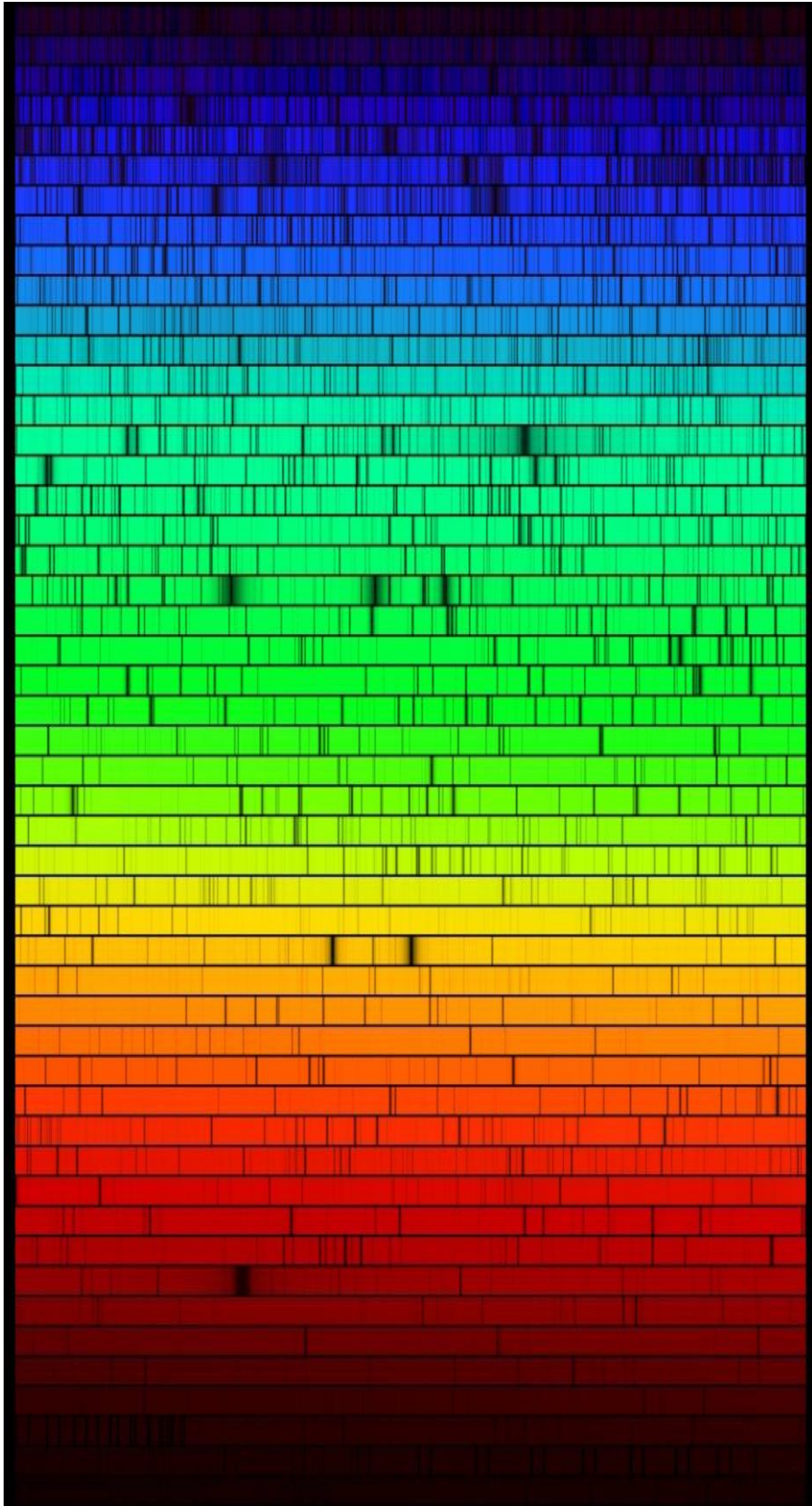


**Figure A.16:** *High resolution solar irradiance spectral bands photography.*  
*[Figure adapted from reference shown in ANNEX F]*



## B. LIGHT AS WAVE

### 1. THEORETICAL SUPPORT

The fact that light is a part of electromagnetic spectrum as it is shown in Chapter 1 Fig. 2 to Fig. 5 implies that, for Electromagnetic Theory, light as well as the whole electromagnetic spectrum is described as waves.

#### Maxwell's Equations

The foundations of Electromagnetic Theory are Maxwell's Equations: [11]

#### *Maxwell's Equations*

$$(1) \quad \nabla \cdot \mathbf{E} = \frac{\rho}{\epsilon_0}$$

$$(2) \quad \nabla \times \mathbf{E} = - \frac{\partial \mathbf{B}}{\partial t}$$

$$(3) \quad \nabla \cdot \mathbf{B} = 0$$

$$(4) \quad c^2 \nabla \times \mathbf{B} = \frac{\partial \mathbf{E}}{\partial t} + \frac{\mathbf{j}}{\epsilon_0}$$

(B.1)

Where:

$E$	Electric Field	[V/m]
$B$	Magnetic Field	[T]
$\rho$	Charge Density	[C/m <sup>3</sup> ]
$j$	Current Density	[A/m <sup>2</sup> ]
$t$	time	[s]
$\epsilon_0$	Permittivity constant	= 8.854E-12 [F/m]
$c$	Speed of light in vacuum	= 299.8E6 [m/s]

Maxwell's Equations are a **vector system of partial differential equations**.

## Electromagnetic waves

When these equations are applied to a region of “**free space**”, as example vacuum, this means a region where neither electric charges nor currents exist ( $\rho = 0 ; j = 0$ ), Maxwell’s equation take the form:

$$\begin{aligned}
 \text{I. } & \nabla \cdot \mathbf{E} = 0 \\
 \text{II. } & \nabla \times \mathbf{E} = - \frac{\partial \mathbf{B}}{\partial t} \\
 \text{III. } & \nabla \cdot \mathbf{B} = 0 \\
 \text{IV. } & c^2 \nabla \times \mathbf{B} = \frac{\partial \mathbf{E}}{\partial t}
 \end{aligned}
 \tag{B.2}$$

When these equations are solved then, the **wave equation** is obtained for  $\mathbf{E}$  as well as for  $\mathbf{B}$ :

$$\nabla^2 \mathbf{B} - \frac{1}{c^2} \frac{\partial^2 \mathbf{B}}{\partial t^2} = 0.
 \tag{B.3}$$

$$\nabla^2 \mathbf{E} - \frac{1}{c^2} \frac{\partial^2 \mathbf{E}}{\partial t^2} = 0.
 \tag{B.4}$$

This means that  $\mathbf{E}$  and  $\mathbf{B}$  behave as waves, they are electromagnetic waves.

Solutions for Eq. (6) and Eq. (7) are **traveling waves** that propagate at the speed of light. See Fig. B.1

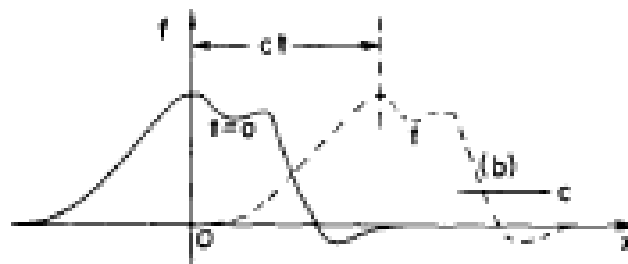


**Figure B.1:** The function  $f(x - ct)$  represents a constant “shape” that travels toward positive  $x$  with speed  $c$ .  
 [Figure adapted from reference shown in ANNEX F]

Electromagnetic waves once generated from accelerated charges propagate in free space as independent entities.

**Due to vector characteristic of electromagnetic waves the following features are deduced from the system of equations (5):**

- The relation between E and B in a electromagnetic wave in free space is

$$|E| = c|B| \quad [V/m] \quad (B.5)$$

- Electric Field  $E$  and magnetic field  $B$  in an electromagnetic wave are oscillating vector fields, perpendicular to each other interchanging energy at a frequency  $f$  and propagating in a direction perpendicular to them. The magnitude defined by vector  $S$  or Poynting's vector. So light is a transversal wave. See Fig. B.2.

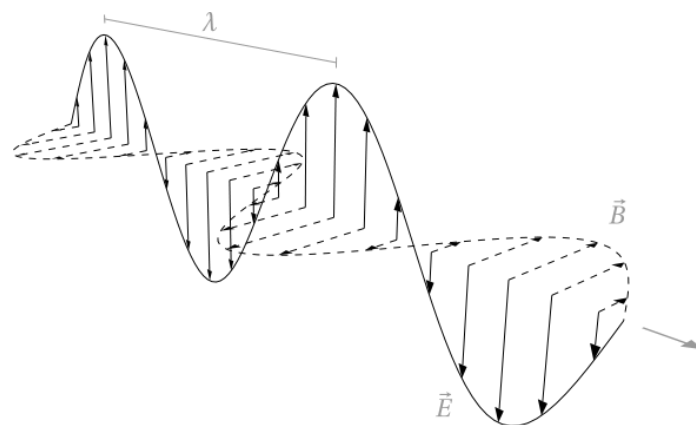


**Figure B.2:** Graphical description of an EMG wave.  
[Figure adapted from reference shown in ANNEX F]

- The Poynting vector  $S$  is proportional to the cross product of E and B.

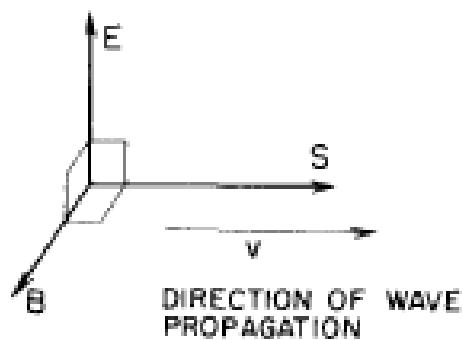


**Figure B.3:** Poynting vector  $S$  defines the direction of propagation of light.  
[Figure adapted from reference shown in ANNEX F]

$$S = \epsilon_0 c^2 E \times B. \quad [W/m^2] \quad (B.6)$$

$$S = \epsilon_0 c E^2. \quad [W/m^2] \quad (B.7)$$

- Electromagnetic Waves transport Energy.

Since Electromagnetic Waves propagate in free space there is an **electromagnetic energy density**  $u$  and in a volume of free space there is an **energy**  $U$

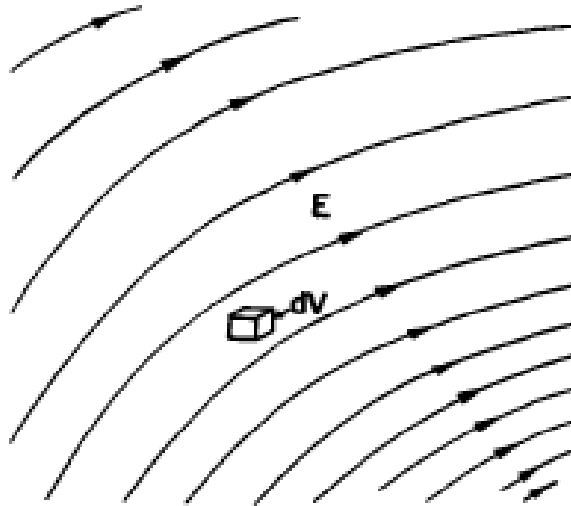


**Figure B.4:** Every volume element in space has an energy density  $u$   
[Figure adapted from reference shown in ANNEX F]

$$u = \frac{\epsilon_0}{2} \mathbf{E} \cdot \mathbf{E} + \frac{\epsilon_0 c^2}{2} \mathbf{B} \cdot \mathbf{B} \quad [\text{J/m}^3] \quad (\text{B.8})$$

$$U = \int \left( \frac{\epsilon_0}{2} \mathbf{E} \cdot \mathbf{E} + \frac{\epsilon_0 c^2}{2} \mathbf{B} \cdot \mathbf{B} \right) dV \quad [\text{J}] \quad (\text{B.9})$$

- Electromagnetic waves have momentum density

$$\mathbf{g} = \frac{1}{c^2} \mathbf{S}. \quad [\text{N.s/m}^3] \quad (\text{B.10})$$

- Electromagnetic waves have a momentum

$$\mathbf{p} = \mathbf{U} / c \quad [\text{N.s}] \quad (\text{B.11})$$

## Plane and Spherical Waves

A wave in the far field, i.e. at a big distance from its source – measured in wavelengths – is considered a **plane wave** since its wave front propagates practically on a plane.

Waves proceeding from a source, in general propagate as a **spherical wave**. At distances comparable with few wavelengths their wave front is a spherical surface. See Fig. B.5.

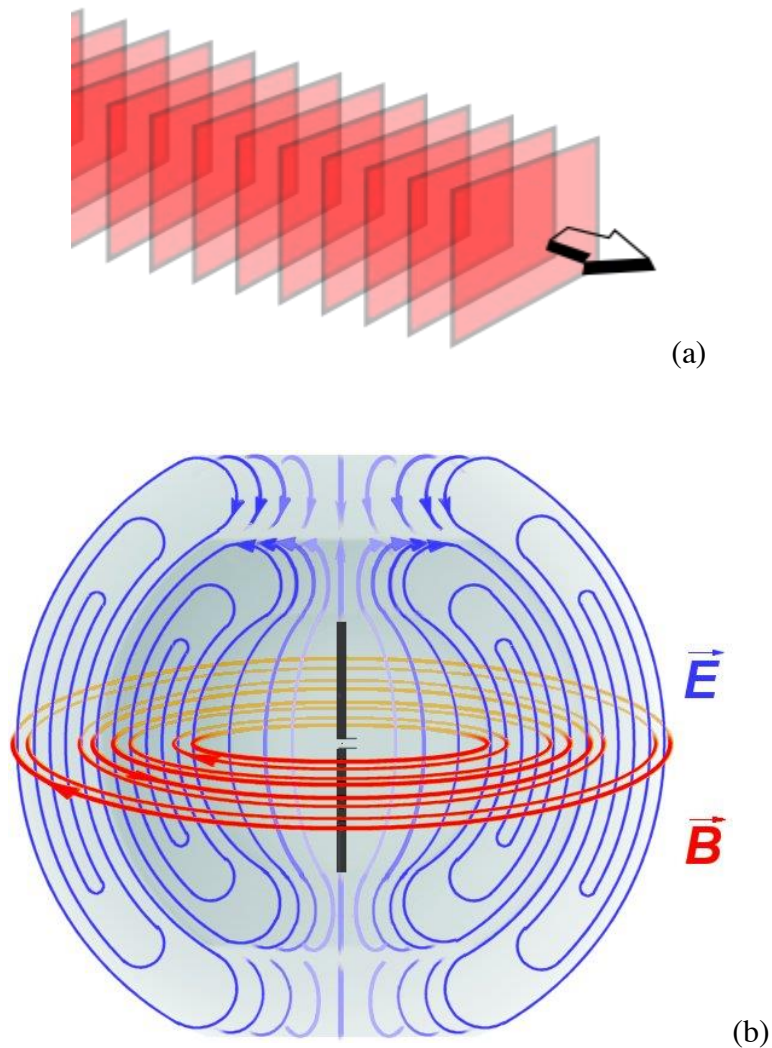


**Figure B.5:** Plane and spherical EMG wavefronts: (a) A plane wave front. (b) A dipole antenna radiates spherical electromagnetic fields. [Figure adapted from reference shown in ANNEX F]

## Plane Waves

The simplest waves are a harmonic plane wave oscillating with an angular frequency  $\omega$ , Eq. (B.11)

$$\begin{aligned}
 E_{\text{PLANE-WAVE}}(x - ct) &= E_0 \cos\left[\frac{2\pi}{\lambda}(x - ct) + \alpha\right] \\
 &= E_0 \cos(k \cdot x - \omega t + \alpha) \quad [\text{V/m}] \quad (\text{B.12})
 \end{aligned}$$

Where:

$E_0$	Electric Field Amplitude	[V/m]
$\lambda$	wavelength	[m]
$r, x$	position	[m]
$c$	speed of light	[m/s]
$t$	time	[s]
$k$	$2\pi/\lambda$ wavenumber	[radians/m]
$\omega$	$2\pi/T = 2\pi f$ angular frequency	[radians/s]
$T$	period	[s]
$f$	frequency	[Hz = 1/s]
$\alpha$	initial phase	[radians]

Main features of a harmonic plane electromagnetic wave are summarized in Fig. B.6

Plane waves are useful in this context to describe interference and diffraction.

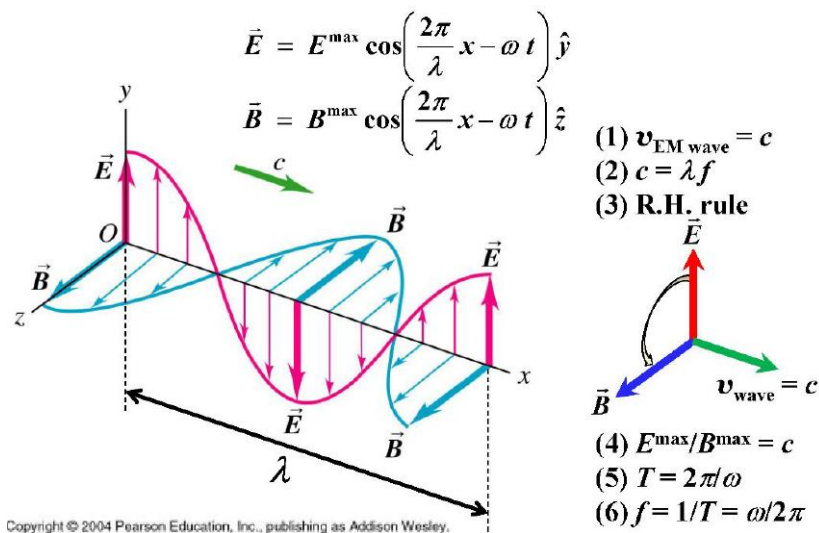


**Figure B.6:** A harmonic plane electromagnetic wave and equations that relate physical parameters.  
 [Figure adapted from reference shown in ANNEX F]

## Spherical Waves

Spherical waves are irradiated from a central source so, it is required to express the wave equation in spherical coordinates. The wave function in spherical coordinates is clearly explained in [12].

Spherical waves are irradiated from a central source so, it is required to express the wave equation in spherical coordinates. See Eq. (6), Eq. (7).

$$\nabla^2 \psi(r, t) - \frac{1}{c^2} \frac{\partial^2}{\partial t^2} \psi(r, t) = 0. \quad (\text{B.13})$$

so, an expression  $\psi(r, t)$  that complies with Eq. (B.12) is required.

Ref. [2] demonstrates that operator  $\nabla^2$  for spherical coordinates that are only function of  $r$  is:

$$\nabla^2 \psi = \frac{1}{r} \frac{d^2}{dr^2} (r\psi). \quad (\text{B.14})$$

So, Eq. (B, 13) is written as:

$$\frac{1}{r} \frac{\partial^2}{\partial r^2} (r\psi) - \frac{1}{c^2} \frac{\partial^2}{\partial t^2} \psi = 0. \quad (\text{B.15})$$

If Eq. (B.15) is multiplied by  $r$ ,

$$\frac{\partial^2}{\partial r^2} (r\psi) - \frac{1}{c^2} \frac{\partial^2}{\partial t^2} (r\psi) = 0. \quad (\text{B.16})$$

This equation expresses that function  $r\psi$  satisfies one dimensional wave equation for the variable  $r$ . This implies that the solution has the form:

$$r\psi(r, t) = f(r - ct). \quad (\text{B.17})$$

then

$$\psi = \frac{f(t - r/c)}{r}. \quad (\text{B.18})$$

Eq. (B.18) represents a general spherical wave travelling outward from the origin at the speed  $c$ . Factor  $r$  in the denominator, implies that **wave decreases in proportion to  $1/r$  when it propagates**. So **there is a difference with a plane wave in which the amplitude remains constant when it propagates**.

This effect is easy to understand if Fig. A.13 is reviewed and, recalling from Eq. (B.8) that **energy density  $u$  in a wave depends on the square of the wave amplitude**. As the wave spreads, its energy is spread over larger and larger areas proportional to the radial distance squared. If the total energy is conserved, the energy density must decrease as  $1/r^2$ , and the amplitude of the wave must decrease as  $1/r$ .

## 2. LIGHT SOURCES

Light comes from an enormous variety of light sources. Natural or man-made sources. Sunlight, electric lamps, flames, explosive chemical reactions or phosphorescent insects are just few examples.

However, light radiation coming from any source can be displayed as a **spectrum** or in a **distribution of light intensities versus wavelength**. See Figs. A.2, A.3, A.4, A.5.

In general, a light source has several wavelength-bands with different light intensities, then it radiates a **polychromatic spectra**.

However there are light sources that emit radiation in a narrow band with no other bandwidths present in the spectrum, this spectrum is called a **monochromatic spectrum**. **Light Emitting Diodes** or simply **LEDS** are good examples of almost **monochromatic sources** with a narrow bandwidth. See Fig. B.7

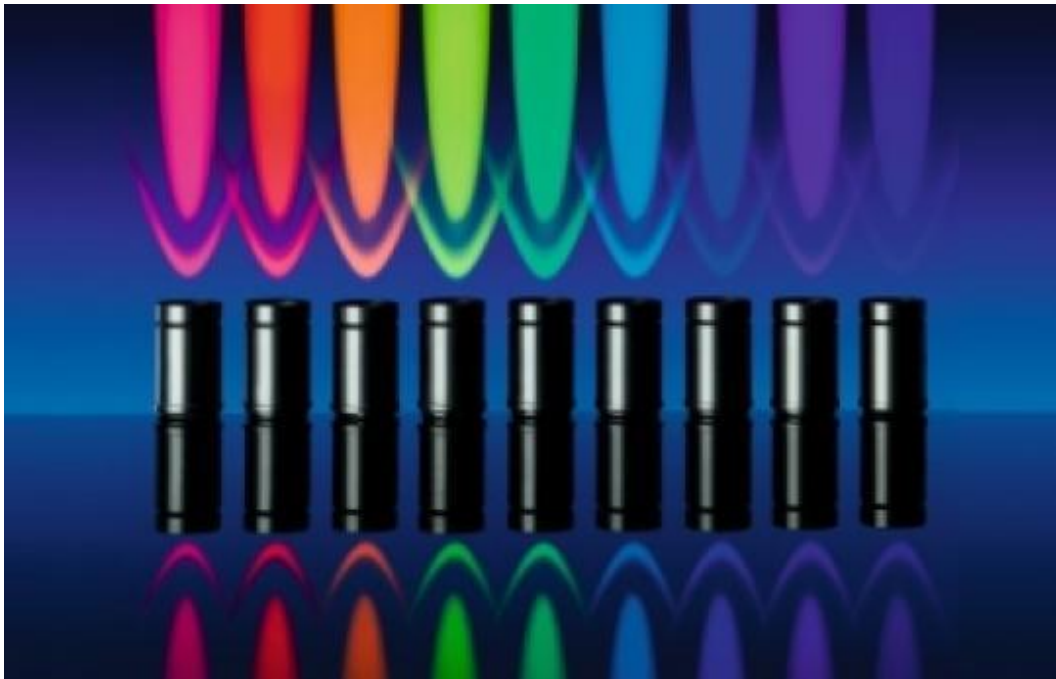


**Figure B.7:** LEDs are examples of quasi-monochromatic light sources.  
[Figure adapted from reference shown in ANNEX F]

**Laser emitting diodes** besides a better monochromaticity than LEDs have an additional characteristic. In general, light from Lasers is a **coherent light**. **Laser coherence** means that laser light differs from conventional light in that all the light waves are in phase with each other. One consequence is a minimum divergence from the constant diameter of the beam over a long distance. See Fig. B.8



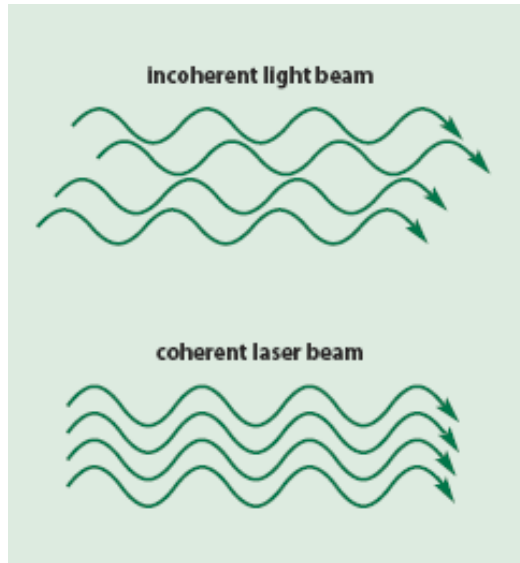


**Figure B.8:** *Coherent and incoherent beams graphical description.*  
*[Figure adapted from reference shown in ANNEX F]*

Solid State Lasers can be used as **wavelength calibration standards**. See Table 1

**Table B.1:** **Solid state lasers and their wavelengths**

Colour Range	Wavelength [nm]
Violet-Blue	405
Blue	445
Green	460
Yellow	473
Red	532
Infrared	589
	635
	650
	808
	980
	1064

### 3. LINEAR ARRAY OF COHERENT SOURCES

Coherent light sources are a useful tool to experiment with essential components of instruments to measure light parameters as are **optical slits** and **diffraction grids**.

Equations for optical slits and diffraction grids are obtained from the analysis of linear arrays of coherent sources in the **far field**. Criterion to distinguish near and far field is found in [13]

#### Single monochromatic source

The wave equation for a single spherical monochromatic source is obtained from Eq. (B.12) and Eq. (B.18):

$$\mathbf{E}(\mathbf{r}, t) = \hat{\mathbf{e}}_r [E_0/r] \cos(\mathbf{k} \cdot \mathbf{r} - \omega t + \alpha) \quad [\text{V/m}] \quad (\text{B.19})$$

Where:

$\mathbf{E}(\mathbf{r}, t)$	Electric field vector as function $\mathbf{r}$ and $t$	[V/m]
$\hat{\mathbf{e}}_r$	Unitary vector in $\mathbf{r}$ direction	[dimensionless]
$E_0$	Electric field module at the source	[V/m]
$\mathbf{k}$	wave vector, $ \mathbf{k}  = k = 2\pi/\lambda$	[radians / m]
$\mathbf{r}, r$	position vector with respect to the source	[m]
$\omega$	angular frequency $2\pi/T = 2\pi(c/\lambda)$	[radians/s]
$T$	period	[s]
$t$	time	[s]
$f$	frequency $1/T$	[Hz = 1/s]
$\alpha$	initial phase	[radians]

From Eq. (9) and Eq. (10), the **Poynting vector**, named also as **Intensity** or **Irradiance** is:

$$\begin{aligned} \mathbf{S}(\mathbf{r}, t) &= \hat{\mathbf{e}}_r \varepsilon_0 c \mathbf{E}(\mathbf{r}, t) \cdot \mathbf{E}(\mathbf{r}, t) = \hat{\mathbf{e}}_r \varepsilon_0 c E^2(\mathbf{r}, t) \\ &= \varepsilon_0 c \frac{1}{r^2} E_0^2 (\cos(\mathbf{k} \cdot \mathbf{r} - \omega t + \alpha))^2 \quad [\text{W/m}^2] \end{aligned} \quad (\text{B.20})$$

#### Phasor representation of a monochromatic source

A harmonic wave as Eq. (B.18) can be expressed as a **phasor**. [14]

The Electric field phasor  $\tilde{\mathbf{E}}(\mathbf{r}, k)$  for Eq. (B.19) that represents a spherical wave is:

$$\tilde{\mathbf{E}}(\mathbf{r}, k) = \text{Real} [\mathbf{E}(\mathbf{r}) e^{j \mathbf{k} \cdot \mathbf{r}}] = \mathbf{E}(\mathbf{r}) \cos(\mathbf{k} \cdot \mathbf{r} + \alpha) = \mathbf{E}(\mathbf{r}) \cos(\Theta(\mathbf{r})) \quad (\text{B.21})$$

Where:

$$\mathbf{E}(\mathbf{r}) = \left(\frac{E_0}{r}\right) \quad [\text{V/m} \cdot \text{m}] \quad (\text{B.22})$$

$\mathbf{E}(\mathbf{r})$  represents the magnitude of the Electric field in position  $\mathbf{r}$  taking as reference its magnitude at the source. The source is placed at the origin O.

and

$$\theta(\mathbf{r}) = (\mathbf{k} \cdot \mathbf{r} + \alpha) \quad [\text{radians}] \quad (\text{B.23})$$

$\theta(\mathbf{r})$  is the angular phase. Since  $k = 2\pi/\lambda$  it has information of wavelength. Since  $r$  is the position of point observation  $P$ , the dot product  $\theta = \mathbf{k} \cdot \mathbf{r}$  represents the direction from the source to the observation point  $P$  in the coordinates frame.

### Physical interpretation

For a sphere that radiates spherical waves. See Eq. (B.18):

$\mathbf{E}(\mathbf{r})$  Describes amplitude of the electric field taking as reference  $E_0$ , the Electric field at the source.

$\theta(\mathbf{r})$  Describes the change of phase with distance. This means that if it were possible to have a “frozen image” of the whole wave at instant  $t_i$ , it would be possible to observe that the amplitude is constant, but its phase changes continuously and steadily along the distance at a rate of  $2\pi/\lambda$ . A vector with constant amplitude that changes its phase is a **phasor**. It is a vector that rotates continuously as increases the distance from the source. A complete rotation represents  $\lambda$ . See Fig. B.9.

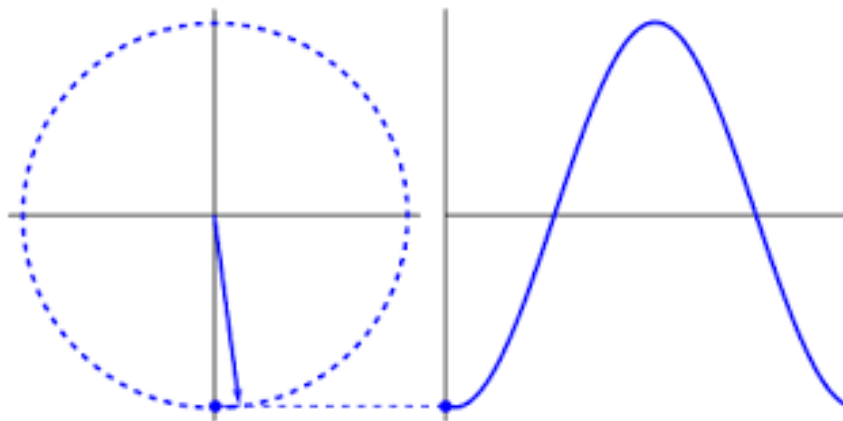


**Figure B.9:** A harmonic change of amplitude along displacement is interpreted as a rotating vector of constant amplitude.  
[Figure adapted from reference shown in ANNEX F]

## Two coherent sources

A detailed description of the behaviour of two or more coherent sources separated a short distance  $d$  when they are observed in the far field and its generalization to a discrete number of sources is found in [15]. Reference [16] describe this phenomenon using phasors in a simpler way.

These ideas are summarized in Figs. B.10, B.11 and B.12

From Eq. B.21, Irradiance is obtained from the Electric Field.

## Irradiance

Irradiance is obtained from Eq. (10)

$$\langle S \rangle = \frac{c}{4\pi} \langle \mathbf{E}^2 \rangle, \quad (\text{B.24})$$

This is:

$$\begin{aligned} \langle \mathbf{E}^2 \rangle &= \langle [A(r, \theta) \cos(\omega t + \varphi_{av} - kr)]^2 \rangle \\ &= \frac{1}{2} A^2(r, \theta), \end{aligned} \quad (\text{B.25})$$

Where:

$$A^2(r, \theta) = \{2A(r) \cos[\frac{1}{2}(\varphi_1 - \varphi_2) + \frac{1}{2} \Delta\varphi]\}^2. \quad (\text{B.26})$$

**Comment:** the term that has the information about interference is  $\frac{1}{2} \Delta\varphi^2$

Fig. B.10 is the intensity in the far field due to coherent oscillating sources.  $d \gg \lambda$

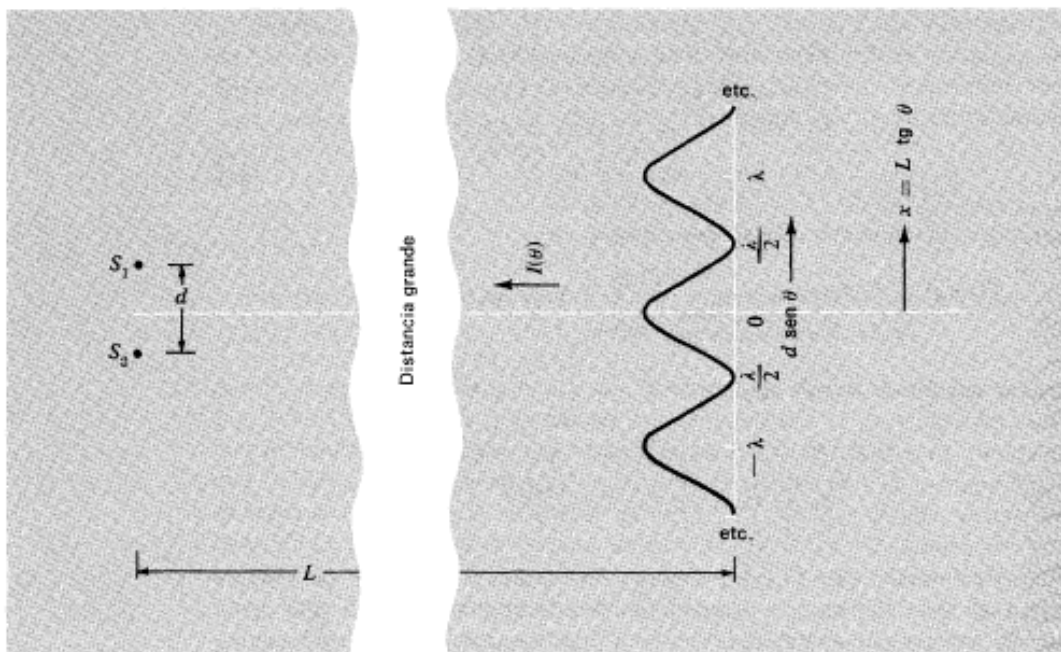


**Figure B.10:** Intensity due to oscillation of two coherent sources in the far field. [Figure adapted from reference shown in ANNEX F]

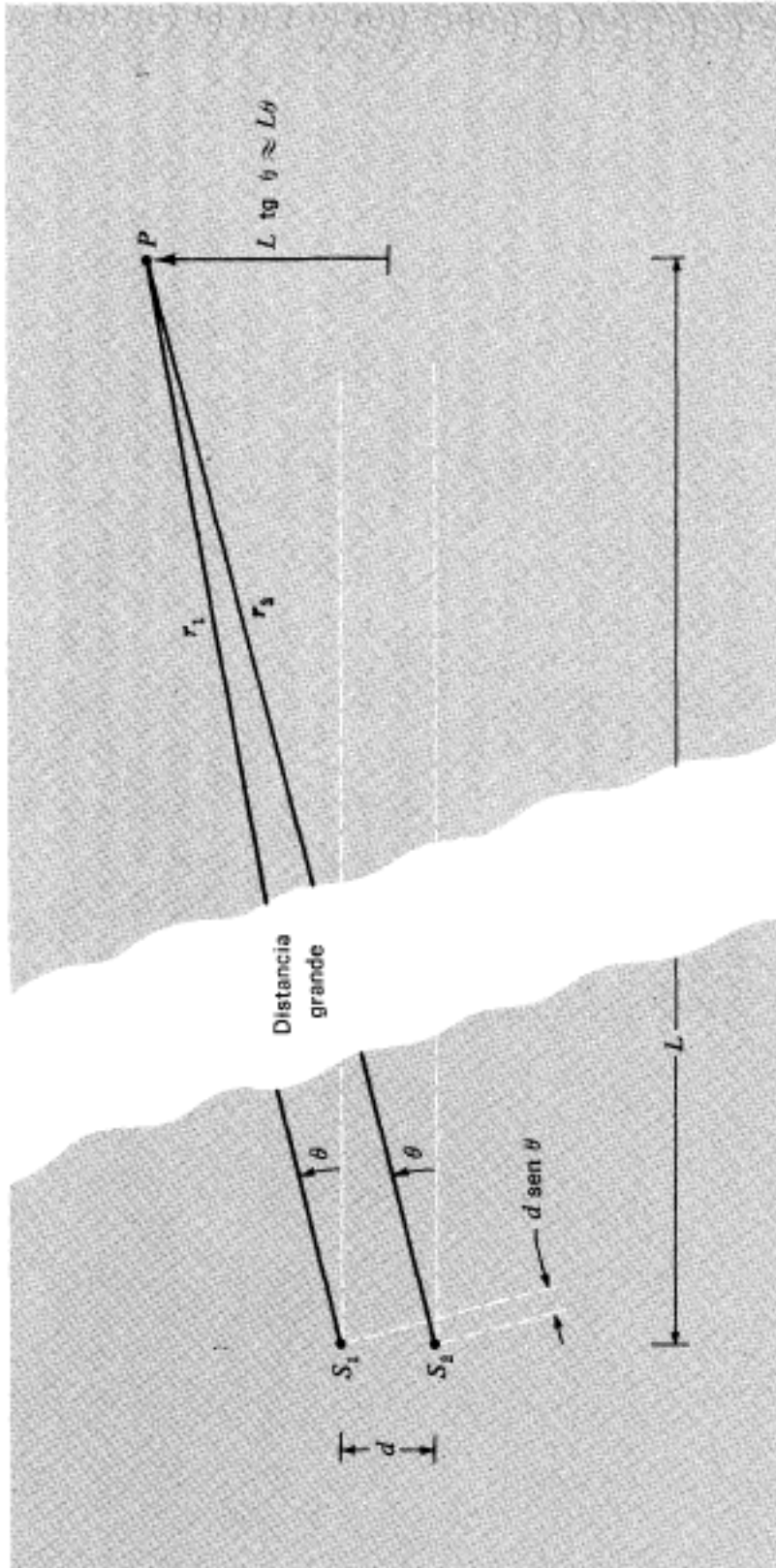


**Figure B.11:** Two point sources radiating waves that are detected in the far field at  $P$ . [Figure adapted from reference shown in ANNEX F]

Interference due to a discrete linear array of coherent sources

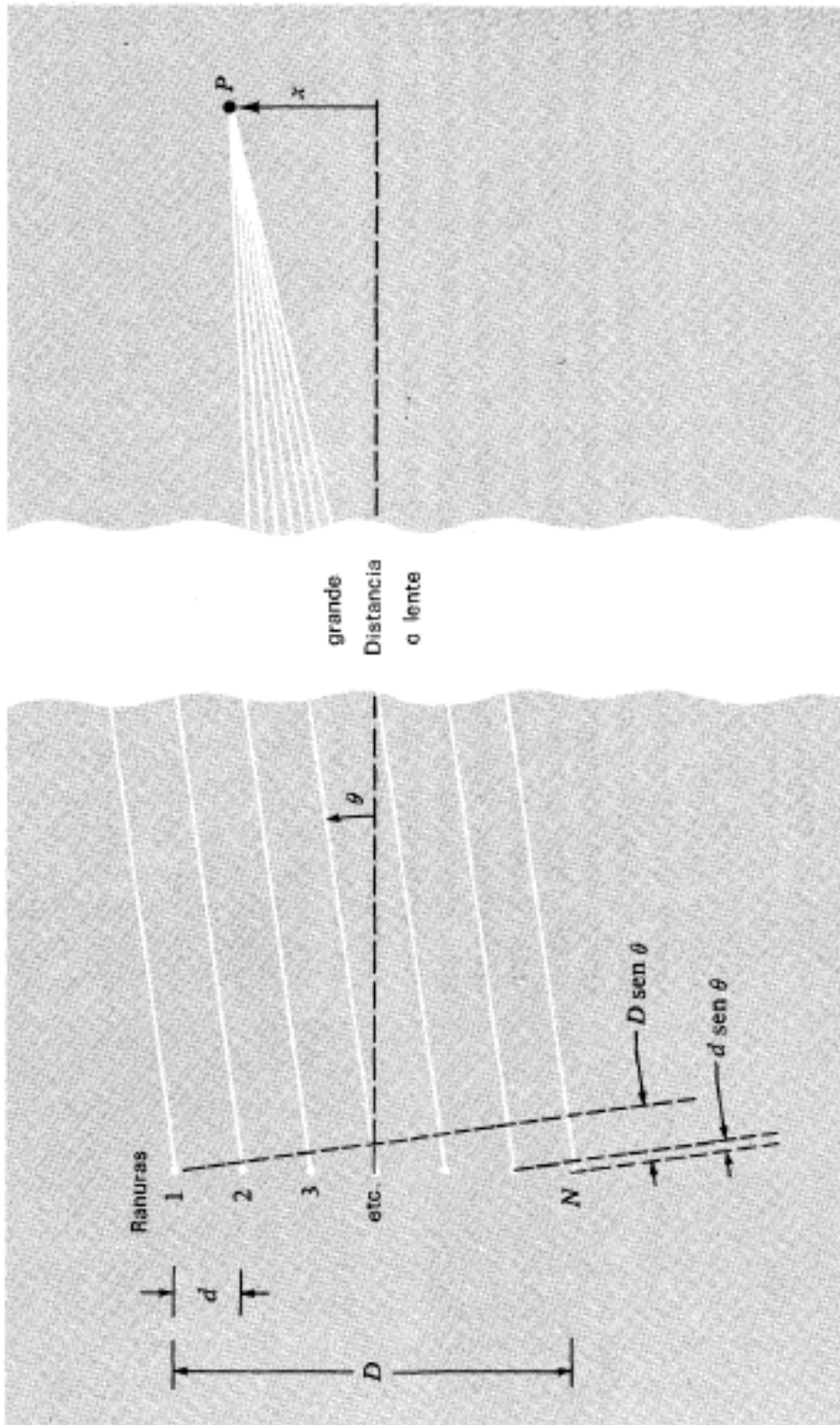


**Figure B.12:** Array of  $N$  coherent sources.  
[Figure adapted from reference shown in ANNEX F]



$$A_R = A \frac{\sin n\phi/2}{\sin \phi/2}. \quad (\text{B.29})$$

The Intensity  $I$  is proportional to the square of  $A_R$ :

$$I = I_0 \frac{\sin^2 n\phi/2}{\sin^2 \phi/2}. \quad (\text{B.30})$$

Fig. B.14.a shows function  $A_R / A$ . Fig. 14.b function  $I / I_0$ .

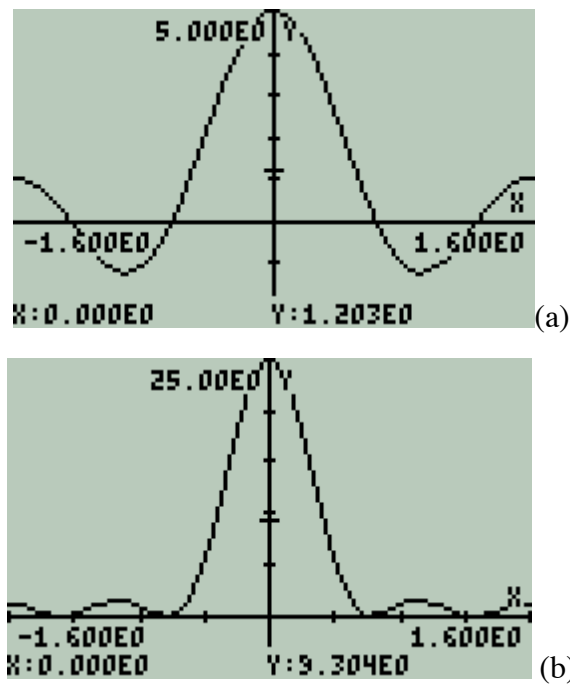


**Figure B.14:** Functions (a)  $A_R / A$  and (b)  $I / I_0$  for  $n = 5$

\* Comments: Roots of these functions are periodic for  $\pm\pi$

(a) Amplitude is proportional to  $n$

(b) Amplitude is proportional to  $n^2$

### Interference for a linear array of many coherent sources

If in Eq. (B.30) the number of coherent sources is increased but maintaining constant the length  $D$  in Fig. B.12, necessarily the angle  $\phi / 2$  decreases and the regular polygon from Fig. B.13 tends to a circumference.



Under those circumstances the angular factor in Eq. (B.31) tends to Eq. (B.32) since  $\sin u \rightarrow u$  when  $u \rightarrow 0$ .

$$A_R = A \frac{\sin n\phi/2}{\sin \phi/2}. \quad (\text{B.31})$$

Is equivalent to Eq. (B.31):

$$I = I_0 \frac{\sin^2 n\phi/2}{\sin^2 \phi/2}. \quad (\text{B.32})$$

$$A_R = \frac{\sin \frac{n\phi}{2}}{\sin \frac{\phi}{2}} \rightarrow \frac{\sin \frac{n\phi}{2}}{\frac{\phi}{2}} \quad (\text{B.33})$$

So 
$$A_R = \text{sinc} \left( \frac{\phi}{2} \right) = A \frac{\sin \frac{n\phi}{2}}{\frac{\phi}{2}} \quad (\text{B.33.a})$$

$$A_R^2 = \text{sinc}^2 \left( \frac{\phi}{2} \right) = A^2 \left( \frac{\sin \frac{n\phi}{2}}{\frac{\phi}{2}} \right)^2 \quad (\text{B.33.b})$$

In general, this expression is known as  $\text{sinc}(u)$  ; its square is  $\text{sinc}^2(u)$ . Fig. B, 15 and Fig. B.16 are their plots in the range  $[- 2\pi \leq u \leq +2\pi]$ , respectively.

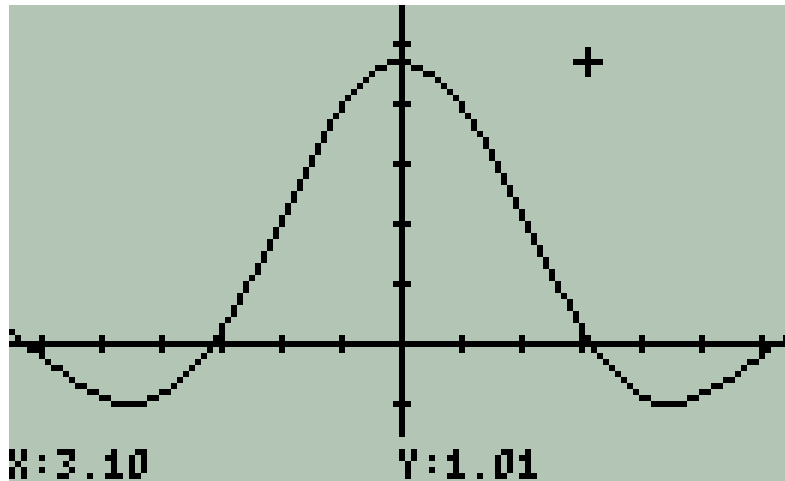


**Figure B.15:** Function  $\text{sinc}[u]$  in the range  $[- 2\pi \leq u \leq +2\pi]$ .

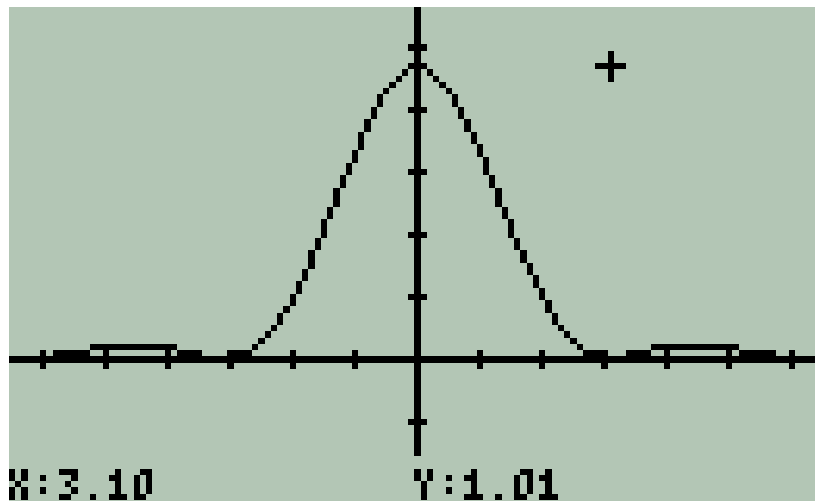


**Figure B.16:** Function  $\text{sinc}^2 [u]$  in the range  $[- 2\pi \leq u \leq +2\pi]$ .

### Main characteristics of $\text{sinc}^2 [u]$

- Maxima and minima abscissas

The derivative of  $\text{sinc}^2 [u]$  with respect to  $u$  equals to zero gives these results:

$$\frac{d(\text{sinc}^2(u))}{du} = \frac{2\sin(u) \cdot (u \cdot \cos(u) - \sin(u))}{u^3} = 0 \quad (\text{B.34})$$

**Minima occurs** when  $\sin(u) = 0$  and  $u \neq 0$  this is when

$$u = \pm m\pi ; m = 1, 2, 3, \dots \quad (\text{B.35})$$

**Maxima occurs** when

$$(u \cdot \cos(u) - \sin(u)) = 0 \text{ or } \tan(u) = u \quad (\text{B.36})$$

See Fig. B.17.

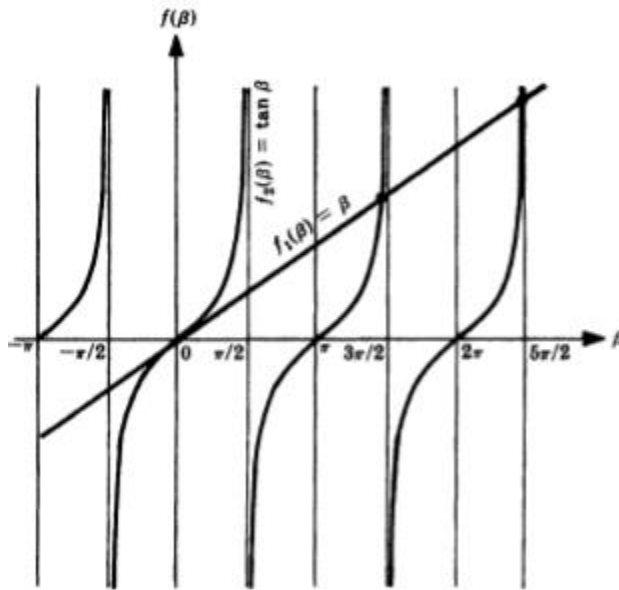


**Figure B.17:** Plot of  $\tan(u) = u$   
 [Figure adapted from reference shown in ANNEX F]

The intersections except zero are:

$$u_1 = \pm 1.43029665312 \pi$$

$$u_2 = \pm 2.45902403296 \pi$$

$$u_3 = \pm 3.47088972434 \pi$$

...

(B.37)

Comment: These values are not periodic

## C. PHOTONS

### 1. PHOTOELECTRIC EFFECT

#### Beginnings of Photoelectric Effect

Experimental support to the idea that light is composed of corpuscles have their beginning in the Einstein's proposition in **1905**: [17]

*“For a monochromatic beam light arrives in portions of magnitude  $hf$ ”. This quantum of energy is completely transferred to an electron.”*

Where  $f$  is frequency.

The famous Einstein's Equation is:

$$E_{KINETIC} = hf - W \quad (C.1)$$

Where:

$E_{KINETIC}$  Kinetic Energy of an emitted electron

$hf$  Photon's Energy completely transferred to the electron

$W$  Constant work energy for the pure alkaline metal coating the surface

And in **Millikan's Experiment** in **1916**. Millikan made experimental observations of photoelectric effect that allowed obtain Planck's constant.

$$V_0 = \left(\frac{h}{e}\right) f - \frac{W}{e} \quad (C.2)$$

This is an equation of a straight line where:

$V_0$ , the stopping voltage is the dependent variable and is a function of the chemical element [V]

$f$  is the frequency of light, independent variable [Hz]

$W/e$  is the voltage potential to extract an electron from a metallic surface, it is a constant for a pure metal [V]

$W$  The bind energy of electrons in a material [J]

$h/e$  is the slope of the curve. [V.s]

## PHOTONS CHARACTERISTICS

In Section B, main characteristics for electromagnetic fields were defined. Here, the correspondent characteristics for photons are summarized.

### The wave – particle duality

Light has a dual behaviour as a wave and as a particle. This is a general property common to elementary particles and atoms at quantum level.

Light as a wave has a wavelength.

$$\lambda = c/f \quad (C.3)$$

Where:

$\lambda$	wavelength	[m]
$c$	speed of light	= 299.8E6 [m/s]
$f$	frequency	[Hz]

Light as a particle (photon) has momentum  $\vec{p}$  and energy  $E$ .

$$\vec{p} = \hbar \vec{k} \quad [\text{N}\cdot\text{s}] \quad (C.4)$$

$$E = h \cdot f \quad [\text{J}] \quad (C.5)$$

Where:

$\vec{p}$	momentum	[N.s]
$\hbar$	hbar or Dirac's constant	= $h / 2\pi = 105.5\text{E-}36$ [J*s]
$\vec{k}$	wavenumber	[1/m]
$E$	Energy	[J]
$h$	Planck's constant	$662.6\text{E-}36$ [J*s]

For a photon, the relationship between energy and wavelength is

$$E = h \cdot c/\lambda \quad (C.6)$$

So energy and wavelength are inversely proportional. This means that the higher the wavelength the lower the energy and, vice versa; the higher photon energy the lower the wavelength.

## SPECTRAL REGION OF INTEREST AND PHOTONS ENERGY

The **Spectral Region of Interest – ROI** for the present work is the electromagnetic region in the Visible, Near Infrared and Near Ultraviolet bands. Specific details follow.

### Connection of Energy and Wavelength in a Photon

In Section A.1. a brief introduction to light was presented. Let's start this topic with the equation of energy for a photon.

Every photon has energy, so light is an expression of energy. The SI unit for Energy is the Joule [J].

$$E_{PHOTON} = h.f \quad [J] \quad (C.7)$$

Where:

$h$  is the **Planck's constant: 6.63E-34\_J\*s**

$f$  is frequency [Hz]

The connection between energy  $E_{PHOTON}$  and wavelength  $\lambda_{PHOTON}$  is easily obtained from

$$\lambda_{PHOTON} . f = c \quad [m] \quad (C.8)$$

Where:

$c = 299.8E6\_m/s$  is the speed of light

Light and, in general, Electromagnetic Fields have a speed  $c = 299.8E6\_m/s$ .

So

$$E_{PHOTON} = h.c / \lambda_{PHOTON} \quad [J] \quad (C.9)$$

### The electron volt [eV] definition

Electric energy [J] is the product of electric charge [C] by a Potential Difference [V].

A non [SI] energy unit comfortable to deal with electrons and photons is the **electron volt [eV]**.

The **electronvolt** (symbol **eV**; also written **electronvolt**<sup>[1][2]</sup>) is a unit of energy equal to approximately  $1.6 \times 10^{-19}$  joules (symbol J). By definition, it is the amount of energy gained (or lost) by the charge of a single electron moved across an electric potential difference of one volt. Thus it is 1 volt (1 joule per coulomb, 1 J/C) multiplied by the elementary charge ( $e$ , or  $1.602176565(35) \times 10^{-19}$  C). Therefore, one electron volt is equal to  **$1.602176565(35) \times 10^{-19}$  J**.<sup>[3]</sup> [18]

The conversion factor with the SI unit [J] is:

$$1[\text{J}] = 6.242\text{E}18_{\text{eV}} \quad (\text{C.10})$$

### Wavelength ranges of interest and the corresponding energies

Table C.1 presents energy and wavelength ranges for the Region of Interest – ROI for this project. These Total ROI is subdivided in three sub-regions: visible, near infrared and near ultraviolet. Sub-ranges are divided taking into account the design of simple spectrometers in next chapter.

**Table C.1: Energy Ranges in [eV] corresponding to the Wavelength Ranges in [nm] in the Region of Interest**

<b>Total Range of Interest</b>	<b>400</b>	<	$\lambda$	<	<b>2600 [nm]</b>
	<b>3.10</b>	>	U	>	<b>476.9E-3 [eV]*</b>
<b>Visible Range Spectrometer</b>	<b>400</b>	<	$\lambda$	<	<b>700 [nm]</b>
	<b>3.10</b>	>	U	>	<b>1.77 [eV]</b>
<b>Near Infrared Spectrometer</b>	<b>650</b>	<	$\lambda$	<	<b>2600 [nm]</b>
	<b>1.91</b>	>	U	>	<b>476.9E-3 [eV]</b>
<b>Near UV Spectrometer</b>	<b>300</b>	<	$\lambda$	<	<b>460 [nm]</b>
	<b>4.13</b>	>	U	>	<b>2.70 [eV]</b>

\* Comment on exponential notation: In this work exponential notation is expressed using capital E. As example:

$$476.9\text{E-}3 [\text{eV}] = 476.9 \times 10^{-3}[\text{eV}] = 0.4769 [\text{eV}]$$

## 2. SEMICONDUCTOR LIGHT DETECTORS

### SILICON AND GERMANIUM PHOTODIODES

#### Energy Gap for Silicon and Germanium

The **energy gap** is the difference of energy between the conduction band and the valence band for electrons in a crystalline solid. For values below about 2eV the substance is considered to be a semiconductor whilst for higher values it is considered to be an insulator.

Table C.2 shows the Energy Gaps for the most used semiconductors Si and Ge and the corresponding photon wavelengths.

**Table C.2: Energy Gap [eV] for Si and Ge and the corresponding wavelengths**

	Temperature [K]	Energy [eV]	Wavelength [nm]
<b><u>Silicon</u></b>	0	<b>1.17</b>	<b>1060</b>
	300	<b>1.11</b>	<b>1117</b>
<b><u>Germanium</u></b>	0	<b>0.74</b>	<b>1675</b>
	300	<b>0.66</b>	<b>1879</b>

So:

For **Silicon**, at room temperature [300 K], photons with a wavelength smaller than 1117 [nm] - or with an energy higher than 1.17 [eV] are able to transfer an electron from the valence band to the conduction band.

For **Germanium**, at room temperature, photons with a wavelength smaller than 1879 [nm] are able to transfer an electron from the valence band to the conduction band.

In this interaction the photon annihilates and transfers its energy to an electron.

Photons with wavelengths of 1879 [nm] and 1117 [nm] are in the **Infrared Region**.

**This implies that, in principle, Si and Ge photodiodes and phototransistors are useful components as photon detectors in the Infrared and Visible Ranges.**

From this description, any photon with a higher energy than the energy gap would be able to transfer an electron from the valence band to the energy gap [19]. This ideal situation is illustrated in Fig. C.1



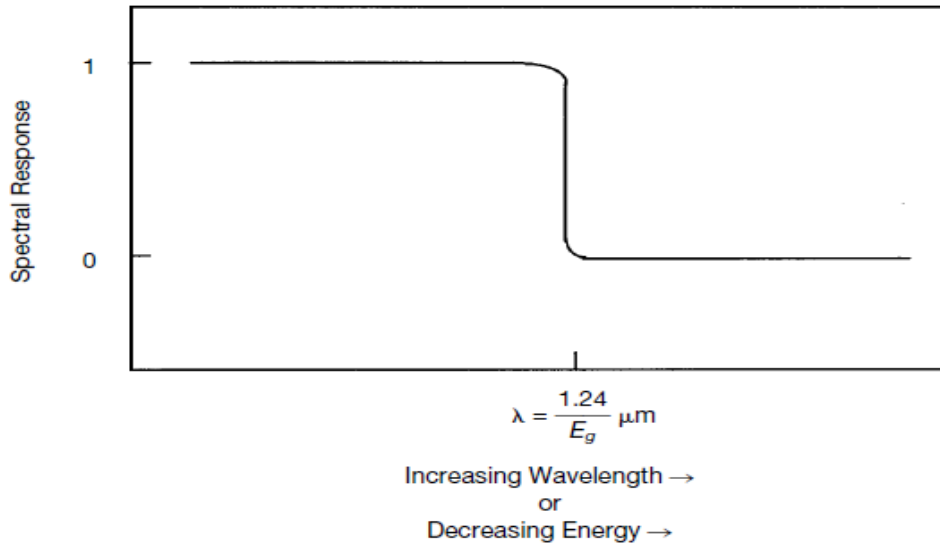


**Figure C.1:** *Idealized Spectral Response photodiode.*  
 $S(E) = 1$  if the photon energy is greater than the band gap. Otherwise  $S(E) = 0$   
 [Figure adapted from reference shown in ANNEX F]

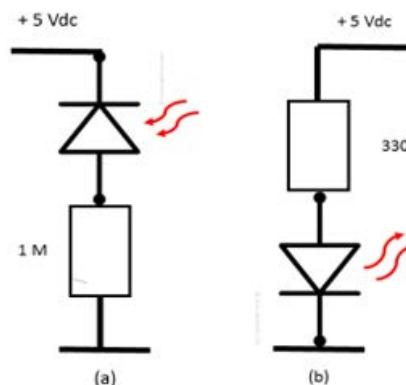
However, real situation is not so simple. Experimental results follow.

### LEDs as Light detectors

In subsection B.2 **Light Emitting Diodes or LEDs** were introduced as **approximately monochromatic sources**.

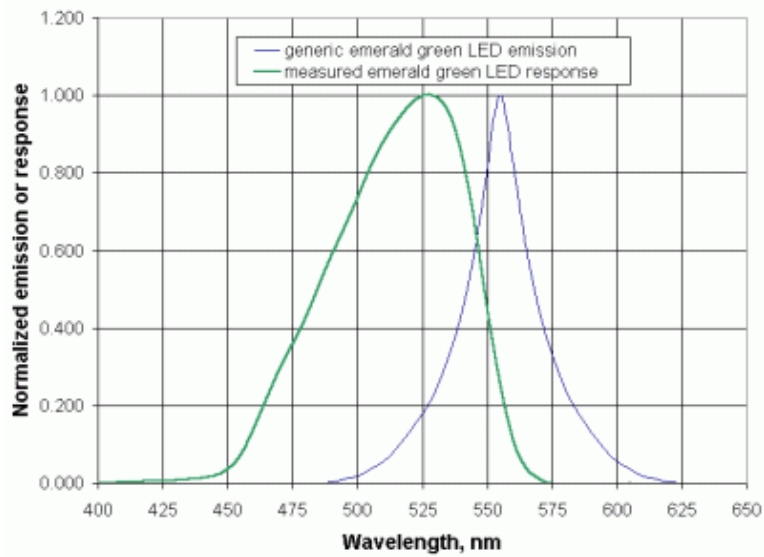
However it is possible to use **LEDs as Light Detectors**.

Fig. C.2 (a) shows a **Reversed Biased LED as a Light Detector** and Fig. C.2 (b) a **Forward Biased LED as a Light Source**.



**Figure C.2:** (a) *A Reverse Biased LED is a Light Detector*  
 (b) *A Forward Biased LED is a Light Source.*

Fig. C.3 shows the spectral bandwidth that emits as a Green Color LED as Light Source and the Spectral Response of this diode. In general, a frequency shift and a frequency enhancement are observed.



**Figure C.3:** *Spectrum of a LED acting as a Light Source and as a Light Detector are not identical and they do not overlap.*  
*[Figure adapted from reference shown in ANNEX F]*

### A simple Experiment on Photons Energy using LEDs

Take two LEDs that emit light at different color; i.e. different Energy or Wavelength.

- Use the LED that emits photons at a higher frequency (energy) as Light Source and the LED that emits photons at a lower energy as Light Detector. By measuring the voltage drop on  $R_{\text{DETECTOR}}$  a current is observed.
- Reverse the situation: Use the LED that emits photons at a lower frequency (energy) as Light Source and the LED that emits photons at a higher frequency (energy) as Light Detector. By measuring the voltage drop on  $R_{\text{DETECTOR}}$ , this time, no voltage drop is detected no matter how intense is the Light Source.

### 3. RESPOSITIVITY

#### Responsivity [20]

A photodiode could be considered as a transducer that converts light in electric charges

$$(Photon's Energy) \leftrightarrow (Photoelectrons) \quad (C.11)$$

Photoelectrons are a function of photons energy and light intensity.

By comparing Fig. C.1 and Fig. C.3, we realize that there are many differences:

- Photodiodes are not pure materials but are doped with impurities to characterize the junction. This implies that The energy gaps for pure materials are only referential values
- Due to impurities introduced in a semiconductor, the energy gap is not a sharp transition
- Only a fraction of incident photons are converted to electric carriers
- The photodiode response is a limited band. There are another factors – that are out the reach of this work than inhibit Photo conversion into charge carriers

In order to overcome this situation **an experimental approach has been taken as an alternative.**

A photodiode is exposed to a known light spectrum and the actual current is measured. The quotient:

$$\textit{(Photoelectrons measured)} / \textit{(Irradiance)} \quad [\text{A/W}] \quad (\text{C.12})$$

as a function of wavelength is reported.

Certainly:

- The quotient is expressed in units of [A/W], but corresponds to the actual active area of the photodiode.
- The quotient depends on the photodiode material
- The quotient is a characteristic of the junction.

This parameter is named **Responsivity**  $R_p$  and represents the experimental photocurrent of the photodiode per Irradiance vs wavelength.

$$R_p = \frac{I_p}{W_p} ; [A / W] \quad (\text{C.13})$$

### **Responsivity depends on wavelength**

A photodiode has a null Responsivity for wavelengths bigger than the corresponding to the Energy Gap, then increases up to a maximum, again decreases when wavelength decrease. There is a range of short wavelengths where photocurrent generation ceases or is extremely low in spite of the photons energy is enough to generate electric carriers. The causes for this behaviour are out of the reach of this document.

## Responsivity of Si and Ge Photodiodes

For this work, initially, two photodiodes widely used are chosen. They are Si and Ge photodiodes. Fig. C.4 and Fig. C.5 show independently Si and Ge responsivities. In Fig. C.6 responsivities of Si, Ge and InGaAs photodiodes are overlapped in a common reference frame, this allows to have an objective vision of their responsivities.

**Chp. 1 ANNEX 2** and **Chp. 1 ANNEX 3** provide **Responsivity Data** from a Manufacturer for Si and Ge photodiodes vs wavelength with resolutions of 5 and 10 [nm]. [21]

**Chp. 1 ANNEX 4** Is the Standard Tungsten Filament light spectrum for  $T = 2856$  [K]. i.e.: standardized to 1 or  $F0\lambda(2856, \lambda)$  in the region of interest – ROI and with a resolution of 10 [nm].

**Chp. 1 ANNEX 5** are technical parameters for Si and Ge photodiodes. These data is useful for circuit design.

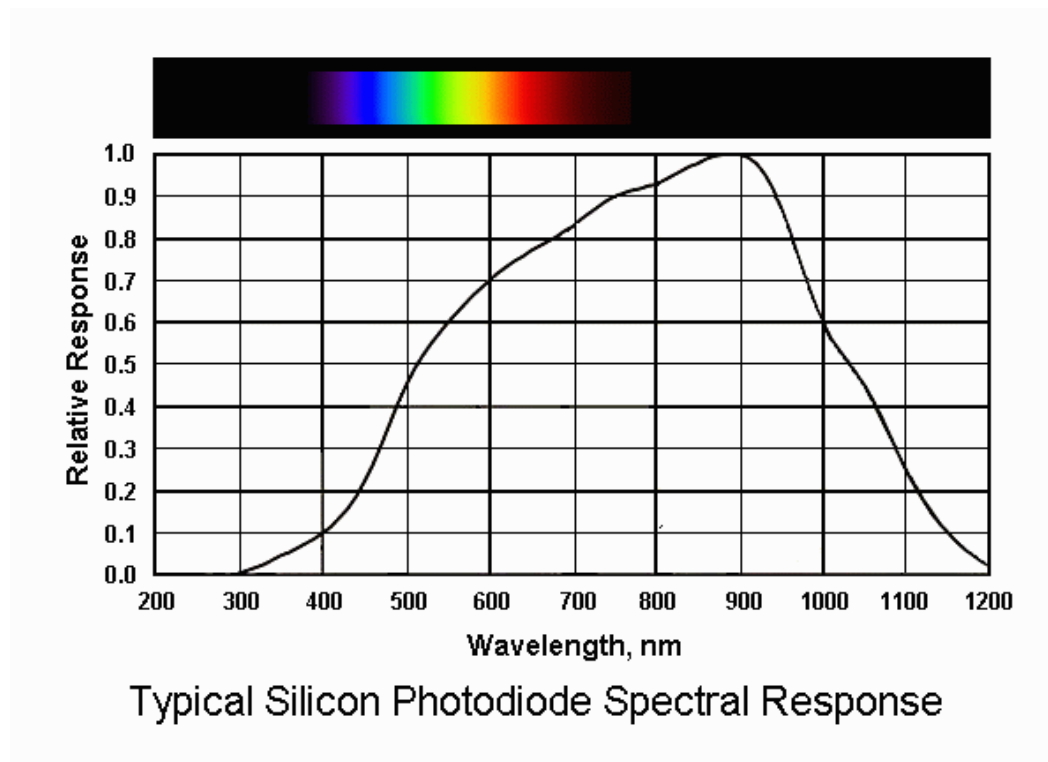


**Figure C.4:** *Typical responsivity for a Si photodiode.*  
[Figure adapted from reference shown in ANNEX F]

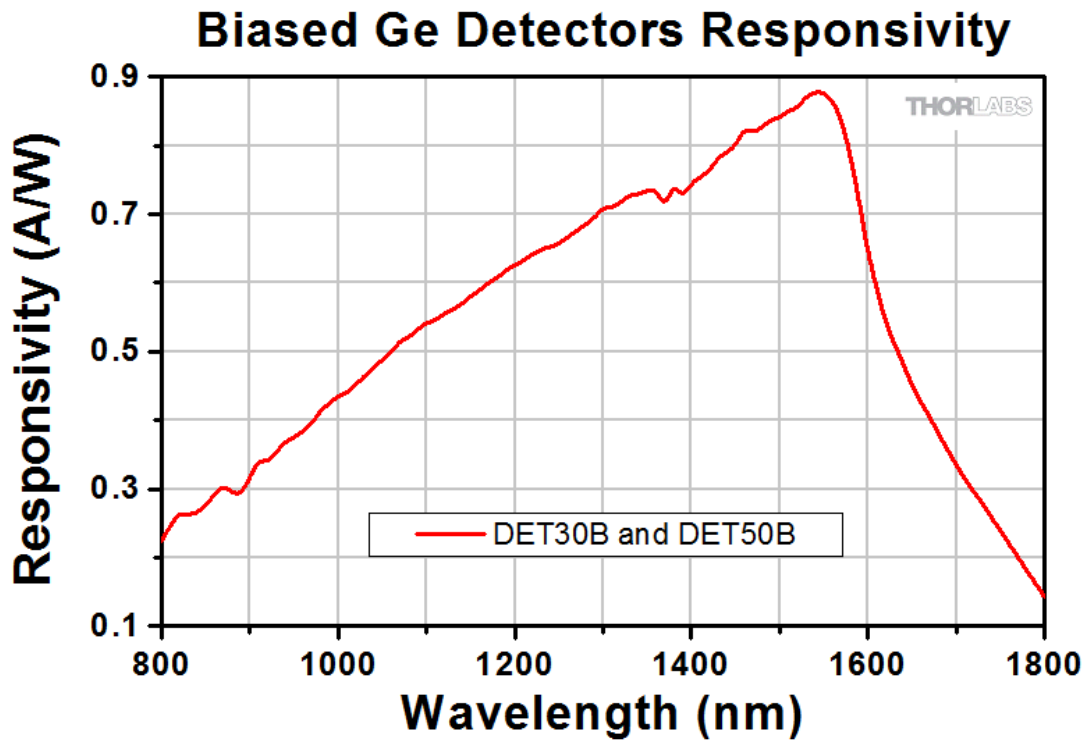


**Figure C.5:** Typical responsivity for a Ge photodiode.  
 [Figure adapted from reference shown in ANNEX F]

### Absolute Spectral Response

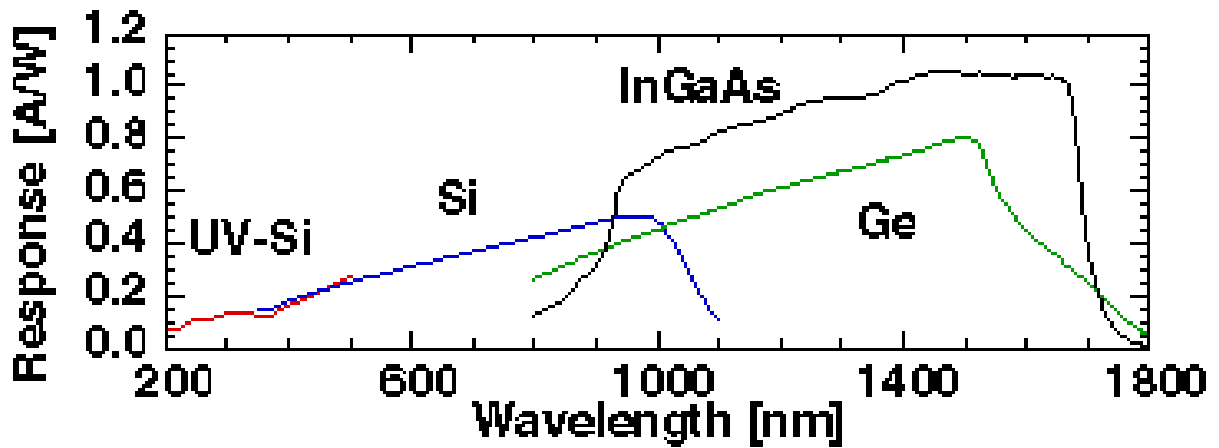


**Figure C.6:** Responsivity for Si, Ge and InSb on a common reference frame.  
 [Figure adapted from reference shown in ANNEX F]

## Responsivity of LEDs

Fig. C.7 is the Responsivity of a GaP photodiode in the UV Region.

In general information on responsivity for LEDs is not provided by fabricants. If one needs this information one has to obtain it experimentally. See Chpt. 4 Section D.

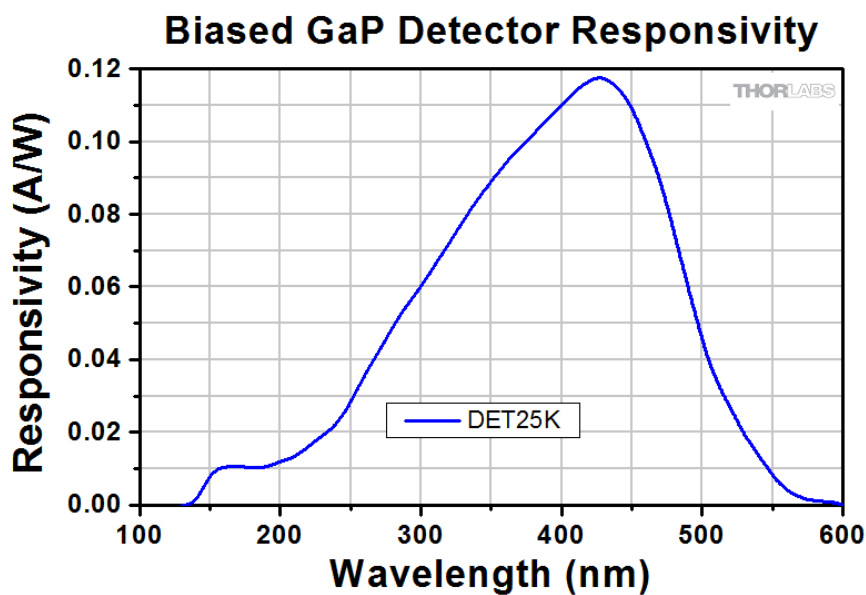


**Figure C.7:** Responsivity of a blue emitter photodiode.  
[Figure adapted from reference shown in ANNEX F]

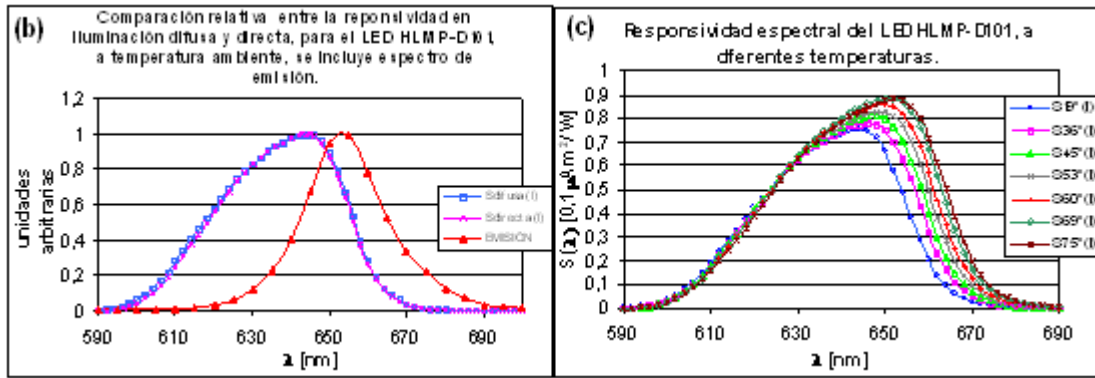
One should realize that **Responsivity is essentially an experimental and statistical physical parameter.**

**Chp. 1 ANNEX 5** offers information related with design parameters and error in percentage for individual photodiodes.

### Ambient Temperature affects Responsivity

Fig. C.8 (a) reports that Responsivity is not affected if direct or diffuse light sources are used for experiment.

Fig. C.8 (b) shows that a Si photodiode is more sensitive to temperature in its longer wavelength sub-band.



(a)

(b)

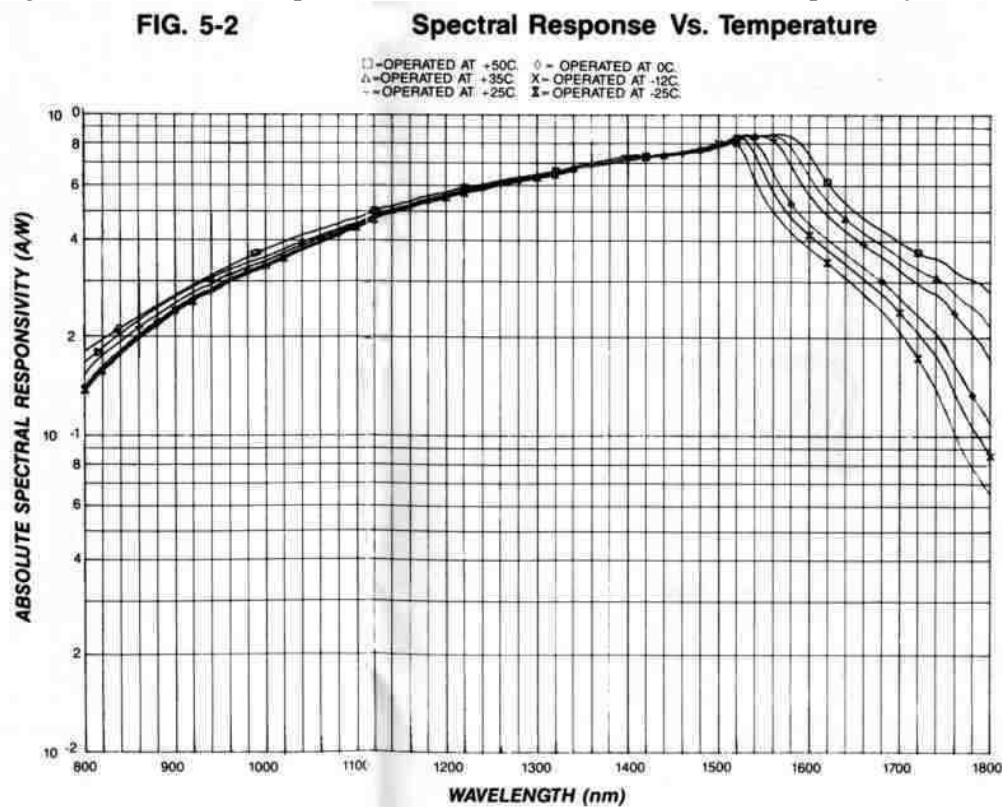
**Figure C.8:** (a) LEDs responsivity for direct and diffuse light.

(b) Temperature dependence of LEDs responsivity.

[Figure adapted from reference shown in ANNEX F]

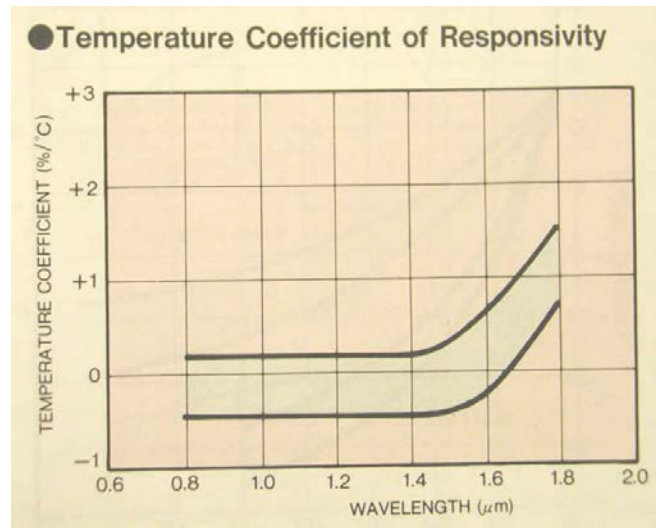
Fig. C.9 shows similar results for Ge photodiodes. These devices are sensitive to operation temperature mainly in its longest wavelength sub-range.

Fig. C.10 shows the Temperature coefficient for Ge Photodiodes Responsivity



**Figure C.9:** Germanium photodiode spectral temperature sensitivity response (typical, used for bands in the 1100-1720 nm range).

[Figure adapted from reference shown in ANNEX F]



**Figure C.10:** *Ge photodiode temperature coefficient of responsivity.*  
 [Figure adapted from reference shown in ANNEX F]

These Temperature Related data allows conclude that:

- If possible, Photodiodes for photovoltaic measurements should be used in a stable temperature environment, as example in the Laboratory Temperature.
- Otherwise, instruments should contain a thermometer. Then temperature correction through software could be applied to data.

These measures should be taken in order to obtain data repeatability from measurements.

#### 4. INCANDESCENT LIGHT SOURCES

**Incandescent light sources** are essentially light emitters of thermal radiation; i.e.: the Spectral Irradiance from these sources closely follows Planck's equation. A tungsten filament lamp, an X-Ray tube, an electric heater are examples of thermal radiation sources.

##### The Tungsten Filament Lamp

For the Visible range, near UV range and near Infrared range: Tungsten halogen lamps are the “work horse” as light sources. [22]

Halogen lamps are incandescent lamps. A metallic filament is heated by an electric current. By far the greater part of the electrical power consumed by the incandescent wire is converted into electromagnetic radiation output.



Total radiation increases as the fourth power of the material temperature. The spectral distribution of the radiation; i.e. its distribution over the ultraviolet, visible and infrared (heat) ranges, shifts to shorter wavelengths in a kind of bell shaped curve as the temperature increases. The peak moves out of the infrared towards the visible region (See Fig. C.11). Unfortunately the melting point of tungsten does not permit to shift the peak into the visible region of spectrum.

At the highest practicable temperature, this peak is at about 850 nm (nanometres). The visible range ends at 750 nm. In this case about 20 % of the total radiation is in the visible region, about 0.3% in the UV region, and the remaining percentage (the majority) as heat.

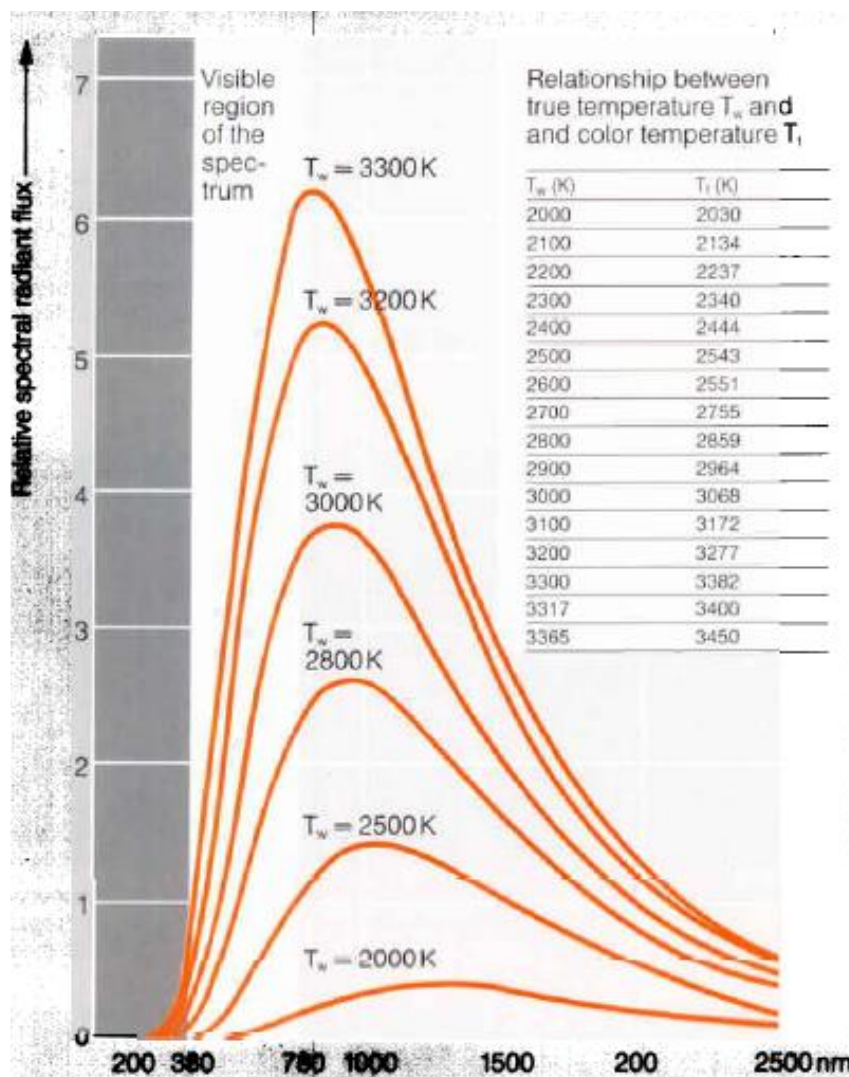


**Figure C.11:** Relative spectral radiant flux for tungsten filaments at different true temperatures. Table comparing “true temperature” with “colour temperature”. [Figure adapted from reference shown in ANNEX F]

## **Tungsten temperature and Colour temperature [23]**

For an ideal “blackbody” (in the physical sense) **the colour temperature is equal to the true temperature** and it is measured in Kelvin [K]. The higher the colour temperature, the whiter irradiated light; the lower the colour temperature, the more yellowish and reddish radiated light is observed.

Tungsten however is not a “blackbody”; its emissivity is less; i.e. the total radiation emitted is less than the ideal case. One could say that tungsten is a gray-body radiator. But even that would be a half – truth, because in the short wave region tungsten is a better emitter – though still not as good as the ideal blackbody – than in the long-wave red region. This variation of the emission coefficient has a positive effect on the radiation characteristics of tungsten in that its colour temperature is higher than its equivalent true body temperature. In the region of interest for lamp technology around 3000 [K], this amounts to 60 – 80 [K]. See Table in Fig. C.11.

An upper limit for the colour temperature is given by the melting point of tungsten and the requirement for minimum lamp life. It lies at about 3550 [K].

## **Recommended Standard Colour Temperature**

Three recommended values for Colour Temperature follow:

- Laboratory Use Temperature 3000 K
- CIE Recommendation Temperature 2854 K
- International Light: Temperature 2856 K

In this work the CIE\* recommendation is used.

\* CIE: International Commission on Illumination

## **5. CALIBRATION OF Si AND Ge PHOTODIODES USING A STANDARD TUNGSTEN FILAMENT LIGHT SOURCE**

In this Section, a detailed description to calibrate a commercial Si or Ge photodiode is explained.

Si and Ge photodiodes have been selected for the following reasons:

- Spectral response of Si and Ge photodiodes, practically cope the wavelength region of interest – ROI for this project. A third photodiode is required for the UV band.
- Since Si and Ge semiconductors are among the purest materials and the doping procedures to make the junctions are very established a similar spectral response is expected from the low cost commercial components compared with Si and Ge photodiodes used for light measurements with the exception of a smaller active area.

- Si and Ge Photodiodes used in this project are low cost, “off the shelf” components.

This Section takes as main reference the Responsivity Data for Si and Ge Photodiodes provided by THOR, manufacturer of this devices.

### Laboratory room temperature

The calibration process is carried out at a **Laboratory Temperature** of **300 [K]**

### Criteria for Calibration

- The main application of this work is for **solar parameters measurement, solar cells characterization, solar cells development and education.**
- To be practical in calculations the **total solar irradiance reference is approached to 1 Technical sun irradiance; i.e.:** :

$$\lambda = [1\text{KW} / \text{m}^2] = [1 \text{mW} / \text{mm}^2] \quad (\text{C.15})$$

Also, it is evident that:

$$[1\text{A} / 1 \text{W}] \equiv [1\text{mA} / 1 \text{mW}] \quad (\text{C.16})$$

- Calculations for sensors are made for:

$$\text{Sensor Active Area} = 1 [\text{mm}^2] \quad (\text{C.17})$$

- Taking as Reference **CIE Recommendations:**

**(International Commission on Illumination - CIE)**

$$\text{Planck's Spectral Standard Temperature} = 2856 [\text{K}] \quad (\text{C.18})$$

- The **Normal Planck's Distribution function** has been calculated in the Spectral Region of Interest [ROI] using the function  $F_0\lambda$ , it has a total bandwidth:

**Total bandwidth:**

$$200\text{E-9} \leq \lambda \leq 3000\text{E-9} [\text{m}] \quad (\text{C.19})$$

$$\text{with a Resolution of } 10\text{E-9} [\text{m}] \quad (\text{C.20})$$

This bandwidth encompasses almost the 88% of the spectral distribution:

$$\sum_{200E-9[m]}^{3000E-9[m]} (F0\lambda_{std}(2856, \lambda)) = 0.877756011195 \quad (C.21)$$

- **Sub-Bandwidths from the Normal Planck's Distribution function** have been obtained **matching the Responsivity Bandwidths for Silicon and Germanium Photodiodes**, with identical resolutions and wavelengths.
- **Silicon and Germanium Photodiodes** have been selected as **light detectors**.
- **Spectral Responsivity** has been obtained from **Manufacturers**. See [**Chp. 1 Annex 1**]. Their Bandwidth Responsivity is:

**For Si:**

$$\text{Bandwidth:} \quad 400.0E-9 \leq \lambda \leq 1100.0E-9 \quad [m] \quad (C.22)$$

$$\text{Resolution:} \quad 10.0E-9 \quad [m] \quad (C.23)$$

$$\sum_{400E-9[m]}^{1100E-9[m]} (F0\lambda_{Si}) = 0.310135167086 \quad (C.24)$$

**For Ge:**

$$\text{Bandwidth:} \quad 800.0E-9 \leq \lambda \leq 1800.0E-9 \quad [m] \quad (C.25)$$

$$\text{Resolution:} \quad 10.0E-9 \quad [m] \quad (C.26)$$

$$\sum_{800[nm]}^{1800[nm]} (F0\lambda_{Ge}) = 0.537314422209 \quad (C.27)$$

- **Total bandwidth encompassed by both detectors is:**

**Total Bandwidth:**

$$400.0E-9 \leq \lambda \leq 1800.0E-9 \quad [m] \quad (C.28)$$

This bandwidth is almost the 66% of the spectral distribution:

$$\sum_{400E-9 [m]}^{1800E-9 [m]} (F0\lambda(\text{Si} + \text{Ge})) = 0.653027805924 \quad (\text{C.29})$$

- There is an **overlap of both sensors in the bandwidth:**

**Overlap Bandwidth:**  $800E-9 \leq \lambda \leq 1100E-9$  [m]

that represents **almost the 20% of the total spectral band**

$$\sum_{800E-9 [m]}^{1100E-9 [m]} (F0\lambda(\text{Ge} - \text{Si})) = 0.194421783371 \quad (\text{C.30})$$

- **Responsivities are obtained experimentally and represent the photodiodes spectral response to light.**

**Standard Light Source [24]**

A standard lamp at the standard spectral temperature is used:

**Standard lamp:** Tungsten halogen lamp type FEL

**CIE Standard Spectral Temperature:** 2856 [K]

## PROCEDURE

**Total Irradiance measured at photodiode position**

A **Standard Pyrometer** is carefully placed facing perpendicularly the light source. Its thermopile array sensor is positioned in the same coordinates where the test-photodiode is going to be placed. **The standard pyrometer reports a total irradiance of 1 technical sun.**

**Total Irradiance**

$$= [1\text{KW} / \text{m}^2] = [1 \text{mW} / \text{mm}^2] \quad (\text{C.31})$$

## Positioning the photodiode

Now, let's place a Si Photodiode in the same coordinates (position) where standard pyrometer was placed. The Photodiode **active area is 1 [mm<sup>2</sup>]** and it is facing perpendicularly the light source. So, the Total Irradiance impacting on the Photodiode is:

$$\begin{aligned} \text{Total Irradiance on Photodiode} \\ = [1 \text{ mW} / \text{mm}^2] \end{aligned} \quad (\text{C.32})$$

So, the Light Power on the Photodiode is:

$$\text{Total Light Power on Photodiode} = [1 \text{ mW}] \quad (\text{C.33})$$

## LIGHT SPECTRAL DISTRIBUTION

**Function  $F_0\lambda(T, \lambda)$  for Standard the Temperature 2856 [K]**

Light spectral distribution for the standard tungsten halogen lamp is given by the **Normal Planck's Function**

$$\text{F}_0\lambda_{\text{std}} \text{ for a Spectral Temperature 2856 [K]} \quad (\text{C.34})$$

This function has been calculated for the Bandwidth:

$$\begin{aligned} \text{Bandwidth:} \\ 200\text{E-9} \leq \lambda \leq 3000\text{E-9} \text{ [m]} \end{aligned} \quad (\text{C.35})$$

with a Resolution:

$$\text{Resolution:} \quad 10.0\text{E-9} \text{ [m]} \quad (\text{C.36})$$

**Chp.1 Annex 3** shows numerical values for the Spectral Bandwidth with the specified resolution. The corresponding plot is Fig. C.12.

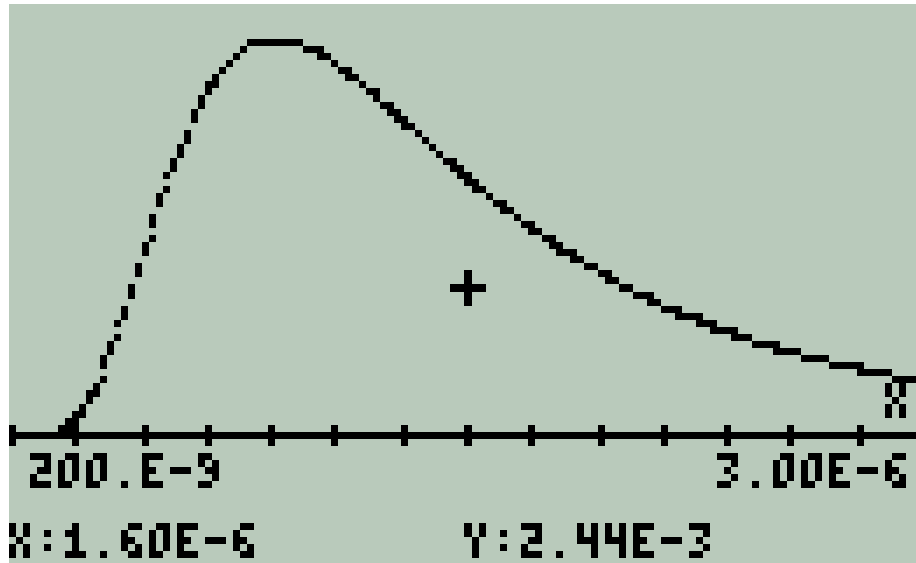


**Figure C.12:** *Standard lamp spectral distribution for  $T = 2856$  [K]*  
*Spectral band:  $200 \leq \lambda \leq 3000$  [nm]. Resolution 10 [nm].*

### The normalized Spectral Distribution

The normalized spectral distribution is defined by the function  $F0\lambda$ . This function generates a value for the Planck's Equation as a function of spectral temperature T [K] and its wavelength  $\lambda$  [m].

This is a **normalized function**, this is:

$$\sum_0^{\infty} (F0\lambda\text{std}(2856, \lambda)) = 1.000000000000 \quad (\text{C.37})$$

For the Spectral Region of Interest – ROI defined in Table C.1 where the limited bandwidth is:

$$\text{Region of Interest Bandwidth: } 200 < \lambda < 3000 \text{ [nm]} \quad (\text{C.38})$$

The correspondent summation is only:

$$\sum_{200E-9 [m]}^{3000E-9 [m]} (F0\lambda\text{std}(2856, \lambda)) = 0.877756011195 \quad (\text{C.39})$$

and, certainly, for the Si and Ge photodiodes sub-ranges are even lower as it is shown here bellow.

## 6. SPECTRAL RESPONSIVITY OF A Si AND Ge PHOTODIODES

Experimentally we know the **responsivity** for a **silicon photodiode** is **RSi10**. So **this responsivity is assumed for the photodiode**. Fig. C.13 is the responsivity for a Silicon Photodiode. **Chp.1 Annex 3** shows this responsivity vs wavelength with a resolution of 10 [nm].

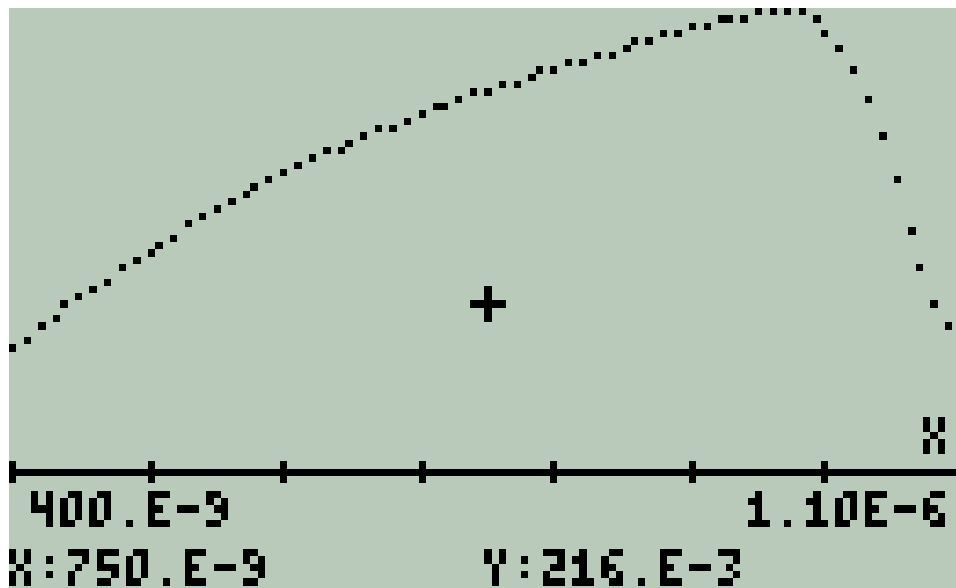


**Figure C.13:** *Spectral Responsivity for a Si Photodiode.*  
*This sensor is practical in the range  $400 \leq \lambda \leq 1100$  [nm].*

$$\text{Si Photodiode Responsivity} = \text{RSi10} \quad [\text{A} / \text{W}] \quad (\text{C.40})$$

it has a Bandwidth:

**RSi10- Bandwidth:**

$$400.0\text{E-}9 \leq \lambda \leq 1100.0\text{E-}9 \quad [\text{m}] \quad (\text{C.41})$$

it has been calculated with a

$$\text{Resolution of } 10.0\text{E-}9 \quad [\text{m}] \quad (\text{C.42})$$



### Sub-band that interacts with a Si Photodiode

The light bandwidth that interacts with the Si Photodiode is defined by Eq. (C.19). So only this sub-bandwidth from  $F0\lambda_{std}(2856, \lambda)$  will interact with the Si Photodiode. This Spectral fragment is  $F0\lambda_{Si}$ . Fig. C.14 shows this spectral fragment. [Chp.1 Annex 4-a](#) is the list of normalized irradiance values vs wavelength is provided with a resolution of 10 [nm]. Eq. (C.43) is the corresponding summation for the sub-band.

$$\sum_{400E-9 [m]}^{1100E-9 [m]} (F0\lambda_{Si}) = 0.310135167086 \quad (C.43)$$

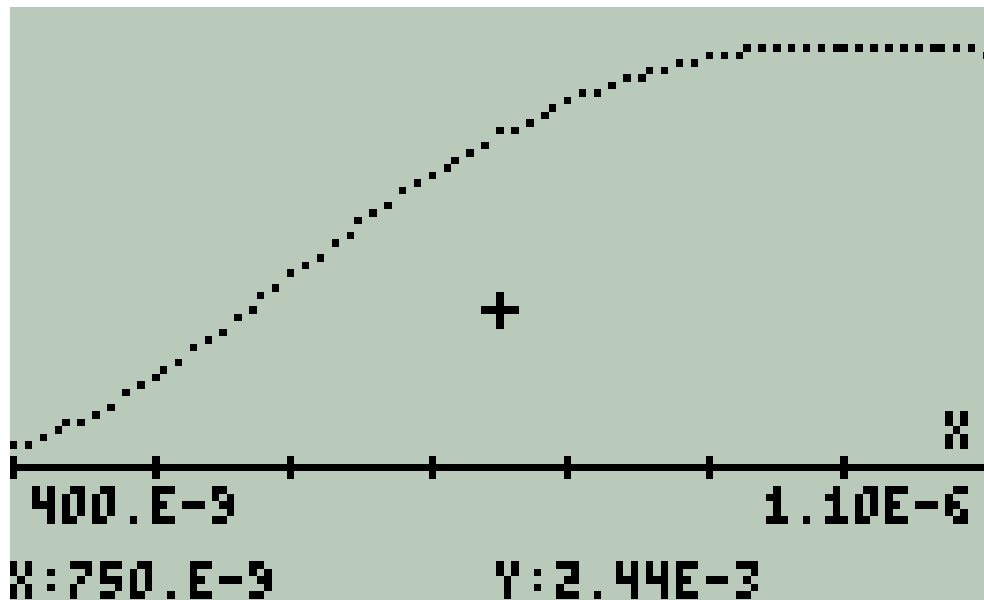


**Figure C.14:** *Fragment of normalized light spectrum that interacts with the Si photodiode*

### Incident Spectral Power on a 1mm<sup>2</sup> Active Area Si Photodiode

Due to Eq. (C.29) and Eq. (C.30), all these magnitudes – and their components inside each array that represent the spectral distribution– are considered as if they were defined in [mW]

So, only **0.310 [mW]** from the **1.000 [mW]** of Light Power impacting the Photodiode will affect the 1 mm<sup>2</sup> sensor.

This is equivalent to  $(1E-3) \cdot (F0\lambda_{Si})$  when the same magnitude is expressed in microwatts.

$$\text{Light Power} = 310.135167086 \text{ } [\mu\text{W}] \quad (\text{C.44})$$

This Light Power is distributed in the Sub-Band  $F0\lambda\text{Si}$ .

$$\text{Light Power in the Sub-Band} = 1\text{E-}3 (F0\lambda\text{Si}) \text{ } [\mu\text{W}] \quad (\text{C.45})$$

### Spectral Photocurrent obtained from the 1mm<sup>2</sup> Active Area Si Photodiode

The current from the 1 mm<sup>2</sup> active area Si Photodiode is obtained from its **responsivity**. No other factor is in between since Responsivity is an experimental parameter as result of how much current is obtained from the photodiode when it is directly and perpendicularly irradiated by a light source.

It is claimed that other parameters as **Quantum Efficiency**, this is, the ratio between the number of photons incident on the photodiode active area divided by the number of electric carriers i.e. electrons effectively generated; or **Internal Quantum Efficiency** this is the ratio between the number of photons that effectively create electron – hole pairs in the photodiode junction and the number of electrons actually measured. In the last case light reflection from the photodiode surface should be subtracted from calculation among other possible factors.

However **responsivity** as a direct experimental result does not consider these factors.

Since Responsivity is defined as:

$$R_P = \frac{I_P}{W_P} \quad [\text{A} / \text{W}] \quad (\text{C.46})$$

And its ratio is known [See Chp. 1 Annex 2]. The Electric Current Distribution  $I_P$  and its Summation Total Current  $I_{P\text{-TOTAL}}$  are, respectively:

$$I_P = ((F0\lambda\text{Si}) 1\text{E} - 3 \text{ } [\text{W}]) \cdot ((R\text{Si}10) \cdot [\text{A} / \text{W}]) \quad (\text{C.47})$$

$$I_P = ((F0\lambda\text{Si}) \text{ } [\text{W}]) \cdot ((R\text{Si}10) \cdot 1\text{E} - 3 \text{ } [\text{A}]) \quad (\text{C.48})$$

$$I_{P\text{-TOTAL}} = \sum I_P \quad [\text{A}] \quad (\text{C.49})$$

Explicit expressions for  $I_P$  and  $I_{P\text{-TOTAL}}$  are shown in Table C.3.

**Table C.3: PHOTOCURRENT DISTRIBUTION AS FUNCTION OF  $\lambda$  FOR 1mm<sup>2</sup> ACTIVE AREA OF A Si PHOTODIODE WHEN IT IS IRRADIATED BY 1mW TOTAL IRRADIANCE FROM A STANDARD TUNGSTEN FILAMENT LAMP AT THE REFERENCE SPECTRAL TEMPERATURE OF 2856 [K]**

$\lambda$ [m]	I [A]
400.0E-9	57.1E-9
410.0E-9	72.2E-9
420.0E-9	95.0E-9
430.0E-9	118.E-9
440.0E-9	146.E-9
450.0E-9	176.E-9
460.0E-9	213.E-9
470.0E-9	252.E-9
480.0E-9	296.E-9
490.0E-9	345.E-9
500.0E-9	397.E-9
510.0E-9	453.E-9
520.0E-9	514.E-9
530.0E-9	585.E-9
540.0E-9	653.E-9
550.0E-9	727.E-9
560.0E-9	805.E-9
570.0E-9	884.E-9
580.0E-9	966.E-9
590.0E-9	1.05E-6
600.0E-9	1.14E-6
610.0E-9	1.23E-6
620.0E-9	1.32E-6
630.0E-9	1.41E-6
640.0E-9	1.50E-6
650.0E-9	1.60E-6
660.0E-9	1.69E-6
670.0E-9	1.78E-6
680.0E-9	1.87E-6
690.0E-9	1.97E-6
700.0E-9	2.06E-6
710.0E-9	2.15E-6
720.0E-9	2.25E-6
730.0E-9	2.34E-6
740.0E-9	2.43E-6
750.0E-9	2.51E-6
760.0E-9	2.60E-6
770.0E-9	2.68E-6
780.0E-9	2.77E-6

790.0E-9	2.84E-6
800.0E-9	2.92E-6
810.0E-9	3.00E-6
820.0E-9	3.07E-6
830.0E-9	3.14E-6
840.0E-9	3.21E-6
850.0E-9	3.28E-6
860.0E-9	3.34E-6
870.0E-9	3.41E-6
880.0E-9	3.46E-6
890.0E-9	3.52E-6
900.0E-9	3.58E-6
910.0E-9	3.63E-6
920.0E-9	3.67E-6
930.0E-9	3.72E-6
940.0E-9	3.76E-6
950.0E-9	3.79E-6
960.0E-9	3.81E-6
970.0E-9	3.80E-6
980.0E-9	3.81E-6
990.0E-9	3.76E-6
1.000E-6	3.67E-6
1.010E-6	3.53E-6
1.020E-6	3.34E-6
1.030E-6	3.10E-6
1.040E-6	2.78E-6
1.050E-6	2.41E-6
1.060E-6	2.01E-6
1.070E-6	1.68E-6
1.080E-6	1.42E-6
1.090E-6	1.18E-6
1.100E-6	956.E-9

Then, the total current obtained from the photodiode is its summation:

$$\mathbf{I_{P-TOTAL} = \sum I_P = 144.70218504 \text{ } [\mu\mathbf{A}] \quad (C.50)}$$

Fig. C.15 is a plot of the obtained results:

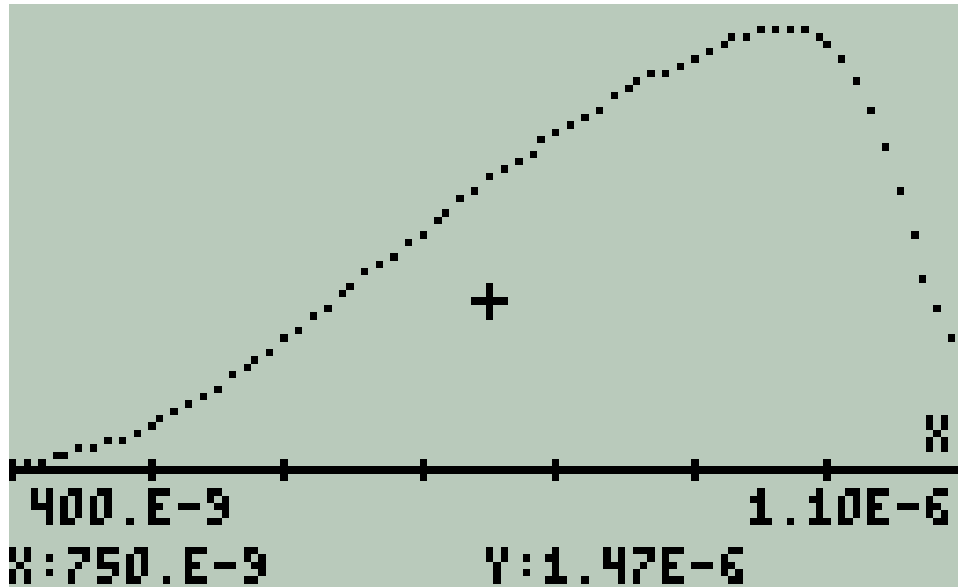


**Figure C.15:** *Electric current from a 1mm<sup>2</sup> silicon photodiode when it is irradiated with 1 KW / m<sup>2</sup> Planck's light source with a standard spectral temperature = 2856 [K]*

### Interpretation of Results

In order to evaluate this answer, let's calculate  $R_{P-TOTAL}$ :

$$\begin{aligned}
 R_{P-TOTAL} &= I_{P-TOTAL} / \text{Light Power} \\
 &= 144.73338E-6 \text{ [A]} / 310.135167086 \text{ [1E-6W]} \\
 &= 0.466678388523 \text{ [A/W]} \quad (C.51)
 \end{aligned}$$

Also, since there are 71 elements in the list  $RSi10$ , let's evaluate its mean value:

$$\begin{aligned}
 R_{P-MEAN} &= (1/71)(\sum_1^{71} RSi10) = 29.846 / 71 \\
 &= 0.420366197183 \text{ [A/W]} \quad (C.52)
 \end{aligned}$$

We realize that result from Eq. (53) is consistent with result from Eq. (54).

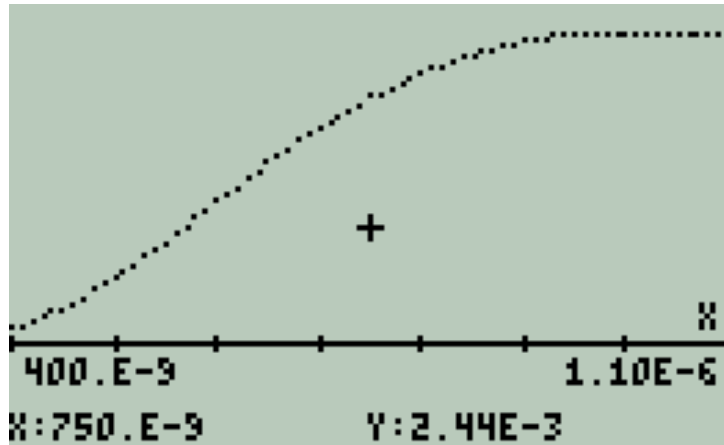
On the other hand, by observing data from Chp. 1 Annex 2 and Chp. 1 Annex 3, the maximum value for Responsivity is

$$\mathbf{R_{P-MAX}} = \mathbf{0.5886 \text{ for } \lambda = 980 \text{ [nm]}} \quad (\text{C.53})$$

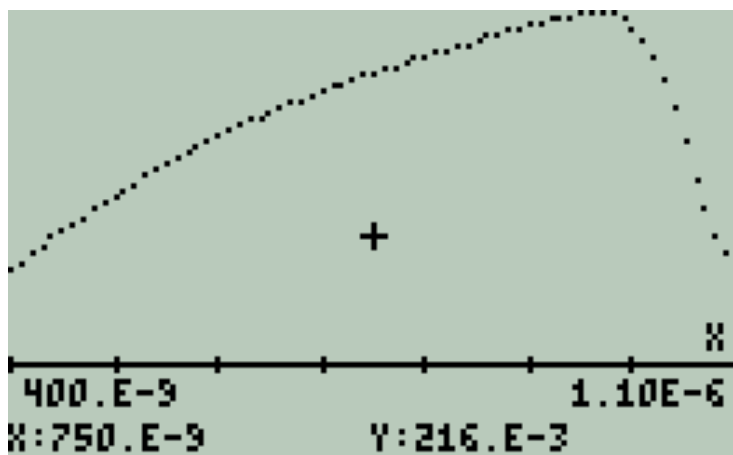
This result is also consistent. So, in general it could be claimed that, in this calculation,

**all this figures are consistent**

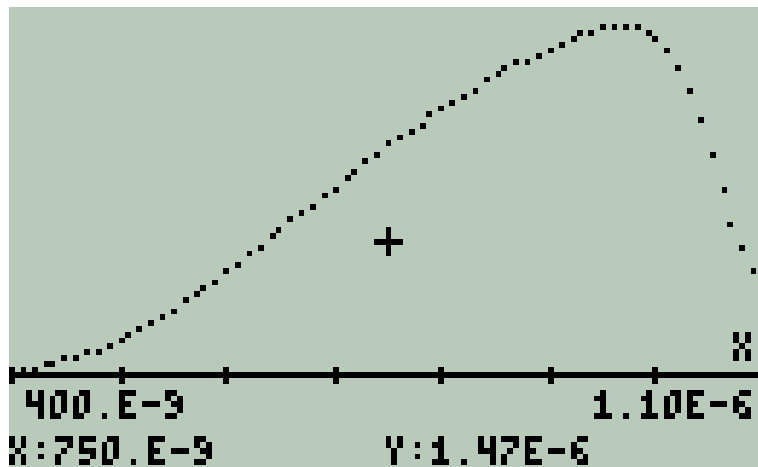
To conclude, in Fig. C.16, the Standard Spectral Irradiance, The Responsivity and the Photodiode Current graphics are presented.



(a) Total Irradiance [ $\text{mW}/\text{mm}^2$ ] vs  $\lambda$  [ $\text{m}$ ]



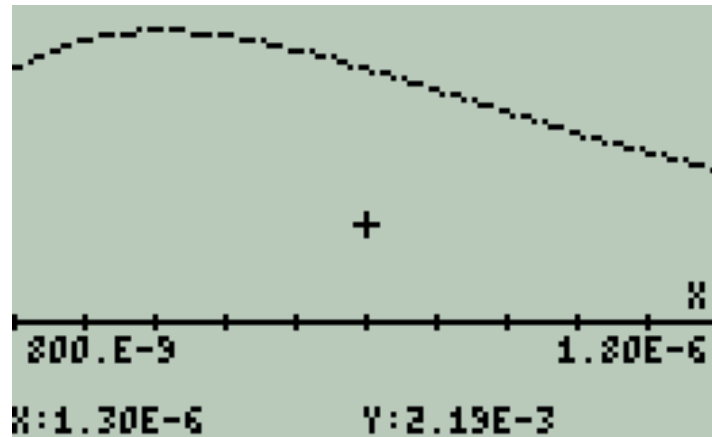
(b) Responsivity [ $\text{A}/\text{W}$ ] vs  $\lambda$  [ $\text{m}$ ]



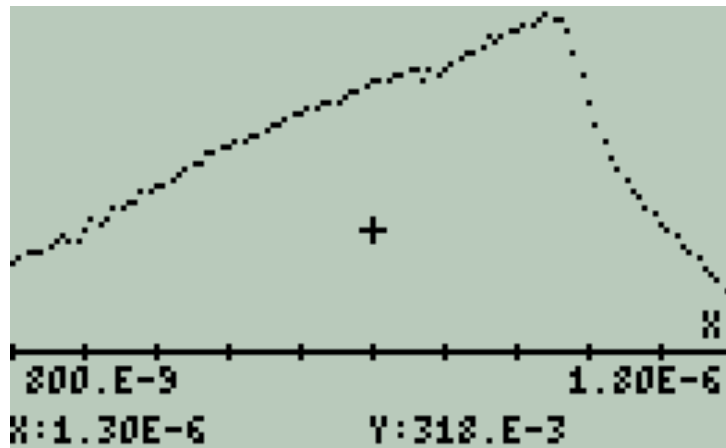
(c) Photocurrent [ $\text{A}$ ] vs  $\lambda$  [ $\text{m}$ ]

**Figure C.17:** Irradiance, Responsivity and Photocurrent for a  $1 \text{ mm}^2$  Si photodiode exposed to an spectral irradiance of  $1 \text{ Kw}/\text{m}^2$  with a spectral  $T$  of  $2856 \text{ [K]}$

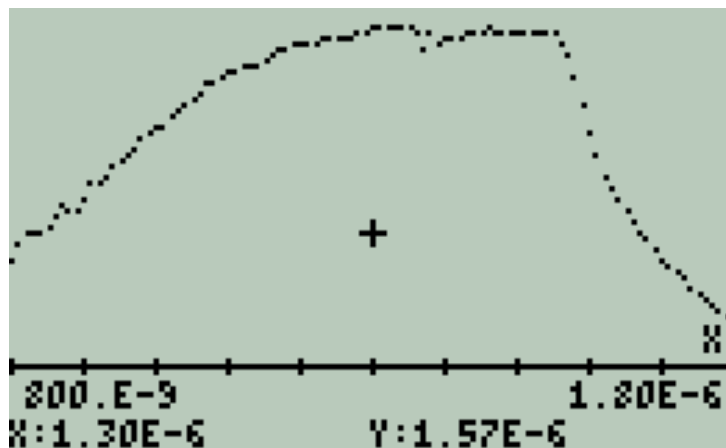
Following an identical procedure, the results obtained for a **Ge photodiode** are summarized in Fig. C.18



(a) Total Irradiance [ $\text{mW}/\text{mm}^2$ ] vs  $\lambda$  [ $\text{m}$ ]



(b) Responsivity [ $\text{A}/\text{W}$ ] vs  $\lambda$  [ $\text{m}$ ]



(c) Photocurrent [ $\text{A}$ ] vs  $\lambda$  [ $\text{m}$ ]

**Figure C.18:** Irradiance, Responsivity and Photocurrent for a  $1 \text{ mm}^2$  Ge photodiode exposed to an spectral irradiance of  $1 \text{ Kw}/\text{m}^2$  with a spectral T of  $2856 \text{ [K]}$ .



## **CONCLUSIONS**

- In this Chapter an introduction to Photons and Photon Detectors is presented.
- Responsivity of Photodiodes is described
- Si and Ge Photodiodes have been chosen as light detectors in the Visible and Infrared Ranges as the simplest options.
- A method to calibrate a photodiode against a known Spectrum from a Standard Tungsten Filament Lamp has been developed.
- The results here obtained permit to detect and measure Light Irradiance in the IR and Visible Ranges.

## **FURTHER ACTIVITIES**

- With the procedure here described, it is possible to determine Responsivity for a Sensor in the IR and UV ranges.
- Si and Ge photodiodes are sensitive to temperature in their long wavelength range. Temperature correction is required.
- At present, there is enough information to design and implement simple instruments as the immediate activity. See Chapter 2.

## D. OBJECTIVES AND SCOPE OF THE PRESENT WORK

### 1. GENERAL OBJECTIVE

This work is related with the development of **virtual instrumentation** to measure **photovoltaic parameters**.

**Virtual instrumentation** is the use of customizable software and modular measurement hardware to create user-defined measurement systems, *called virtual instruments*.

*The primary difference between hardware instrumentation and virtual instrumentation is that software is used to replace a large amount of hardware.*

This work has as general objective to develop virtual instruments to measure the main parameters of light as the primary source for photovoltaic applications.

The virtual instruments developed are:

- **Thermometer** based on a Si pn junction and Ebers – Moll equation.
- **Spectral temperature meter** for thermal radiation sources based two LEDs of different color characterized as photocurrent detectors and several algorithms.
- **Irradiance meter** for thermal radiation sources based on a Si commercial photodiode, spectral temperature and several algorithms. Spectral temperature and irradiance are concomitant parameters for the same thermal radiation source.
- **Current – Voltage response for single solar cell prototypes** and related parameters based in a front end circuit conformed by the tested cell itself and a N-channel JFET transistor acting as a controlled variable potentiometer and several algorithms.

- Also the calculated parameters to build a **simple spectrometer and monochromator** are presented.

The work departs from the physical principles and simple low cost electronic components.

Simple front end circuits are used to detect the physical parameters of interest. These circuits are connected to a microcontroller board (IOIO OTG) for data acquisition.

The microcontroller board is interface-able to either to a PC or to an Android device.

A mathematical emulator (EMU 50G) is embedded in the PC or Android device.

Developed routines – i.e.: the software part of each virtual instrument – is able to process the acquired data and display numeric and/or graphic results of the measurements in the appropriate [SI] units.

These instruments are initially intended as useful tools in a laboratory where photovoltaics measurements are a routine or where solar cells prototypes are developed, though there are other activities in which they are also applicable.

It is thought that the general idea of virtual instruments is applicable mainly for educational purposes to provide affordable experimental tools to students in science and fields of engineering to ease their experimental skills and knowledge background.

## 2. SPECIFIC OBJECTIVES

### Chapter 1:

- a) Summarize: the **physical principles of light either as wave or as photon**.
- b) Introduce the concept of **responsivity** for photodiodes and LEDs as light detectors and correlate it with the **measured photocurrent** and **irradiance** when these detectors are exposed to **thermal radiation sources**.
- c) Establish the **objectives and scope of this thesis work**.

### Chapter 2:

- d) Develop simple spectrometer and monochromator for visible range, near UV range and near IR range. Design procedures are detailed and results are shown as Tables. A prototype has been assembled for the visible range.
- e) Summarize electronic components light detectors, and front end circuits applicable to the tasks exposed as general objective.

- f) Show developed front end circuits used in this work for: environmental thermometer, spectral temperature meter (pyrometer), irradiance meter (pyranometer), and single solar cell current-voltage generator (I-V curve generator).

### **Chapter 3:**

- g) Introduce: the microcontroller board IOIO OTG used in this project, its characterization and interfacing.
- h) Introduce Android Studio, the freeware official Android devices programmer established by Google to program the Android Device in order to control IOIO OTG. So electric signals from front end circuits are converted into data and stored in memory files of the Android device.
- i) Show the interconnections of the microcontroller board with front the end circuits to detect the physical parameters in this work
- j) Briefly describe the Android ↔ Windows transparency for data transfer and data use by the emulator routines that conform each virtual instrument..

### **Chapter 4:**

- k) Mathematical emulator HP 50G as a tool to characterize virtual instruments is introduced.
- l) Introduce common topics to develop algorithms that implement virtual instruments
- m) Explain the algorithms that conform the virtual instruments in this work.

### **Chapter 5:**

- a) Describe calibration methods for the virtual instruments in this work.
- b) Show preliminary measurements made with the developed prototype and intercompare these results with those obtained using the Laboratory equipment.
- c) Provide a list of the electronic components, microcontroller board and freeware used in this project.

### 3. SCOPE OF THE WORK

The present work is an effort to put together knowledge from several disciplines to obtain as result simple and affordable **virtual instruments for photovoltaic measurements**.

This work contains five chapters, conclusions and recommendations.

Each chapter ends with **bibliography** numbered in [...] and **basic references** numbered in | ... |.

**Annexes** corresponding to each chapter are presented at the end of the work.

**Chapter 1** introduces preliminary topics and basic definitions, the Electromagnetic Spectrum, the Planck's Equation and Sunlight. Then summarizes the description of Light as Wave and Light as Photon. Responsivity for LEDs as sensors and photodiodes is correlated with photocurrents and irradiance for thermal radiation sources. Annex 1 for Chapter 1 is a paper written by the author that procures conciliate this two descriptions using equations from electromagnetic theory and the basic equations for photons.

**Chapter 2** introduces essential optical components and. procedures to design a simple spectrometer and monochromator. Useful electronic components, common light sensors and useful electronic stages for photovoltaic measurements are described. Finally, practical front end circuits used in this work are exposed.

**Chapter 3** is related with data acquisition and control using microcontrollers and a pc or an android device. Preliminary Topics, IOIO-OTG – the microcontroller board – characterization and interfacing, Programming Android devices as measuring instruments, interfacing front end circuits with the microcontroller and the transparency Android ↔Windows data transfer are the topics dealt in this chapter.

**Chapter 4** introduces the mathematical and graphic emulator used to develop the routines that are part of the proposed virtual instruments. Then common algorithms for this project are described. Finally the algorithms for individual virtual instruments are described.

**Chapter 5** contains: The calibration procedures and preliminary measurements made with the virtual instrument prototype in the Laboratory. In this chapter stands out the intercomparison of results between the developed prototype and the equipment of the Nanostructured Materials for Photovoltaic Applications – ICN2. Finally a description of the materials and freeware employed in the prototype are listed.

**Conclusions and Recommendations** are presented at the end.

Every Chapter ends with the corresponding Bibliography: numbered in [] and Basic References: numbered in {}. Annexes for all chapters are at the end of the work.

## BIBLIOGRAPHY

- [1] Feynman Richard      The Lectures on Physics. Vol. 1. Mechanics and Thermodynamics. Chp. 41 The Brownian Motion
- [2] Wikipedia              [http://en.wikipedia.org/wiki/Solar\\_radius](http://en.wikipedia.org/wiki/Solar_radius)
- [3] Wikipedia              [http://en.wikipedia.org/wiki/Earth's\\_orbit](http://en.wikipedia.org/wiki/Earth's_orbit)
- [4] Wikipedia              <http://en.wikipedia.org/wiki/Sunlight>
- [5] Wikipedia              <http://en.wikipedia.org/wiki/Insolation>
- [6] Wikipedia              [http://en.wikipedia.org/wiki/Solar\\_simulator](http://en.wikipedia.org/wiki/Solar_simulator)
- [7]                              [http://en.wikipedia.org/wiki/Ozone-oxygen\\_cycle](http://en.wikipedia.org/wiki/Ozone-oxygen_cycle)
- [8]                              <http://chinook.kpc.alaska.edu/~ifafv/lecture/fraunhofer.htm>
- [9] Hewlett Packard      HP 50 Advanced User Reference Manual, pg. 202
- [10] L. A. Sena              Unidades de las Magnitudes Físicas y sus Dimensiones.  
Cap. 8: Unidades de Radiación. Sección 8.2 Características Energéticas de la Radiación. Pgs. 248 – 254. Editorial MIR, Moscú 1979
- [11]. Feynman Richard      The Feynman's Lectures on Physics Vol.2  
Mainly Electromagnetism and Matter  
Adisson Wesley 1964
- [12] ídem 1                      Vol. 2. Chp. 20: Solutions of Maxwell's Equations  
In Free Space. Sect. 20.4.: Spherical Waves.
- [13] Frank Crawford      Ondas Capítulo 9: Interferencia y Difracción. 9.2 Interferencia entre dos fuentes puntuales coherentes. Campo Cercano y Campo Lejano. Pág. 484. Berkeley Physics Course Vol. 3. Editorial Reverté 1994 Barcelona.
- [14] Okan K. Ersoy              Diffraction, Fourier Optics and Imaging.  
Chp. 3: Fundamentals of wave propagation.  
Sect. 3.4 Phasor Representation.  
John Wiley & Sons 2007

- [15] Frank Crawford Ondas. Berkeley Physics Course Vol. 3. Capítulo 9: Interferencia y Difracción. 9.2. Interferencia ente dos fuentes puntuales coherentes. Págs. 482 – 495. Editorial Reverté 1994 Barcelona.
- [16] ídem 1 Vol. 1. Chapter 30 Diffraction. 30.1: The resultant amplitude of n equal oscillators. 30.2: Diffraction Grating. 30.3: The resolving power of a grating.
- [17] Eyvind H. Wichmann Física Cuántica. Berkeley Physics Course – Vol. 4 Chp. 1: Introduction 41 -46 Photoelectric Effect. Pgs: 31-36. Edit. Reverté 1986 Barcelona
- [18] Wikipedia Word: Electronvolt
- [19] Thomas Pearsal Photonics Essentials An Introduction with Experiments. Section 2: Photonic Devices. Chapter 3: Photodiodes. Pag. 37-58 Mc. Graw Hill 2003
- [20] Wei-Chih Wang Optical Detectors  
Department of Mechanical Engineering  
University of Washington ME557  
<http://depts.washington.edu/mictech/optics/sensors/detector.pdf>
- [21] THOR High-Speed Photodetectors
- Note:** In this page there are links like:
- Click [Here](#) to have access to this information.
- Where Data on Responsivity for Photodiode Detectors is available with resolutions of 5 or 10 [nm]  
[http://www.thorlabs.com/newgrouppage9.cfm?objectgroup\\_id=1295](http://www.thorlabs.com/newgrouppage9.cfm?objectgroup_id=1295)
- [22] INTERNATIONAL LIGHT
- Tungsten Halogen Lamps - Technical / Application Information
- <http://www.intl-lighttech.com/applications/light-sources/tungsten-halogen-lamps>
- [23] OSRAM Technology and Application
- TUNGSTEN HALOGEN LOW VOLTAGE LAMPS PHOTO OPTICS
- [https://assets.sylvania.com/assets/documents/ENGR\\_BLTN9.9ecc8e28-950e-4995-a67e-ceedfc343c65.pdf](https://assets.sylvania.com/assets/documents/ENGR_BLTN9.9ecc8e28-950e-4995-a67e-ceedfc343c65.pdf)
- [24] Wikipedia Word: CIE Standard Illuminant
- [https://en.wikipedia.org/wiki/Standard\\_illuminant](https://en.wikipedia.org/wiki/Standard_illuminant)

## Basic References

- [1] **Feynman Richard    The Feynman's Lectures on Physics Vols. 1, 2, 3**  
**Adisson Wesley 1964**

**Note:**

An organized sequence of related topics consulted in the Feynman's Book are summarized here below.

**The Feynman's Lectures on Physics.**

**Vol. 1. Mechanics and Thermodynamics.**

Chp. 41 The Brownian Motion

**Vol. 2: Electromagnetism and Matter.**

Chp. 18: The Maxwell Equations.	Sect. 18.4: A travelling field
Cap. 13: Magnetostatics.	13.1 The Magnetic Field
Chp. 15: The potential vector $\mathbf{A}$ .	Section 15.6: What is true for statics is false for dynamics
Chp. 18: The Maxwell Equations.	Section 18.4: A travelling field
Chp. 18: The Maxwell Equations.	Section 18.5: The speed of light.
Chp. 8: Electrostatic Energy.	Section 8.5 Energy in the electrostatic field.
Chp. 15: The vector potential.	Section 15.3 The energy of steady currents
Chp. 15: The vector potential.	Section 15.6: What is true for statics is false for dynamics; Table 15.1
Chp. 17: The Laws of Induction.	Section 17.8: Inductance and Magnetic Energy.
Chp. 27: Field Energy and Field Momentum.	Section 27.3: Energy Density and Energy Flow in the Electromagnetic Field.

- [2] **Frank Crawford    Ondas**  
**Berkeley Physics Course Vol. 3.**  
**Editorial Reverté 1994 Barcelona**



---

*CHAPTER 2*

*OPTICAL*

*AND ELECTRONICS*

*ESSENTIAL COMPONENTS*



## OUTLINE OF THE CHAPTER

### A) ESSENTIAL OPTICAL COMPONENTS

1. DESIGN PARAMETERS FOR A SPECTROMETER
2. "DARK ROOM"
3. OPTICAL SLIT
4. DIFFRACTION GRID
5. SIMPLE SPECTROMETER AND MONOCHROMATOR DESIGN PARAMETERS
6. SIMPLE SPECTROMETER AND MONOCHROMATOR DESIGN

### B) USEFUL ELECTRONIC COMPONENTS

1. PN JUNCTIONS AS TEMPERATURE SENSORS
2. FIELD EFFECT TRANSISTORS – FETs
3. OPERATIONAL AMPLIFIERS – OPAMPs

### C) COMMON LIGHT SENSORS

1. LIGHT EMITTING DIODES – LEDs
2. SILICON PHOTODIODES
3. Si AND Ge SIGNAL DIODES

### D) USEFUL ELECTRONIC STAGES FOR PHOTOVOLTAIC MEASUREMENTS

1. JFET CURRENT SOURCE
2. VOLTAGE FOLLOWER
3. OPAMPs AMPLIFIERS
4. PHOTOCURRENT TO VOLTAGE CONVERTER

### E) FRONT END CIRCUITS

1. ENVIRONMENTAL THERMOMETER
2. SIMPLE SPECTROPHOTOMETER AND MONOCHROMATOR
3. PYROMETER (SPECTRAL TEMPERATURE METER)
4. PYRANOMETER (IRRADIANCE METER)
5. SOLAR CELL I – V CURVE GENERATOR

## Bibliography

### Basic References

### Annexes Chapter 2 (Shown at the end of this work)

ANNEX 1: A DISGRESSION ON FOURIER TRANSFORMS



## **CHAPTER 2: OPTICAL AND ELECTRONIC ESSENTIAL COMPONENTS**

This chapter provides information about the optical and electronic components useful for the project. Simple optical instruments are designed and the analog circuit board for the virtual instruments is presented.

This chapter is divided in five sections.

### In Section A:

Essential optical devices as slits, “dark room”, and diffraction grids are introduced. Then, as a direct application of Chp. 1 Section B: Light as wave simple spectrometer and monochromator for visible range, near UV range and near IR range are developed. Design procedures are detailed and results are presented as Tables. Finally, a prototype assembled for the visible range is shown.

### In Section B:

Electronic components useful for this project are introduced. Silicon PN junctions or Si diodes are useful temperature sensors; using Ebers – Moll equation are excellent thermometers for environmental and cryogenic temperature ranges. Bipolar Field Effect transistors are useful components to assemble current sources and to act as controlled variable resistors when they are used in the linear range. Operational amplifiers – OPAMPs, in particular FET input OPAMPs as useful components to handle small currents signals.

### In Section C:

Common light sensors are introduced: Light emitting diodes - LEDs are useful quasi monochromatic light sources or narrow window light sensors. Si and Ge photodiodes are broad band light sensors in the visible and near infrared regions. Si and Ge glass encapsulated signal diodes are also light sensors.

### In Section D:

Useful electronic stages for this project are presented: A simple constant current source using a JFET transistor. Finally, four stages using OPAMPs: voltage follower, inverting and noninverting amplifiers and, in particular, photocurrent to voltage converters that as excellent ammeters in the nano-amperes range are introduced.

### In Section E:

Includes the front end circuits to detect the physical parameters required in this project. These front end circuits are: thermometer, spectrophotometer light detector stage, spectral temperature meter, irradiance meter and solar cell I-V curve generator.



## A. ESSENTIAL OPTICAL COMPONENTS

In this section the optical components for this project are described.

As a prerequisite, the design parameters for the optical Instruments i.e.: spectrophotometer, monochromator; are firstly established. These parameters are the wavelength ranges. These ranges are the start point to design the instruments

Then an approach to the essential optical components is developed taking as reference the theoretical support in Chapter 1, Section B.

Since the simple instruments proposed require only a “Dark Room”, Slits and Grids if the Front End Circuit to detect Light is excluded; then it is possible to calculate at, once, the Design Parameters for the Spectrophotometer, Monochromator. So, they are included as well in the last numeral in this Section.

There are four optical components that are critical in these instruments:

### “Dark Room”

Experiment with light, in general, requires a dark empty volume to observe light – related phenomena.

### Slits

**Entrance slit** and **exit slit** collimate the light beam that enters the instrument and its spectral output.

### Diffraction Element

It is the device that unfolds light in its wavelengths. The most commonly used component is a **diffraction grid** or simply a **grid**.

Essentially, two types of grids will be used:

- **Transmissive grids**: They are transparent grids
- **Reflective grids** are mirror like grids

### Light Detectors

They are the light sensors that obtain the spectral information as an electrical signal. Light detectors are part of Section C.

Optical lenses are excluded in these simple prototypes.

## 1. DESIGN PARAMETERS FOR A SPECTROMETER

Let's apply now the information from Chapter 1 to design simple instruments to measure Light wavelength.

### Wavelength Range of Interest for this Project

The proposed instruments are for solar spectrum measurements and solar cells development. With this objective in mind and taking as reference solar irradiance spectrum, Please, refer to Fig. A.15 in Chapter 1, the Wavelength Region of Interest is defined as:

$$\begin{array}{c} \text{Wavelength Region of Interest} \\ 300 < \lambda < 3000 \text{ [nm]} \end{array}$$

(A.1)

By considering several factors mainly:

- Slit widths range
- Available diffraction grids
- Dimensions for the proposed equipment
- Type of light detectors to be used
- Design optimization in order that the prototype could be used for different ranges
- Availability of low cost local components

The Wavelength Region of Interest defined in Eq. (A.1) has been subdivided in three sub-ranges. These Sub-ranges are shown in Table A.1.



**Table A.1: Ranges of Wavelengths for the Proposed Instruments\***

---

<b>Total Range of Interest</b>	<b><math>300 &lt; \lambda &lt; 3000</math> [nm]</b>
<b>Visible Range Spectrometer</b>	<b><math>400 &lt; \lambda &lt; 700</math> [nm]</b>
<b>Near Infrared Spectrometer</b>	<b><math>650 &lt; \lambda &lt; 2600</math> [nm]</b>
<b>Near UV Spectrometer</b>	<b><math>300 &lt; \lambda &lt; 460</math> [nm]</b>

---

**\* Important Comment:** The criteria for defining these sub-ranges will become evident through the design procedure. However it is considered indispensable to have these initial sub-ranges to start the design.

### Proposed Instruments

Two type of instruments are proposed to measure wavelength:

A **Spectrometer**, displays wavelengths versus intensity on a screen or detectors array. In general their parts are fixed and the spectral band or spectral range bandwidth is specified.

A **Monochromator** is a dispositive with one movable or rotating part, it allows to select a narrow wavelength band from the whole spectrum to leave the instrument through the exit slit.

### Span to Display Spectra

For the spectrometer, as well as for the photometer, a common length (width)  $D_{SPAN}$  to display the whole spectrum on a horizontal fringe is defined:

$$D_{SPAN} = 2.00 \text{ [cm]} \tag{A.2}$$

### Applications of linear arrays of coherent sources

Ideas on linear arrays of coherent sources from Chapter 1 B.3 are directly applicable to describe optical diffraction grids and optical slits.

## 2. “DARK ROOM”

If we are interested in observing Light or to experiment with it, it is better to set an appropriate environment for the purpose by surrounding an empty volume – in the order of 1 cubic decimetre – by opaque walls, a “dark room” or dark place is obtained. Fig. A1.

This “dark room” or “dark volume” has to be designed as a prerequisite. It also defines the geometry and its walls are useful to “fix the position” of internal components.

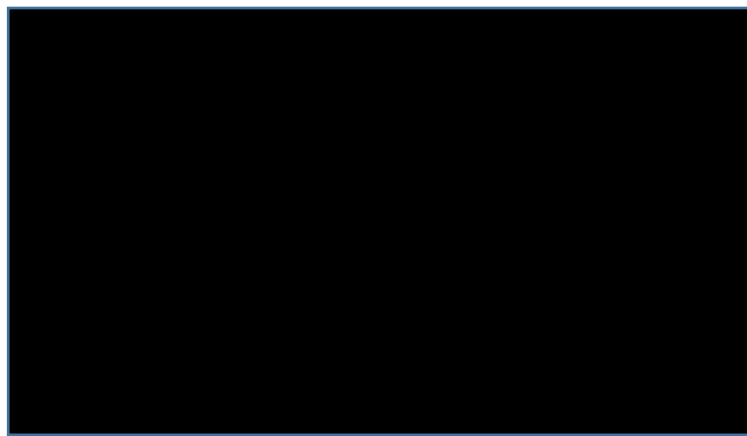


**Figure A.1:** *An isolated environment to observe Light is an empty volume or “dark room” surrounded by opaque walls*

## 3. OPTICAL SLIT

### PHYSICS OF A SINGLE OPTICAL SLIT

A **slit** is a narrow rectangular aperture that behaves as light input or output for an optical instrument as a spectrometer or monochromator.

In spite of its simplicity a slit is an essential component in the above mentioned optical instruments since it defines the amount of light that enters – or leaves – the instrument.

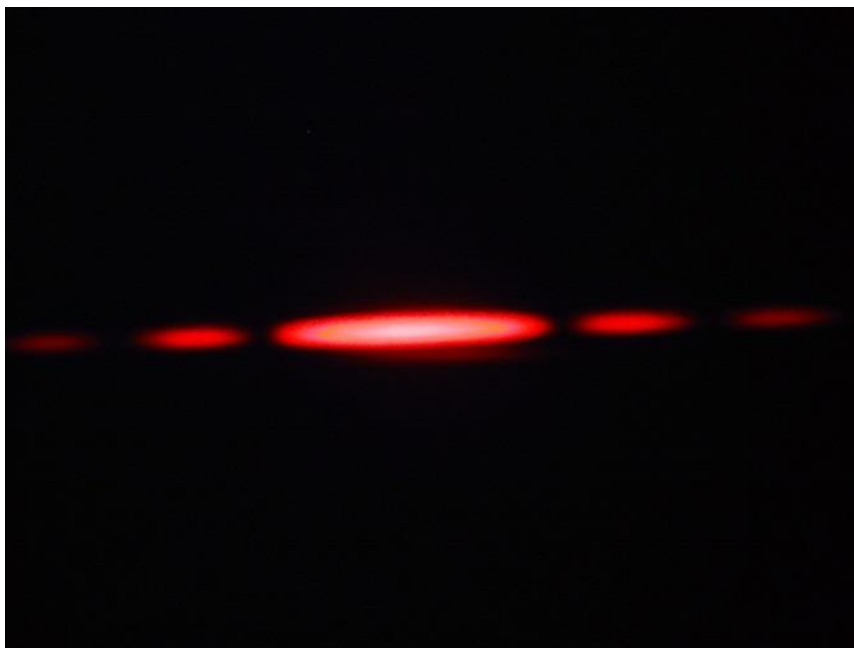
Slits must be properly sized and placed in these instruments.

Fig. A.2 shows a picture of a simple slit.



**Figure A.2:** *Image of a vertical narrow optical slit.*  
*[Figure adapted from reference shown in ANNEX F]*

If a small portion of the vertical narrow slit is illuminated with a red laser beam 650 [nm] coming from a simple pointer, the horizontal pattern observed on the opposite wall of our “dark room” is shown in Fig. A.3



**Figure A.3:** *Horizontal Light Pattern observed on the bottom wall of our “dark room” when a small section of the Narrow Vertical Slit is illuminated by a red laser beam coming from an external pointer when Light impacts perpendicularly on the slit.*  
*[Figure adapted from reference shown in ANNEX F]*

If a monochromatic green light 532 [nm] passes through the **whole vertical slit** a pattern like the one shown in Fig. A.4 is observed on a screen placed few centimetres away (far field).

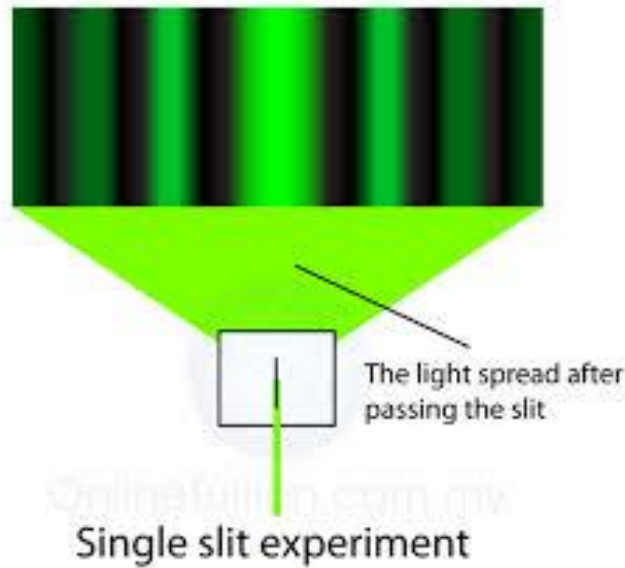


**Figure A.4:** Light pattern observed on a screen from a beam coming from a vertical narrow slit when a monochromatic light crosses through the **whole slit**. [Figure adapted from reference shown in ANNEX F]

It is important to realize that Light Intensity in Fig. A.3 and Fig.A.4 have a wavelike behaviour. Compare the intensity along a fringe and observe their similarity with Eq. (B.32.b) and Fig. B.16 in Chapter 1.

Let's consider a narrow section of a vertical slit illuminated by a laser beam. Fig. A.5

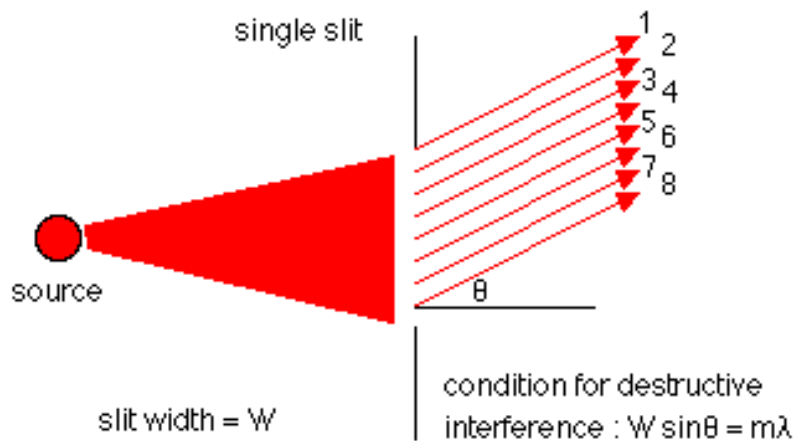


**Figure A.5:** Every point along the slit width is considered as a source of spherical secondary wavelets of the same frequency as the primary wave. The optical field at any point beyond an obstruction is the superposition of all such wavelets reaching that point. (Huygens – Fresnel Principle). [Figure adapted from reference shown in ANNEX F]

Since the spherical secondary wavelets in the slit are originated from a coherent source, let's consider them as identical in amplitude, frequency and phase.

For  $\theta = 0$ , this is the maximum intensity point in Fig. A.3 and Fig. A.4; there is a maximum central intensity. It implies that **wavelets arriving to the central point are in phase**. When  $\theta$  increases, intensity diminishes up to zero. Then it starts again increasing up to a next maximum of lower intensity and so forth.

The mathematical approach to this problem is to consider **a phase difference from a discrete identical wavelets coming from different points along the slit. The phase difference depends on the path of each of them to the observation point P.**

### The Fraunhofer diffraction by one narrow slit [1]

With the phasors approach introduced previously, (Chpt. 1, Section 3), let's obtain an expression for light diffraction through a narrow slit. See in Chapter 1 Eqs. (B.18 – B.19) and Eqs. (B.26 to B.29).

If a monochromatic light of wavelength  $\lambda$  crosses through a narrow slit of width  $a$  divided in  $\Delta y$  differential increments, then light intensity at point P is the resultant of wavelets coming from each element  $\Delta y$  in the slit.

Geometry for this deduction is shown in Fig. A.5 and Fig. A.6.

Note that the “lens” in Fig. A.6 is just an “optical resource” to observe diffraction in the “far field” in a shorter distance from the slit to the observation point P. Compare Fig. A.19 in this Section with Fig. B.11 and Fig. B-12 in Chapter 1. An important point that is highlighted is that diffraction is observed in the “far field” region.

At the observation point P, there is a phase shift  $\Delta\beta$  from wavelets coming from two neighbour source elements separated  $\Delta y$ .

$$\Delta\beta = \frac{2\pi}{\lambda} \Delta y \cdot \sin\theta \quad (\text{A.3})$$

The total phase difference for the whole slit is

$$\beta = N\Delta\beta = \frac{2\pi}{\lambda} \cdot (N \cdot \Delta y) \cdot \sin\theta = \frac{2\pi}{\lambda} \cdot a \cdot \sin\theta \quad (\text{A.4})$$

When  $\Delta y \rightarrow 0$  and  $N \rightarrow \infty$  the discrete phasors become an arc length which magnitude is  $R \cdot \beta$ . Compare Fig. B.13 Chpt. 1 (discrete case) with Fig. A.7 Chpt. 2 (continuous case).

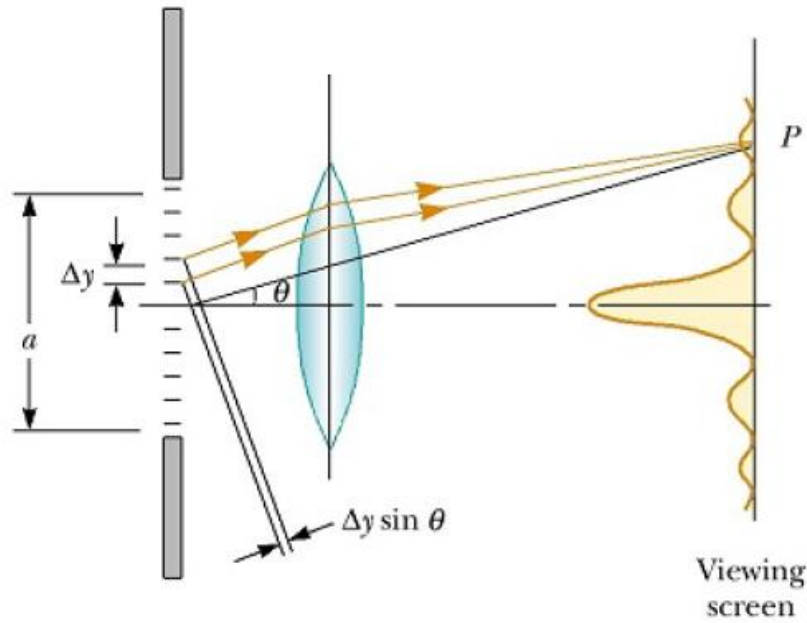


**Figure A.6:** Fraunhofer diffraction by a single slit. The light intensity at point  $P$  is the resultant of all the incremental electric field magnitudes from the slit-zones of width  $\Delta y$ .  
 [Figure adapted from reference shown in ANNEX F]

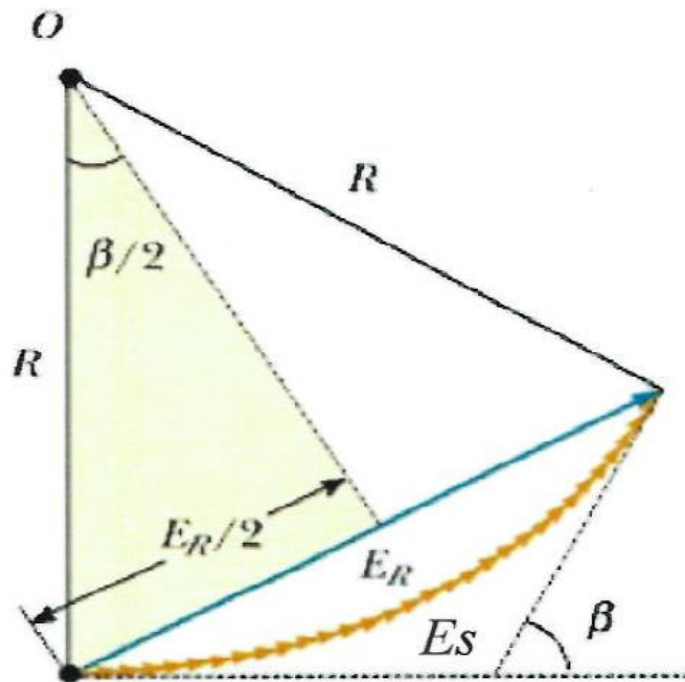


**Figure A.7:** Phasor diagram for large number of coherent sources. The locus of phasors is then the arc of radius  $R$ . The resultant electric field magnitude  $E_R$  is the length of the chord length.  
 [Figure adapted from reference shown in ANNEX F]

The magnitude of  $E_R$  is the chord length (see Fig. A.7)

$$\sin\left(\frac{\beta}{2}\right) = \frac{(E_R/2)}{R} \quad (\text{A.5})$$

where  $R$  is the radius of curvature.

However **the radius of curvature  $R$  and the arc  $E_S$  are related** by

$$E_S = \beta \cdot R \quad (\text{A.6})$$

where  $\beta$  is measured in radians.

Substituting  $R$  from (A.6) in (A.5):

$$E_R = E_S \left[ \frac{\sin(\beta/2)}{\beta/2} \right] \quad (\text{A.7})$$

How could  $E_S$  be understood?

From Eq. (A.7),  $E_S$  would be equal to  $E_R$  when

$$\left[ \frac{\sin(\beta/2)}{\beta/2} \right] = 1 \quad \text{or} \quad \sin(\beta/2) = \beta/2$$

It implies that  $\beta = 0, \pm\pi, \pm2\pi, \pm n\pi$

It means that there are not phase shifts among all phasors along the slit. The first solution that meets this condition is when

$$E_S = E_{R-MAXIMUM} = E_0 \quad (\text{A.8})$$

**Irradiance  $I_\theta$**  at the observation point P is proportional to  $E^2$ ; this is when:

$$I_R = I_0 \left[ \frac{\sin(\beta/2)}{\beta/2} \right]^2 \quad (\text{A.9})$$

### Expressions for the Electric Field and Irradiance

When definition for  $E_0$  from Eq. (A.8) is replaced in Eq. (A.7), the magnitude of the phasor observed at any point P is obtained.

However:

- $E_0$  is  $(1/R) \cdot E_{00}$ , where  $E_{00}$  is the magnitude of the electric field from the horizontal strip of width  $a$  in the slit.
- The phasor varies its amplitude harmonically; i.e. as

$$e^{i[\vec{k} \cdot \vec{r} - \omega t]} \quad ; \quad k = 2\pi / \lambda \quad (\text{A.10})$$

- So, the total expression for the **Electric Field** is

$$E_R = (1/R)E_{00} e^{i[\vec{k} \cdot \vec{R} - \omega t]} \left[ \frac{\sin(\beta/2)}{\beta/2} \right] \quad (\text{A.11})$$

where:

$$k = 2\pi/\lambda \quad \text{wavenumber} \quad (\text{A.12})$$

and

$$\beta = k \cdot a \cdot \sin\theta \quad (\text{A.13})$$

where:

*a* is the slit width

and

$\theta$  is the angle  $R$  makes with the perpendicular to the screen  
(See Fig. A.6)

- And the total expression for **Irradiance** is

$$I(\theta) = \varepsilon_0 \cdot c [E_R \cdot E_R^*] = \varepsilon_0 \cdot c \cdot [E_{00}/R]^2 \cdot [\sin(\beta/2)/(\beta/2)]^2 \quad (\text{A.14})$$

Recall that the characteristics of  $\left[ \frac{\sin(\beta/2)}{\beta/2} \right]$  and  $\left[ \frac{\sin(\beta/2)}{\beta/2} \right]^2$ ; functions that are named *sinc* $[\beta/2]$  and *sinc*<sup>2</sup> $[\beta/2]$ , respectively were explained in “**Interference for a linear array of many coherent sources**”.

See Chapter 1: Eqs. (B.30 to B.35) and Figs. B.15 to B-17.

## OPTIMIZATION OF OPTICAL SLIT WIDTH

In order to allow Light to enter – or leave – the closed “dark room” shown in Fig. A.1, a narrow **slit** is required. See Fig. A.2.

### Slit Width Importance

*In spite of its simplicity a slit is an essential component in optical instruments since it defines the amount of light that goes in – or goes out – the instrument.*

*Slits must be properly sized and properly placed in these instruments to observe the appropriate beam of interest, as example, to limit the main lobe.*



## Observations

From Chapter 1, Fig. B.16:

- The main lobe contains about the 90 % of Irradiance
- The Full Width at Half Maximum – FWHM for every lobe contains about the 80% of irradiation of that lobe
- Irradiance decreases abruptly in the main lobe from its FWHM to its minimum.

## Optimization Criterion

*Slit width must be sized to capture main lobe, or the lobe range of interest.*

## The Observation Point $P$ and the Main Irradiance Lobe

From Chapter 1, Fig. B.12 and Chapter 2 Fig. A.6

- The observation point  $P$  depends on the Deviation Angle  $\theta$ .
- For a monochromatic wavelength, there is a central maximum where the phase shift from wavelets coming from the slit is negligible only for small deviations from the observation point  $P$ . In other words, the **observing angle  $\theta$  must be small** and **copies maximum Irradiance**
- From Fig. A.6 and Eq. (A.4), the angle  $\beta/2$  is:

$$\beta/2 = (\pi \cdot a/\lambda) \cdot \sin(\theta) \quad (\text{A.15})$$

However,  **$\theta$  must be small**, so a good approximation for Eq. (A.15) is

$$\beta/2 = (\pi \cdot a/\lambda) \cdot \theta \quad (\text{A.16})$$

From Chapter 1: Eqs. B.35 and B.26:

- Half angle  $u_{1/2}$  for the main peak is ( $\approx 1.39$  [radians]). Note from Fig. A.7 that angle  $u_{1/2}$  is  $\beta/2$ . When replacing these **Angular width at half maxima for the first lobe** in Eq. (A.16), **one half of the  $\theta$  angle  $\theta_{1/2}$  is calculated**; this is:

$$1.39 \approx \frac{\pi \cdot a}{\lambda} \cdot \theta_{1/2} \quad \text{or} \quad \theta_{1/2} \approx 0.442 (\lambda/a) \quad (\text{A.17})$$

Now, the total angle  $\theta$  is

$$\theta = 2 \cdot \theta_{1/2} = 0.884 (\lambda/a) \approx (\lambda/a) \quad (\text{A.18})$$

**This is an important conclusion:**

*For a monochromatic wavelength:*

*The width of the diffraction peak varies inversely with the width of the slit.*

Fig. A.8 illustrates this idea.

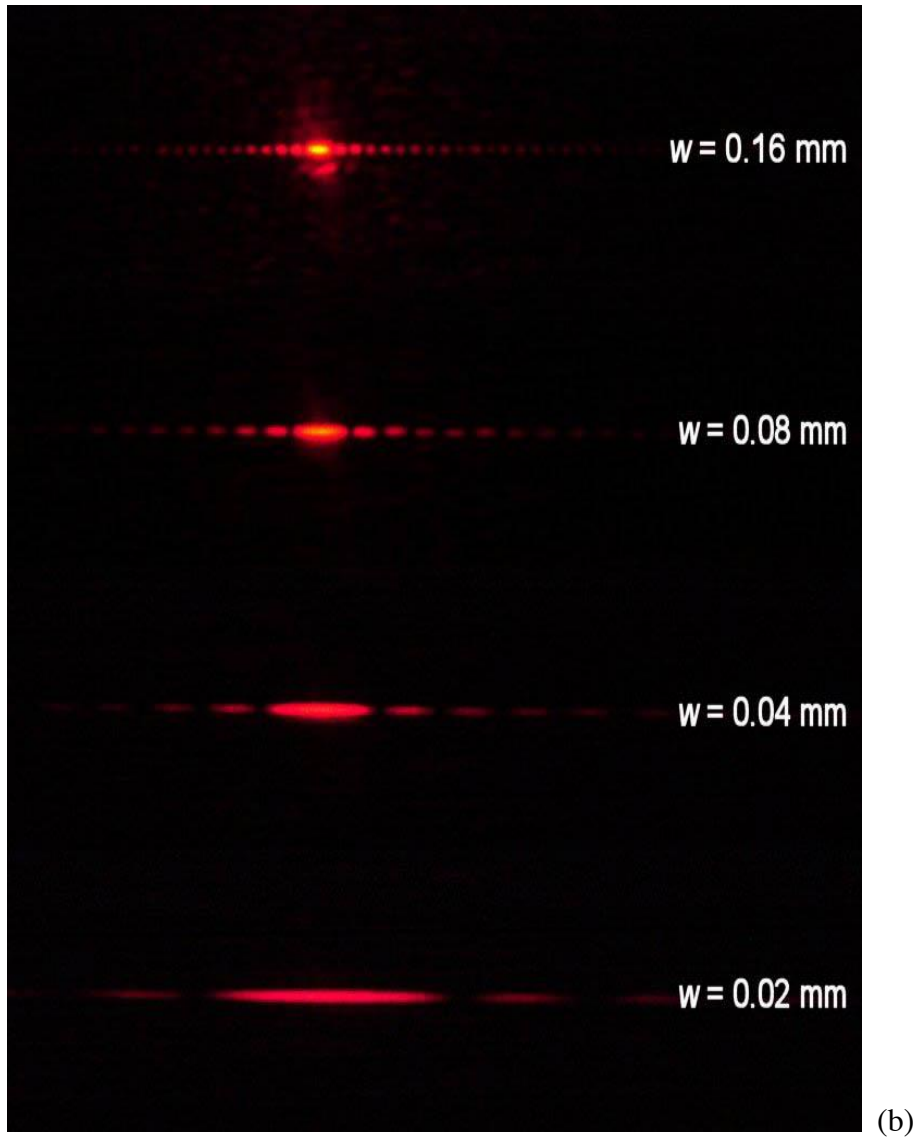
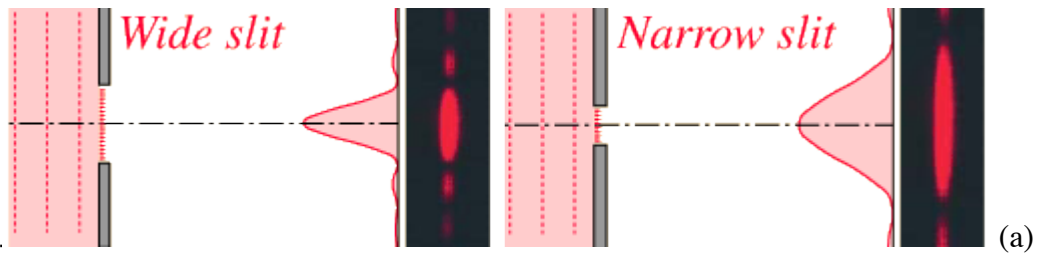


**Figure A.8:** *The width of the diffraction peak varies inversely with the slit width. [Figure adapted from reference shown in ANNEX F]*

**Comment:**

This is related with the Scaling Property of Fourier Transforms:

$$f(at) \leftrightarrow \frac{1}{|a|} F\left(\frac{\omega}{a}\right)$$

See **Chp. 2 ANNEX 1: A digression on Fourier transforms**. One realizes that light intensity distribution of a monochromatic beam passing through a slit is also obtained using Fourier transforms.

### Optimum Slit Width

The process to optimize the slit width is described:

- 1) Geometry of the array is described by Fig. A.6.
- 2) Eq. (A.19) defines the relation among parameters for a narrow slit. It is important to realize that this is a “phase relation” or “angular relation”:

$$\beta = \frac{2\pi}{\lambda} \cdot a \cdot \sin\theta \quad [\text{radians}] \quad (\text{A.19})$$

where:

$\beta$  phase at observation point  $P$  due to the a monochromatic source slit passing through a slit placed at the origin of coordinates [radians]

$a$  slit width [m]

$\lambda$  monochromatic wavelength [m]

$\theta$  Observation angle in the “far field” taking as vertex the midpoint in the slit. The starting side of Angle  $\theta$  is the perpendicular line to the slit from its centre to the parallel plane to the slit that contains the Observation Point  $P$ . [radians] See (Fig. A.6)

Note:  $k = 2\pi / \lambda = \text{wave number}$  [1/m]

Its dimension is reciprocal to the slit width  $a$

- 3) We are interested to observe only the main lobe for a monochromatic wavelength. So, Angle  $\theta$  deviates at most up to the first minima of the  $\text{sinc}(\beta/2)$  function. See Eq. (A.7) and Fig. B.16 in Chapter 1.
- 4) The first minima for  $\text{sinc}(\beta/2)$  correspond to  $\beta = \pm \pi$  so the main lobe of interest is encompassed by the angle  $\beta_{TOTAL} = 2\pi$ .
- 5) Suppose that the slit width  $a$  is any “reasonable” initial value; say 0.5 [mm].

From Eq. (A.19) calculate the correspondent angle  $\theta$  for two monochromatic wavelengths that are the extreme wavelengths for the

**Visible Range Spectrometer:**  $400 < \lambda < 700$  [nm]

defined in **Table A.1**. These values are:

$$\begin{aligned}
\text{For } \lambda_{\text{MAX}} = 700 \text{ [nm]} & \quad \rightarrow \quad \theta_{\text{MAX}} = 1.4\text{E-}3 \text{ [radians]} \\
\text{For } \lambda_{\text{MIN}} = 400 \text{ [nm]} & \quad \rightarrow \quad \theta_{\text{MIN}} = 0.8\text{E-}3 \text{ [radians]} \quad (\text{A.20})
\end{aligned}$$

These first results conduce us to the following conclusion:

**Conclusion:**

*$\lambda_{\text{MAX}}$  copes an angle  $\theta_{\text{MAX}}$  ;*

*$\lambda_{\text{MIN}}$  copes an angle  $\theta_{\text{MIN}}$  ;*

*$\theta_{\text{MAX}} > \theta_{\text{MIN}}$*

*In other words:*

*For any wavelength range, the wavelength  $\lambda_{\text{MAX}}$  defines the slit width  $a$ . The Observation Angle  $\theta_{\text{MAX}}$  copes the whole band  $\lambda_{\text{MIN}} < \lambda < \lambda_{\text{MAX}}$ .*

- 6) Since Eq. (A.4) is an “angular equation” it is necessary to obtain an expression that makes an equation in which “length magnitudes” are involved. Now, let’s imagine that the “angular spot” from the slit is going to be observed on a plane screen perpendicular to the beam at a distance  $X$  as in Fig. A.9. Then, the displacement  $\Delta Y$  is related with the Observation Angle  $\theta$  by Eq. (A.21):

$$\text{tg} \left( \frac{\theta}{2} \right) = \frac{(\Delta y/2)}{X} \quad (\text{A.21})$$

where:

$\theta$  is the deviation angle, in [radians].  $\theta_{\text{MAX}}$  or  $\theta_{\text{MIN}}$  are obtained for  $\beta = 2\pi$  the angle between the two minima for the first lobe in  $\text{sinc}(\beta/2)$ .

$X$  is the distance between slit position and observation plane [m]

Note that Eq. (A.4) and Eq. (A.6) conform a system of Equations.

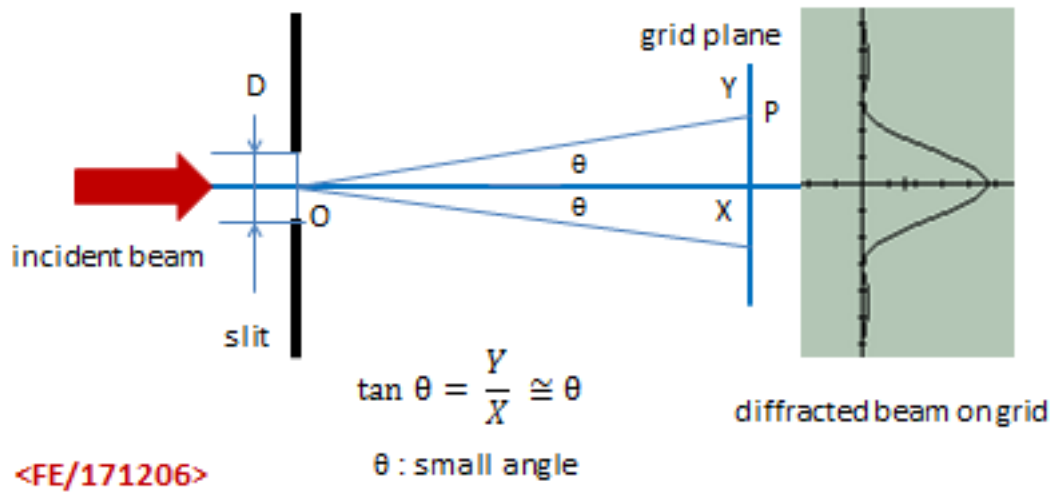


Figure A.9  
Span displacement  $\Delta y$  at distance  $X$  for the Observation Angle  $\theta$

- 7) Choosing an appropriate length  $X$  for the prototype, say 30 cm, the wavelength, as example  $\lambda_{MAX}$ , and  $\beta_{TOTAL} = 2\pi$ , then the slit width  $a$  is calculated.
- 8) Simple routines have been implemented to solve the system of Eq. (A.4) and Eq. (A.6) for the wavelength sub-ranges defined in Table A.1.
- 9) Table A.2 shows the slit widths and related parameters for the **ranges of wavelengths for the proposed instruments**. See Table 4.

### Optimization criterion

From this point it is possible to optimize the slit width. The procedure is shown through an example:

Optimization Example:

Which is the slit width  $a$  for a near IR instrument in order to have a span  $\Delta Y_{MAX}$  of two millimetres using the Common Parameters from Table A.2

The critical parameter to define the slit width in a range of wavelengths is  $\lambda_{MAX}$ . Let's consider two wavelengths 3000 and 2600 [nm].

From Eq. (A.6):

$$X = 0.30 \text{ [m]} \text{ and } \Delta Y_{MAX} = 2000 \text{ [\mu m]}; \text{ so, } \theta_{MAX} = 6.666\text{E-}3 \text{ [radians]}.$$

From Eq. (A.4),

$$\text{for } \lambda_{MAX} = 3000 \text{ [nm]}, \text{ a} = 0.450 \text{ [mm]}$$

$$\text{for } \lambda_{MAX} = 2600 \text{ [nm]}, \text{ a} = 0.390 \text{ [mm]}$$

**Table A.2: Slit Widths for three selected ranges of Wavelengths**

<b>Common Parameters</b>							
Slit – Central Observation Point Distance <b>X</b>				0.30 [m]			
Total Phase Angle $\beta_{TOTAL}$				$2\pi$ [radians]			
<b>Wavelength Range</b>	$\lambda_{MAX}$ [nm]	$\lambda_{MIN}$ [nm]	$\theta_{MAX}$ [radians] x1E-3	$\theta_{MIN}$ [radians] x1E-3	$\Delta Y_{MAX}$ [μm]	$\Delta Y_{MIN}$ [μm]	<b>Slit Width [mm]</b>
Visible	700	400	2.800	1.600	840	480	0.25
Near UV	460	300	1.840	1.200	552	360	
Near IR	3000 2600	650	1.200 1.040	2.600	3600 3120	780	
Near IR	3000 2600	650	6.000 5.200	1.300	1800 1560	390	0.50

**Conclusions:**

**A method to calculate and optimize the slit width for an optical instrument has been developed.**

**The calculated parameters:**

**distance X = 0.300 [m], distance**

**Span apertures  $\Delta Y_{MAX}$  in the order of 1 [mm]**

and Slit widths in the order of 0.5 [mm]  
are manageable parameters in order to develop a prototype of a simple instrument to measure wavelengths in the visible range.

#### 4. DIFFRACTION GRIDS

##### PHYSICS OF DIFFRACTION GRIDS

A **diffraction grid** is a ruled surface at small distances equally spaced.

Fig. A.10 is a microscopic photograph of a grid.

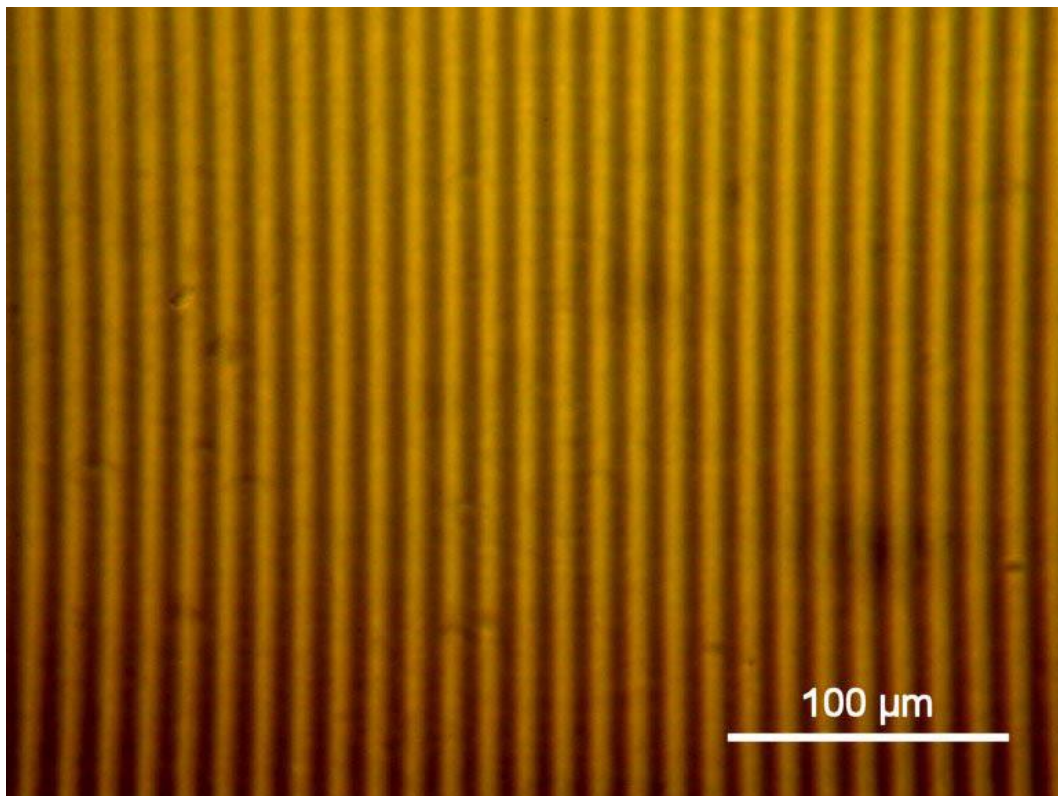


**Figure A.10:** *Microphotography of a diffraction grid.*  
*[Figure adapted from reference shown in ANNEX F]*

The most common diffraction grids for optical applications are shown in the first part of Table A.3. The second part of this Table gives information of the lines/mm in the spiral curve in CDs and DVDs

**Table A.3: Diffraction Grids for Optical Applications**

Grating	lines/mm	grating separation ( $d$ )* [nm]
Lab grade diffraction gratings	150	6667
	300	3333
	600	1667
	900	1111
	1000	1000
	1200	833
	1800	556
CD**	625	1600
DVD**	1350	741

\* Note: **Example:** If there are, by, 150 [lines/mm] then the distance between two lines is  $(1/150)[\text{mm}] = 6.667\text{E-}3$  [mm]. To convert this value to nanometres it should be multiplied by a factor of  $1\text{E}6$ ; then distance between two lines is 6667 [nm]. Calculation is identical for the other grids.

\*\*Note: Distance between two lines in a CD and a DVD are comparable with those Lab grade diffraction grids, so they are useful for diffraction purposes and very easily obtained. The interline distances  $d_{\text{CD}} = 1600$  [nm] corresponds to the IR region and  $d_{\text{DVD}} = 741$  [nm] corresponds also to the IR very close to the visible red band. See Chp 1 Figs A.4 and A.5.

Now, let's compare the grating separation ( $d$ ) with two wavelengths taken from the extremes in the visible range: Violet 450 [nm] and Red 700 [nm]. Table A.4.

**Table A.4: Diffraction Grids for Optical Applications compared with  $\lambda_V$  and  $\lambda_R$**

Grating	grating separation ( $d$ ) [nm]	$\lambda$ Violet $d[\text{nm}] / 450$ [nm]	$\lambda$ Red $d[\text{nm}] / 700$ [nm]
Lab grade diffraction gratings	6667	14.815	9.524
	3333	7.407	4.761
	1667	3.704	2.381
	1111	2.469	1.587
	1000	2.222	1.429
	833	1.851	1.190
	556	1.236	0.794*
CD	1600	3.556	2.286
DVD	741	1.647	1.059



Observations:

- Grating separation is bigger and comparable with the visible wavelengths with one exception\*
- No one of the quotients in columns 3 and 4 matches exactly with wavelengths

Comment:

In order to describe diffraction grids let's take as reference a diffraction grid made with a CD.

## Geometry for the transmissive grid

### Experimental Observation

If a pointer red laser ( $\lambda = 650$  [nm]) perpendicularly crosses a transparent grid made of a piece of CD ( $d = 1600$  [nm]), several symmetric red dots are diffracted on a screen placed on the opposite side. The dots appear in a perpendicular direction of the ruled lines of the grid. See Fig. A.11



**Figure A.11:** A 650 nm red laser crossing a grid with  $d = 1600$  nm produces several symmetric dots on an opposite screen. The central mode corresponds to  $m=0$ . Lateral points correspond to orders  $m1 = \pm 1$  and  $m2 = \pm 2$ .  
[Figure adapted from reference shown in ANNEX F]

Geometry for the transmissive grid of this array is shown in Fig. A.12

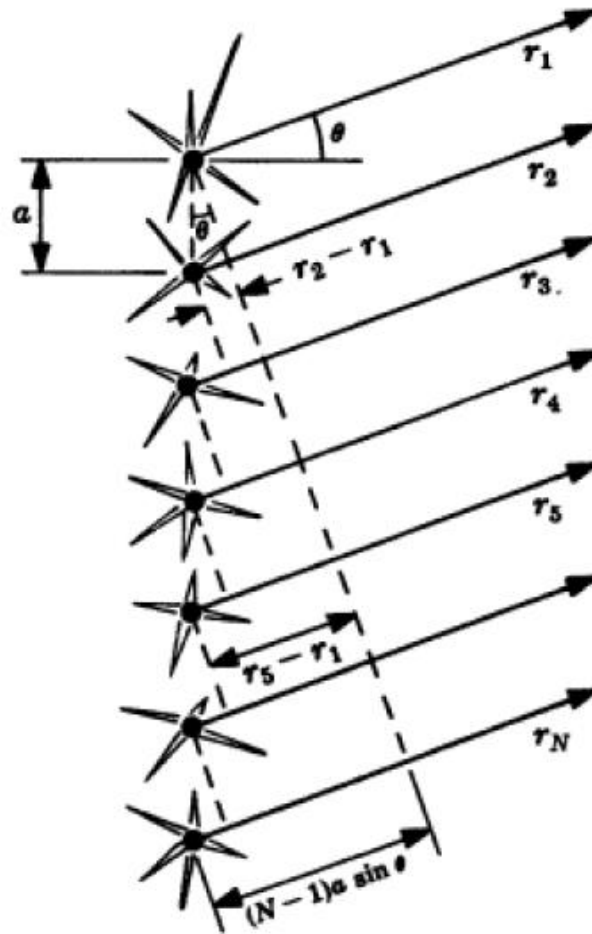


**Figure A.12:** Angle  $\theta$  is the angle of diffraction for a beam crossing a grid. At the observation point P, in the far field, all rays make a maximum for angle  $\theta = \theta_m$

this means that they are in phase to interfere constructively in direction  $\theta_m$ . In other words the path-difference among them must be an integer number of wavelengths.

As example, the path difference between the first and last coherent sources is  $(N-1).a.\sin \theta$

Diffraction plane is aligned with the incident beam coming from left side and perpendicular to the grid.

[Figure adapted from reference shown in ANNEX F]

## DESIGN CONSIDERATIONS FOR DIFFRACTION GRIDS

### DESIGN EQUATIONS

Equation (A.22) or **grating relationship** and its variant Eq. (A.23) are the grid basic equations to develop simple instruments to measure wavelength.

$$d \sin \theta_m = m\lambda \tag{A.22}$$

where: The diffracted light will have maxima at angles  $\theta_m$

- $d$  is the grating separation [m]
- $\lambda$  is the monochromatic wavelength [m]
- $m$  is the order of the diffracted beam ( $m = 1, 2, 3, \dots$ );  
 $m = 1$  corresponds to the maximum closer to the axis of symmetry
- $\theta_m$  is the angle that the maximum <sub>$m$</sub>  makes with the axis of symmetry [radians]

Its variant is a useful expression since it defines the feasible number of modes when a monochromatic beam of wavelength  $\lambda$  impinges on the grid:

$$\theta_m = \arcsin\left(\frac{m\lambda}{d}\right) \tag{A.23}$$

Comment: Since it is easier to visualize angles in Sexagesimal Degrees this units are used in this section.

For our example:

$$\theta_m = \arcsin\left(\frac{m\lambda}{d}\right)$$

$m = 1$	$\pm 23.97^\circ$
$m = 2$	$\pm 54.34^\circ$
$m = 3$	$\pm 69.84^\circ$
.....	.....

### Geometry for the reflective grid

#### Experimental Observation

If a pointer red laser ( $\lambda = 650$  [nm]) is oriented to a reflective diffraction grid making an elevation angle with the grid of about  $30^\circ$ , the reflected beam presents modes similar to those in Fig. A.13.

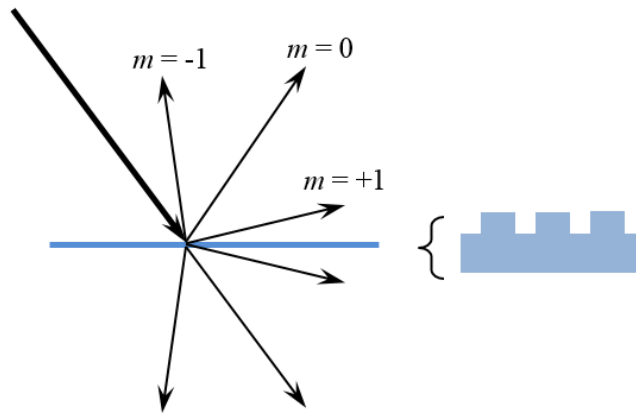


**Figure A.13:** A 650 nm red laser reflected on a grid with  $d = 1600$  nm also produces several symmetric dots on an opposite screen.  
 [Figure adapted from reference shown in ANNEX F]

### Experimental Observation

If a polychromatic points to a grid it is decomposed in its spectrum. The shortest wavelengths are closer to the diffraction plane for the possible modes. This occurs for a reflective or transmissive grid. Fig. A.14

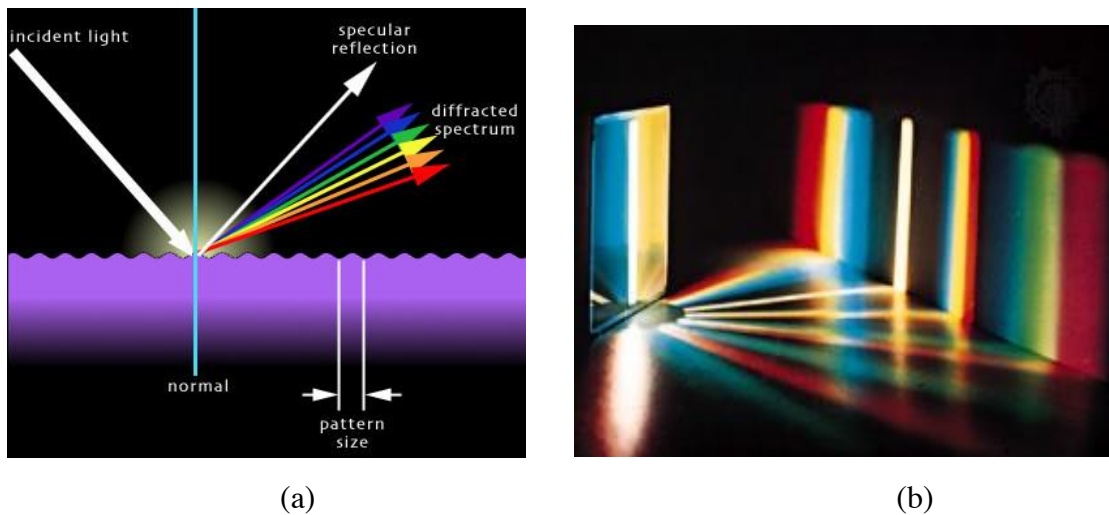


**Figure A.14:** A polychromatic beam is decomposed in its spectrum. The smaller wavelength are closer to the diffraction plane for every mode.  
 (a) Reflective grid. (b) Transmissive grid.  
 [Figure adapted from reference shown in ANNEX F]

Geometry for reflective grid is shown in Fig. A.15.

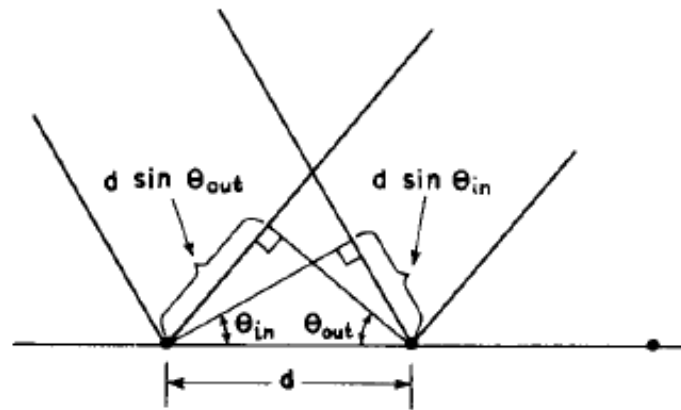


**Figure A.15:** The path difference for rays scattered from adjacent rulings of a grating is:  $d \cdot \sin \theta_{OUT} = d \cdot \sin \theta_{IN}$ .  
 [Figure adapted from reference shown in ANNEX F]

In order to have a  $\theta_m$  maximum for a wavelength  $\lambda$  the sum of the path differences for rays arriving to two neighbour rules at a distance  $d$  should be an integer nonzero  $m$  number of wavelengths.

$$d (\sin \theta_i + \sin \theta_m) = m\lambda \quad (\text{A.24})$$

When solved for the diffracted angle maxima, the equation is:

$$\theta_m = \arcsin \left( \frac{m\lambda}{d} - \sin \theta_i \right) \quad (\text{A.25})$$

### Diffraction Power

Resolving power of the grating is its capability to distinguish two wavelengths that are very close to each other. **Rayleigh criterion** is used: **Maximum of one pattern should sit on minimum of the other.** If so, which is the difference in wavelength between two distinguishable wavelengths?

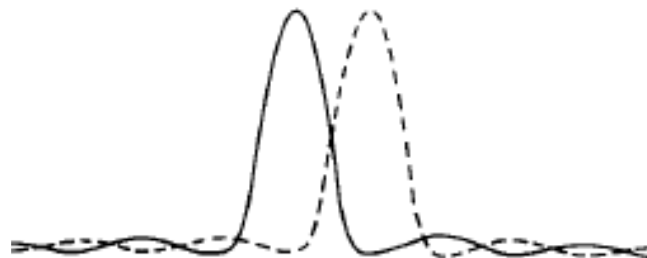


**Figure A.16:** Illustration of the Rayleigh criterion.  
 The maximum of one pattern falls on the first minimum of the other.  
 [Figure adapted from reference shown in ANNEX F]

In order to have a **maximum** for  $\lambda'$ , the distance  $\Delta$  must be  $n\lambda'$  (Fig. A.16); or, if the order is  $m$ , must be  $n(m\lambda')$ .

Now, for the neighbour wavelength  $\lambda$ , we want to have a **minimum** for the same angle.

With the array in Fig. A-17, the diffraction power is deduced.

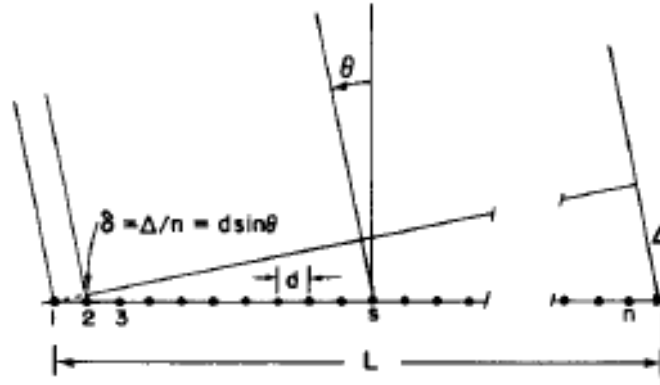


**Figure A.17:** A linear array of an equal oscillators, driven with phases  $\alpha_s = s.\alpha$  [Figure adapted from reference shown in ANNEX F]

In Fig. A.17, grid is represented as a horizontal set of dots. It has a length  $L$ . The distance between 2 lines in the grid is  $d$ . The beam emerging from the grid makes an angle  $\theta$  with the perpendicular to the grid.

If the direction  $\theta$  corresponds to a maximum, the secondary emitters i.e., the emitter dots from the grid must be in phase. The route difference between the emitter 1 and emitter  $n$  is  $\Delta$ , where the line of reference from emitter 1 to the last ray is perpendicular to the rays so it also makes an angle  $\theta$  with the grid in vertex 1.

In this array, the geometric relations are:

$$\delta = \Delta/n$$

$$\sin\theta = \delta/d \Rightarrow \delta = d.\sin\theta$$

$$\sin\theta = \Delta/L = \Delta/nd$$

The Rayleigh criterion implies that if for the same direction  $\theta$  two neighbour wavelengths  $\lambda$  and  $\lambda'$  are going to be distinguishable they should differ in one wavelength, i.e.:

$$\lambda' = (n + 1)\lambda$$

For a maximum direction  $\theta_M$  for  $\lambda'$ :  $\Delta = n(m\lambda')$  where  $m$  is the order. This means that:

$$\Delta = m\lambda' = n.\delta = n.d.\sin\theta$$

For a minimum direction  $\theta_m$  for  $\lambda$ , which is identical to  $\theta_M$  for  $\lambda'$ ,

$$\Delta = n(m\lambda) + \lambda = n(m\lambda')$$

If  $\lambda' = \lambda + d\lambda$  is replaced in the previous equation, it implies that

$$d\lambda/\lambda = 1/n.m \tag{A.26}$$

Ratio  $d\lambda/\lambda$  is called the **resolving power of a grating and it is equal to the reciprocal of the total number of lines in the grating times the order.**

This formula is equivalent to the formula that the error in frequency is equal to the reciprocal time difference between extreme paths that are allowed to interfere:

$$df = 1/T \tag{A.27}$$

In our case  $T = \Delta/c = n(m\lambda)/c$  where  $c$  is the speed of light. The frequency  $f = c/\lambda$ , so, its derivative is  $df = c.d\lambda/\lambda^2$

Comment:  $n(m\lambda) = \lambda$  corresponds to the number of lines in the grid that are in fact interacting with the light beam.

A detailed information on Diffraction Gratings is found in [2], [3].

**Calculation of Transmitted Diffraction Parameters for the Visible Range Spectrometer**

**Diffraction parameters** for the **visible range spectrometer** are calculated in detail. Since the procedure is the same for the other instruments can be easily implemented it is omitted here.

From Table A.1, the **spectral range** for this spectrometer is defined as:

$$400 < \lambda < 700 \text{ [nm]} \tag{A.28}$$

Diffraction parameters calculation for the wavelengths  $\lambda_{max} = 700 \text{ [nm]}$  and  $\lambda_{min} = 400 \text{ [nm]}$  in this range follow.

**Diffraction grid** selected for this Spectrometer is a piece of transparent CD.

**Incident beam** to be measured is oriented **perpendicularly to the grid.**

Since a **horizontal diffraction** is required, then the **grid lines** must be **vertically oriented.**

From Table 3, the **number of lines** for a CD are **625 lines / mm**, so the distance  $d_{CD}$  between two neighbour lines is  $d_{CD} = 1600 \text{ [nm]}$ .

- For  $\lambda_{max} = 700 \text{ [nm]}$  and  $d_{CD} = 1600 \text{ [nm]}$  at once, the maximum angles  $\theta_m$  for the feasible modes  $m$  are obtained from Eq. (A.23)

For:

$$m = 1 \quad \theta_m = 25.94^\circ$$

$$m = 2 \quad \theta_m = 61.04^\circ$$

.....

- For  $\lambda_{min} = 400$  [nm] and  $d_{CD} = 1600$  [nm] at once, the maximum angles  $\theta_m$  for the feasible modes  $m$  are obtained from Eq. (A.23)

For:

$m = 1$	$\theta_m = 14.48^\circ$
$m = 2$	$\theta_m = 30.00^\circ$
$m = 3$	$\theta_m = 48.59^\circ$
$m = 4$	$\theta_m = 90.00^\circ$ (Not practical angle)
.....	.....

Fig. A.18 summarizes these results.

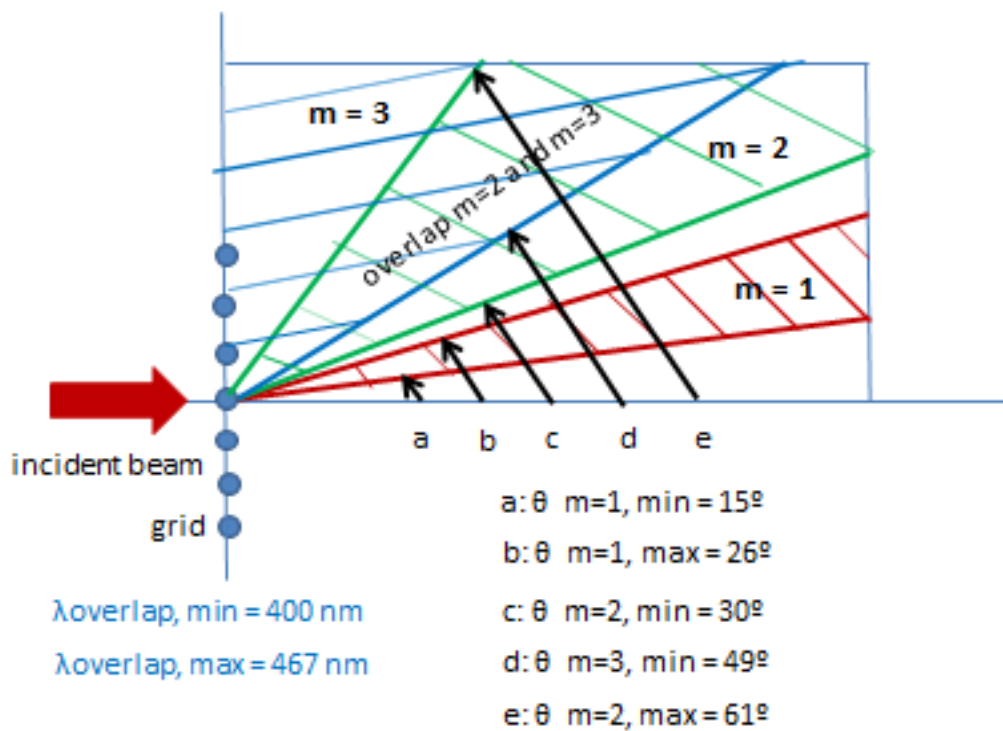


**Figure A.18:** Span of the angle of diffraction vs mode  $m$  for this example. Mode  $m=1$  does not overlap with mode  $m=2$ . Mode  $m=2$  overlaps with mode  $m=3$ .



## Conclusions

From these results we conclude:

- For  $m = 1$  the total angle  $\theta_{SPAN}$  in which the spectrum is diffracted is

$$\theta_{SPAN} = 25.94^\circ - 14.48^\circ = 11.46^\circ$$

- The smallest wavelength is closer to the plane of symmetry ( $14.48$ ) and the bigger one makes a bigger angle ( $25.94^\circ$ ).
- For  $m = 2$  total angle  $\theta_{SPAN}$  in which spectrum is diffracted is

$$\theta_{SPAN} = 61.04^\circ - 30.00^\circ = 31.04^\circ$$

- Again, the smallest wavelength is closer to the plane of symmetry ( $30.00^\circ$ ) and the bigger one makes a bigger angle ( $61.04^\circ$ ).
- There are not more options to diffract completely the incident beam with the above defined bandwidth with this diffraction slit.
- Though  $\theta_{SPAN}$  for  $m = 2$  is almost 3 times wider than  $\theta_{SPAN}$  for  $m = 1$ , There is a partial overlap with the spectral  $\theta_{SPAN}$  for  $m = 3$ . This overlap starts at  $\theta_m = 48.59^\circ$  for  $\lambda_{min} = 400$  [nm] and above as wavelength increases. The corresponding wavelength for  $m = 3$  and  $\theta_m = 61.04^\circ$  is  $\lambda_{max-overlap} = 466.64$  [nm] in the blue-green band.
- So the situation is a compromising one: For  $m = 1$  there is not overlapping but resolution is about 1/3 than for  $m = 2$ . On the other hand, for  $m = 2$  resolution is better, however a partial overlapping for the band corresponding to  $m = 3$  occurs. This overlap starts with  $\lambda_{min}$  for  $m = 3$  at  $\theta_m = 48.59^\circ$  and continues with increasing wavelengths. Finally  $\lambda_{max}$  for  $m = 2$  is overlapped with  $\lambda_{max-overlap} = 466.64$  [nm] in the blue-green band.

All these preliminary conclusions are useful to optimize the spectrometer design.

### Length L-span to collect the Diffracted Beam

As defined in Eq. 72; for design purposes, for every instrument to be designed, a constant Lspan = 2 cm has been selected.

$$Lspan = 20 \text{ [mm]} \quad (\text{A.29})$$

Fig. A.19 shows the geometry of the incident beam, the grid,  $Lspan$  and the distance R from the middle of the grid to the screen where the diffracted beam is collected.

Screen is perpendicular to the line from the middle of the grid to the screen.

Screen is placed making an angle  $\theta_{mean}$  for the mode  $m$ :

$$\theta_{mean} = (1/2)(\theta_{max} + \theta_{min}) \quad (A.30)$$

$$tg(\theta_{mean}) = (1/2)(L_{SPAN}/R)$$

i.e.:  $R = (1/2)(L_{SPAN}/tg(\theta_{MEAN} - \theta_{min})) \quad (A.31)$

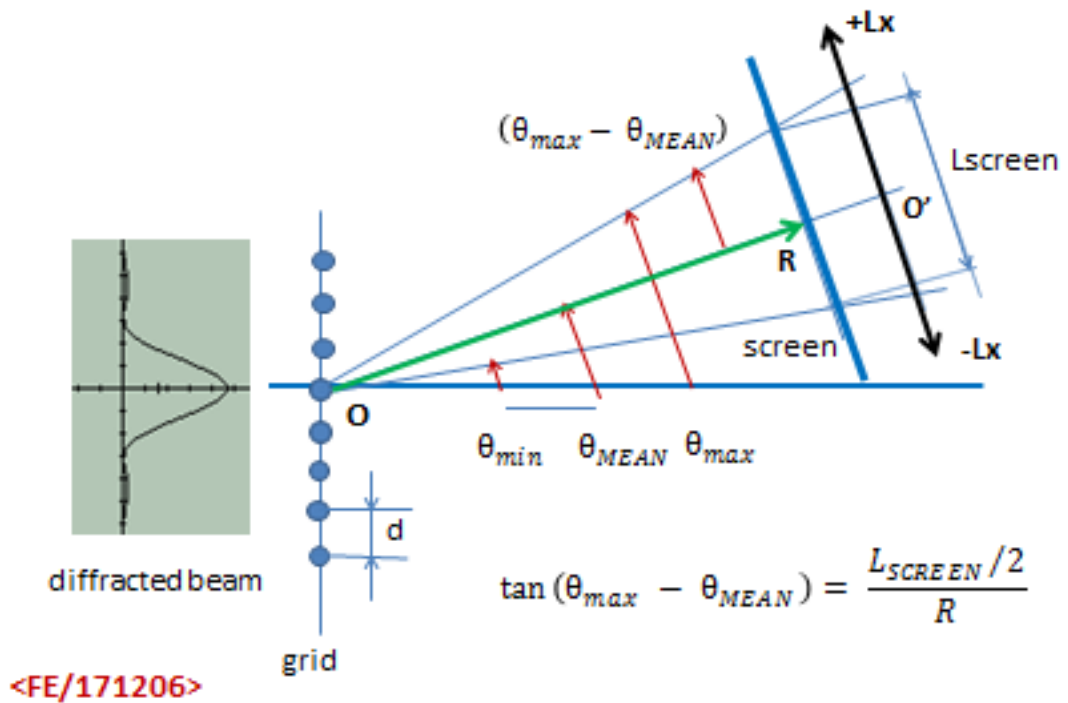


**Figure A.19:** Geometry showing the useful size of a screen with distance from the grid and the optimal angle that makes the grid with the screen

### Angle between the grid and the screen

*Conclusion: If instead of a screen in front of the slit, a grid is placed; diffracted beams of order  $m_1$  and  $m_2$ , etc. will appear on the other side of the grid with angles previously calculated.*

From Fig. A.19 it is also straightforward to conclude that **the angle that makes the grid with the collecting screen is  $\theta_{MEAN}$ .**

*Conclusion: The calculated parameters are for a span of 2cm. This allows place a focused camera to implement a Spectrometer or a slot to implement a monochromator.*

As example, for  $L_{SPAN} = 20$  [mm]

$$\text{For } m=1 \quad \theta_{mean} = 20.21^\circ \quad \theta_{min} = 14.48 \quad R = 99.66 \text{ [mm]}$$

$$\text{For } m=2 \quad \theta_{mean} = 45.52^\circ \quad \theta_{min} = 30.00 \quad R = 36.01 \text{ [mm]}$$

### Resolution Power or (Angular Dispersion)

From Eq. (53), renaming  $d = a$  to avoid confusion with the derivative,

$$a \sin \theta = m \lambda$$

Taking the derivative

$$d(a \sin \theta) = d(m \lambda)$$

$$a \cdot \cos \theta \cdot d\theta = m \cdot d\lambda$$

$$\text{then,} \quad D = d\theta/d\lambda = m/a \cdot \cos \theta \quad [\text{radians/nm}] \quad (\text{A.32})$$

where:  $D$  is the dispersive power.

In our example  $d = a$  the dispersive power  $D$  is:

$$\text{For } m = 1 \text{ and } \theta_{min} = 14.48^\circ \quad D = 645.50 \quad [\text{Radians / mm}]$$

$$\text{For } m = 1 \text{ and } \theta_{max} = 25.94^\circ \quad D = 695.02 \quad [\text{Radians / mm}]$$

$$\text{For } m = 2 \text{ and } \theta_{min} = 30.00^\circ \quad D = 1443.38 \quad [\text{Radians / mm}]$$

$$\text{For } m = 2 \text{ and } \theta_{max} = 61.04^\circ \quad D = 2581.58 \quad [\text{Radians / mm}]$$

## Conclusions

- The **angular dispersion** or **dispersive power**  $D$  is measured in [Radians / unit of Length]. Common units of length to express  $D$  are: [cm] or [mm]. It is referred to a monochromatic wave.
- The name **angular dispersion** Seems to be more appropriate.
- **Angular dispersion**  $D$  increases with the angle  $\theta$  and with the mode  $m$ .

## Minimal distinguishable wavelengths

From Eq. (A.26) here repeated:

$$d\lambda/\lambda = 1/n.m \quad (\text{A.26})$$

### Reflection:

First of all,  $d\lambda/\lambda$  is a dimensionless number. On the other hand  $n$  is the number of lines and  $m$  is the order. And the product  $n.m$  is the extension of the grid. It implicitly involves a magnitude of length. One should think that the length of the grid is not “any length” since the number would be arbitrary. It may mean either “the number of lines in a unit of length”, as example 1 mm; or “the number of lines that effectively are illuminated by the incident beam” though, this is a “vague” definition. **Both approaches coincide if the beam illuminates 1 mm on the grid.** This is more objective and standardized since this is the usual way the grid is defined.

So, for 1 mm of perpendicularly incident beam, for a monochromatic wave length of 700 nm, for  $m = 1$ , strikes a span of 625 [lines/mm]. See Table 2.

**Note** that 625 [lines/mm] implies a distance of separation of 1600 [nm] between 2 lines. So for  $m = 1$ :  $d\lambda/\lambda = 1/1600$ .

Then, for  $\lambda = 700$  [nm];  $d\lambda = 700$  [nm]/1600  $\left[\frac{nm}{line}\right] = 0.44$  [line] = 704 [nm] since the distance between 2 lines is 1600 [nm].

### Comment:

This result is consistent with the idea that the grid should be able to exactly resolve one wavelength.

Now, what is the case for  $m = 1$  and  $\lambda = 400$  [nm]?

Answer: It is about the same. It is able to resolve 1 wavelength. The only difference is that the diffraction angle is different.

What is the case for  $m = 2$  and  $\lambda = 700$  [nm]?

Answer:  $d\lambda = \lambda/2$

And for  $m = 3$  and  $\lambda = 700$  [nm]?

Answer:  $d \lambda = \lambda/3$

And so forth for any mode  $m$  the resolution increases.

But, at the same time, Overlapping also increases and noise also increases. So, always there is a compromising situation.

### Summary of Parameters

The parameters so far obtained for Visible range spectrometer are summarized in Table A.5

**Table A.5: Summary of parameters for the Visible Range Spectrometer (Transmissive Diffraction Grid);  $400 < \lambda < 700$  [nm]**

Instrument	Spectrometer, Monochromator
Wavelength Range	$400 < \lambda < 700$ [nm]
Grid	CD
Number of lines / mm	665 [lines/mm]
Interline Distance	1600 [nm]
<u>Mode 1</u>	<u><math>m = 1</math></u>
$\theta_m$ maximum	25.94° (Red)
$\theta_m$ minimum	14.48° (Violet)
$\theta_{SPAN} = \Delta\theta$	11.46°
$\theta_{mean}$	20.21°
Overlapping with $m=2$	No
$L_{SPAN}$	20 [mm]
R	99.66 [mm]
Resolution	$1\lambda$ in the whole range
<u>Mode 2</u>	<u><math>m = 2</math></u>
$\theta_m$ maximum	61.04° (Red)
$\theta_m$ minimum	30.00° (Violet)
$\theta_{SPAN} = \Delta\theta$	31.04°
$\theta_{mean}$	45.52°
Overlapping with $m=3$	Yes
$\theta_{overlap}$ – minimum	48.59°
$\lambda_{overlap}$ – minimum	400 [nm]
$\lambda_{overlap}$ for $\theta_m$ maximum	466.64 [nm] (blue-green band)
$L_{SPAN}$	20 [mm]
R	36.01 [mm]
Resolution	$\lambda/2$ in the whole range

## CALCULATION OF REFLECTED DIFFRACTION PARAMETERS FOR THE SPECTROMETER IN THE VISIBLE RANGE

For a **Reflective Instrument**. Using the array shown in Geometry Fig.23 and routines for Eq. (55), Eq. (56). Following a similar procedure than the one used for the transmissive diffraction grid; **the reflective diffraction grid parameters have been calculated.**

### Incident and Emerging beam angles

After preliminary considerations, the angle of incidence of the beam to be diffracted has been defined in this way:

- **The input angle for IR is - 45°. The incident angle for VIS and UV is - 30° in the second quadrant. These input angles are fixed angles.**
- **The output angle spans in the first quadrant**

They are summarized in Table A.6.

**Table A.6: Summary of parameters for the Visible Range Spectrometer (Reflective Diffraction Grid) ;  $400 < \lambda < 700$  [nm]**

Instrument	Spectrometer, Monochromator
Wavelength Range	$400 < \lambda < 700$ [nm]
Grid	CD
Number of lines / mm	665 [lines/mm]
Interline Distance	1600 [nm]
<u>Mode 1</u>	<u>m = 1</u>
$\theta_{IN}$	- 30°
$\theta_m$ maximum	69.64° (Red)
$\theta_m$ minimum	48.59° (Violet)
$\theta_{SPAN} = \Delta\theta$	21.05°
$\theta_{mean}$	59.11°
Overlapping with m=2	No
$L_{SPAN}$	20 [mm]
R	53.85 [mm]
Resolution	$1\lambda$ in the whole range

Note: Only for Mode 1

## DIFFRACTION PARAMETERS FOR IR AND UV INSTRUMENTS

Following a similar procedure, the diffraction parameters for the UV and IR instruments have been calculated.

## TRANSMISSIVE GRID AND REFLECTIVE GRID INSTRUMENTS GEOMETRY

Fig. A.20.a shows the geometry for a transmissive grid geometry device. Fig. A.20.b is the geometry for a reflective grid device.

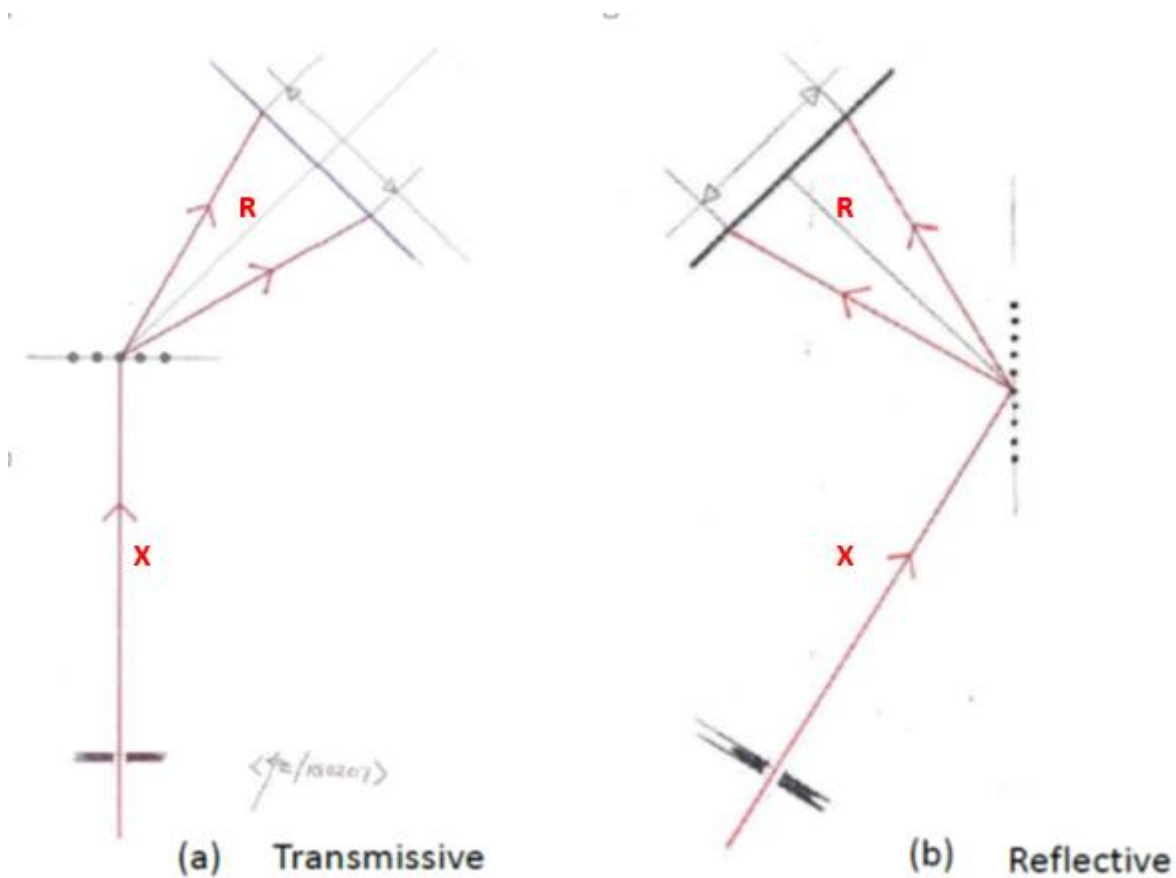


**Figure A.20:** Geometries for Transmissive and Reflective Spectrophotometers.

## 5. SIMPLE SPECTROMETER AND MONOCHROMATOR DESIGN PARAMETERS

Table A.1 shows the total range of interest for the present work and the Visible, Near Infrared and Near Ultraviolet subranges for which simple spectrophotometers have been designed.

**Table A.1: Ranges of Wavelengths for the Proposed Instruments**

---

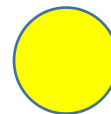
<b>Total Range of Interest</b>	<b><math>400 &lt; \lambda &lt; 2600</math> [nm]</b>
<b>Visible Range Spectrometer</b>	<b><math>400 &lt; \lambda &lt; 700</math> [nm]</b>
<b>Near Infrared Spectrometer</b>	<b><math>650 &lt; \lambda &lt; 2600</math> [nm]</b>
<b>Near UV Spectrometer</b>	<b><math>300 &lt; \lambda &lt; 460</math> [nm]</b>

---

Tables A.7, A.8 and A.9 show the design parameters for these three subranges. Visible and Infrared design parameters are defined for Transmission Type instruments. The Near UV spectrometer was designed as a Reflective Spectrometer.

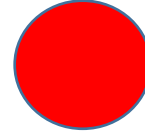


**Table A.7: Summary of parameters  
for the Visible Range Spectrometer  
(Transmission Type)**



Instrument	Spectrometer, Monochromator
Wavelength Range	$400 < \lambda < 700$ [nm]
Grid	CD
Number of lines / mm	665 [lines/mm]
Interline Distance	1600 [nm]
<u>Mode 1</u>	<u>m = 1</u>
$\theta_m$ maximum	25.94° (Red)
$\theta_m$ minimum	14.48° (Violet)
$\theta_{SPAN} = \Delta\theta$	11.46°
$\theta_{mean}$	20.21°
Overlapping with m=2	No
$L_{SPAN}$	20 [mm]
R	99.66 [mm]
Resolution	$1\lambda$ in the whole range
<u>Mode 2</u>	<u>m = 2</u>
$\theta_m$ maximum	61.04° (Red)
$\theta_m$ minimum	30.00° (Violet)
$\theta_{SPAN} = \Delta\theta$	31.04°
$\theta_{mean}$	45.52°
Overlapping with m=3	Yes
$\theta_{overlap}$ – minimum	48.59°
$\lambda_{overlap}$ – minimum	400 [nm]
$\lambda_{overlap}$ for $\theta_m$ maximum	466.64 [nm] (blue-green band)
$L_{SPAN}$	20 [mm]
R	36.01 [mm]
Resolution	$\lambda/2$ in the whole range

**Table A.8: Summary of parameters  
Near Infrared Range Spectrometer  
(Transmission Type)**



Instrument	Spectrometer, Monochromator
Wavelength Range	$650 < \lambda < 2600$ [nm]
Grid	Low cost plastic grid
Number of lines / mm	300 [lines/mm]
Interline Distance	3333 [nm]
<u>Mode 1</u>	<u><math>m = 1</math></u>
$\theta_m$ maximum	$51.27^\circ$ (Infrared, 2600 nm)
$\theta_m$ minimum	$11.25^\circ$ (Red Laser 650 nm)
$\theta_{SPAN} = \Delta\theta$	$40.02^\circ$
$\theta_{mean}$	$31.26^\circ$
Overlapping with $m=2$	No
$L_{SPAN}$	20 [mm]
R	99.66 [mm]
Resolution	$1\lambda$ in the whole range

Note: Only Mode 1

Note: A “calibration channel” is left for a  $\theta_m$  maximum corresponding to a red laser (650 nm). For this calculation a grid with 300 lines/mm is considered. A CD (665 lines/mm) a grid is not practical since the distance  $d = 1600$  [nm] is smaller than the maximum wavelength required (2600 nm).



**Table A.9: Parameters for the UV Range Spectrometer (CD) REFLECTIVE**

The following Table shows the parameters for a Spectrometer that has as reference a “channel” for a blue laser (460 nm) and displays the UV spectra up to 300 nm

Instrument	Spectrometer, Monochromator
Wavelength Range	$300 < \lambda < 460$ [nm]
Grid	CD
Number of lines / mm	665 [lines/mm]
Interline Distance	1600 [nm]
<u>Mode 1</u>	<u>m = 1</u>
$\theta_m$ maximum	51.95° (Blue Laser 460 nm)
$\theta_m$ minimum	43.43° (UV 300 nm)
$\theta_{SPAN} = \Delta\theta$	8.52°
$\theta_{mean}$	47.69°
Overlapping with m=2	No, 300 nm makes 61.04°
LSPAN	20 [mm]
R	134.25 [mm]
Resolution	$1\lambda$ in the whole range

\*Note: Calculations are only for Mode 1.

## 6. SIMPLE SPECTROPHOTOMETER AND MONOCHROMATOR DESIGN

As it has been described in this chapter, **wavelength information of a spectrum depends mainly on the geometry of the device**, i.e.: on the **entrance slit**, the **grid** and the **output slit geometry**. Then **spectrum is displayed on the screen plane** with a **span  $L_{SPAN}$** .

### Spectrophotometer

As example, a visible range spectrometer prototype was built using the calculated parameters from Table 7, standard PVC 32 mm pipes and accessories. Slits were made using thin metallic blades. Grids were implemented with grids slides for didactic instruction. A photography of this prototype is Fig. A.21.



Figure A.21

*Picture of the optical spectrometer prototype*

Visible Spectrum range is observable on a thin translucent screen at the output. It's more, it could be observed on a PC screen using a focused webcam matched to the output and its standard software.

Near Infrared spectrum is detectable using a modified webcam where the interior IR filter in its optical system has been removed [12], [13].

Near UV range is detectable using an UV LED as sensor. See Chp. 1, Section 2 and Section 3.

Visible, Near Infrared and Near Ultraviolet subranges for which simple spectrophotometers have been designed are calibrated and displayed using one application from Public Laboratory Org. ([www.publiclaboratory.org](http://www.publiclaboratory.org)) and one of their magnificent projects, **Spectral Workbench** ([www.spectralworkbench.org](http://www.spectralworkbench.org)). It is a free software for educational and community services purposes [14], [15], [16], [17].

Fig. A.22 is an example of Spectral Work Bench display for a user's spectra observable in a PC, Tablet, or Smartphone connected to internet and interfaced to the spectrometer prototype as explained.

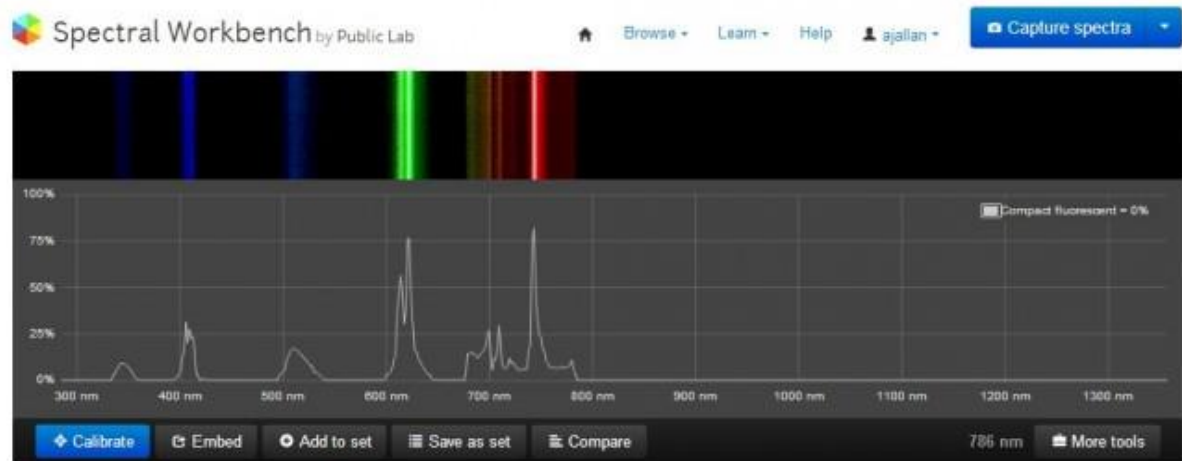


**Figure A.22:** *Spectral Work Bench display for a user's spectra.  
[Figure adapted from reference shown in ANNEX F]*

## Monochromator

A monochromator is a device able to select a narrow band of the whole spectrum displayed on the screen plane.

The sensor is a Si photodiode, a Ge photodiode or an UV LED reverse biased depending on the observed spectrum range.

The front end circuit is a photocurrent to voltage converter. See Chapter 2, Section D.4.

In order to detect a narrow wavelength band, a narrow slit is prepended to the sensor. To select a narrow band of the spectrum a mechanical linear displacement of the sensor along the screen plane must be provided. This mechanism could be controlled from a microcontroller through a stepper motor [18].

The algorithm to control detect and measure is deduced from Sections 4 and 5 in this chapter.

These topics are out of the scope of the present work.

## FINAL COMMENT

The subject related to simple spectrophotometer and monochromator prototypes concludes with this section.

In Chapter 4, new virtual instruments related with thermal radiation, temperature measurement and single solar cell's I-V curve response prototypes are exposed.

## B. USEFUL ELECTRONIC COMPONENTS

### 1 PN DIODES AS TEMPERATURE SENSORS

Signal silicon diodes or the base – collector junction of low power Si metallic case transistors are excellent sensors to measure temperature.

Temperature is a fundamental physical magnitude. In the International System of Physical Units [SI], the fundamental physical magnitudes are: length [m], time [s], mass [kg], temperature [K], electric current [A], luminous Intensity [Cd] and amount of substance [mole].

In a range from low temperatures up to  $\approx 500$  [K] – about  $250$  °C – it is possible to make an absolute measurement of temperature using a Si PN junction (a signal Si diode). Although Si melts at  $1414$  °C, it is not practical to measure temperatures higher than  $\approx 250$  °C due to the way the diode itself is assembled. However, a Si diode is an excellent sensor to measure temperature (room, environmental or cryogenic temperature ranges).

Since many instruments require a temperature correction for accurate measurements, in general, a PN junction thermometer is a useful laboratory tool.

The **Ebers – Moll equation** describes the Voltage – Current – Temperature for a PN junction. A complete expression for this equation is in Reference [4]:

$$I = I_o \left( e^{V/\eta V_\tau} - 1 \right) \quad (\text{B.1})$$

For Si:

$$I_o = k_2 T^m e^{-V_{GO}/2V_\tau} \quad (\text{B.2})$$

and, in general:

$$V_\tau = \bar{k}T/e^{(-)} \quad (\text{B.3})$$

Where:

$I_o$ : Reverse Saturation current, [A]

$V_\tau$ : Temperature equivalent Voltage, [V]

Definition of parameters follow:

$V$  Junction Voltage, [V]

$T$  temperature [K]

$e^{(-)}$  electron charge ;  $e^{(-)} = 1.60219 \times 10^{-19}$  [C]

$\bar{k}$  Boltzmann Constant ;  $\bar{k} = 1.381 \times 10^{-23}$  [J/K]

$V_{G0}$  Equivalent Voltage Energy Band Gap [V]

$k_2$  Material Constant, temperature independent [A/K]

For Silicon, the remaining parameters are:

$$V_{G0} = 1.21 \quad \eta = 2 \quad m = 1.5 \quad (\text{B.4})$$

A temperature sensor can be characterized using a direct biased signal Silicon diode. A constant current source in the order of  $10 \mu\text{A}$  through the diode characterizes it as a temperature sensor since, under this condition, from Evers Moll equation, it is deduced that the voltage drop through the junction depends basically on Temperature.

## 2. FIELD EFFECT TRANSISTORS – FETs

Field effect transistors or FETs are components with a conduction channel for electric current from two electrodes named **source** and **drain**; however these conduction is controlled by an electric field applied to a third electrode named as **gate**. Reference [5] is an excellent introduction to field effect transistors.

FETs are excellent candidates to be part of a circuit where control and high input impedance are required.

There are two polarities for FETs n-channel and p-channel.

FETs can be made with two different kinds of gates using junctions or isolators. So, there are **junction field effect transistors or JFETs** and **metal oxide semiconductor field effect transistors or MOSFETs**, also known as IGFETs (Insulated Gate FETs).

Finally, FETs conduction is controlled either by *depletion mode* or by *enhancement mode*. For more information consult [5] or any other appropriate reference.

In this project, N Channel Junction Bipolar Field Effect transistor or N-JFET is used as the main component in a Front End Circuit to obtain the Current – Voltage curve of a single solar cell. For that purpose, the N-JFET is characterized in its linear region. A summary of this component follows.

### N-JFET field effect transistor

As an example of FETS, the N – channel bipolar junction JFET transistor is explained in more detail. The N – JFET is the component with more similarities in its behaviour compared with the usual NPN bipolar transistor. This component will be applied in several stages in the instrumentation shown in this chapter so more attention is paid to this component.

Reference [6] is a practical experimental approach to n-JFETs.

Fig. B.1 shows a family of curves for the drain current  $I_D$  [mA] vs the drain – source voltage  $V_{DS}$  [V] for a set of constant values of the gate – source Voltage  $V_{GS}$  [V]. It is observed that the gate – source Voltage  $V_{GS}$  [V] exerts control on the drain current  $I_D$  [mA] when it goes negative and increases its magnitude.

Fig.B.2 shows  $I_D$  vs  $V_{DS}$  for  $V_{GS}$  constant for any FET transistor. It defines a border between the **linear region** and the **saturation region** modes of operation of a FET transistor. In

connection with Fig. B.2 also are introduced Eq. (B.5) and Eq. (B.6). These equations are known as the universal FET drain current formulas either for the linear region or the saturation region. See Reference [5].

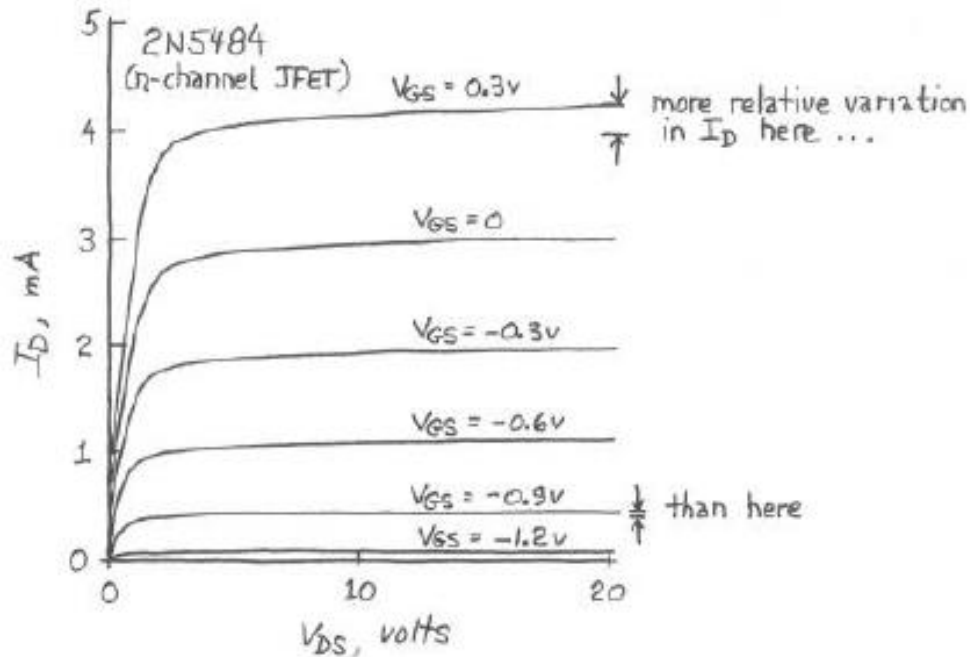


**Figure B.1:** Family of curves  $I_D$  vs  $V_{DS}$  for  $V_{GS}$  constant for 2N5484 JFET. When  $V_{GS}$  is more negative the current  $I_D$  decreases, so  $V_{GS}$  exerts control on  $I_D$ . Note also that  $V_{GS}$  reverse biased improves a current source. [Figure adapted from reference shown in ANNEX F]

$$I_D = 2k[(V_{GS} - V_T)V_{DS} - V_{DS}^2/2] \quad \text{(linear region)} \quad \text{(B.5.a)}$$

$$I_D = k(V_{GS} - V_T)^2 \quad \text{(saturation region)} \quad \text{(B.5.b)}$$

Where:

$k$  Constant to be defined experimentally [ $1 / \Omega \times V$ ]

$V_T$  “Threshold Voltage” or “Pinch off Voltage” [V] \*

The remaining parameters are defined in Fig. B.3.



## FETs as variable resistors

For  $V_{DS}$  close to the origin there is a region where the slope changes depends on  $V_{GS}$ . This operation region in the  $I_D$  vs  $V_{DS}$  family of curves is named **linear region since the FET behaves approximately as a variable resistor.** [7]

The behaviour of FETs as variable resistors is obtained from Eq. (B.5a). This expression is rewritten as Eq. (B.6).

$$\frac{I_D}{V_{DS}} = \frac{1}{R_{DS}} = 2K \left[ (V_{GS} - V_T) - \frac{V_{DS}}{2} \right] ; [1 / \Omega] \quad (B.6)$$

This equation describes the FET as a variable resistor controlled by the  $V_{GS}$  voltage when the FET is working in the linear region. The term  $(V_{DS} / 2)$  is the term that affects linearity. Depending of the control voltage  $V_{GS}$  the variable resistance takes values as close to zero ohms for Power MOSFETS or as high as mega ohms though the change is not strictly linear.

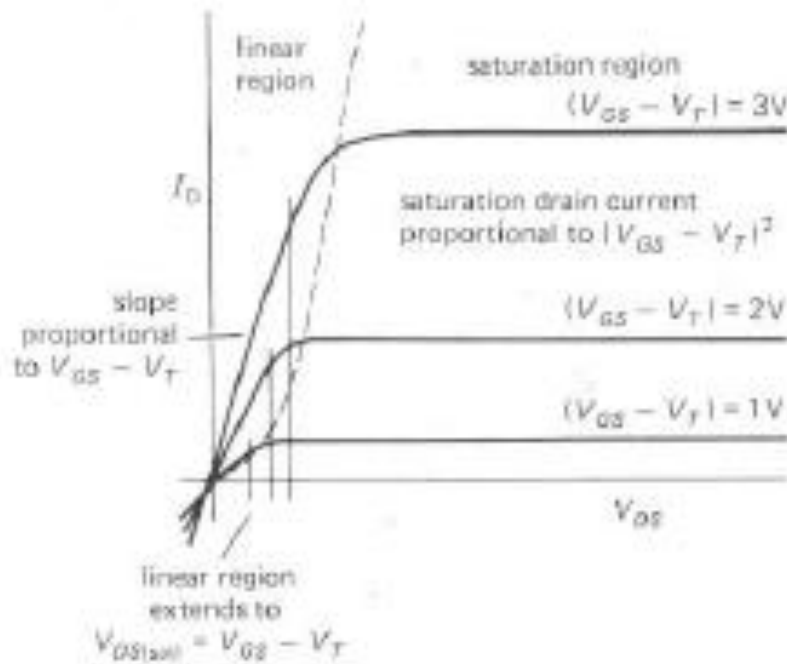


**Figure B.2:** FET transistor family of curves  $I_D$  vs  $V_{DS}$  for  $V_{GS}$  constant. Two operation regions are defined: The Linear Region for low  $V_{DS}$  voltages ( $\approx 1$  V) and the Saturation Region for  $V_{DS}$  higher. [Figure adapted from reference shown in ANNEX F]

$V_T$  and  $I_{DSS}$  two important parameters for FETs

Fig. B.3 shows the code, physical aspect, electronic symbol and the work regions for a N-Channel JFET field effect transistor.

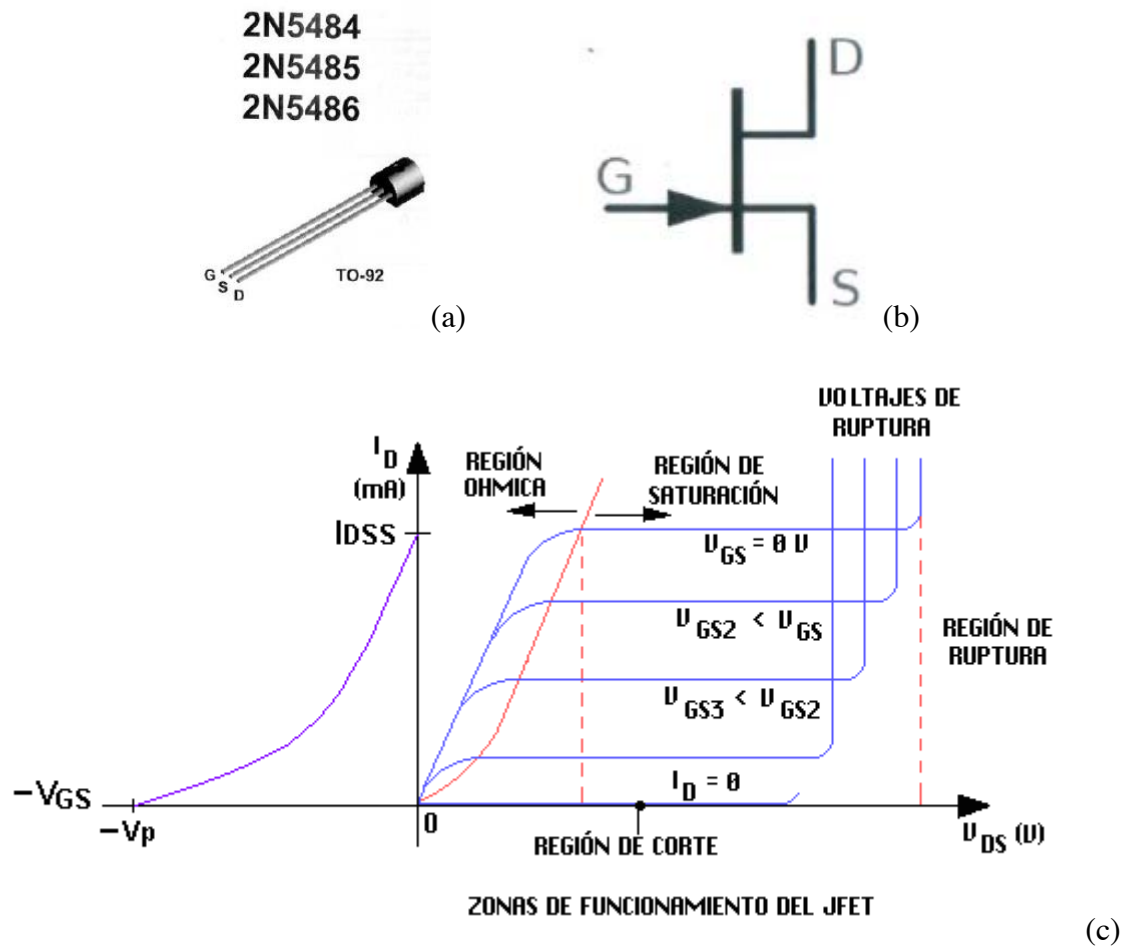


**Figure B.3:** *N-Ch JFET Field Effect Transistor (a) Physical aspect and code number (b) Electronic Symbol (c) Work Regions and main parameters  $I_{DSS}$  and  $V_P$ . [Figure adapted from reference shown in ANNEX F]*

**Important:** Note that

$I_{DSS}$  is the current value for  $V_{GS} = 0$

and

$V_P$  is  $V_{GS}$  for  $I_D = 0$

$I_{DSS}$  and  $V_P$  are two essential parameters for FET transistors and are unique for any FET.

**Note:**  $V_T$  and  $V_P$  are essentially the same parameter referred to JFETS or MOSFETS.

Since for many applications like to obtain the I – V Curve for a solar cell, it is necessary to measure  $I_{DSS}$  and  $V_P$  for the JFET used in the circuit for calibration purposes. Two simple methods to measure these parameters follow.

Fig. B.4 the circuit diagram to measure  $I_{DSS}$  followed (Method 1).

Fig. B.5 shows two alternative circuit diagram and procedure to measure  $V_T$ . (Method 2)

**Procedure Method 1**

- In a circuit as shown in Fig. 5 measure  $V_0$  and calculate  $I_{DSS}$ .

**Procedure Method 2**

- Start decrementing  $V_{GS}$  from 0 [V] to negative values.
- With a Voltmeter observe  $V_0$ . It will decrease since  $I_D$  decreases
- When  $V_0 = 0$  implies that  $I_D = 0$ .
- On this condition, measure  $V_{GS}$ . This particular value of  $V_{GS}$  is  $V_P$

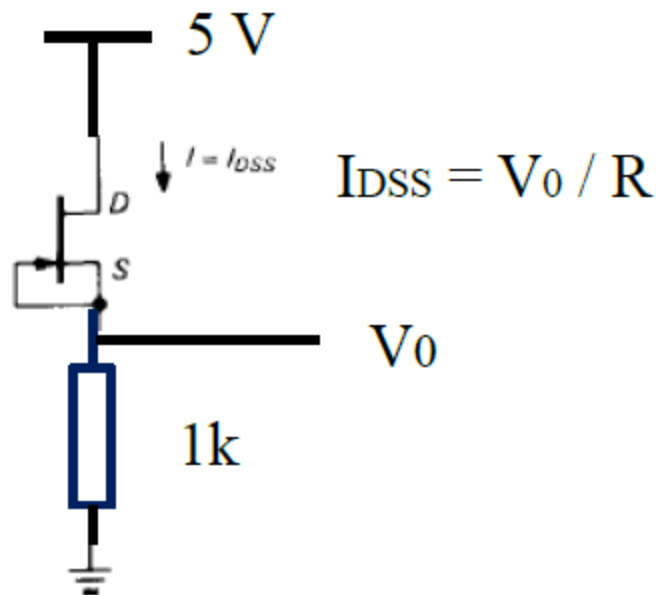


**Figure B.4:** Circuit diagram to measure  $I_{DSS}$ .

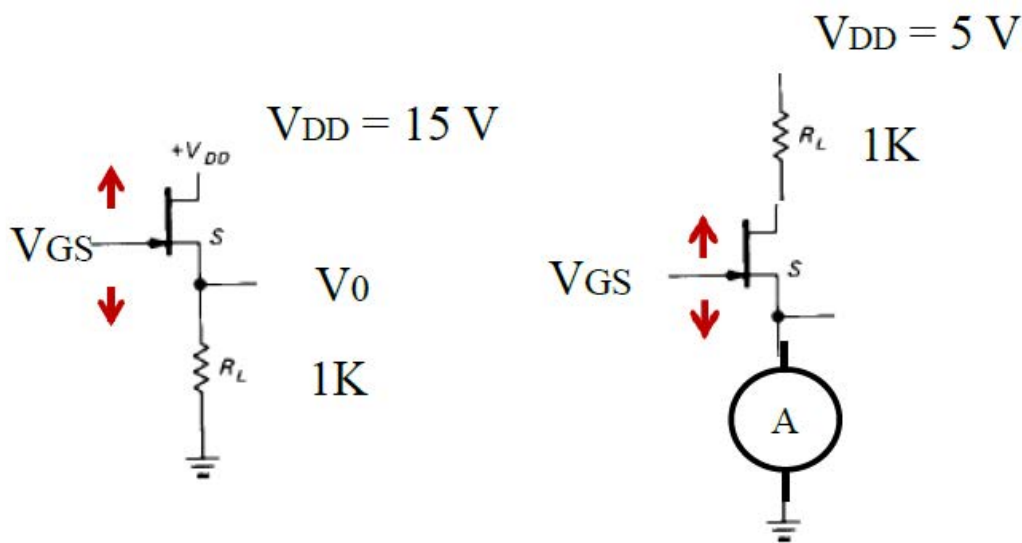


**Figure B.5:** *Alternative circuits to measure  $V_p$*

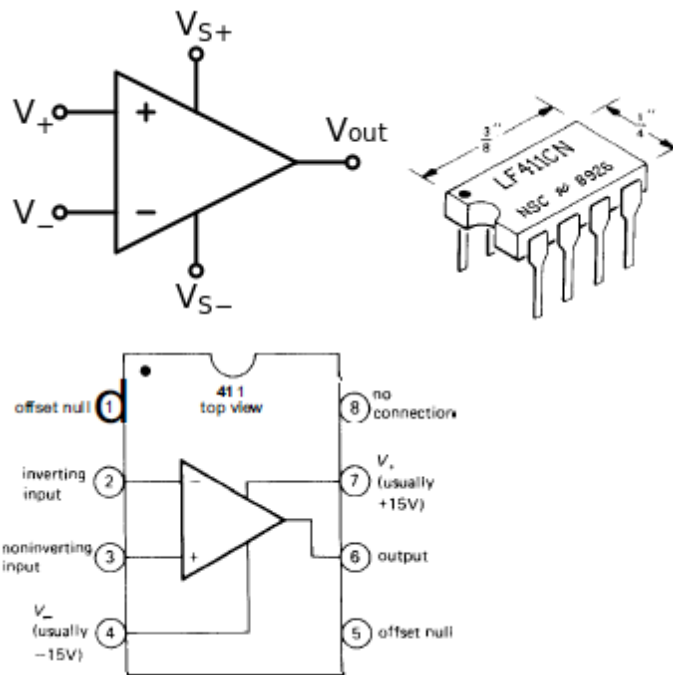
### 3. OPERATIONAL AMPLIFIERS – OPAMPS

An **operational amplifier** ("op-amp") is an integrated circuit able to amplify dc voltage signals about hundred thousand times the potential difference between its input terminals. When a feedback loop – as a conductor or a circuit – is connected from its output to its input, gain can be controlled and the output depends in a specific manner on: the input signal and the feedback loop circuit. [8]

Around an Op Amp circuits that process electric signals can be built independently and then, these stages can be interconnected to obtain a required response.

Op-amps are among the most widely used electronic devices today, being used in a vast array of consumer, industrial, and scientific devices. Many standard IC op-amps cost only a few cents in moderate production volume, though some specialized op amps may be more expensive. Op-amps may be packaged as components, or used as elements of more complex integrated circuits.

Fig. B.6 shows the symbol used for Op Amps, its physical aspect as a mini-DIP integrated circuit and the orientation to recognise the pin number and its function to use this integrated circuit.



a) Op Amp Symbol    b) Mini Dip Integrated Circuit    c) Top View showing pin distribution

**Figure B.6:** Symbol, physical image and pin distribution for an Op Amp.  
 [Figure adapted from reference shown in ANNEX F]

To have an idea of the versatility of Op Amps, References [4], [5], [6] and [7] are collections of circuits made with Op Amps where hundreds of applications are shown.

### FET Op Amps

FET Op Amps are a type of Op Amp that is made using JFET transistors as its (+) and (-) inputs. Due to the very high input impedance of JFET transistors, the Op Amp itself presents as characteristic an input impedance in the range of ( $\approx 10^{12} \Omega$ ) besides the general advantages of a general purpose Op Amps made with NPN transistors. Fig. B.7 shows the circuit schematic of a JFET Op Amp.

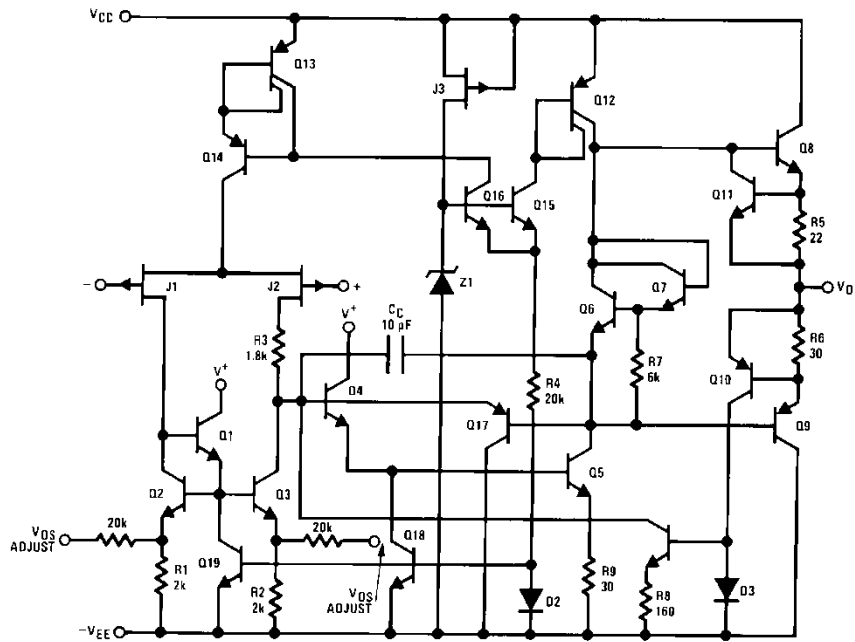


**Figure B.7:** JFET input Op Amp schematic. Its input impedance is in the order of  $10^{12} \Omega$ . Inputs (+) and (-) in this Op Amp are J1 and J2, they are JFET transistors. [Figure adapted from reference shown in ANNEX F]

Fig. B.8 is a simplified schematic of Fig. B.7

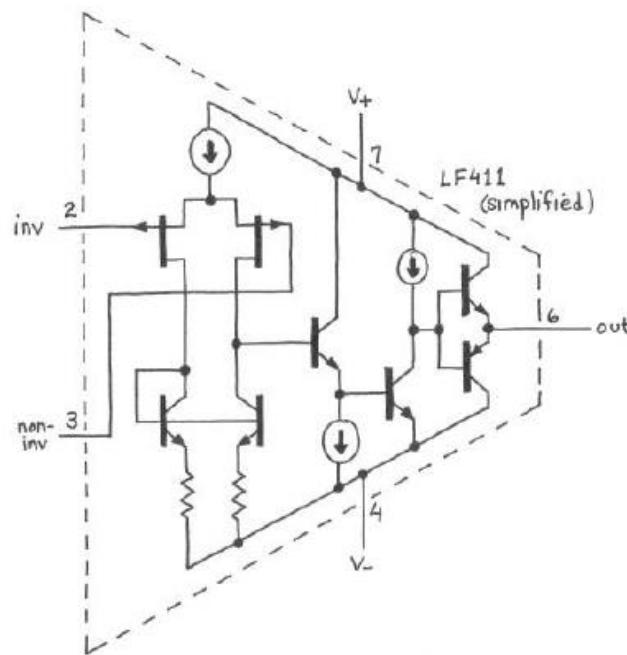


**Figure B.8:** Simplified diagram for a JFET input Op Amp. [Figure adapted from reference shown in ANNEX F]

Due to these characteristics JFET Op Amps are excellent candidates to detect very small currents like those produced in light transducers.

## C. COMMON LIGHT SENSORS

### 1. LIGHT EMITTING DIODES – LEDs

A **light-emitting diode (LED)** is a two-lead semiconductor light source. It is a p-n junction diode, which emits light when activated.<sup>[4]</sup> When a suitable voltage is applied to the leads, electrons are able to recombine with electron within the device, releasing energy in the form of photons. This effect is called electroluminescence, and the color of light (corresponding to the energy of the photon) is determined by the energy band gap of the semiconductor.

An LED is often an small area (less than 1 mm<sup>2</sup>) and integrated optical components may be used to shape its radiation pattern.<sup>[5]</sup> [9]

Fig. B.7 in Chapter 1 is a picture of several LEDs emitting light at different wavelengths.

However **LEDs are used also as light detectors**.

Fig. C.1 (a) shows a **reversed biased LED as a light detector** and Fig. C.1 (b) a **forward biased LED as a light source**.

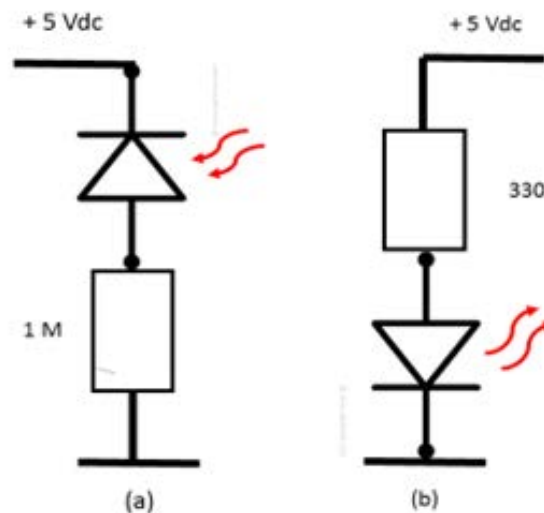


**Figure C.1:** (a) A Reverse Biased LED is a Light Detector  
(b) A Forward Biased LED is a Light Source.

## 2. SILICON PHOTODIODES

A **photodiode** is a semiconductor device that converts [light](#) into [electric current](#). The current is generated when photons are absorbed in the photodiode. A small amount of current is also produced when no light is present. Photodiodes may contain [optical filters](#), built-in lenses, and may have large or small surface areas. Photodiodes usually have a slower response time as their surface area increases. The common, traditional [solar cell](#) used to generate electric [solar power](#) is a large area photodiode.

Photodiodes are similar to regular [semiconductor diodes](#) except that they may be either exposed (to detect [vacuum UV](#) or [X-rays](#)) or packaged with a window or [optical fiber](#) connection to allow light to reach the sensitive part of the device. Many diodes designed for use specifically as a photodiode use a [PIN junction](#) rather than a [p-n junction](#), to increase the speed of response. A photodiode is designed to operate in [reverse bias](#).<sup>[1]</sup> [10]

Fig. C.2 shows typical photodiodes and its electric symbol.

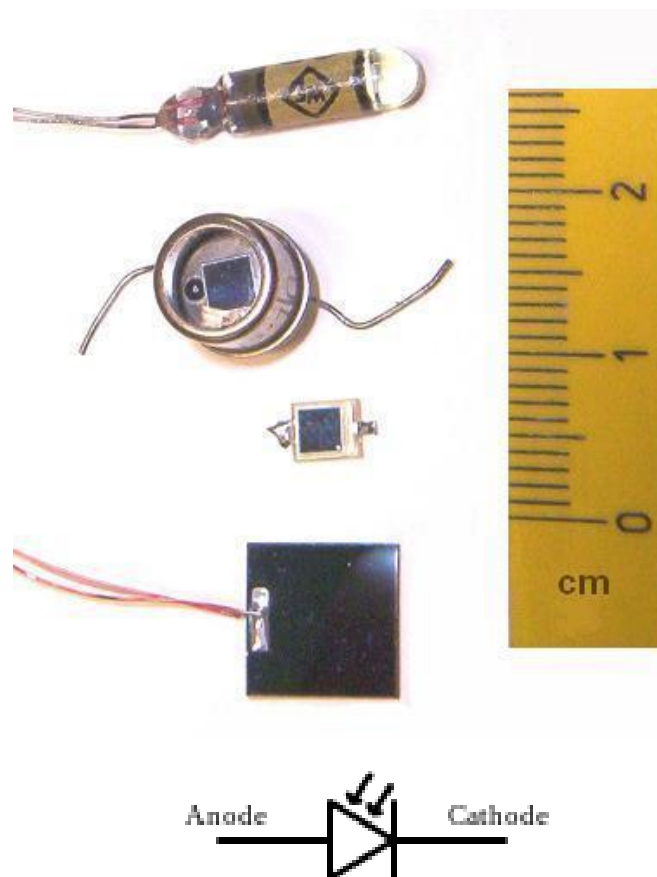


**Figure C.2:** Pictures of several photodiodes and its electronic symbol.  
[Figure adapted from reference shown in ANNEX F]



### 3. Si and Ge SIGNAL DIODES

Low power signal Si and Ge diodes glass encapsulated can also be used as light sensors when they are reverse biased. Fig. C.3 shows a picture of this diodes.

Si and Ge photodiode responsivities are shown in Chapter 1, Figs. C.4 to C.6.

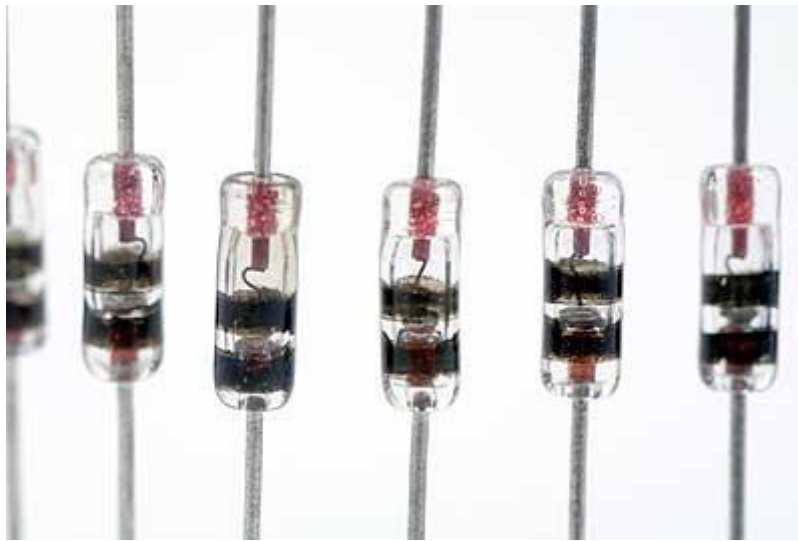


**Figure C.3:** *Low power Si or Ge signal diodes glass encapsulated can also be used as light sensor. [Figure adapted from reference shown in ANNEX F]*

## D. USEFUL ELECTRONIC STAGES FOR PHOTOVOLTAIC MEASUREMENTS

### 1. JFET CURRENT SOURCE

The current source with a N – channel JFET is shown in Fig. D.1 (a) a symbol for a current source is presented. Fig. D.1 (b) is a current source made with a JFET it needs no gate bias (it is a depletion mode) works reasonably for a  $V_{DS}$  greater than 2 volts. At higher voltages is more stable. The current provided by the source is the characteristic  $I_{DSS}$  current of a JFET, it depends on the transistor and has a magnitude from 1 mA to 5 mA. Fig. D.1 (c) is a variant that allows to decrease  $I_D$  from  $I_{DSS}$  to the “pinch off voltage” i.e., to fractions of  $\mu A$  or even lower.

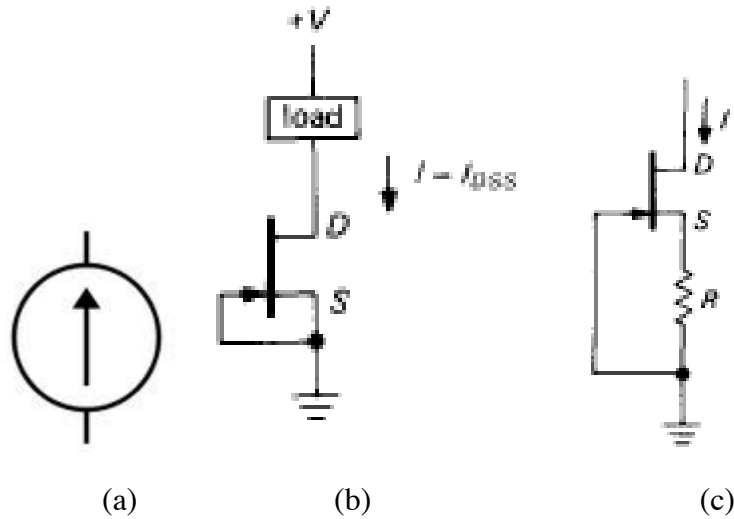


**Figure D.1:** *Current sources with a n-JFET*  
 (a) Current Source circuit symbol. (b)  $I_{DSS}$  current source.  
 (c) A self-biasing current source,  $I_D < I_{DSS}$ .  
 [Figure adapted from reference shown in ANNEX F]

## 2. VOLTAGE FOLLOWER

Fig. D.2 shows probably the simplest circuit using an Op Amp. It is useful to obtain an output to the same  $V_{in}$  with the advantage of not representing any load to the stage from where  $V_{in}$  is measured due to the negligible current required for the Op Amp at the input.

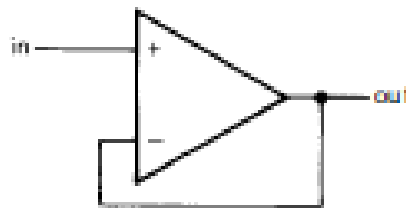
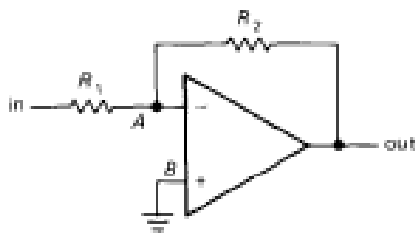


**Figure D.2:** *Voltage Follower.*  $V_{OUT} = V_{In}$   
 [Figure adapted from reference shown in ANNEX F]

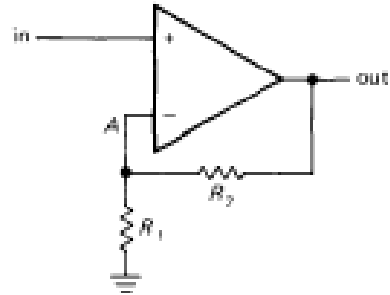
## 3. INVERTER AND NON INVERTER OPAMPs AMPLIFIERS

Fig. D.3 shows the basic configurations for amplifiers using Op Amps. There are Inverting and Noninverting amplifiers. An Inverter amplifier has its output with opposite polarity referred to its input. The gain of these amplifiers is defined by the values  $R_2$  and  $R_1$ .



voltage gain =  $V_{out}/V_{in} = -R_2/R_1$

(a)



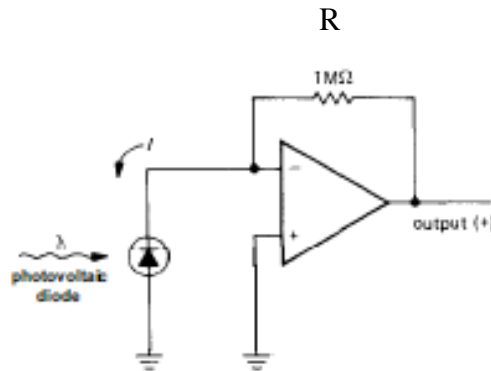
gain =  $V_{out}/V_{in} = 1 + R_2/R_1$

(b)

**Figure D.3:** Amplifiers using Op Amps: (a) Inverting and (b) Non Inverting. [Figure adapted from reference shown in ANNEX F]

#### 4. PHOTOCURRENT TO VOLTAGE CONVERTER

Fig. D.4 shows a useful circuit to convert current to voltage. The Op Amp (+) input and the photodiode – or the cell – cathode are connected to ground. The relation photocurrent  $I$  to the output voltage  $V_{OUT}$  is also shown.



$I = - V_{OUT} / R$

**Figure D.4:** Photocurrent to Voltage Converter using Op Amps. [Figure adapted from reference shown in ANNEX F]

This circuit constitutes an excellent **photocurrent ammeter** where small currents in the order of few Nano Amperes ( $1 \times 10^{-9}$  Amperes) are easily measured using FET OpAmps.

## E. FRONT END CIRCUITS

In this section front end circuits for the proposed instruments are described only from a viewpoint of their electronic components. The way each circuit behaves to measure the target – parameter is explained in Chapter 4 Section B where the algorithms for each instrument are described.

### 1. ENVIRONMENTAL THERMOMETER

A low power Si signal diode directly biased connected in series to a constant current source is the front end circuit to measure Temperature. Output signal is the voltage drop in the junction. See Fig. E.1

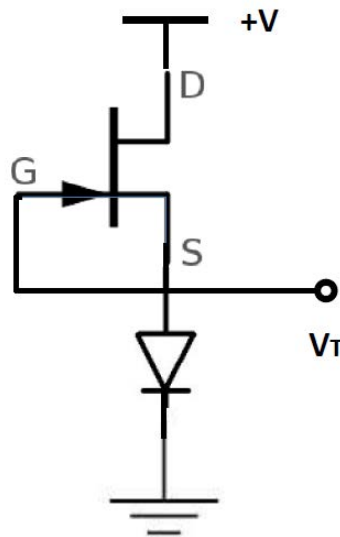


**Figure E.1:** *Thermometer front end circuit*

### 2. SIMPLE SPECTROPHOTOMETER AND MONOCHROMATOR

Spectrophotometers and monochromators have a photocurrent to voltage converter as the front end circuit. The key factor of these instruments is its wavelength resolution and depends mainly on the geometry of the instrument, the sensor's active area or mechanical or electromechanical accessories to displace the sensor facing the scattered beam or vice versa. For the circuit diagram refer to Fig. D.4. For detector's spectral response refer to Chapter 1 Section C.2 and C.3.

### 3. PYROMETER (SPECTRAL TEMPERATURE METER)

Front end sensor for a Pyrometer is a photocurrent to voltage converter. To measure Spectral Temperature of Planck's type sources two or more sensors are required. The key factor is that sensors have a narrow band responsivity. Colour LEDs, Infrared LEDs are good candidates for this application. See Fig. E.2

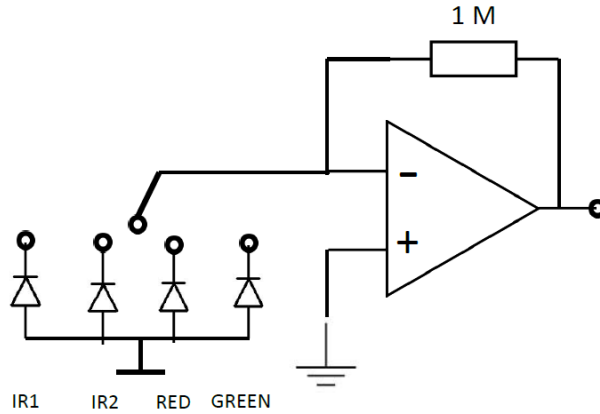


**Figure E.2:** *Pyrometer Front End Circuit.*

### 4. PYRANOMETER (IRRADIANCE METER)

Front end sensor for a Pyranometer, again is a photocurrent to voltage converter. To measure Irradiance, the key factor is the sensor responsivity. A broadband sensor responsivity is desirable. Si and Ge photodiodes are good candidates. Si photodiodes are preferable for the visible range. Ge photodiodes are better for the infrared range. See Fig. E.3.

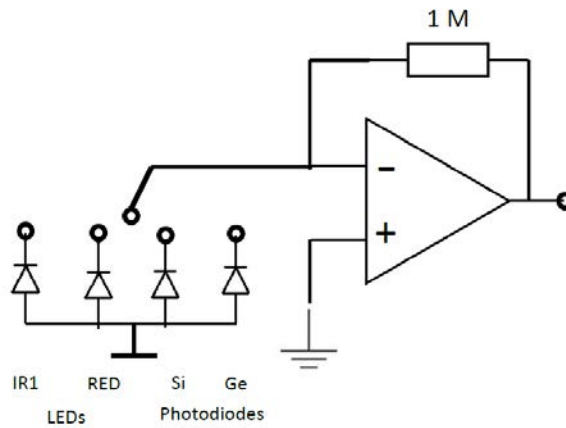


**Figure E.3:** *Pyranometer Front End Circuit.*

## 5. SOLAR CELL I – V CURVE GENERATOR

The sensor for this circuit is the tested solar cell itself. The front end circuit is the tested solar cell biasing a JFET N-Ch transistor operating in its linear region. The Voltage – Current relationship to generate the curve is controlled by the negative Gate – Source Voltage. See Fig. E.4

To measure the cell's short circuit current – or maximum current  $I_{SC}$ , a photocurrent to voltage is used. The circuit diagram is Fig. D.4.

To measure the cell's open voltage  $V_{OC}$  an opamp voltage follower or a non-inverting amplifier with appropriate gain is used. See Fig. D.2 and Fig. D.3.

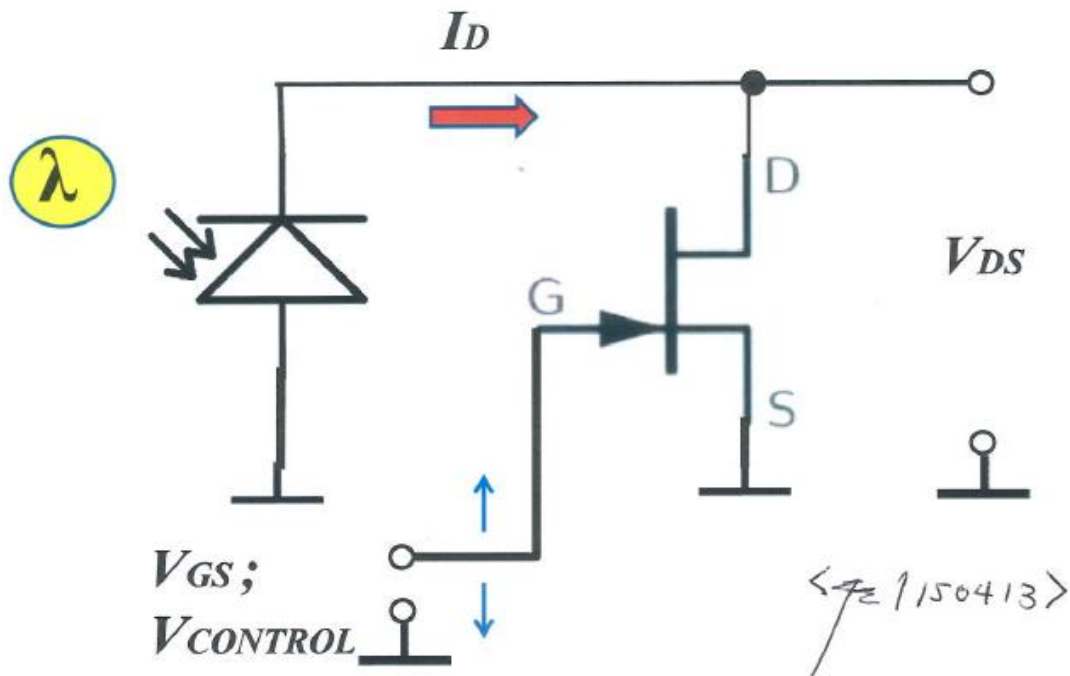


**Figure E.4:** Basic circuit diagram a solar cell connection with a JFET transistor showing.

## BIBLIOGRAPHY

- [1] KSHITIJ EDUCATION INDIA  
Diffraction from narrow slits  
<http://www.kshitij-iitjee.com/diffraction-from-narrow-slits>
- [2] THORLABS Diffraction Gratings  
<https://www.thorlabs.com/catalogpages/802.pdf>
- [3] PHYSICS PAGES Diffraction Gratings in Spectroscopy.  
<http://www.physicspages.com/2015/07/23/diffraction-gratings-in-spectroscopy/>
- [4] Millman J., Halkias C.: Electronic Devices and Circuits.  
Chp. 6: Semiconductor – Diode Characteristics. Seccs. 6.6, 6.6. 6.7.  
págs. 124 – 132. Mc. Graw Hill Inc. 1967
- [5] Paul Horowitz THE ART OF ELECTRONICS 2<sup>nd</sup>. Edition  
Winfield Hill Chapter 3: FIELD EFFECT TRANSISTORS  
Pgs. 113-174. Cambridge University Press 1990
- [6] Iku.edu.tr JFET Characteristics  
[http://web.iku.edu.tr/courses/ee/ee425/PDF/EE%20425\\_Exp\\_7.pdf](http://web.iku.edu.tr/courses/ee/ee425/PDF/EE%20425_Exp_7.pdf)
- [7] Idem [5] FET as Variable Resistors Chapter 3: FIELD EFFECT TRANSISTORS  
Pgs. 138-140.
- [8] Idem [5] FEEDBACK AND OPERATIONAL AMPLIFIERS  
Pgs. 175 - 251.
- [9] Wikipedia Word: LED  
[https://en.wikipedia.org/wiki/Light-emitting\\_diode](https://en.wikipedia.org/wiki/Light-emitting_diode)
- [10] Wikipedia Word: Photodiode  
<https://en.wikipedia.org/wiki/Photodiode>
- [11] Instructables.com Infrared (IR) Webcam  
<http://www.instructables.com/id/Infrared-IR-Webcam/?ALLSTEPS>
- [12] thenakedscientists.com Make an Infra-Red Camera  
<http://www.thenakedscientists.com/HTML/experiments/exp/make-an-infra-red-camera/>
- [13] Agilent G2721AA/G2733AA  
Spectrum Mill MS Proteomics Workbench  
[http://www.chem.agilent.com/Library/usermanuals/Public/G2721-90036\\_SpectrumMill\\_QuickStart.pdf](http://www.chem.agilent.com/Library/usermanuals/Public/G2721-90036_SpectrumMill_QuickStart.pdf)[15] Spectral Workbench calibration  
<http://publiclab.org/wiki/spectral-workbench-calibration>
- [14] Spectral Workbench usage <http://publiclab.org/wiki/spectral-workbench-usage>

- [15] Setup for UV Testing with Spectrometer  
<http://publiclab.org/notes/show/1833>
- [16] Escuela Politécnica Nacional – EPN Quito – Ecuador  
Tesis de Grado en Ingeniería Electrónica  
Título: DISEÑO Y CONSTRUCCION DE UN SISTEMA  
PARA LA GENERTACIÓN Y CONTROL  
DE MICROGIROS EN UN MOTOR DE PASOS  
Graduando: Mario Oswaldo Loza Vega  
Proponente y Director de Tesis: Fernando Echeverría Troya  
Fecha: Octubre 1997

## **Basic References**

- [1] **Frank Crawford**  
**Ondas**  
**Berkeley Physics Course Vol. 3.**  
**Editorial Reverté 1994 Barcelona.**
- [2] **Okan K. Ersoy**  
**Diffraction, Fourier Optics and Imaging**  
**John Wiley & Sons 2007**
- [3] **Paul Horowitz**  
**Winfield Hill**  
**THE ART OF ELECTRONICS 2<sup>nd</sup>. Edition**  
**Cambridge University Press 1990**



---

*CHAPTER 3*

*DATA ACQUISITION*

*AND CONTROL*

*USING*

*MICROCONTROLLERS*

*AND ANDROID DEVICES*

---



## OUTLINE OF THE CHAPTER

### A) PRELIMINARY TOPICS

1. MEASUREMENT
2. VIRTUAL INSTRUMENTATION
3. PHYSICAL PHENOMENA AND ANALOG FRONT END CIRCUITS
4. MICROCONTROLLERS
5. ANDROID DEVICES
6. ANDROID OPEN ACCESSORIES
7. PROGRAMMABLE AND GRAPHIC CALCULATOR EMULATORS

### B) IOIO OTG CHARACTERIZATION AND INTERFACING

1. IOIO OTG: DESCRIPTION
2. IOIO OTG: CHARACTERIZATION
3. IOIO OTG: INTERFACING

### C) ANDROID STUDIO AND IOIO OTG: PROGRAMMING ANDROID DEVICES AS MEASURING INSTRUMENTS

1. ANDROID STUDIO
2. INSIDE ANDROID STUDIO
3. DEVELOPING IOIO OTG APPLICATIONS FOR ANDROID DEVICES OR PC
4. IOIOLib ANDROID PACKAGE
5. REQUIRED COMMANDS FOR THE PRESENT APPLICATION

### D) INTERFACING FRONT END CIRCUITS WITH THE MICROCONTROLLER

1. FRONT END CIRCUITS INPUTS AND OUTPUTS
2. SCHEMATIC DIAGRAMS
3. DATA STORAGE FOR EACH APPLICATION

### E) ANDROID ↔ WINDOWS DATA TRANSFER TRANSPARENCY

## Bibliography

## Basic References

Annexes Chapter 3 (Shown at the end of this work)

#### ANNEX 1:

DESCRIPTION OF ALGORITHM TO  
MEASURE A PHYSICAL MAGNITUDE

#### ANNEX 2:

ANDROID RELATED COMMAND SEQUENCES

#### ANNEX 3:

REQUIRED COMMANDS FOR THE PROJECT (CANONICAL FORM)



## **CHAPTER 3: DATA ACQUISITION AND CONTROL USING MICROCONTROLLERS AND ANDROID DEVICES**

This Chapter is a brief though necessary description of the microcontroller board (IOIO OTG), its interface with an Android device – smartphone or tablet – and related software. The connection of the front end circuits with the microcontroller board ends this chapter.

This chapter is divided in five sections:

### Section A:

Preliminary topics are presented: physical measurement, virtual instrumentation, physical phenomena and analog front end circuits, microcontrollers and Android devices – among others.

### Section B:

Deals about the microcontroller (IOIO OTG) used in this project. Its description, characterization and interfacing.

### Section C :

It is a brief introduction to Android Studio, the freeware official Android devices programmer established by Google. Android Studio supports the instructions to program the Android Device to control IOIO OTG. The required canonical instructions for the microcontroller for the present work are also provided.

### Section D:

The interconnections of the microcontroller board with front end circuits to detect the physical parameters in this work are shown in this section.

### Section E:

Briefly deals with an approach to solve the problem of transparency in data transfer between Android and Windows, the operative systems used in this project.



## A. PRELIMINARY TOPICS

### 1. MEASUREMENT

In general, a measuring instrument is a device – simple or complex – to evaluate the magnitude of a physical or physical – chemistry phenomenon expressed in the corresponding units of the Metric International System [SI].

The SI – units are standardized and the relationship among the whole set of physical or physical – chemistry units is determined by the **Equations of Theoretical Physics** and the **Universal Physical Constants**. So, the SI –Units is a powerful and consistent system of units.

All measuring instruments are subject to varying degrees of [instrument error](#) and [measurement uncertainty](#)

So, to measure any physical magnitude means an [experimental procedure](#) to find the relationship between the unknown or measured magnitude and the corresponding unit of measurement. Certainly a measure includes inherently the instrument error and the measurement uncertainty. [1]

During the measurement of a magnitude – that remains “constant” in principle – “fluctuations” are observed. These fluctuations can be handled using **statistical criterion**. [2]

**Chp. 3 ANNEX 1** is a description of the statistical criterion to measure a physical magnitude.

### 2. VIRTUAL INSTRUMENTATION

A **measuring instrument** is a device for measuring a [physical quantity](#). In [physical sciences](#), [quality assurance](#), and [engineering](#); [measurement](#) is the activity of obtaining and comparing [physical quantities](#) of real-world [objects](#) and [events](#). Established standard objects and events are used as [units](#), and the process of measurement gives a number relating the item under study and the referenced unit of measurement. Measuring instruments, and formal [test methods](#) which define the instrument's use, are the means by which these relations of numbers are obtained.

In Science and Engineering and many other human activities a vast range of instruments is used to perform [measurements](#). These instruments may range from simple objects such as [rulers](#) and [stopwatches](#) to [electron microscopes](#) and [particle accelerators](#). [Virtual instrumentation](#) is widely used in the development of modern measuring instruments. [3]

**Virtual instrumentation** is the use of customizable software and modular measurement hardware to create user-defined measurement systems, *called virtual instruments*.

Traditional hardware instrumentation systems are made up of pre-defined hardware components, such as [digital multimeters](#) and [oscilloscopes](#) that are completely specific to their stimulus, analysis, or measurement function. Because of their hard-coded function, these systems are more limited in their versatility than virtual instrumentation systems. **The primary difference between hardware instrumentation and virtual instrumentation is that software is used to replace a large amount of hardware.** The software enables complex and expensive hardware to be replaced by already purchased computer hardware; e. g. [analog-to-digital converter](#) can act as a hardware complement of a virtual [oscilloscope](#), a [potentiostat](#) enables [frequency response](#) acquisition and analysis in [electrochemical impedance spectroscopy](#) with virtual instrumentation. [4]

### 3. PHYSICAL PHENOMENON AND ANALOG FRONT END CIRCUITS

**Physical Phenomenon** natural [phenomenon](#) involving the physical properties of matter and energy [5]

**Analog front-end (AFE or analog front-end controller AFEC):** is a set of analog signal conditioning circuitry that uses sensitive analog amplifiers, often operational amplifiers, filters, and sometimes [application-specific integrated circuits](#) for sensors, radio receivers, and other circuits to provide a configurable and flexible electronics functional block, needed to interface a variety of sensors to an, antenna, [analog to digital converter](#) or in some cases to a [microcontroller](#). [6]

**Sensor:** In the broadest definition, a **sensor** is an object whose purpose is to detect events or changes in its environment, and then provide a corresponding output. A sensor is a type of [transducer](#); sensors may provide various types of output, but typically use electrical or optical signals. For example, a [thermocouple](#) generates a known voltage (the output) in response to its temperature (the environment) [7]. It is a device which [detects](#) or measures a [physical](#) property and records, indicates, or otherwise [responds](#) to it. [8]

A **transducer** is a device that [converts](#) one [form of energy](#) to another. Usually a transducer converts a [signal](#) in one form of energy to a signal in another.<sup>[1]</sup>

Transducers are often employed at the boundaries of [automation](#), [measurement](#), and [control systems](#), where electrical signals are converted to and from other physical quantities (energy, force, torque, light, motion, position, etc.). The process of converting one [form of energy](#) to another is known as [transduction](#) [9].

Nowadays there is a broad set of sensors – many of them are low cost – to detect almost any physical parameter.

An important set of sensors and transducers used in instrumentation are those that convert a physical phenomenon or a physical magnitude into an electric signal (charge, current, voltage) with the enormous advantage to handle this signal using electronic components: single as a transistor, or chips as analog circuits (operational amplifiers, comparators, phase locked loops, etc.), or digital ones (from simple logic gates to microcontrollers). These options offer a versatile approach to handle signals from sensors as electric signals.



**Physical Phenomena facing a front end circuit:** It is important also to highlight that in spite of a sensor may have a nonlinear behaviour, a limited range of detection, DC offset, noise at low level signals, **there is a one to one correspondence between the physical phenomena and the signal from the sensor.** The main link between the phenomenon and signal are the equations that describe the physics of the transducer. Linearization, Amplification, Offset Suppression, Signal Filtration, etc. are resources from electronic design of the front end circuit. Numerical Analysis of Data are alternatives to handle Data through a software approach.

#### 4. MICROCONTROLLERS

A **microcontroller** (or **MCU**, short for *microcontroller unit*) is a small computer (SoC) on a single integrated circuit containing: a processor core, memory, and programmable input/output peripherals. Program memory in the form of Ferroelectric RAM, NOR flash or OTP ROM is also often included on chip, as well as a typically small amount of RAM. Microcontrollers are designed for embedded applications, in contrast to the microprocessors used in personal computers or other general purpose applications consisting of various discrete chips. [10]

Among the programmable input/output peripherals inside a microcontroller are: **programmable counters** (circuits able to count periodic and aleatory pulses), **programmable timers** (circuits able to generate periodic pulses or to count precise time intervals), **analog to digital converters A/D** (circuits able to take an amplitude-sample of analogue voltage signal during a short time-interval and convert it into a binary number among an ordered interval of numbers with a given resolution), **digital to analog converters D/A** (circuits able to generate a voltage signal with an amplitude and resolution in a voltage range corresponding to a binary number at its input), several **programmable circuits for intercommunication** with other microcontrollers or microprocessors (USB, I2C, UART, others); etc.

The Microcontroller chosen for this Project is a **16-bit MCUs - PIC24, dsPIC**. The criteria for this selection will be apparent throughout this chapter. Complete information about this microcontroller is found in **Basic Reference | 5 |** at the end of this chapter.

#### 5. ANDROID DEVICES

**Android** is a mobile operating system developed by Google, based on the Linux kernel and designed primarily for touchscreen mobile devices such as smartphones and tablets. Android's user interface is mainly based on direct manipulation, using touch gestures that loosely correspond to real-world actions, such as swiping, tapping and pinching, to manipulate on-screen objects, along with a virtual keyboard for text input. In addition to touchscreen devices, Google has further developed Android TV for televisions, Android Auto for cars, and Android Wear for wrist watches, glasses, each with a specialized user interface. Variants of Android are also used on notebooks, game consoles, digital cameras, and other electronics.

Android has the largest installed base of all operating systems of any kind. Android has been the bestselling OS on tablets since 2013, and on smartphones it is dominant by any metric. [11]

## 6. ANDROID OPEN ACCESSORIES

**Android Open Accessory (AOA)** support allows external USB hardware (Android USB accessories) to interact with Android-powered devices in *accessory mode*. When an Android-powered device is in accessory mode, the connected accessory acts as the USB host (powers the bus and enumerates devices) and the Android-powered device acts as the USB accessory.

Android USB accessories are designed to attach to Android-powered devices. Such accessories adhere to AOA, enabling them to detect Android-powered devices that support accessory mode, and must provide 500mA at 5V for charging power. Some previously-released Android-powered devices are capable of acting only as a USB device and cannot initiate connections with external USB devices. AOA support overcomes this limitation, enabling you to build accessories that can initiate connections and interact with an assortment of Android-powered devices.

**Note:** Accessory mode is dependent on device hardware; not all devices support accessory mode. Devices that support accessory mode can be filtered using a `<uses-feature>` element in the corresponding application's Android manifest. For details, see the [USB Accessory](#) developer guide.

AOA has two versions that support different types of communication:

- **AOAv1.** Supports generic accessory communication and adb debugging. Available in Android 3.1 (API Level 12) and higher and supported through an [Add-On Library](#) in Android 2.3.4 (API Level 10) and higher.
- **AOAv2.** Supports audio streaming and human interface device (HID) capabilities. Available in Android 4.1 (API Level 16). [12]

There are several brands that support Android Open Accessory (AOA): Arduino or IOIO brands are commercially available. An illustrative and extensive explanation about this topic can be found in Reference [13]

For this project the AOA chosen device is IOIO OTG based on the microcontroller PIC 24 family.

**Basic Reference** | 4 | provides information on the microcontroller PIC 24 family.

## 7. PROGRAMMABLE AND GRAPHIC CALCULATOR EMULATORS

Once measured data has been acquired by the Android Device through the AOA device, it has to be handled by a specific program as data. This process is made by dedicated routines. Due to the versatility and enormous popularity of HP 48GX and HP 50G graphical and programmable calculator-emulators have been chosen for this purpose. There are two more advantages for this election: Emulators EMU 48, as they are known, are freeware. There are Android versions for EMU48 (Droid 48; Go49). **Chapter 4 is dedicated to expose the topic to handle measured data in order to obtain a measurement.**

## B. IOIO OTG CHARACTERIZATION AND INTERFACING

### 1. IOIO OTG: DESCRIPTION

Fig. B1 is a picture of IOIO OTG. The IOIO OTG board is accessible by other circuits through its 46 pins that can be characterized by software as Inputs or Outputs. A detailed description of this device is found in [14].

**Input / Output pins** the IOIO OTG board connects with external circuits through its pins. These are Input (I) and Output (O) pins. The function of a pin is characterized from software. Depending of software, a pin is able to play different roles at different instants. Several pins stand up to 3.3 V. Others stand up to 5.0 V. Several pins are used as A/D conversion inputs or PWM outputs. See Reference [14]

There are several types of outputs and Inputs:

**Digital (logic-level) input and output** is the most basic building blocks of digital hardware systems. It is also commonly referred to as General Purpose Input Output – GPIO. A logic-level signal has two states: LOW and HIGH, respectively 0 and 1 or false and true. In practice, any pin of IOIO OTG can be software characterized as a Digital Input or Output. [15]

**Analog Input** In many real-life situations we want to measure voltage. Ever so often, it is not the voltage itself we care about, but some other physical quantity that has been converted to voltage by some sort of sensor or transducer. IOIO has 16 pins, commonly known as "Analog Inputs", which are capable of measuring voltage levels between 0V-3.3V, with a precision of about 3mV. [16]

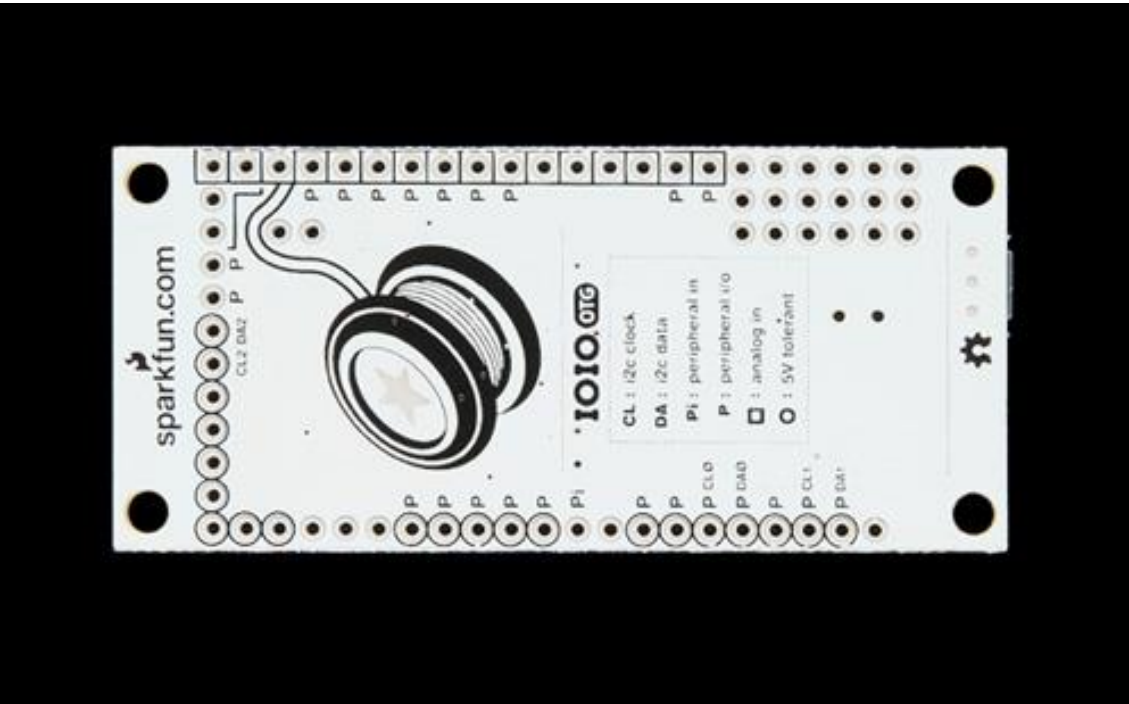
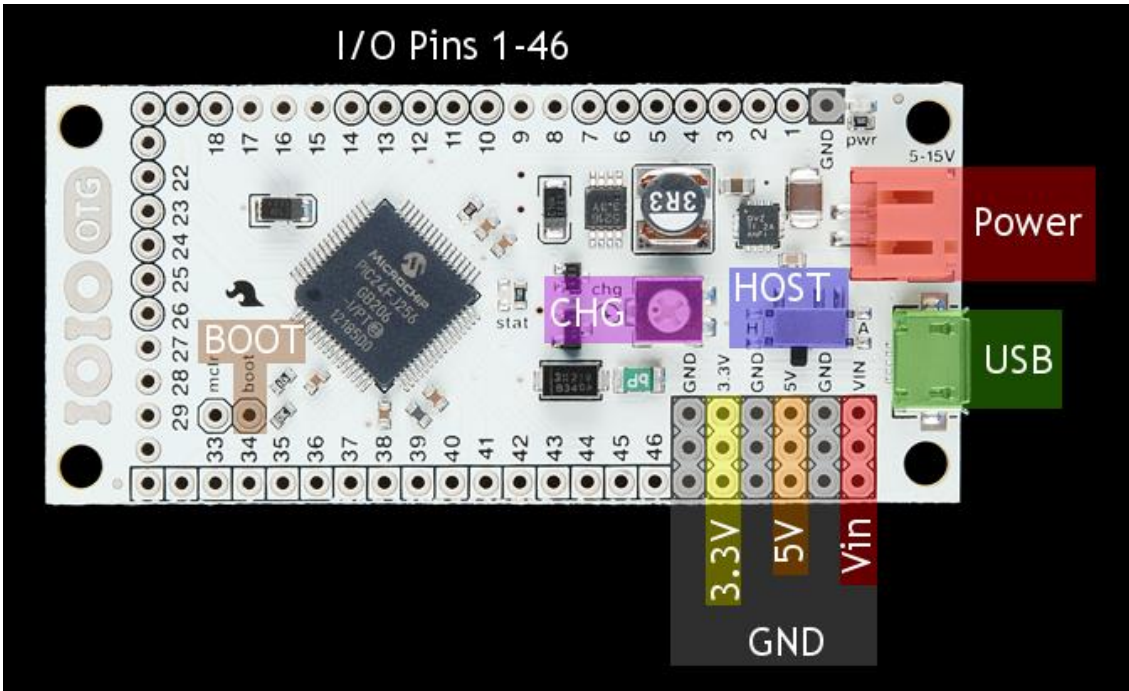
**Pulse Width Modulation** A Pulse Width Modulation (PWM) signal is a kind of a digital output, which has a certain structure in its temporal behaviour. Specifically, the signal has a fixed period. Every time a period starts, the signal moves from LOW to HIGH. Then it stays HIGH for a certain duration, called the *pulse width*, after which it becomes LOW again for the rest of the period. The pulse width may change over time, but the period stays the same. PWM is a method to generate a Digital to Analog Conversion D/A. [17]

IOIO OTG is able to manage up to nine A/D inputs and up to nine PWM outputs.

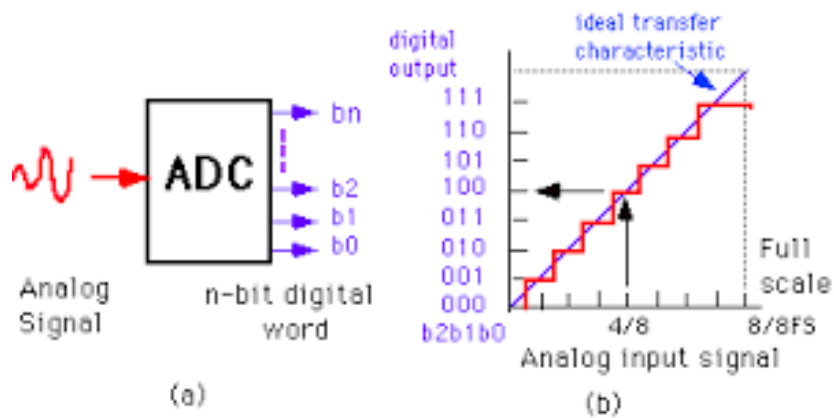
Fig. B2.a illustrates the concept of A/D conversion; an analogue input is converted in a binary count in an amplitude interval with a predetermined resolution.

Fig. B2.b is a schematic representation of the A/D converter circuit.

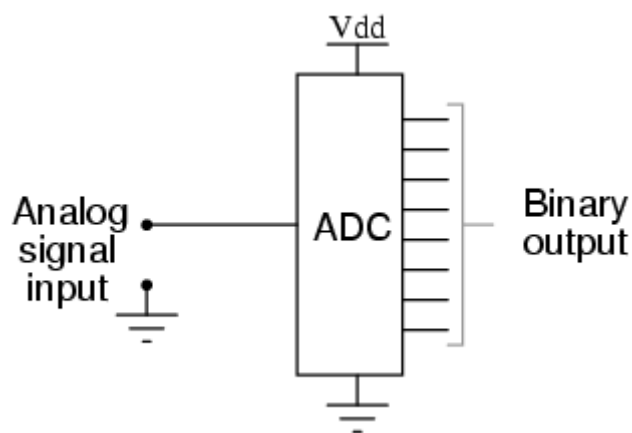
Fig. B2.c is a schematic representation of the D/A converter circuit i.e.: the complementary process when a binary number generated in the microcontroller produces an analog output voltage within a voltage range and with a predetermined resolution.



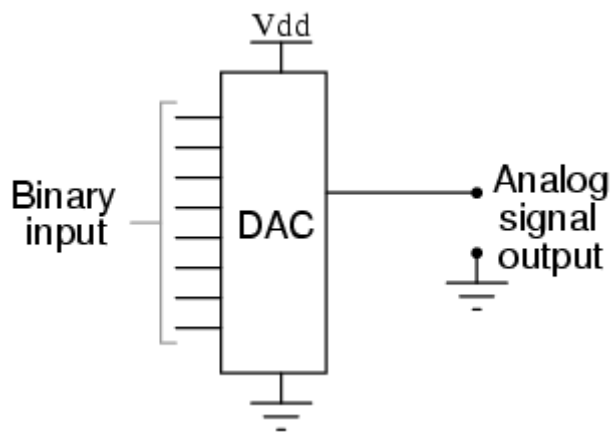
**Figure B.1:** Front and Back sides of the microcontroller board (IOIO OTG). [Figure adapted from reference shown in ANNEX F]



(a)



(b)



(c)

**Figure B.2:** (a) Illustration of Analog to Digital Conversion (b) Schematic of A/D Conversion Circuit. (c) Schematic of D/A Conversion Circuit. [Figure adapted from reference shown in ANNEX F]

## 2. IOIO OTG: CHARACTERIZATION

### a. Loading IOIO OTG Drivers to PC (Windows)

The first action to enable IOIO OTG board for any application of this board interfaced with a PC is to install the IOIO OTG Drivers. The Windows drivers are downloaded from [18], Section Drivers, Subsection Windows.

Two procedures to download the drivers are detailed in **Chp. 3 ANNEX 2.1**.


Once drivers are installed in the PC and the IOIO OTG board is interfaced with it through the appropriate USB connector – or two connectors – from the micro USB from the IOIO OTG to a USB port in the PC, the PC recognizes this board as it is shown in Fig. B.3

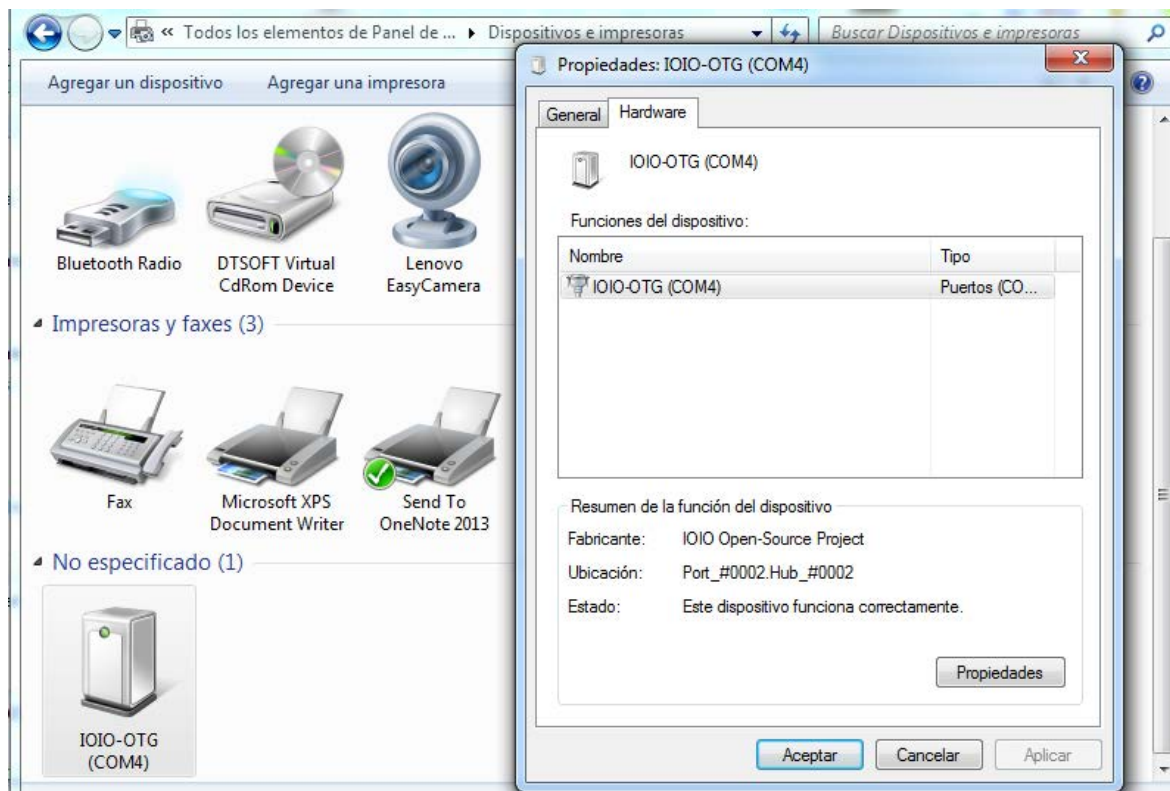


**Figure B.3:** Screen shot showing that IOIO OTG is recognized by the PC when drivers are installed.

### b. Updating Firmware in IOIO OTG

The second action to enable IOIO OTG for applications using Android Studio is to upgrade its firmware to the version IOIO0505, or more recent. The most recent version is downloaded from [19], Section Client Software and IOIO Application Firmware Images. Fig. B.3 shows the corresponding row. The download is made by clicking the third column. The process to update firmware on the board is detailed in **Chp. 3 ANNEX 2.2**.

5.06 / 5.05 <b>(recommended)</b>	App- IOIO0505.zip	 App- IOIO0506.ioioapp	<ul style="list-style-type: none"> <li>• IOIO0021</li> <li>• IOIO0022</li> <li>• IOIO0023</li> <li>• IOIO0030</li> </ul> (Bootloader V3.x, Device Bootloader V4.x)	A new way to build applications, based on Gradle, Maven and Android Studio. Improved reliability of OpenAccessory connections. See <a href="#">release notes</a> .
-------------------------------------	----------------------	---	--	--

**Figure B.4:** The most recent version to Upgrade IOIO OTG is downloaded from the third column. [Figure adapted from reference shown in ANNEX F]

The procedure to upgrade this board is explained in [20]

### c. The Command Line

In IOIO OTG documents the “Command Line” expression is found very often. The command line is referred also as the **command screen** or a **text interface**, the **command line** or **Windows command line** is a [user interface](#) that is navigated by typing commands at [prompts](#), instead of using the mouse. For example, the Windows folder in a Windows command line ([MS-DOS](#)) is C:\Windows>

A preliminary approach to the command lines is found in [21].

Fig. B.5 is a screenshot of the command line.

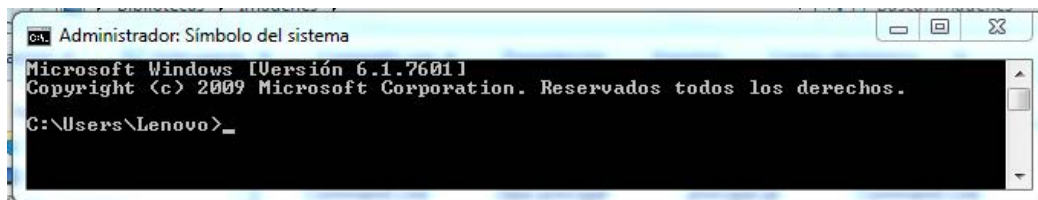


**Figure B.5:** Screenshot of the command line.

### 3. IOIO OTG: INTERFACING

#### a. Ways to interface IOIO OTG

The IOIO OTG board offers a broad set of alternatives to be interfaced with a PC or an Android device. So it is a versatile device in what interface is concerned. The alternatives are summarized and references are included.

IOIO OTG is compatible with different operative systems: Windows, Linux, OSX and Android. [22]

IOIO OTG can be interfaced with a PC [22], or an Android Tablet or Mobile

IOIO OTG can be interfaced over Bluetooth either with an Android Device [23] or with a PC [24].

IOIO OTG also can be interfaced with an Android Device either in USB Debugging Mode [25] or in Open Accessory Mode [26].

#### b. Interfacing IOIO OTG as Host with an Android Device

Although there are several alternatives to interface IOIO OTG either with a PC or an Android Device, in this work, the option to interface an IOIO OTG as HOST and the Android Device as ACCESSORY is explained in major detail since it is representative and has all the requirements for the purpose to develop virtual instruments.

The HOST and ACCESSORY modes are referred to the USB interface between two devices – as example, the Android Device and the IOIO OTG board.

When the Android –powered device is in **host mode**, it acts as the USB host and powers the bus.

When the Android-powered device is in USB **accessory mode**, the connected USB hardware (an Android accessory in this case) acts as the host and powers the bus [27].

*Host mode* is a name for when a device is acting as a host. Every USB connection has exactly one device in *host mode*. PCs always run in host mode. (You wouldn't usually call it that for a PC, because it's not really a "mode", it's always like that.)

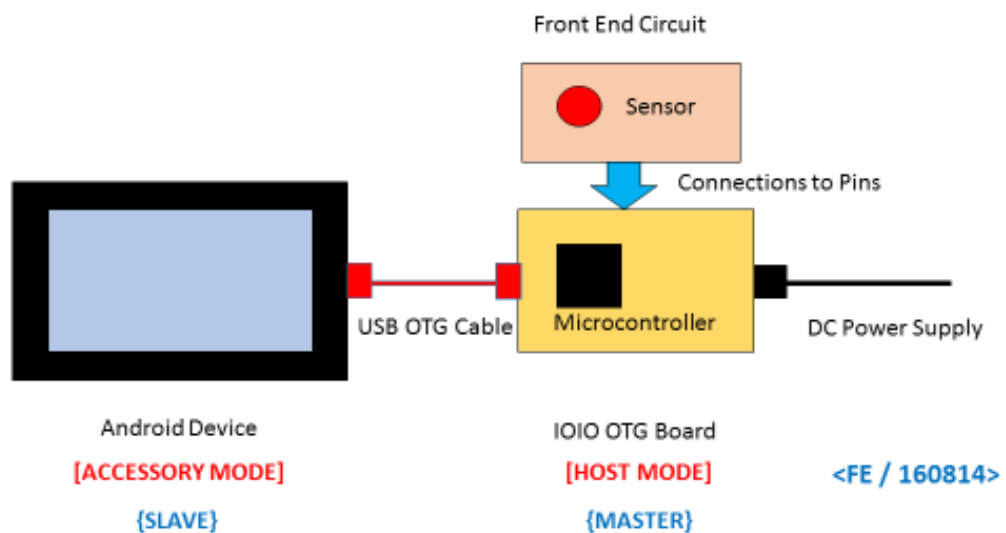
A phone is a bit different, though. Sometimes you want it to act as a peripheral: for example, so you can plug it into a PC, so the PC can access the phone's storage. Sometimes you want it to act as a host: for example, to connect a physical keyboard or mouse to it. This is why many Android devices now support USB host mode as well as USB peripheral mode: they can act in either role. But how can you make this work, when a host's USB socket is different from a peripheral's?



This is where *USB-on-the-go (OTG)* comes in. It adds an extra pin to the micro-USB socket. If you plug a normal A-to-B USB cable, the device acts in peripheral mode. If you connect a special USB-OTG cable, it has the pin connected at one end, and the device at that end acts in host mode.

This can be a little confusing if one cable has seemingly identical plugs at either end, which do different things. But cables with USB-OTG at both ends are uncommon: it's more common to use an adaptor, which has a host-mode USB-OTG plug at one end, and a rectangular USB-A socket on the other. You can plug a normal USB cable into this adaptor, and it will work normally. [28]

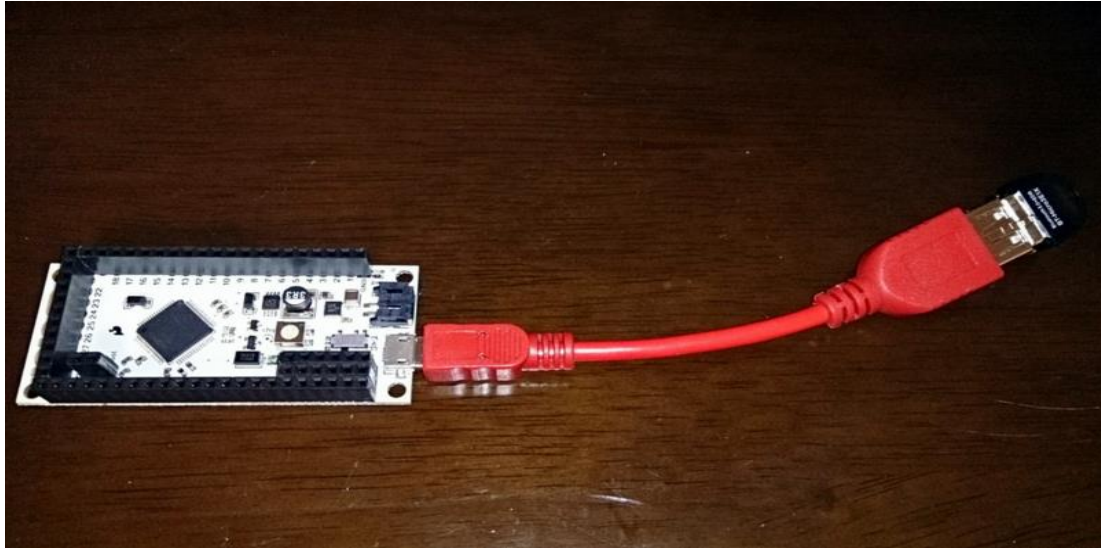
Fig. B.6 illustrates these ideas:



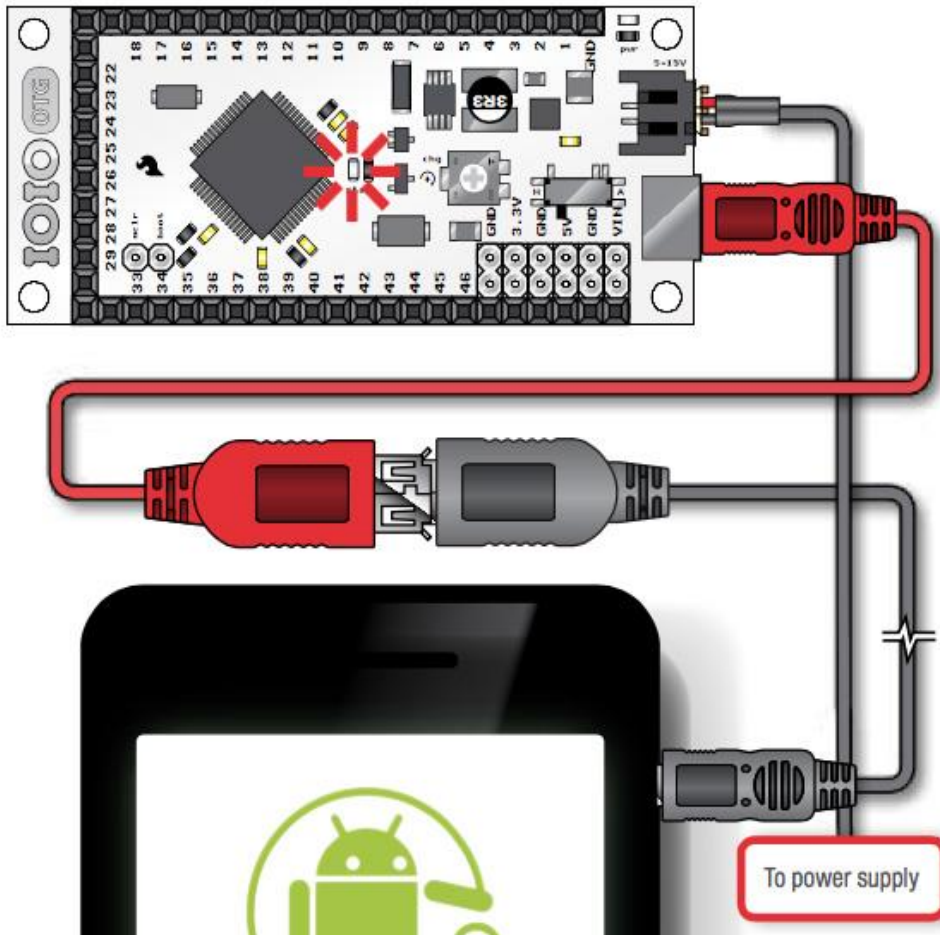
**Figure B.6:** Schematic diagram showing IOIO OTG card connected in host mode to an Android Device. A front end circuit also is connected to the IOIO OTG board.

Fig. B.7 is a photography of an IOIO OTG board connected with an USB OTG cable at its micro USB input.

Finally, Fig. B.8 shows the interface of the IOIO OTG board with an Android Device through a USB OTG cable (the red cable) connected to a rectangular USB cable (the black cable) that ends in the micro USB port of the Android Device. The power supply is connected to the IOIO OTG board that is in HOST MODE. The Android Device is in ACCESSORY MODE, it is powered through the USB bus from the IOIO OTG.



**Figure B.7:** *Photography of IOIO OTG connected with USB OTG cable. [Figure adapted from reference shown in ANNEX F]*



**Figure B.8:** *IOIO OTG board (in Host Mode) interfaced to an Android Device (in Accessory mode). The red cable is a USB OTG cable. The power supply is connected to the IOIO OTG board. [Figure adapted from reference shown in ANNEX F]*

## C. ANDROID STUDIO AND IOIO OTG: PROGRAMMING ANDROID DEVICES AS MEASURING INSTRUMENTS

### 1. ANDROID STUDIO

**Android Studio** is the official [integrated development environment](#) (IDE) freeware for [Android](#) platform developed by Google..

Fig. C.1 is the logotype of this Integrated Development Environment – IDE.



**Figure C.1:** *Android Studio Logo.*  
[Figure adapted from reference shown in ANNEX F]

Android Studio was announced on May 16, 2013 at the [Google I/O](#) conference. Android Studio is freely available under the [Apache License 2.0](#).<sup>[31]</sup>

Android Studio was in early access preview stage starting from version 0.1 in May 2013, then entered beta stage starting from version 0.8 which was released in June 2014.<sup>[51]</sup> The first stable build was released in December 2014, starting from version 1.0.<sup>[61]</sup>

Based on [JetBrains' IntelliJ IDEA](#) software, Android Studio is designed specifically for Android development.<sup>[71]</sup> It is available for download on [Windows](#), [Mac OS X](#) and [Linux](#),<sup>[81][91]</sup> and replaced [Eclipse Android Development Tools](#) (ADT) as Google's primary IDE for native Android application development. [29]

The actual stable version of Android Studio is Version 2.0. It was released on 07 April 2016. [30]

Android Studio for Windows is free downloaded from [30].

Java Development Kit (JDK) 8 has to be installed previously in the PC it is free downloaded from [31]. Android Studio by itself has been developed in Java Programming Language.

The process to install and characterize Java Development Kit (JDK) 8 is detailed in **Chp. 3 ANNEX 2.3.**

The process to install Android Studio is detailed in **Chp. 3 ANNEX 2.4.**

**Basic Reference | 3 | : Android Studio User Guide** is an extensive and structured document intended as a complete reference for Android Studio users.

**Basic Reference | 7 | : The Java™ Tutorials** is a page where a user can learn or consult topics on this Programming Language.

## 2. INSIDE ANDROID STUDIO

**Android Studio** is the Official Integrated Developing Environment – IDE for Android Platform Development.

Android Studio has been developed using Java Programming Language.

Android Studio stands on **Java Development Kit**. A Java Development Kit (JDK) is a program development environment for writing [Java applets](#) and applications. It consists of a runtime environment that "sits on top" of the [operating system](#) layer as well as the tools and programming that developers need to compile, debug, and run applets and applications written in the Java language.

In December 2014, Google announced version 1.0 of [Android Studio](#), an [open source](#) IDE for [Android](#) apps, based on the open source community edition of **IntelliJ IDEA**.

**IntelliJ IDEA** (pronounced /ɪnˈtɛlɪ dʒeɪ aɪˈdɪə/) is a [Java integrated development environment](#) (IDE) for developing computer software. It is developed by [JetBrains](#) (formerly

known as IntelliJ), and is available as an [Apache 2 Licensed](#) community edition,<sup>[11]</sup> and in a [proprietary](#) commercial edition. Both can be used for commercial development.<sup>[2]</sup>

The first version of IntelliJ IDEA was released in January 2001, and was one of the first available Java IDEs with advanced code navigation and [code refactoring](#) capabilities integrated.<sup>[3][4]</sup>

In a 2010 *Infoworld* report, IntelliJ received the highest test centre score out of the four top Java programming tools: [Eclipse](#), IntelliJ IDEA, [NetBeans](#) and [JDeveloper](#).<sup>[5]</sup>[32]

Embedded in **Android Studio** there are two programmes: **Gradle** and **Maven**. It is more: [Starting from Version IOIO0505, IOIO OTG has adopted Android Studio as its Official Integrated Developing Environment – IDE.](#)

Let's develop this paragraph in more detail to foresee its implications:

**Gradle** is a state-of-the-art Application Programming Interface – API that easily supports customizations and is widely used in the Java world. The Android plug-in for Gradle adds a wide range of features specific to Android apps, including build types, flavours, signing configurations, library projects, and more.

Using Gradle, software can easily be built, tested and published via a simple command-line interface, but Gradle is also tightly integrated into various Integrated Developing Environments – IDEs, making the IDE understand the structure of the project, simplify editing of build scripts and execute different build tasks from a Graphic User Interface – GUI.

**Basic Reference | 8 |** : **Gradle Beyond the Basics** First Edition July 2013

and

**Basic Reference | 9 |** : **Gradle Recipes for Android** First Edition June 2016

Are very recent references to learn Gradle and to apply it to Android Studio.

**Maven** is a [build automation](#) tool used primarily for [Java](#) projects. The word *maven* means "accumulator of knowledge" in [Yiddish](#).<sup>[31]</sup> Maven addresses two aspects of building software: first, it describes how software is built, and second, it describes its dependencies. Contrary to preceding tools like [Apache Ant](#), it uses conventions for the build procedure, and only exceptions need to be written down. An [XML](#) file describes the software project being built, its dependencies on other external modules and components, the build order, directories, and required [plug-ins](#). It comes with pre-defined targets for performing certain well-defined tasks such as compilation of code and its packaging. Maven dynamically downloads [Java](#) libraries and Maven plug-ins from one or more repositories such as the Maven 2 Central Repository, and stores them in a local cache.<sup>[41]</sup> This local cache of downloaded [artefacts](#) can also be updated with artefacts created by local projects. Public repositories can also be updated. [33]

**Maven Repository** is a place i.e. directory where all the project jars, library jar, plugins or any other project specific artefacts are stored and can be used by Maven easily.

Maven repository are of three types

- local
- central
- remote

#### Local Repository

Maven local repository is a folder location on your machine. It gets created when you run any maven command for the first time.

Maven local repository keeps your project's all dependencies (library jars, plugin jars etc.). When you run a Maven build, then Maven automatically downloads all the dependency jars into the local repository. It helps to avoid references to dependencies stored on remote machine every time a project is build.

Maven local repository by default get created by Maven in `%USER_HOME%` directory. To override the default location, mention another path in Maven settings.xml file available at `%M2_HOME%\conf` directory.

When you run Maven command, Maven will download dependencies to your custom path.

#### Central Repository

Maven central repository is repository provided by Maven community. It contains a large number of commonly used libraries.

When Maven does not find any dependency in local repository, it starts searching in central repository using following URL:<http://repo1.maven.org/maven2/>

#### Key concepts of Central repository

- This repository is managed by Maven community.
- It is not required to be configured.
- It requires internet access to be searched.

To browse the content of central maven repository, maven community has provided a URL: <http://search.maven.org/#browse>. Using this library, a developer can search all the available libraries in central repository.

## Remote Repository

Sometime, Maven does not find a mentioned dependency in central repository as well then it stopped build process and output error message to console. To prevent such situation, Maven provides concept of **Remote Repository** which is developer's own custom repository containing required libraries or other project jars.

For example, using below mentioned POM.xml, Maven will download dependency (not available in central repository) from Remote Repositories mentioned in the same pom.xml. [34]

**IOIO OTG**, starting at release 5.05 of the IOIO software, the recommended way to build IOIO applications is using the [Gradle build system](#). To those not familiar with Gradle, it is a flexible build tool that is becoming very popular among Java developers and has been adopted by the Android SDK as the official way to build Android applications. Using Gradle, software can easily be built, tested and published via a simple command-line interface, but Gradle is also tightly integrated into various IDEs, making the IDE understand the structure of the project, simplify editing of build scripts and execute different build tasks from a GUI. The official IDE of choice for Android development is [Android Studio](#), which, despite its name, is a general purpose Java IDE, based on the popular [IntelliJ IDEA](#). Starting at release 5.05 of the IOIO software, this is the official IDE for developing IOIO based applications for either Android or PC.

Moreover, along with this change the IOIO libraries are no longer needed to be built by users, but rather made available on [Maven Central](#). Maven Central is a universal repository of canonically named and versioned software packages including meta information such as their source code, documentation and dependencies on other packages. Maven Central is supported by many build tools and IDEs, typically requiring a user of those components to merely state the name ("coordinates") and version of the component they want to use, thus greatly reducing the complexity of distributing and using those components. Specifically, using Maven packages is seamlessly integrated into the Gradle build system mentioned above. [35]

In short features:

*Android Studio, supported by Google, is the official Integrated Development Environment program dedicated to be a platform to develop applications for Android Devices. Its first version appeared in 2014. It is written in Java Programming Language and stands on the program **Java Development Kit**. Android Studio has been developed based on the open source community edition of **IntelliJ IDEA**, a leader promoter of Java Integrated Development Environment whose first version appeared 13 years before.*

*Embedded in Android Studio there are two programmes: **Gradle** and **Maven** as plugins; these programs interact with each other and with the **Project** under development. **Gradle** is a state-of-the-art Application Programming Interface that allows built, test and publish applications via a simple command-line interface; Gradle is also tightly integrated into various Integrated Developing Environments – IDEs, making the IDE understand the structure of the project, simplify editing of build scripts*

and execute different build tasks from a Graphic User Interface – GUI. On the other hand, **Maven** is a build automation tool used primarily for Java projects; The core of this program is the **Maven 2 Central Repository** provided by Maven community and accessible through Internet ; Maven Central is a universal repository of canonically named and versioned software packages including meta information such as their source code, documentation and dependencies on other packages.

Then: using Android Studio for Android Applications allows their development almost automatically obtaining as the final product an **Application Plugin** that is directly applicable to an Android Device of the corresponding - or newer – model.

**IOIO OTG** – starting from version IOIO 0505 – has adopted Android Studio as its official Integrated Development Environment taking advantage of all the previously described benefits.

These ideas are summarized in the schematic drawing shown in Fig. C.2

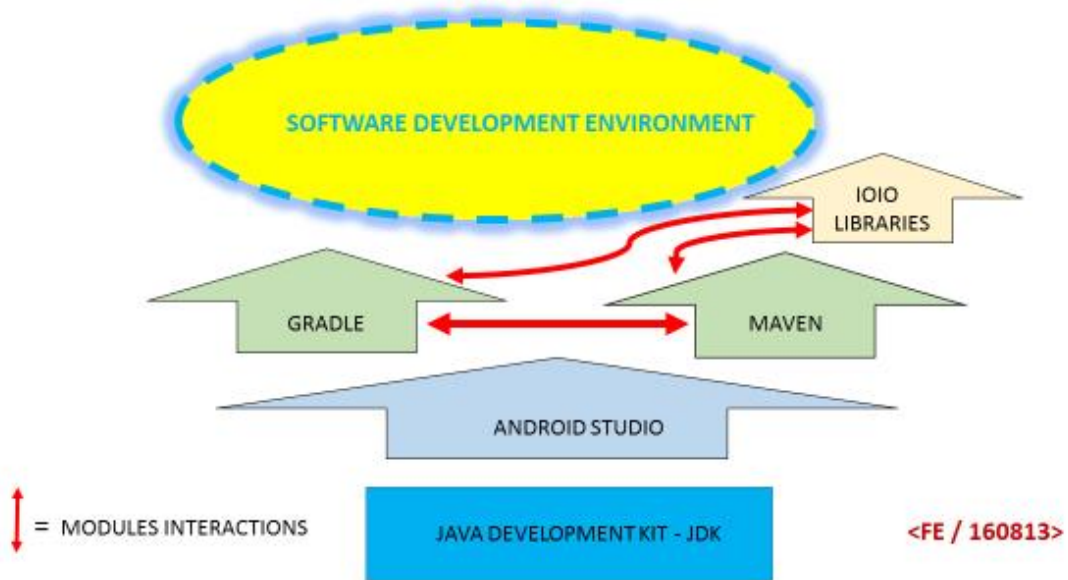


**Figure C.2:** *Android Studio and IOIO OTG Libraries plugin. Schematic representation of the main components and their interactions.*



### **3. DEVELOPING IOIO OTG APPLICATIONS FOR ANDROID DEVICES OR PC**

As it was mentioned in section B.3.a, IOIO OTG board is a versatile device. It can be interfaced directly to a PC. It can be interfaced to an Android device or; through Bluetooth, it can be interfaced either to a PC or an Android Device. However, all these possibilities imply different software approaches and subtleties.

This section seeks to clarify these matters. A forty-pages formidable Reference that introduces IOIO OTG and the ways to interface it in a practical way is [36].

#### **a. Interfacing IOIO OTG to a PC**

It is possible to work with IOIO OTG card directly interfaced with a PC. If one wishes to work exclusively with a PC then it is not necessary to install Android Studio. A fraction of it is only required. This is Android SDK (Software Development Kit). Android SDK is downloadable from the same page Android Studio. It is available in the Section Different Platforms at the end of that page (android-studio-bundle-143.2915827-windows.exe). Since Android SDK is going to be used with the Command Line, it is necessary to add Android SDK Platform Tools folder to your \$PATH.

Gradle Open Source binary version is required to compile the code. It is necessary to add the Gradle bin folder to your path.

A Java Editor is also required.

Then IOIO OTG board is connected to an USB in the PC and turns on its red led. Certainly IOIO OTG drivers must be previously installed in your PC.

Besides Basic Reference [2] to Download Android SDK, useful References arte: [36] and [22].

#### **b. Interfacing IOIO OTG to an Android Device**

In order to run an IOIO OTG Application in an Android Device it is required previously to program – or to transfer – the Application to the Android Device from the PC.

The Application is developed in the PC using Android Studio.

Once the Application has been developed, the Android Device is connected to the PC in “Debugging Mode” and the Application is transferred – uploaded – to the Android Device.

Then, the Android Device is unplugged from the PC keeping the micro USB OTG cable attached.

Connect the IOIO OTG to the Android Device as shown in Fig. B.8 providing the power to IOIO OTG (in Host Mode) and open the IOIO Application following identical procedure as any Android application.

For details of the procedure, refer to: [36], [25].

#### **c. Android Debug Bridge – ADB**

For development purposes, it is possible to connect the IOIO OTG and the Android Device to the PC at the same time in a configuration named IOIO Bridge using an additional subroutine named also IOIO Bridge. This configuration allows develop Applications and Test them using the IOIO OTG board at once.

For details of the procedure, refer to: [36], [37].

#### **d. Going wireless with Bluetooth**

It is possible to connect wireless IOIO OTG either to a PC or an Android Device using low cost Bluetooth Dongles and specific additional open software.

For details of the procedure, refer to: [36], [23], and [24].

#### **e. Interfacing IOIO OTG with an Android Device as Open Accessory**

IOIO OTG also can be interfaced with an Android Device in Open Accessory Mode.

For details of the procedure, refer to [26].

### **4. IOIOLib ANDROID PACKAGE**

The software that supports the use of IOIO OTG board is organized in Libraries and are attached to Android Studio as a Plugin for IOIO firmware versions IOIO0505 or higher. It is also available from the Maven Central repository.

Either to develop IOIO OTG applications for a PC or an Android device one needs use these Libraries. The basic information is found in [37].

The main Libraries are:

### a. IOIOLib Application Framework

The ways IOIO OTG is interfaced and operates as described in Section C.3 must be software supported. This set of programmes is organized in a Library named IOIOLib Application Framework.

For information about this Library refer to [38]

### b. IOIOLib Core API

Regardless of whether you are developing Android applications or PC applications, the [IOIOLib Core API](#) is exactly the same and the provided application frameworks share many of the concepts and code.

The `IOIO` interface is the heart of the IOIOLib. An instance of this interface represents a physical IOIO board, and through its methods you can control its various functions, such as reading or writing values to individual physical pins.

Once established the interface with a PC or Android Device through the **IOIOLib Application Framework**, the physical control of the IOIO OTG board is achieved through instances of the **IOIOLib Core API**.

For information about this Library refer to [39]

Fig. C.3 is a screenshot of the IOIOLib Core.

For information about any command shown in Fig. C.3 please start the search in the right hand side of Reference [40].

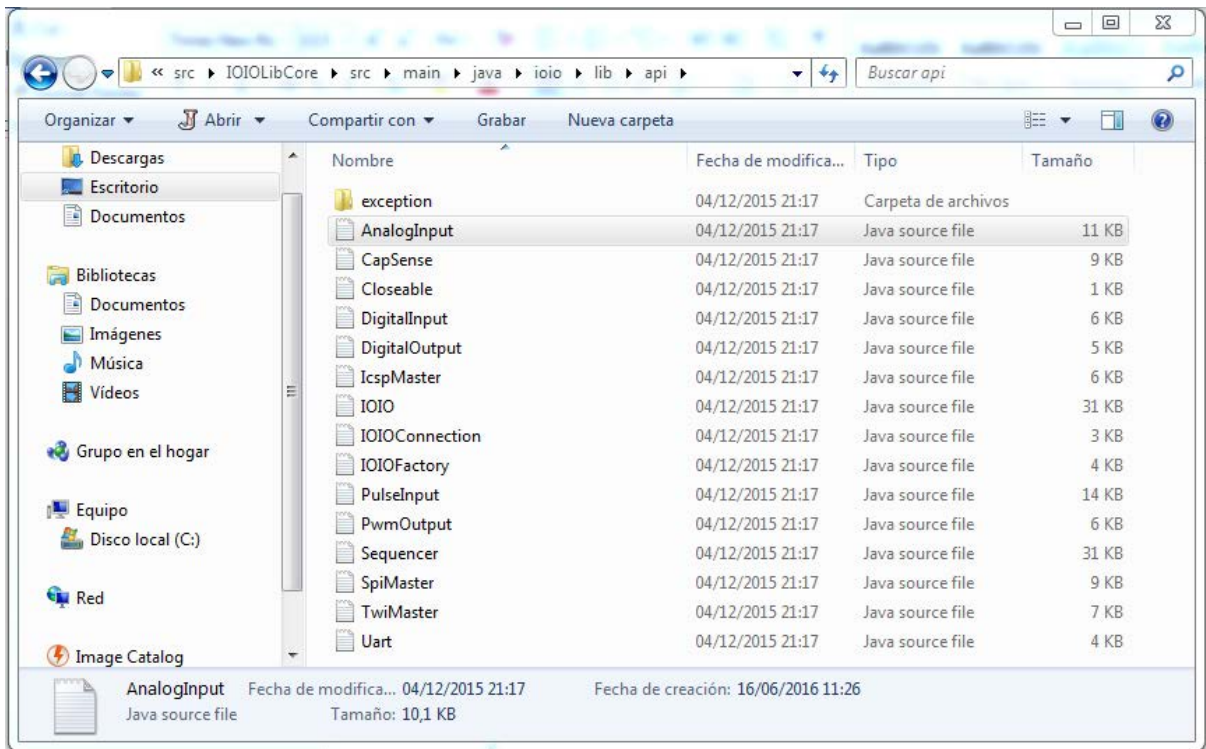


**Figure C.3:** *IOIOLib API screenshot*

## 5. REQUIRED COMMANDS FOR THE PRESENT APPLICATION

The interface Commands to control IOIO OTG board from the Android Device are:

- Digital Input
- Digital Output
- Analog Input
- Pwm Output

These Commands written in Canonical Form are shown in **Chp. 3 ANNEX 3**

Next Section D summarizes the way these commands are used for each measurement in the Project.

## D. INTERFACING FRONT END CIRCUITS WITH THE MICROCONTROLLER

In this Section, the interface between the Front End Circuits and the Microcontroller is exposed.

### 1. FRONT END CIRCUITS INPUTS AND OUTPUTS

Table D.1 summarizes the Front End circuits in this work, their input and output parameters and the required microcontroller commands. The Commands are deferred to the IOIOLib API.

**TABLE D.1: FRONT END CIRCUITS INPUTS, OUTPUTS AND REQUIRED IOIO OTG COMMANDS**

Front End Circuit	Input	Output	Command
Voltmeter	---	DC Volts	A/D
Thermometer	Temperature	DC Volts	A/D
Photocurrent to Voltage Converter	Light	DC Volts	A/D
JFET Solar Cell I – V Curve Generator	Light		
	Gate – Source Voltage (Control Voltage)		D/A
		DC Volts	A/D
			I , O *

\* See correspondent explanation in Chapter 4

Note that the Front End circuits are used with different sensors or in different applications.

If the Front End Circuits signals are properly matched with the microcontroller specifications for Input and Output signals i.e.: (Maximum Amplitude lower than 5.0 Vdc or 3.3 Vdc depending on the

IOIO OTG card pin. Positive Input signals. Required currents smaller than 10 mA), then Front End circuits are connected directly to the microcontroller.

## 2. SCHEMATIC DIAGRAMS

In Fig. D.1 are shown schematic diagrams for the Thermometer, Optical Pyrometer and Optical Pyranometer.

All these Front End Circuits have as outputs a DC Voltage signal and are connected to an Analog / Digital converter input at the IOIO OTG Board.

Note that the Temperature Sensor is a Si PN junction directly biased using a constant current source.

The Optical Pyrometer (Spectral Temperature meter) in this example uses two reverse biased LEDs of different colour (wavelength) as sensors.

The Optical Pyranometer (Irradiance meter) uses a reversed biased Si Photodiode as sensor.

Note that for both measuring devices the Front End circuit is a Photocurrent to Voltage Converter.

The IOIO OTG board is able to handle up to nine A/D converters at the same time.

In Fig. D.2 the Solar Cell I-V Curve Generator schematic diagram is shown.

For a constant light source, the maximum current (short circuit current) is measured as a voltage signal using the photocurrent to voltage converter. This measurement corresponds to the coordinate (Zero Volts, I Maximum). This signal is connected to the A/D 1 converter pin in the IOIO OTG board.

Different current – voltage coordinates are obtained by controlling the voltage Gate – Source of a JFET transistor working in the linear region as variable resistor. See Chapter 2, Section E Numeral 5.

The control signal is generated by a D/A output and is a set of predetermined voltages within a range. For each control signal amplitude, the corresponding Voltage Gate Source is measured in A/D 2 converter.

These two sets of measurements and the short circuit current measured previously conform two paired sets of data. From these sets the I-V curve is generated through software. See the corresponding section in Chapter 4.

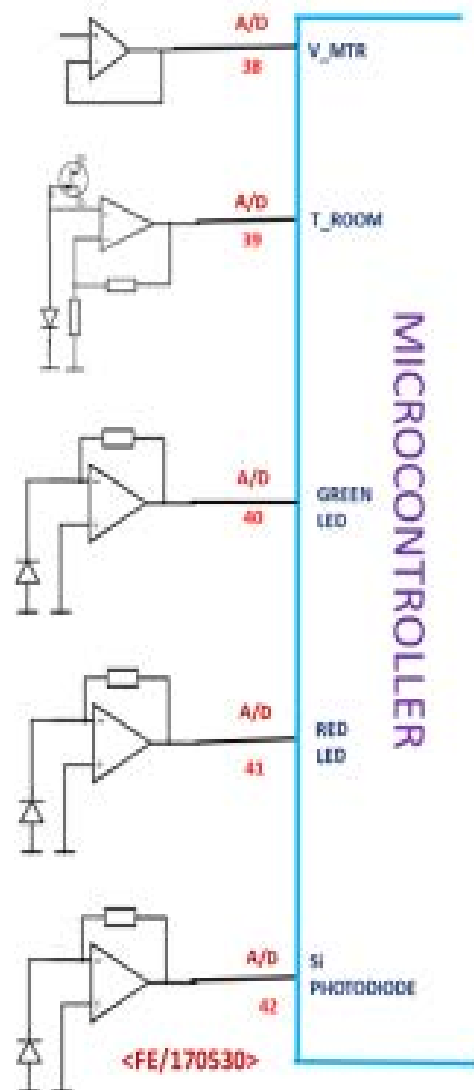


**Figure D.1:** Schematic diagrams for Voltmeter, Thermometer, Spectral Temperature and Irradiance meters.

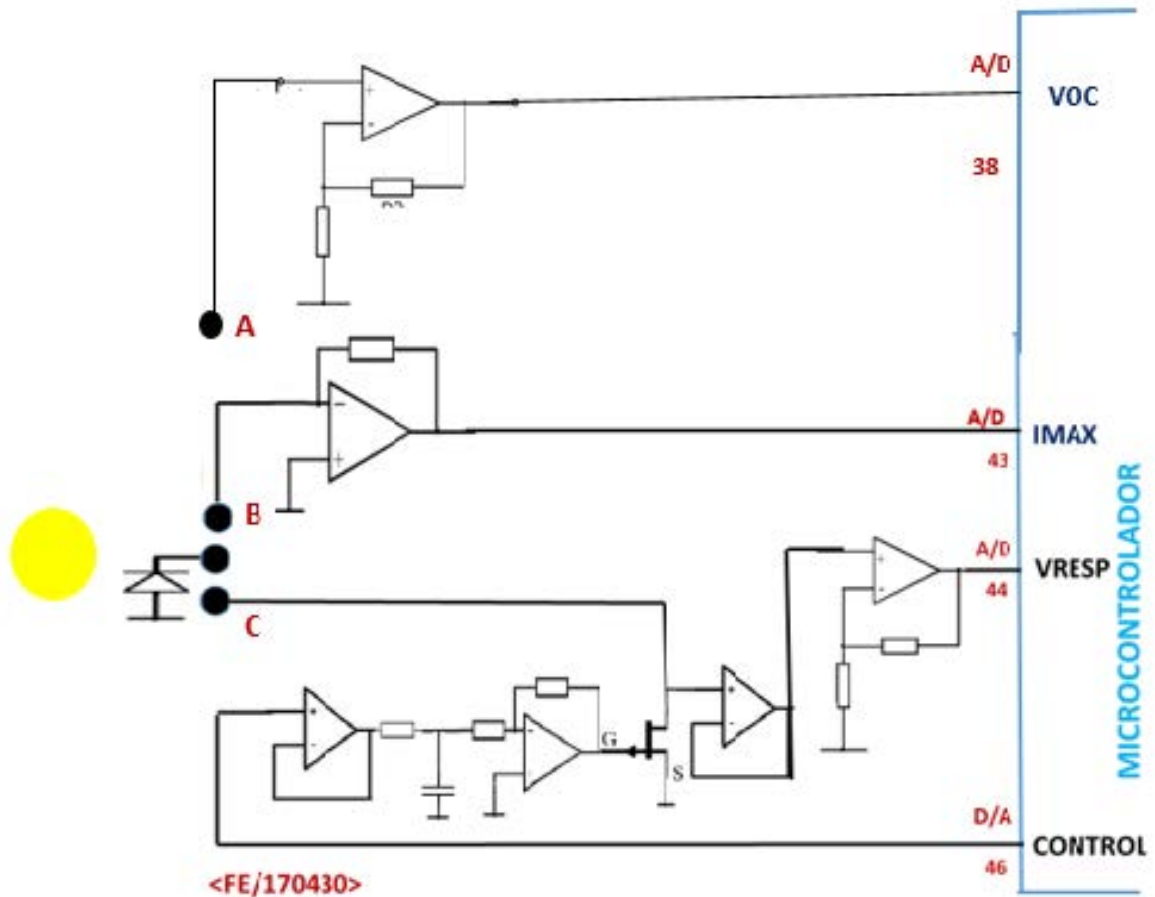


**Figure D.2:** Schematic diagram for the Solar Cell I-V Curve Generator

### 3. DATA STORAGE FOR EACH APPLICATION

Acquisition Data corresponding to those front end circuits here described are obtained through the IOIO OTG board interfaced to an Android Studio Device.

Data is stored in dedicated files for each device. These files are located in Internal Memory or in the SD Card memory plugged in the Android Device.

It is important to highlight that these stored data in the SD Card is also available from the Android HP 48GX or HP 50G emulators embedded in the Android Device.

In those emulators, dedicated routines for each Virtual Instrument have been developed. These routines take acquisition data stored in the SD Card and process it. The final product of the whole process is the corresponding measurement in tabular and / or graphic form.

Chapter 4 deals about this software that completes a set of virtual instruments for photovoltaic measurements.



## E. ANDROID ↔ WINDOWS DATA TRANSFER TRANSPARENCY

During development it was necessary to implement transparency to transfer data from Android operative system to Windows. This task was achieved by superposing operative systems either for an Android device or a PC. Fig. E.1 summarizes these procedures [41], [42], [43], [44].




**Figure E.1:** *Schematic to overlap Android and Windows Platforms*

Nowadays, several software development companies are working to have operative systems that make Windows and Android 100% compatible. These systems will become of general use in the near future [45], [46], [47], [48], [49].



- [14] Ytai / IOIO. Getting To Know The IOIO-OTG Board  
<https://github.com/ytai/ioio/wiki/Getting-To-Know-The-IOIO-OTG-Board>
- [15] Ytai / IOIO Digital I/O  
<https://github.com/ytai/ioio/wiki/Digital-IO>
- 
- [16] Ytai / IOIO Analog Input  
<https://github.com/ytai/ioio/wiki/Analog-Input>
- [17] Ytai / IOIO Pulse Width Modulation Output – PWM  
<https://github.com/ytai/ioio/wiki/PWM-Output>
- [18] Ytai / IOIO. Downloads Drivers Windows  
<https://github.com/ytai/ioio/wiki/Downloads>
- [19] Ytai / IOIO Downloads Section Client Software and IOIO Application Firmware Images  
<https://github.com/ytai/ioio/wiki/Downloads>
- [20] Ytai / IOIO IOIO-OTG Bootloader and IOIODude  
<https://github.com/ytai/ioio/wiki/IOIO-OTG-Bootloader-and-IOIODude>
- 
- [21] lifehacker.com A command Line Primer for beginners  
<http://lifehacker.com/5633909/who-needs-a-mouse-learn-to-use-the-command-line-for-almost-anything>
- [22] Ytai / IOIO. Using IOIO with a PC  
<https://github.com/ytai/ioio/wiki/Using-IOIO-With-a-PC>
- [23] Ytai / IOIO. IOIO Over Bluetooth for Android  
<https://github.com/ytai/ioio/wiki/IOIO-Over-Bluetooth>
- [24] Ytai/IOIO. IOIO Over Bluetooth for PC  
<https://github.com/ytai/ioio/wiki/IOIO-Over-Bluetooth-for-PC>
- [25] Ytai/IOIO Devices With USB OTG Host Mode Support  
<https://github.com/ytai/ioio/wiki/Devices-With-USB-OTG-Host-Mode-Support>
- [26] Ytai/IOIO. IOIO Over OpenAccessory  
<https://github.com/ytai/ioio/wiki/IOIO-Over-OpenAccessory>
- [27] stackoverflow What is the difference between USB host and USB Accessory?  
<http://stackoverflow.com/questions/17140598/what-is-the-difference-between-usb-.host-and-usb-accessory>

- [28] Greg Millette, Professional Android™ Sensor Programming  
Adam Stroud Part II INFERRING INFORMATION FROM PHYSICAL SENSORS  
Chapter 10: Android Open Accessory pgs. 189 – 191  
Published by John Wiley & Sons, Inc. Indianapolis, Indiana  
2012 Available also through: [www.it-ebooks.info](http://www.it-ebooks.info)
- [29] Wikipedia Word: Android Studio  
[https://en.wikipedia.org/wiki/Android\\_Studio](https://en.wikipedia.org/wiki/Android_Studio)
- [30] Android Android Developers Blog  
<http://android-developers.blogspot.com.es/2016/04/android-studio-2-0.html>
- 
- [31] Oracle Java SE Development Kit 8 Downloads  
<http://www.oracle.com/technetwork/java/javase/downloads/jdk8-downloads-2133151.html>
- [32] Wikipedia Word: IntelliJ IDEA  
[https://en.wikipedia.org/wiki/IntelliJ\\_IDEA](https://en.wikipedia.org/wiki/IntelliJ_IDEA)
- [33] Server Side Java Development Kit Definition  
<http://www.theserverside.com/definition/Java-Development-Kit-JDK>
- 
- [34] Wikipedia Word: Maven  
[https://en.wikipedia.org/wiki/Apache\\_Maven](https://en.wikipedia.org/wiki/Apache_Maven)
- [35] Tutorials Point What is a Maven Repository?  
[http://www.tutorialspoint.com/maven/maven\\_repositories.htm](http://www.tutorialspoint.com/maven/maven_repositories.htm)
- 
- [36] Ytai/IOIO. Building IOIO Applications with Gradle  
Ytai Ben-Tsvi edited this page on Aug 20, 2015 · [2 revisions](#)  
<https://github.com/ytai/ioio/wiki/Building-IOIO-Applications-With-Gradle>
- [37] Sparkfun IOIO-OTG Hookup Guide  
CONTRIBUTORS:  [JOEL E. B. YTAI](#)  
<https://learn.sparkfun.com/tutorials/ioio-otg-hookup-guide>

- [38] Ytai/IOIO. IOIO Bridge  
<https://github.com/ytai/ioio/wiki/IOIO-Bridge>
- 
- [39] Ytai/IOIO IOIO Lib Basics  
<https://github.com/ytai/ioio/wiki/IOIOLib-Basics>
- [40] Ytai/IOIO IOIOLib Application Framework  
<https://github.com/ytai/ioio/wiki/IOIOLib-Application-Framework>
- 
- [41] Ytai/IOIO IOIO Lib Core API  
<https://github.com/ytai/ioio/wiki/IOIOLib-Core-API>
- [42] Ytai/IOIO Downloads  
<https://github.com/ytai/ioio/wiki/Downloads>
- [43] REMIX OS <http://www.jide.com/remixos>
- [44] UBUNTU <https://www.ubuntu.com/>
- [45] Wine HQ <https://www.winehq.org/>
- [46] VMware  
[https://my.vmware.com/en/web/vmware/info/slug/desktop\\_end\\_user\\_computing/vmware\\_workstation\\_pro/14\\_0](https://my.vmware.com/en/web/vmware/info/slug/desktop_end_user_computing/vmware_workstation_pro/14_0)
- [47] Wikipedia Word: Cross-platform  
<https://en.wikipedia.org/wiki/Cross-platform>
- [48] Microsoft Cross-platform mobile development in Visual  
<https://msdn.microsoft.com/en-us/library/dn771552.aspx>
- 
- [49] DZone Phone Apps Best Cross-Platform Technologies For iOS, Android, and Windows  
<https://dzone.com/mobile-app-developer-tutorials-tools-news>

## Basic References

- | 1 | Greg Millette, Adam Stroud  
**Professional  
Android™ Sensor Programming**  
Published by John Wiley & Sons, Inc.  
Indianapolis, Indiana 2012  
Available also through: [www.it-ebooks.info](http://www.it-ebooks.info)
  
- | 2 | Android Studio The Official IDE for Android  
<https://developer.android.com/studio/index.html>
  
- | 3 | **Android Studio  
User Guide**  
<https://developer.android.com/studio/intro/index.html>
  
- | 4 | **IOIO  
Documentation**  
<https://github.com/ytai/ioio/wiki>
  
- | 5 | **PIC24F Family Reference Manual | Microchip**  
<http://www.microchip.com/forums/m558417.aspx>
  
- | 6 | **Java SE Development Kit 8 Downloads (JDK)**  
<http://www.oracle.com/technetwork/java/javase/downloads/jdk8-downloads-2133151.html>
  
- | 7 | **The Java™ Tutorials**  
<http://docs.oracle.com/javase/tutorial/>

| 8 | **Gradle Beyond the Basics**

First Edition

**Tim Berglund**

Editorial: O`REILLY July 2013

| 9 | **Gradle Recipes for Android**

First Edition

**Ken Kousen**

Editorial: O`REILLY June 2016

---

*CHAPTER 4*

*MEASUREMENT AND*  
*EVALUATION*

*USING PROGRAMMABLE*  
*GRAPHIC*  
*EMULATOR CALCULATORS*

---





## OUTLINE OF THE CHAPTER

- A) HP 48 GX AND HP 50G AND THEIR EMULATORS
  - 1. HP48 GX AND HP50G CALCULATORS
  - 2. HP48 GX AND HP50G EMULATORS
  - 3. HP48 GX AND HP50G EMULATORS FOR ANDROID DEVICES
- B) COMMON TOPICS RELATED TO ALGORITHMS
  - 1. A/D CONVERSION AND DC VOLTMETER
  - 2. PHOTOCURRENT MEASUREMENTS
  - 3. PHOTOCURRENT TO ENERGY CONVERSION FOR A MONOCHROMATIC SOURCE
  - 4. LIGHT SENSORS ACTIVE AREA
  - 5. LIGHT SPECTRUM PHOTOCURRENTS AND RESPONSIVITY
  - 6. D/A CONVERSION AS A CONTROL TOOL
  - 7. SENSORS AND FRONT END CIRCUITS CALIBRATION
  - 8. VIRTUAL INSTRUMENTS GENERAL SUPPORTS

## DESCRIPTION OF ALGOTRITHMS FOR VIRTUAL INSTRUMENTS

- C) ENVIRONMENTAL THERMOMETER
- D) THERMAL RADIATION: SPECTRAL TEMPERATURE AND IRRADIANCE METERS
- E) SOLAR CELL I – V CURVE GENERATOR
- F) SUMMARY OF VIRTUAL INSTRUMENTS MEASUREMENTS AND EVALUATION

Bibliography

Basic References



## **CHAPTER 4: MEASUREMENT AND EVALUATION USING PROGRAMMABLE – GRAPHIC EMULATOR CALCULATORS**

This Chapter is related to the EMU 50G emulator embedded in the Android Device and describes the algorithms used to handle the data acquired from the front end circuits through the microcontroller and stored in the Android device memory files.

This chapter is divided in six sections.

### **Section A:**

The HP 48 GX and HP 50G programmable and graphical calculator emulators are described.

### **Section B:**

Common topics related to the algorithms used to implement the virtual instruments for this work are presented. Results of measurements are provided either as numerical or as graphical parameters in the appropriate [SI] units.

### **Section C:**

Algorithms to implement the virtual thermometer are explained.

### **Section D:**

Algorithms to implement the virtual instruments to measure thermal radiation are explained. Two concomitant parameters are measured: spectral temperature and irradiance.

### **Section E:**

Algorithms to implement the virtual solar cells I-V curve generators and related parameters are explained.

### **Section F:**

General idea of virtual instrument is summarized.



## A. HP 48 GX AND HP 50G AND THEIR EMULATORS

### 1. HP48 GX AND HP50G CALCULATORS

The **HP 48GX** is a graphical and programmable calculator produced by Hewlett-Packard from 1990 until 2003. It is essentially an advanced and dedicated pocket computer to solve mathematical, mathematical-physics and logical tasks. A summary of its specifications is found in [1].

**Basic Reference | 1 |**: **HP 48G Series User's Guide** is a downloadable complete copy of the eighth edition of the 48G series instruction manual. This PDF document has 612 pages and it is a useful reference to learn how to use this calculator.

**Basic Reference | 2 |**: **HP 48G Series Advanced User's Reference Manual** is also a downloadable and complete copy of the fourth edition of the HP 48G Series Advanced User's Reference Manual. This PDF document has 764 pages and is a reference for programmers, it includes a dictionary-like of the HP 48GX commands and examples of their use.

The **HP 50G** is the actual successor of the HP 48GX. The first calculator of this series, the HP 49G was released on August 1999. A worldwide announcement regarding the availability of this calculator was made by HP in September 2006, and official details are available on the [HP calculator's](#) webpage. The calculator was discontinued in 2015. A summary of its specifications is found in [2].

**Basic Reference | 3 |**: **HP 50g User's Guide** is a downloadable and complete English-language 887-page user's guide for the HP 50g.

**Basic Reference | 4 |**: **HP 50g / 49g+ / 48gII graphing calculator advanced user's reference manual**, Edition 2 HP. Printed Date: 2009/7/14 is a 693 pages advanced manual for programmers.

All these | 1 | to | 4 | **Basic References** are free downloadable manuals.

**Basic Reference | 5 |**: **hpcalc.org**

This site is the main repository of programs and information about hp programmable graphic calculators. It is the premier source of software for and information about the HP Prime, HP 50, HP 49, HP 48, and HP 28 RPN programmable graphic calculators and the HP 38G, HP 39, and HP 40 programmable graphic calculators, with 7625 files by 2307 authors and 3204 screenshots totaling 961.81MB.

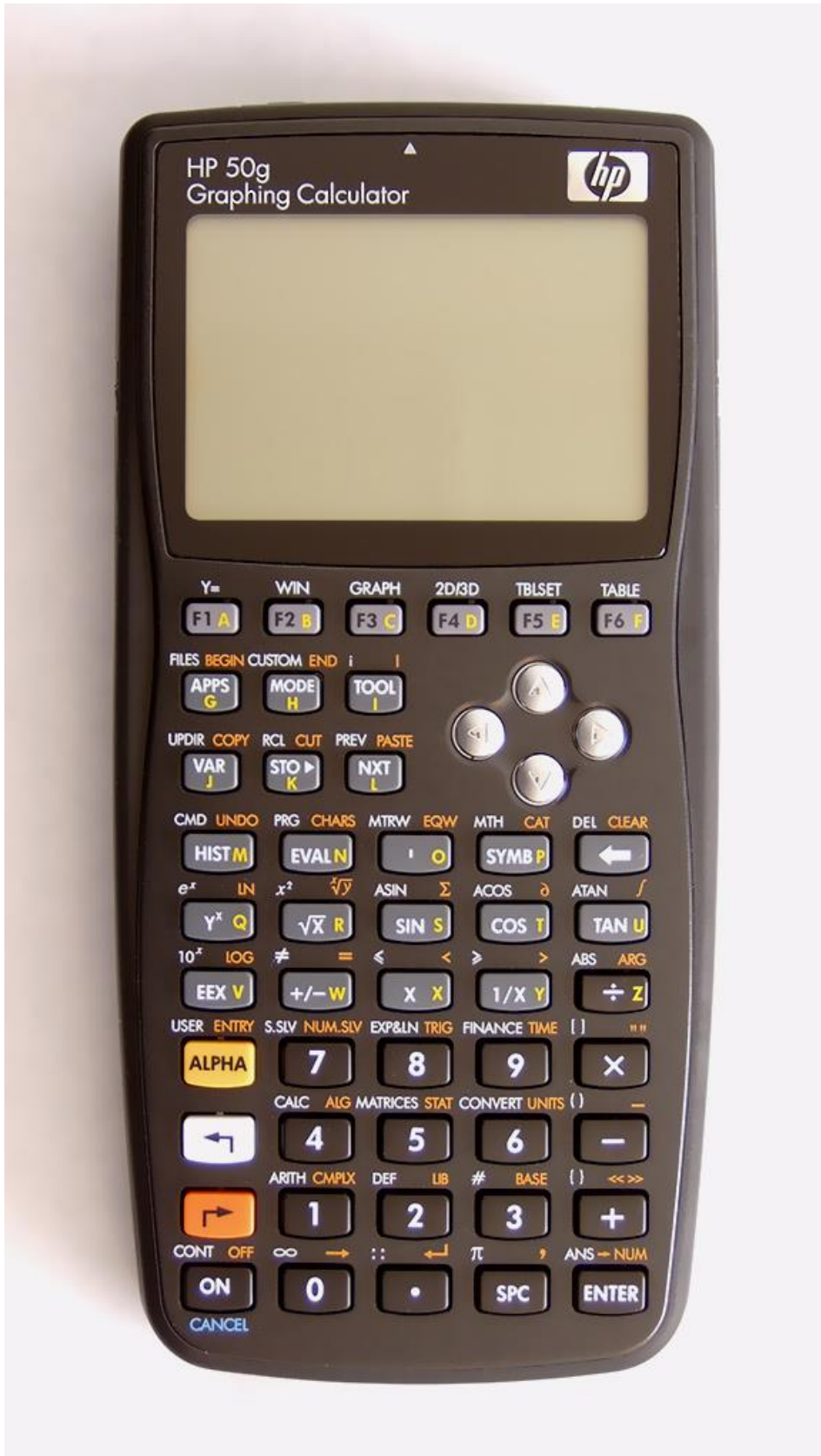
Finally:

Fig. A.1 is a photography of the HP 48GX pocket calculator.

Fig. A.2 is a photography of the HP 50G pocket calculator.



**Figure A.1:** *HP 48GX photography.*  
[Figure adapted from reference shown in ANNEX F]



**Figure A.2:** *HP 48GX photography.*  
[Figure adapted from reference shown in ANNEX F]



## 2. HP48 GX AND HP50G EMULATORS

HP48 GX AND HP50G calculators are available as emulators for several operative systems.

In **computing**, an **emulator** is hardware or software that enables one computer system (called the *host*) to behave like another computer system (called the *guest*). An emulator typically enables the host system to run software or use peripheral devices designed for the guest system. [3]

There are several [emulators](#) available for the HP 49G calculator. A version of EMU48 is available in the Debug4x<sup>[13]</sup> [IDE](#) that allows emulation of most of the features of the 49g+/50g, but will not execute any ARM-based code.

An ARM-based emulator, x49gp,<sup>[14]</sup> has been released and allows the true emulation of the 49g+/50g ARM processor and successfully runs HPGCC 2 and 3 compiled programs. The emulator is only available for [Linux](#) and [Mac OS X](#) and must be compiled from the source. (See [README.QUICKSTART](#) for details.)

The commercial version of the application EMU48 also supports HP 49G. So far, there are no 49g+/50g emulators for smartphones with the exception of HP 50g<sup>[15]</sup> for iPhone and iPad released in October 2012.

An emulator for [Microsoft Windows Mobile](#) (PPC, smartphones) is available.<sup>[16]</sup>

Other 49G/49g+/50g emulators for Android (without ARM support).<sup>[17]</sup>

In 2012, Hewlett-Packard released an emulator named *HP 50g Virtual Calculator* (version 3.1.29/3.1.30 with firmware 2.16 and support for the [StreamSmart 410](#)) for Windows

**Updates:** The 49/50 series allows the user to update the firmware to gain enhanced features or bug fixes. Official firmware updates are released by Hewlett-Packard. Unsupported unofficial firmware updates are also available at sites such as [hpcalc.org](#). [4]

## 3. HP48 GX AND HP50G EMULATORS FOR ANDROID DEVICES

Although there are two emulators for HP 48GX or HP 50G for Android Devices, no explicit instructions to transfer data acquired from Android devices through the microcontroller has been found. This circumstance has oriented our effort to superpose operative systems that allow a transparent flow of data from Android to Windows. See Chapter 3, Section E.

As references two emulators for HP 48GX and HP 50G are mentioned here:

**Droid48** from [Arnaud Brochard](#): Emulator of the HP 48 scientific calculator, using RPN. [5] with its mate **Droid Reader** [6] emulate HP 48GX in Android Devices in a fluent manner. See Fig. A.3.

Emu 50G [7] emulates HP 50G for Windows Devices. See Fig. A.4.

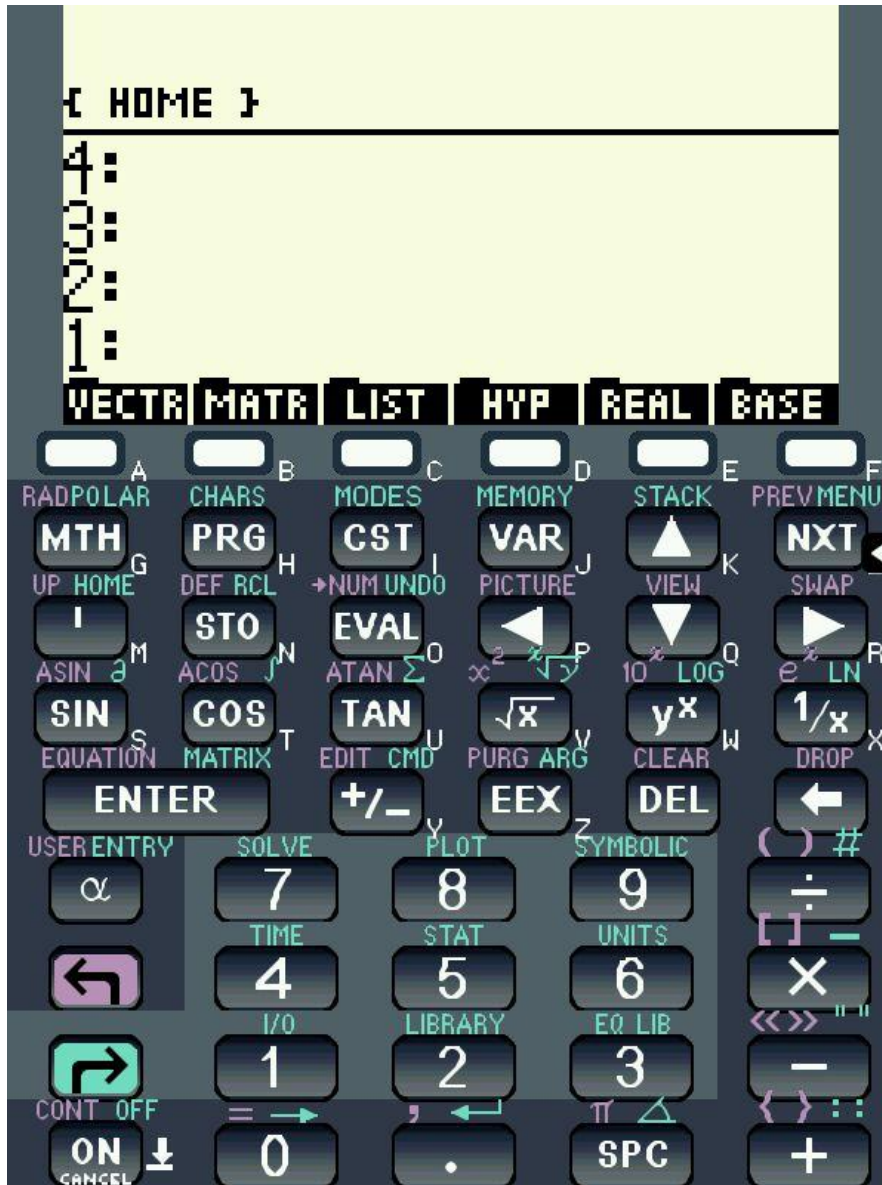


**Figure A.3:** Screenshot of Droid48 mask emulator. Its mate for data/routines transfer is Droid48 Reader.

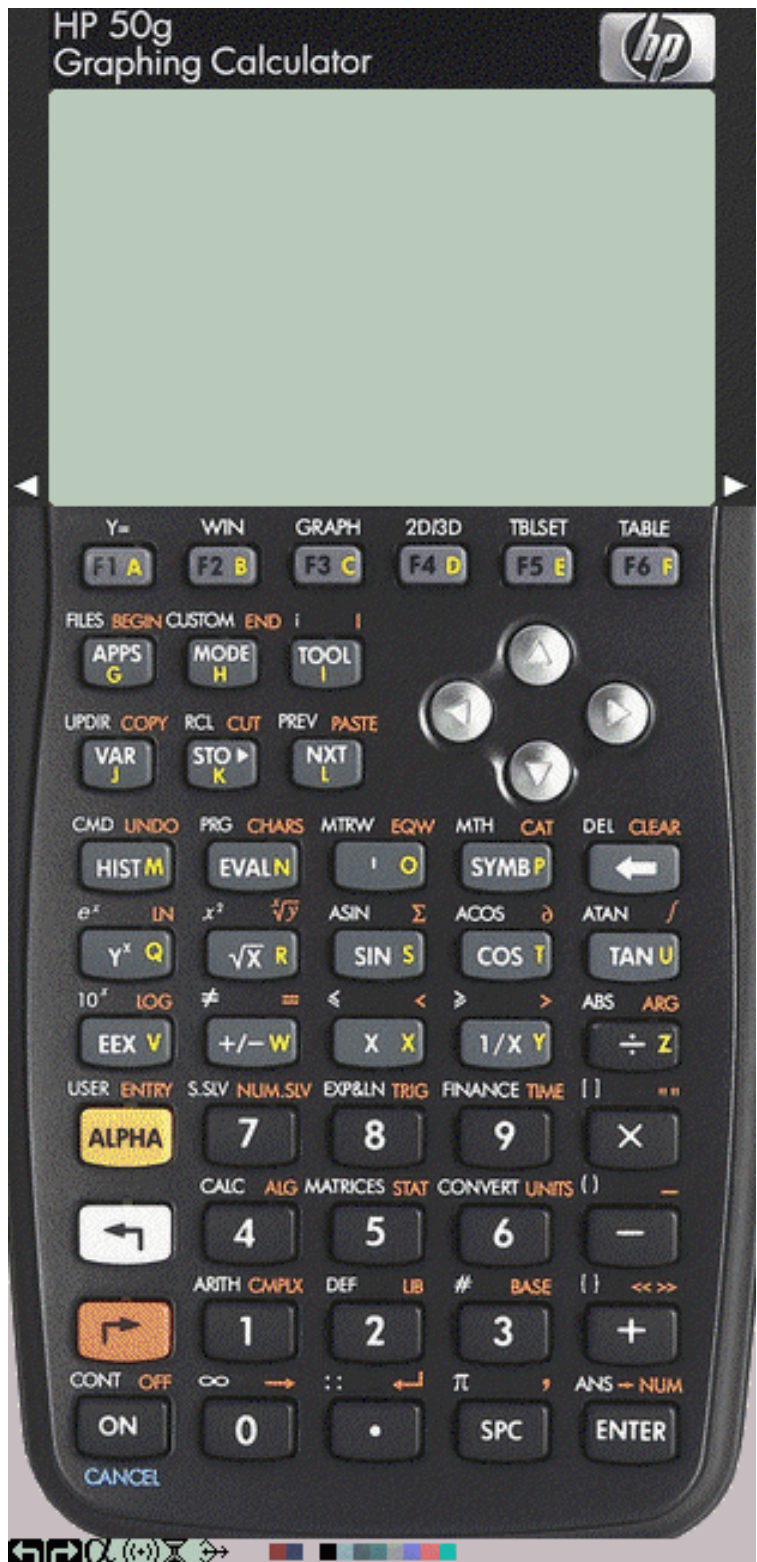


Figure A.4: Screenshot of EMU50G mask for Windows

## **B. COMMON TOPICS RELATED TO ALGORITHMS**

In this Section common issues that concern to algorithms for the virtual instruments developed here are discussed.

In Section C, this preliminary ideas will be referred or developed in more detail in the numeral corresponding to each instrument.

### **1. A/D CONVERSION AND DC VOLTMETER**

#### **G) Data Acquisition Source**

Every instrument in this project depends on a voltage measurement. Front End circuits produce an Analog voltage signal corresponding to the physical parameter being sensed.

#### **H) Data is acquired through A/D Conversion using IOIO OTG board**

An Analog Voltage signals is connected to an A/D input in the IOIO OTG board. This signal is sampled and converted to a digital count or binary number.

The IOIO OTG board is interfaced to an Android Device. Acquired Digital Counts are stored either in the internal memory or external SD Card Flash Memory.

#### **I) Counts to Voltage Conversion and Calibration**

The embedded Emu 48 in the Android device accesses to de acquired data stored in the SD Card Flash Memory and takes it as data to be handled by an appropriate routine to report the measurement in the corresponding SI unit.

Since the relationship between the amplitude of sampled voltage and counts is linear, a preliminary calibration is required to convert counts in a voltage measurement.

This idea is explained in more detail.

#### **The A/D Converter in the PIC 24F microcontroller**

The A/C circuit in the PIC24F microcontroller is a 10 bits A/D converter. This means that there are 1024 levels in 3.3 V or about 1000 levels with a resolution of  $\approx 3$  mV /level.

The 10-bit A/D Converter module accepts a single analog signal at any instant and converts it to a corresponding 10-bit digital value. The microcontroller accommodates up to 16 analog inputs and separate reference inputs; the actual number available on a particular device depends on the software characterization.

The heart of the module is a Successive Approximation Register or (SAR) type of A/D Converter [8]

### The A/D process and Nyquist Sample criterion

An internal Sample-and-Hold (S/H) amplifier acquires a sample of an input signal, then holds that value constant during the conversion process.

Conversion Speeds of up to 500 ksp/s ( $500 \times 10^3$  samples / second) [9]

**Nyquist Criterion** is often stated as

$$f_s > 2B \quad (B.1)$$

Where:

$f_s$  is the sampling frequency [number of samples/s]

$B$  is the Bandwidth of the input signal [Hz = 1/s]

And  $2B$  is called the **Nyquist rate** for functions with bandwidth  $B$ . When the Nyquist criterion is not met ( $B > \frac{1}{2} f_s$ ), a condition called **aliasing** occurs, which results in some inevitable differences between  $x(t)$  and a reconstructed function that has less bandwidth. In most cases, the differences are viewed as distortion. [10]

**Comment:** Since the time varying signals in this project are slow varying signals, their frequency band is very low when comparing these bandwidth with the number with the conversion speed of the A/D converter in the microcontroller, one realizes that the sampled signal distortion is neglect able compared with the analogue input signal. See Fig B.1

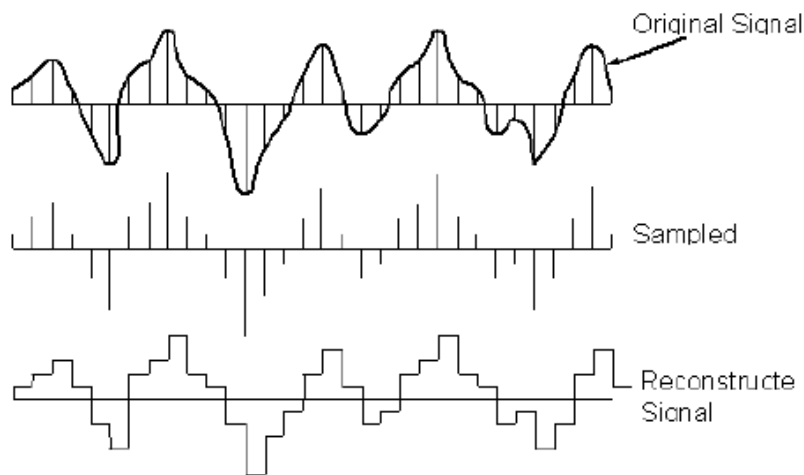


**Figure B.1:** The original signal (analog signal) is sampled and reconstructed from sampled amplitudes. For sampling frequencies higher than twice the frequency band of original signal, the reconstructed signal resembles the original signal (Nyquist sampling criterion). The reconstructed signal distortion is neglect able if sampling frequency is much higher than Nyquist frequency. [Figure adapted from reference shown in ANNEX F]

### Voltage Calibration

By measuring two sets of counts using two stable DC voltages (as example from electrochemical batteries), one corresponding to the lower level (few mVolts) and the other close to 3.0 V, it is possible to calibrate de microcontroller DC voltmeter calculating the slope  $m_0$  and the intersection point with the abscissa  $h_0$  using the equation of a straight line.

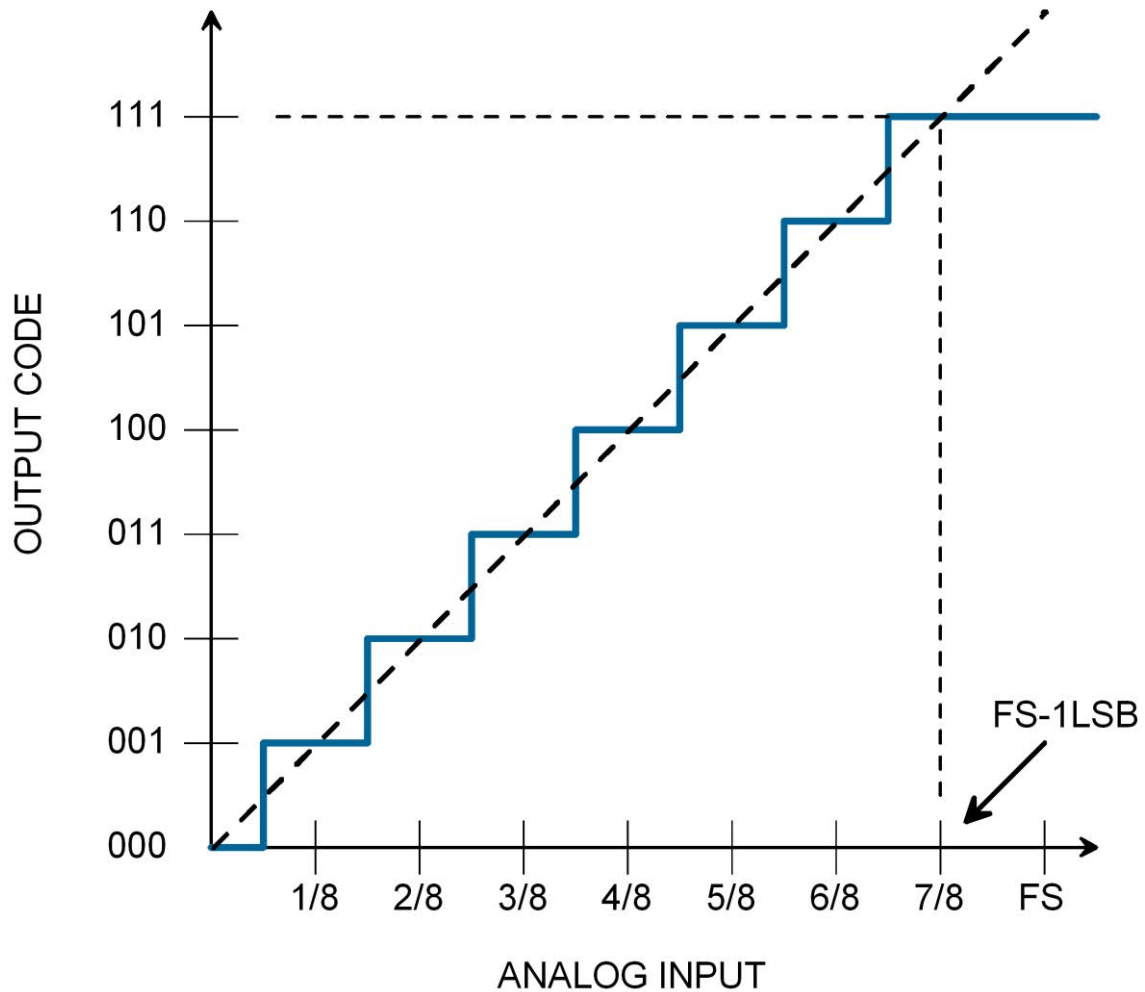


**Figure B.2:** Assuming that the analog input (in volts) is linear with the output code (in counts) Voltage calibration is made obtaining the equation of a straight line  $Voltage = f(counts)$  Then, the slope  $m_0$  and the intersection point with the abscissa  $h_0$  are determined. If  $h_0 < (level\ resolution \approx 3\ mV)$ , then  $h_0$  is neglected. [Figure adapted from reference shown in ANNEX F]

The routine VKLB for Emu 48 has been developed for this purpose.

## Voltage as a fundamental Unit in A/D data acquisition

So, through this procedure, [the fundamental SI unit Volt is established as a measuring unit.](#)

Once the voltmeter has been calibrated it is possible to make voltage measurements. Statistical methods are applicable. See Annex 3.1.

The routine VMTR for Emu 48 has been developed for this purpose.

Many physical units are convertible to Voltage using sensors and front end circuits

It is worthwhile to highlight the fact that many physical units are convertible to voltage through appropriate sensors and front end circuits. The basic relation between the new unit and voltage is obtained from the physics of the sensor and the transfer equations of the front end circuit. These idea is illustrated in Section B in this Chapter.

## 2. PHOTOCURRENT MEASUREMENTS

### a. Voltage to Current Conversion

The Photocurrent to Voltage Converter circuit (See: Chp. 2 Section C.4 and Fig. C.7) produces a voltage output proportional to the input photocurrent. This voltage signal is connected to an A/D input of the IOIO OTG board and it is read as a voltage magnitude following the process explained in previous Section B.1

The Front End circuit transfer function is:

$$I = - V_{OUT} / R \quad (B.2)$$

The emulator Emu48 is able to calculate the photocurrent through a simple subroutine.

### b. Electric Currents expressed through the fundamental electron charge

The electric current SI unit is Ampere. [1 A = 1C / s ]. Where C is the electric charge expressed in Coulombs.

Since the concern of this project is to measure phenomenon related with photoelectric effect, it is useful to express currents using the elementary charge of electrons. The electron's charge  $e^-$  is:

$$e^- = 1.60217733E-19 [C] \quad (B.3)$$

So:

$$I_{(IN\ ELECTRONS / S)} = 6.24150636309 \times 10^{18} [ I_{(IN\ AMPERES)} ] \quad (B.4)$$

### 3. ENERGY OF A PHOTON FOR A MONOCHROMATIC SOURCE

From Chapter 1, Eq. (A.1) and Eq. (A.2), the corresponding energy – in electron-volts – for a photon of a wavelength  $\lambda$  is:

$$E = h \times \left(\frac{c}{\lambda}\right) ; [eV] \quad (B.5)$$

### 4. LIGHT SENSORS ACTIVE AREA

The Active Area of a Light Sensor is the perpendicular surface to an incident light beam in which electric currents are generated by Photoelectric Effect.

#### a. Pre-configuring Active Area in a Light Sensor

Under certain circumstances it is possible to circumscribe the sensor's Active Area by partially covering the sensor with an opaque mask. Then, the sensor Active Area is delimited and its magnitude is known.

#### b. Calculating Active Area in a Light Sensor

On the other hand, there are circumstances in which the sensor's Active Area is not directly measured and it has to be estimated experimentally.

### 5. LIGHT SPECTRUM PHOTOCURRENTS AND RESPONSIVITY

#### a. Light Spectrum of a Planck's Source

It is highlighted that the algorithms developed for light measurement are for thermal radiation sources, i.e.: Light Sources that fulfil the Planck's Equation. Tungsten filament light sources are a good example. See Chapter 1: ANNEX 3.

#### b. Responsivity

Responsivities for Si and Ge photodiodes has been taken from the manufacturer's references. See Chapter 1: ANNEX 1 and ANNEX 2.

Responsivities for LEDs used as sensors have been determined experimentally.

#### c. Photocurrents

Photocurrents have been measured experimentally.

Experimentally measured Photocurrents and Planck's Light Sources Spectra have been correlated through the Sensor's Responsivity equation. See Chapter 1, Section C.3.

$$R_P = \frac{I_P}{W_P} ; [A / W] \quad (B.6)$$



**d. Light Spectrum of a solar simulator lamp**

Fig. B.3 (a) shows the spectrum corresponding to a tungsten filament lamp. In contrast, Fig. B.3 (b) corresponds to the Irradiance obtained from a Xenon arc lamp for a solar simulator [11].

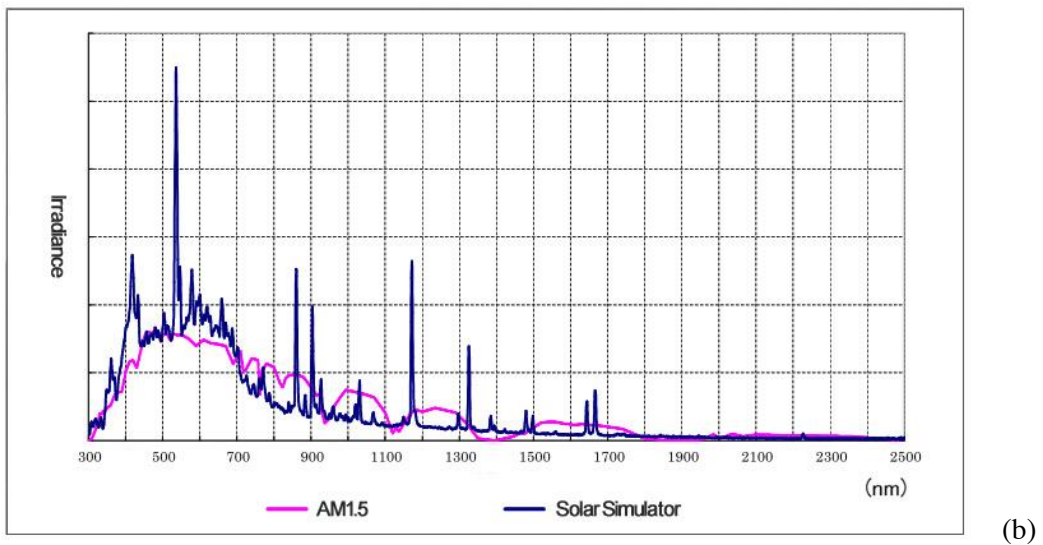
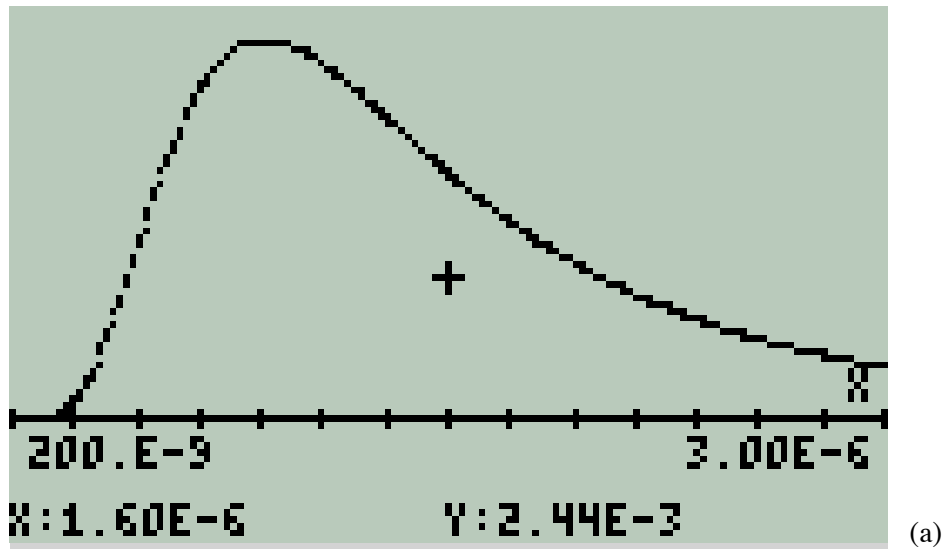


**Figure B.3:** (a) Standard Lamp Spectral Distribution for  $T = 2856$  [K]  
(b) Spectral Irradiance of a Xenon Lamp for Solar Simulator.

It is reasonable to think that Irradiance measurements made for a Xenon lamp spectrum, though representative, should be considered only as referential values.

## **6. D/A CONVERSION AS A CONTROL TOOL**

The possibility to generate a precise and controllable analog output from the microcontroller and apply it to a front end circuit fulfils two purposes: (a) It can be used as a control signal applied to the external circuit. (b) Since it is a precise amplitude signal it can be used as a measurement of the voltage applied to the external circuit pin.

These ideas are applied to the current - voltage curve solar cell circuit.

## **7. SENSORS AND FRONT END CIRCUITS CALIBRATION**

In general, if a sensor or a front end circuit is going to be used as a part of a meter instrument, two criteria prevail:

- Sensors selected for the application from a set of identical specifications (brand, part number, etc.) must have the best measured characteristics in the set.
- Every single sensor or front end circuit must be calibrated individually and have their own calibration constants.

## **DESCRIPTION OF ALGORITHMS FOR VIRTUAL INSTRUMENTS**

Next Sections in this chapter describe or explain the algorithms developed to obtain a measurement of the physical parameter of interest. Algorithms are developed as routines for the programmable and graphic calculator emulator Emu48 embedded in the Android Device. These routines take data from files stored in the SD Card flash memory of the Android Device. Data stored in the SD Card is acquired from a sensor facing the physical phenomenon. The sensor is part of a front end circuit connected to an IOIO OTG board. The IOIO OTG board is interfaced with the Android Device. So data handled by the Emu48 routines are representative numerical values of the physical phenomenon being measured.

**Two common routines to all virtual instruments have been developed they are:**

### **PLOTS2d**

General Program to dimension the HP50G emulator Screen for an X Y Plot in Scattering Mode for two lists of data of equal SIZE. The dimensioning of screen to input data and its display is made automatically.

**vmtr**

This is a simplified routine of VMTR, it is used to measure voltage signals from A/D inputs for the microcontroller. Using **vmtr** allows to obtain calibrated voltage measurements from external analog signals.

**PLOTS2d** and **vmtr** constitute a set of basic routines installed at **HOME DIRECTORY** in the **HP50G** Emulator. They are not a Directory itself. They are just “general purpose loose routines”. Embedded in these “loose routines” are the Directories for individual Virtual Instruments. So the whole set of virtual instruments share these “loose routines”. Notice that routines in HOME Directory can be used by any Directory installed in Home Directory.

Fig. CR.1 summarizes these ideas.

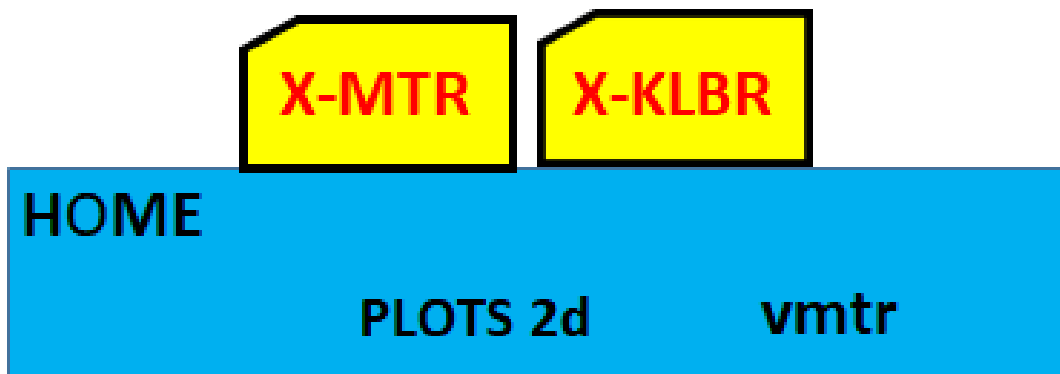


**Figure CR.1:** *PLOTS2d* and *vmtr* are a set of basic routines installed at **HOME DIRECTORY** in the **HP50G** Emulator. They are not a Directory itself. They are just “general purpose loose routines”. Embedded in these “loose routines the Directories” for individual Virtual Instruments are installed.

## C. ENVIRONMENTAL THERMOMETER

### 1. Sensor

Signal diodes or the base – collector junction of low power Si metallic case transistors are excellent sensors to measure temperature.

Recall Chapter 2, Section B.1; Equations (B.1) to (B.4).

### 2. Front End Circuit

A low power Si signal diode directly biased connected in series to a constant current source is the front end circuit to measure temperature.

Recall Chapter 2, Section B.1 and Fig. E.1

### 3. Algorithm Explanation

Starting in equations in Chapter 2, Subsection B.1:

Replace Silicon Parameters from Eq. (B.4) in Eqs. (B.1) to (B.3)

Replace numerical values of physical constants in (B.1) to (B.3)

Substitute Eq. (B.2) and Eq. (B.3) in Eq. (B.1)

The resultant expression is a function of  $I$  (the current through the junction in [A]),  $V$  (the voltage drop along the junction in [V]) and  $T$  (the Absolute Temperature in [K]). This expression depends also of constant  $k_2$ , it is a material's constant independent of temperature.

Measure the current flowing through the junction provided that it is generated from a constant current source and replace its value in the last obtained equation.

Then the present equation depends only on  $V$ ,  $T$  and  $k_2$ .

Following these procedure two routines were developed:

- |          |  |
|----------|--|
| TKLB:    | Routine for temperature calibration  |
| TMTR:    | Routine for temperature measurement once the virtual instrument has been calibrated. |
| Comment: | This thermometer is also useful to measure cryogenic temperatures.                   |

#### 4. Experimental Results

Introduce the junction in an environment where temperature is accurately known and measure the voltage drop in the junction. Under these conditions it is possible to calculate parameter  $k_2$ . Then the temperature front end circuit is calibrated.

Table C.1 shows the voltage drop in the silicon junction for three signal diodes when they are submerged in liquid nitrogen and boiling water as temperature references.

**Table C.1 Junction Voltage for liquid nitrogen  
Temperature and boiling water temperature.**

<b>Junction Code</b>	<b>V<sub>low</sub></b> <b>(77.26[K])</b> <b>[V]</b>	<b>V<sub>high</sub></b> <b>(373.16[K])</b> <b>[V]</b>
A	0.990	0.174
B	0.992	0.176
C	0.983	0.175

Note: For 10  $\mu$ A constant current source

#### 5. Example

For a forward biased Si junction using a constant current source of 9.5  $\mu$ A immersed in an environment at 273.16 K a voltage drop through the junction of 0.722 V was measured. So, the calculated constant is  $k_2 = 3.45047488397 \times 10^{-5}$ . When the junction was exposed to environment and thermal equilibrium was obtained, the voltage drop across the junction was 0.716 V that is equivalent to 294.791 K or 21.63 Celsius.

## **D. THERMAL RADIATION MEASUREMENTS: SPECTRAL TEMPERATURE AND IRRADIANCE METERS**

Irradiance and Spectral Temperature are concomitant parameters. For a Planck's source, if spectral temperature is known, numerical values for the whole irradiance spectrum can be generated using equation  $F_{\lambda}(T, \lambda)$ . If Irradiances are known for delimited Spectral Bands of a Planck's Spectrum then its Spectral Temperature is calculable.

If a light source emits radiation in vacuum only its Irradiance decreases with the square distance from the source, but the spectral distribution remains.

Spectral distribution of light changes when it interacts with matter. Then changes in the spectral distribution of light constitute a valuable tool to learn the mechanisms behind the interaction.

### **D.1. IRRADIANCE METER (PYRANOMETER)**

The purpose of this section is to structure a simple device capable of measuring Irradiance from a light source that meets the Planck distribution. Recall Section B in this Chapter, particularly Subsections B.2 to B.5.

#### **1. Sensors**

Reverse biased LEDs Si or Ge photodiodes used as wide spectral windows are the sensors for this application. A Si photodiode is preferable for the Visible Spectral Region and a Ge photodiode is more appropriate for the Infrared Range. Recall Chapter 2, Sections C.2 and C.3.

Fig. C.6 in Chapter 1 illustrates the Absolute Spectral Irradiance for Si and Ge photodiodes.

In this prototype a Si photodiode has been selected as sensor.

#### **2. Front End Circuit**

It is a photocurrent to voltage converter. See Chapter 2, Section E.4 and Fig. E.3.

#### **3. Algorithm Explanation**

##### **Key Ideas**

Spectral irradiance, sensor's spectral responsivity and measured spectral photocurrents are interrelated parameters through the responsivity equation. Please see Chapter 1, Section C.3.

If spectral irradiance is known as a function of wavelength with high resolution (i.e.: 10 [nm]), total irradiance is, practically, its summation.

Similarly, if spectral photocurrents vs wavelength are known with identical resolution (i.e.: 10 [nm]), for identical wavelength values, then total photocurrent is, practically, its summation.

Measured total photocurrents depend on the sensor's active area.

Total photocurrents measured with photodiodes is linear with light intensity (or total irradiance) in a wide range of several decades. It is limited by noise at its lowest threshold and by saturation at its highest threshold.

For a detailed explanation of this behaviour, please refer to Chapter 1, Sections C.4 and C.5.

### Prerequisites

- Measurement is made with a Si photodiode as example
- Radiation source is a Planck's source
- Spectral temperature is known (either from direct measurement of spectrum as it is explained in Chapter 1, Section C.4. For this Section, the selected Spectral Temperature is  $T_{SP} = 3175$  [K].
- Absolute Responsivity of Si Photodiode is known: Resolution = 10 [nm]. Detection Band  $400 < \lambda < 1100$  [nm]. See Chapter 1, ANNEX 2 and ANNEX 3.

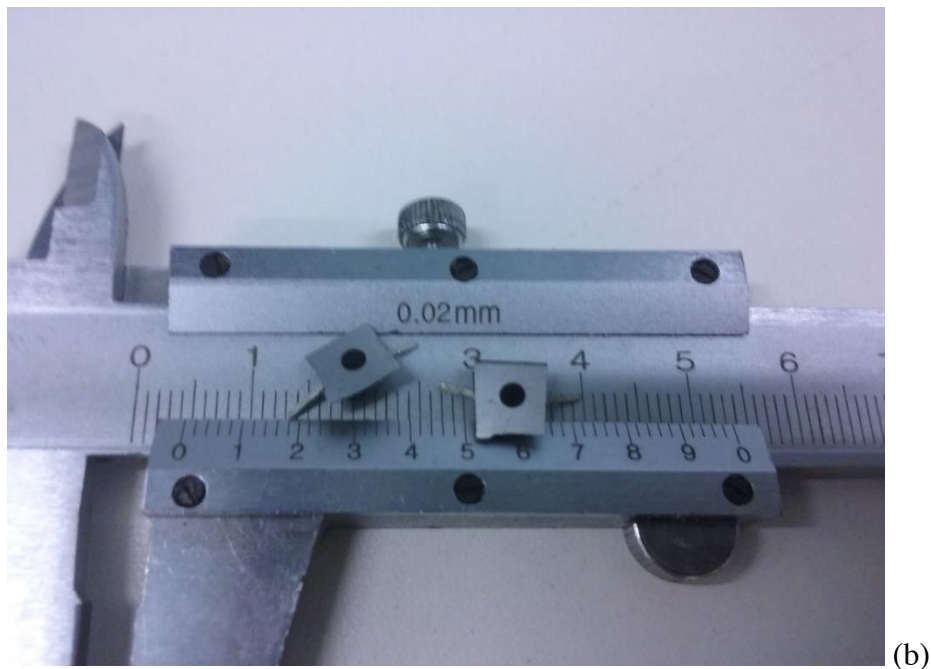


Figure D.1: (a) Planar Si photodiodes. (b) A planar Si photodiode adapted with a mask to measure Total Irradiance.

## Sequence and Results

### Reasoned Sequence Steps

- 1) Total photocurrent is measured using a current to voltage converter
- 2) Photocurrent is scaled to an Active Area = 1 [mm<sup>2</sup>]
- 3) Since Spectral Temperature is known,  $F0\lambda(3175 [K] , \lambda )$  is generated with a resolution of 10 [nm] in the same values of  $\lambda$  than those used to obtain absolute responsivity. This standardized spectrum corresponds to a total Irradiance of 1 [mW / mm<sup>2</sup>] (1 Technical - Sun). This parameter is taken as reference.
- 4) The subset of the standardized spectrum coinciding with the Absolute Responsivity of Si Photodiode is: a) obtained as a sub-array and b) The sub-array summation is evaluated and corresponds to total Irradiance impacting 1mm<sup>2</sup> in the band of active area of the Si photodiode for (1 technical sun) irradiance. This is a fraction of the previous one in step (3).
- 5) The spectral current for 1 sun (technical) Irradiance in the band of active area of the Si photodiode is calculated using equation:

$$I_{p-Si} = W_{p-Si} R_{p-Si} \quad [A]$$

(D.1)

It represents the standardized spectral current. Its summation represents the standardized total current.

- 6) The quotient  $Q_{Ip}$  is calculated by dividing scaled photocurrent from step (2) by standardized total current from step (5) :

$$Q_{Ip} = \frac{\textit{Measured Photocurrent scaled to 1mm}^2}{\textit{Normalized Total Current}} \quad [\textit{Dimensionless}]$$

(D.2)

- 7) Since the photodiode current is linear with incident irradiance; when factor  $Q_{Ip}$  multiplies the subset of spectral current irradiance in the band of active area of the Si photodiode (Step 5), the spectral distribution corresponding to the “actual” measurement is obtained.

$$I_{p-Si-Measured} = Q_{Ip} W_{p-Si} R_{p-Si} \quad [A]$$

(D3)

- 8) The corresponding measured spectral irradiance is



$$\begin{aligned}
W_{p-Measured} &= \frac{I_{p-Si-Measured}}{R_{p-Si}} \\
&= \frac{Q_{Ip} W_{p-Si} R_{p-Si}}{R_{p-Si}} = Q_{Ip} W_{p-Si} \quad [W]
\end{aligned}$$

(D.4)

and its summation is the total measured spectral irradiance.

- 9) As conclusion, the corresponding measured spectral irradiance and total spectral irradiance are obtained by multiplying the factor  $Q_{Ip}$  by the corresponding subset of the Si photodiode normalized spectral or total irradiance.
- 10) Now, since the total irradiance spectrum is a Planck's spectrum, and the measurement is limited by the responsivity of the Si photodiode, the  $Q_{Ip}$  factor could be extrapolated to the complete spectrum. It is more, since the complete spectrum is normalized to 1 [mW / mm<sup>2</sup>], the  $Q_{Ip}$  factor could be "dimensioned" in [mW / mm<sup>2</sup>] providing the measured spectral and total irradiance in the geometry defined for the "actual" measurement.

### Practical Sequence

- 1) The sequence follows identically the steps 1 to 6 in the previous sequence to obtain  $Q_{Ip}$  factor
- 2) Factor  $Q_{Ip}$  in [mW / mm<sup>2</sup>] corresponds to the **measured total irradiance**. Similarly, factor  $Q_{Ip}$  in [mW / mm<sup>2</sup>] multiplied by  $F0\lambda(T [K], \lambda)$  is the **measured total spectral irradiance** in the geometry defined for the "actual" measurement.

### Software Sequence

- 1) Measure **Actual Photocurrent**
- 2) Scale **actual photocurrent** to an active area of 1 [mm<sup>2</sup>] to obtain **actual scaled photocurrent**
- 3) Generate  $F0\lambda(T [K], \lambda)$  for the known spectral temperature  $T = T_{Sp}$
- 4) Obtain the Subset of  $F0\lambda(T [K], \lambda)$  corresponding to the band of Si photodiode

- 5) Obtain the **normalized spectral current** and its summation, the **normalized total current** in the band corresponding to the Si photodiode.

$$I_{p-Si} = W_{p-Si} R_{p-Si} \quad [A] \quad (D5)$$

Then obtain factor:

$$Q_{Ip} = \frac{\text{Measured Photocurrent scaled to } 1\text{mm}^2}{\text{Normalized Total Current}} \quad [\text{Dimensionless}]$$

(D6)

Finally:

Factor  $Q_{Ip}$  in [mW / mm<sup>2</sup>] corresponds to the **measured total irradiance**. Similarly, factor  $Q_{Ip}$  in [mW / mm<sup>2</sup>] multiplied by  $F0\lambda(T [K], \lambda)$  is the **measured total spectral irradiance** in the geometry defined for the “actual” measurement.

#### 4. Routines

- An Emu48 routine to generate standardized spectrum for a predefined Spectral Temperature in the range 250 – 3000 [nm] with a resolution of 10 [nm] has been developed using function F0λ.
- Digital Files for Si and Ge photodiodes responsivities with a resolution of 10 [nm] have been implemented.
- Appropriate routines for calculations related with equation of responsivity and the process here described have been implemented.

#### 5. Calibration

It was observed that individual photodiodes present different yield when exposed to the same light source and geometry. Since photocurrents measurements are trustable and responsivities are provided by the manufacturer, only one inter-comparison of irradiance is required against a secondary standard when the photodiode in the front end circuit and the secondary standard are exposed to the same light source in identical geometry. Calibration was made using the standard pyranometer in the **ICN2 Laboratory of Nanostructured Materials for Photovoltaic Energy**.

## 6. Numerical Example

Table E.1 summarizes the procedure to Measure Total Irradiance.

Since: a) Si – photodiode spectral responsivity is known. b) The light source spectral temperature is known. c) Total irradiance is measured through the process summarized in Table A.

Then: spectral irradiance is calculable in a straight forward way.

**Table D.1: Experimental Results for total Irradiance using Si Photodiode  
T<sub>SP</sub> = 3175 [K]**

---

Sensor Component:	Si Photodiode (Masked)
Si Photodiode Spectral Bandwidth:	400.0E-9 ≤ λ 1100.0E-9 [m]
Masked Si Photodiode Active Area:	4.144 [mm <sup>2</sup> ]
Measured Photocurrent:	185.32E-6 [A]
Photocurrent / mm <sup>2</sup> *	44.817E-6 [A/mm <sup>2</sup> ]
Normalized Photocurrent **	195.54E-3 [mA/mm <sup>2</sup> ] = 195.54E-6 [A/mm <sup>2</sup> ]
Fraction coef ***	229.20E-3 ≈ 0.229 ≈ 23 %
Calculated Irradiance from Measured Irradiance	97.429E-3 [mW/mm <sup>2</sup> ]
Normalized Irradiance	425.07E-3 [mW/mm <sup>2</sup> ]
Fraction coef	229.20E-3 ≈ 0.229 ≈ 23 %

Comment: Identical to current fraction coef.

**Calculated Total Irradiance            0.229 [mW/ mm<sup>2</sup>]**

---

Notes:

\* Measured Photocurrent / Active Area

\*\* Photocurrent Summation. See Numeral (5)

\*\*\* (Photocurrent / mm<sup>2</sup> / standardized photocurrent)

## 7. Intercomparison and Experimental Results

Thermal Radiation Intercomparison and experimental results are presented in chapter 5 Section A.2.

### D.2. SPECTRAL TEMPERATURE METER (PYROMETER)

The purpose of this section is to structure a simple device capable of measuring the spectral temperature from a light source that meets the Planck's distribution. Recall Section C in chapter 1, particularly Subsections C.2 to C.5.

Although the front end circuit is simple, the procedure to measure spectral temperature is more elaborated.

#### 1. Statement of the Problem

In this Section, a procedure to measure spectral temperature of a Planck's source is developed.

For this purpose, a tungsten filament lamp of a known spectral temperature of 3175 [K] under working conditions was taken as reference.

This lamp – under identical working conditions – was used for two different purposes: 1) To measure spectral photocurrents of a red and green LEDs selected as sensors using a monochromator, and 2) To measure total photocurrents from the same LEDs in a fixed geometry where the distance lamp – sensor was constant in a “dark room”.

In this fixed geometry an Irradiance of **0.229 [mW/mm<sup>2</sup>]** was measured at the measuring position to place the LEDs.

Irradiance was measured using the method described in this Chapter, Section D.1.

Preliminary spectral temperature measurements for the reference lamp were made using spectral measurements made with a Si Photodiode using the monochromator. This procedure allows to know wavelengths and photocurrents measured by the Si photodiode. Since absolute spectral responsivity is known for a Si Photodiode it is possible to calculate Spectral irradiance for different narrow bands delimited by wavelengths. Finally, the ratio between irradiances of two delimited bands allow to calculate spectral temperature using the developed virtual pyrometer routine to be explained later in this section.

The point is that if spectral temperature as well as total irradiance at the measuring point are previously known and, if results obtained through the method using a red and green LEDs here explained, produce consistent results then, two advantages are obtained: 1) The validity of both

approaches is demonstrated, and 2) The possibility to measure spectral temperatures using two colour LEDs instead of using a Monochromator is also demonstrated.

## **2. Sensors**

Reverse biased LEDs used as narrow spectral windows are the sensors for this application. Infrared LEDs, Visible range LEDs or UV LEDs are good candidates depending on the spectral region of interest – ROI.

In this prototype a red LED emitting in the 632 [nm] and a green LED emitting in the 569 [nm] have been chosen. Recall Chapter 2, Section C.1.

## **3. Front End Circuit**

It is a Photocurrent to Voltage Converter. See Chapter 2, Section E.3 and Fig. E.2.

## **4. Algorithm Explanation**

### **Key Ideas**

Spectral temperature is measured from a Planck's distribution spectrum. See Chapter 1, Section A.3 and ANNEX 3.

LEDs can be used as light sensors. See Chapter 2, Section C.1.

LEDs are used as spectral windows since their responsivities are delimited to narrow spectral bands when compared with a Planck's Distribution Spectrum.

The spectral response of LEDs as sensors differs from their spectral emission as light emitters. See Chapter 1, Fig. C.3.

The Spectral Responsivity of LED's has to be determined experimentally

The physical magnitudes directly measurable are spectral and total photocurrents through the front end circuit.

Intercomparison of readings from two different LEDs with different bands response implies to know the magnitude of their active areas as an essential prerequisite.

The quotient between two delimited irradiance bands of the same Planck's spectrum determines its spectral temperature univocally. See Chapter 1, Section A.3.

As in previous topics, the procedure is explained through an example.

### Prerequisites

Three important parameters are required for this task:

- The **spectral distribution of photocurrents** for each LED
- The **active area** for each LED
- The **absolute responsivity** for each LED

The procedures to measure these parameters follow.

- **Spectral Distribution of Photocurrents**

Spectral distribution for each LED was measured using a monochromator. Parameters are summarized in Table B.

**Table D.2: Monocromator selected parameters for measurements**

---

Resolution window	2.5	[nm]
Wavelength incremental step	10	[nm]
Lamp spectral temperature	3175	[K]
Measured R from I-V Converter stage	993	[k $\Omega$ ]

---

Fig. F.1 and Table F.2 show results for red LED.

Fig. F.2 and Table F.3 show results for green LED.

- Red LED

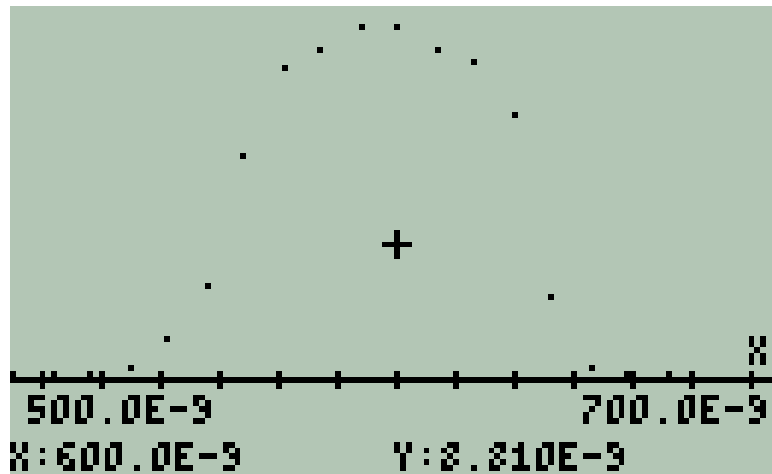


Figure D.2: Red LED spectral distribution

Table D.3: Red LED Current vs  $\lambda$

$\lambda$ [m]	Current B [A]	19.3 x Current B [A]
510.0E-9	404.45E-12	7.797E-9
520.0E-9	505.56E-12	9.766E-9
530.0E-9	1.0111E-9	19.49E-9
540.0E-9	2.7300E-9	52.69E-9
550.0E-9	5.9656E-9	115.2E-9
560.0E-9	14.661E-9	283.7E-9
570.0E-9	20.222E-9	389.9E-9
580.0E-9	21.335E-9	411.1E-9
590.0E-9	22.750E-9	440.0E-9
600.0E-9	22.851E-9	442.0E-9
610.0E-9	21.234E-9	409.2E-9
620.0E-9	20.425E-9	393.7E-9
630.0E-9	17.189E-9	332.0E-9
640.0E-9	5.2578E-9	101.5E-9
650.0E-9	1.0111E-9	19.49E-9
660.0E-9	303.34E-12	5.848E-9
	<b><math>\Sigma I =</math></b>	<b><math>\Sigma I =</math></b>
	<b>177.86E-9</b>	<b>3.43E-6 [A]</b>
	<b>[A]</b>	

\* Red Figures are the current summation

- Green LED

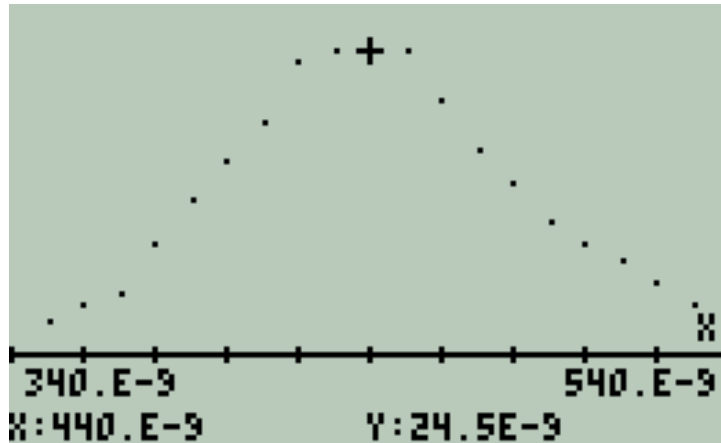


Figure D.3: Green LED spectral distribution

Table D.4: Green LED Current vs  $\lambda$

$\lambda$ [m]	Current B [A]	X 19.3 Current B [A]
350.0E-9	303.30E-12	5.85E-9
360.0E-9	404.40E-12	7.80E-9
370.0E-9	505.60E-12	9.76E-9
380.0E-9	910.00E-12	17.6E-9
390.0E-9	1.3140E-9	25.4E-9
400.0E-9	1.6180E-9	31.2E-9
410.0E-9	1.9210E-9	37.1E-9
420.0E-9	2.4270E-9	46.8E-9
430.0E-9	2.5280E-9	48.8E-9
440.0E-9	2.4270E-9	46.8E-9
450.0E-9	2.5280E-9	48.8E-9
460.0E-9	2.1230E-9	41.0E-9
470.0E-9	1.7190E-9	33.2E-9
480.0E-9	1.4160E-9	27.3E-9
490.0E-9	1.1120E-9	21.5E-9
500.0E-9	910.00E-12	17.6E-9
510.0E-9	808.90E-12	15.6E-9
520.0E-9	606.70E-12	11.7E-9
530.0E-9	404.40E-12	7.80E-9
	<b><math>\Sigma I =</math></b>	<b><math>\Sigma I =</math></b>
	<b>25.986E-9</b>	<b>502.E-9 [A]</b>
	<b>[A]</b>	

\* Red Figures are the current summation



Both spectral photocurrents are shown in the Fig. F.3.

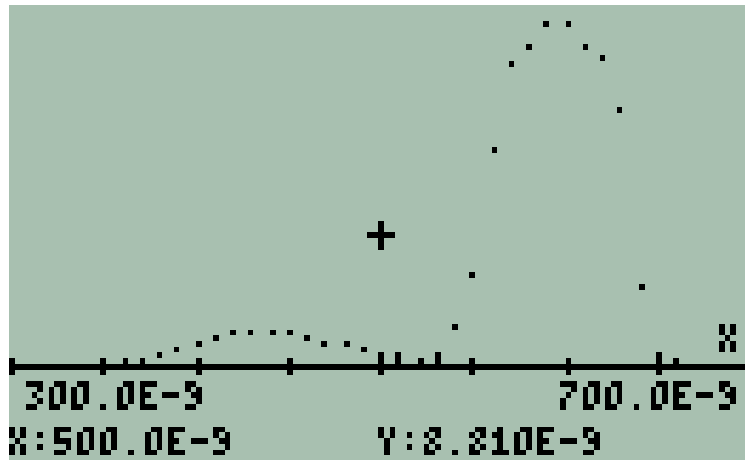


**Figure D.4:** *Spectral photocurrents for LEDs.  
Green LED (left) Red LED (Right).*

So: LEDs spectra are wavelength-bounded:

**Table D.5: Bounded Wavelengths for Red and Green LEDs Spectra**

LED	$\lambda_{\text{MIN}}$ [nm]	$\lambda_{\text{MAX}}$ [nm]
Green	350	530
Red	510	660

Now, since **total photocurrent** as well as **spectral photocurrent** are **scalable** in a wide range of light intensities – several decades limited by saturation of sensor at very high intensities or by noise at very low intensities.

### Measuring Total Photocurrents

Complementing the spectral measurements of photocurrents shown in Table F.2 and Table F.3; total photocurrents using identical light source and a fixed geometry were made.

Under this new condition, LEDs exposed to a light source detect only total photocurrents in the narrow band they are active.

In this example the selected photodiodes were exposed to the same light source than the one was used for the spectral measurements using the monochromator. A fixed geometry – (fixed lamp – photodetector array distance) – was used and total photocurrents were measured. A set of seven measurements (shown in { }) were made and its mean value was calculated, it is shown in **bold letters**.

- **Red LED measurements:**

List of seven measurements of Total Photocurrents made using Fixed Lamp – Photodetector Array

$$\{3.384\text{E-}6 \ 3.404\text{E-}6 \ 3.424\text{E-}6 \ 3.414\text{E-}6 \ 3.444\text{E-}6 \ 3.454\text{E-}6 \ 3.464\text{E-}6 \ 3.474\text{E-}6\} \text{ [A]} \quad (\text{D.1.a})$$

$$\text{Total Photocurrent Mean Value:} \quad \mathbf{3.433\text{E-}6} \text{ [A]} \quad (\text{D.1.b})$$

- **Green LED measurements:**

List of seven measurements of Total Photocurrents made using fixed lamp – photodetector array

$$\{498.3\text{E-}9 \ 500.9\text{E-}9 \ 499.1\text{E-}9 \ 503.6\text{E-}9 \ 500.0\text{E-}9 \ 503.6\text{E-}9 \ 504.4\text{E-}9 \ 502.7\text{E-}9\} \text{ [A]} \quad (\text{D2.a})$$

$$\text{Total Photocurrent Mean Value:} \quad \mathbf{501.6\text{E-}9} \text{ [A]} \quad (\text{D.2.b})$$

- **Current scaling factors between monochromator and (fixed lamp – photodetector array) measurements.**

Since – in general – photocurrents are linear with Light Intensity in a wide range of several decades limited by noise for small intensities and by saturation of detector for very intense light beams; so linearity is assumed for total as well as for spectral photocurrents.

A factor of **19.3** is found between the Total Photocurrent Mean Value and the Current Summation for Red LED and Green LED shown in Table C and Table D, respectively:

$$\text{Red LED} \quad \mathbf{19.3} \quad (19.3027014546) \quad (\text{D3.a})$$

$$\text{Green LED} \quad \mathbf{19.3} \quad (19.3016979647) \quad (\text{D.3.b})$$

\* Note: Scaling Factors are consistent.

- **Scaled Spectra**

If total photocurrents are scalable, then its sub-bands are also scalable. A third column is included in Tables F.2A and F.3. They are multiplied by the scale factor of 19.3.

## Irradiance

The normalized function  $F0\lambda(T, \lambda)$  represents Spectral Irradiance of  $1 \text{ [mW/mm}^2\text{]}$  or its equivalent  $1 \text{ [kW/m}^2\text{]}$  i.e.: the Irradiance for **1 Technical Sun**. Note that the function  $F0\lambda(T, \lambda)$  is Normalized for any value of temperature in [K].

### IMPORTANT

Note that these UNITARY values correspond to the complete spectrum

SUB-BANDS consequently must be obtained from the complete spectrum.

Chp. 1 ANNEX 4 is a Table for  $F0\lambda(3175, \lambda)$  coefficients in the range

$200 < \lambda < 3000 \text{ [nm]}$

$$I(\lambda) = 1 \left[ \frac{\text{mW}}{\text{mm}^2} \right] F0\lambda(T, \lambda) \quad (\text{D.4})$$

As example: The Summation of  $F0\lambda(3175, \lambda)$  with a Resolution of **10 [nm]** in the band  $200 < \lambda < 3000 \text{ [nm]}$  ; i.e.: practically the Complete Spectrum, has as result of one. See Fig. F.4 and Eq. (F.5).

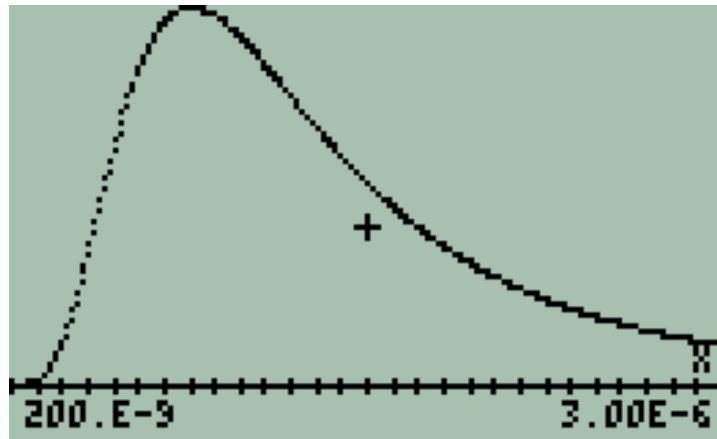


Figure D.5: The function  $F0\lambda(3175, \lambda)$

$200 < \lambda < 3000 \text{ [nm]}$  ; resolution 10 [nm]

$$\sum_{200 [nm]}^{3000 [nm]} F_{0\lambda}(3175, \lambda) = .9999999999995$$

(D5)

Table F.5 and Fig. F.5 show Irradiance for the measured spectral temperature  $T_{SP} = 3175 [K]$ . Two profiles are presented for  $1 [mW/mm^2]$  and for  $0.229 [mW/mm^2]$  i.e.: the irradiance measured in the – (fixed lamp – photodetector array distance) – both in the sub-band applicable to the Red and Green LEDs  $300 < \lambda < 700 [nm]$  and with a resolution of  $10 [nm]$ .

Note that Total Irradiance of  $0.229 [mW/mm^2]$  was measured using the same lamp in identical geometry using the procedure to measure Irradiance (See Section D in this Chapter).

Coefficients for the upper profile shown in Fig. D.6 were taken from **CHAPTER 1 ANNEX 4.1** for the corresponding wavelengths. Coefficients for the lower profile are the coefficients for the upper profile multiplied by the factor  $0.229$ .

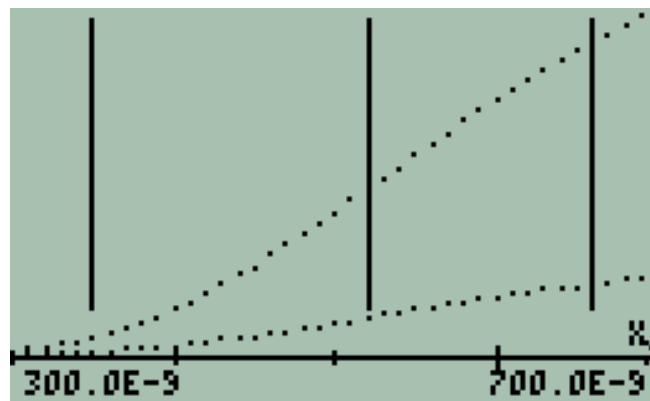


**Figure D.6:** Sub-bands for Red LED and Green LED for  $1 [mW/mm^2]$  (one technical sun) and for  $0.229 [mW/mm^2]$  (actual Irradiance measured in the fixed array). Vertical lines delimit the sub-bands where Green and Red LEDs are photo-sensible

**Table D.6: Irradiance for the measured spectral temperature  $T_{SP} = 3175$  [K] for irradiances of 1 [mW/mm<sup>2</sup>] and 0.229 [mW/mm<sup>2</sup>]**

$\lambda$ [m]	$F0\lambda(3175, \lambda)$ [mW/mm <sup>2</sup> ]	<b>0.229 x</b> $F0\lambda(3175, \lambda)$ [mW/mm <sup>2</sup> ]
300.0E-9	96.27E-6	22.05E-6
310.0E-9	131.2E-6	30.04E-6
320.0E-9	174.7E-6	40.01E-6
330.0E-9	227.5E-6	52.10E-6
340.0E-9	290.6E-6	66.55E-6
350.0E-9	364.6E-6	83.49E-6
360.0E-9	450.1E-6	103.1E-6
370.0E-9	547.4E-6	125.4E-6
380.0E-9	656.7E-6	150.4E-6
390.0E-9	778.2E-6	178.2E-6
400.0E-9	911.5E-6	208.7E-6
410.0E-9	1.056E-3	241.8E-6
420.0E-9	1.213E-3	277.8E-6
430.0E-9	1.379E-3	315.8E-6
440.0E-9	1.556E-3	356.3E-6
450.0E-9	1.741E-3	398.7E-6
460.0E-9	1.935E-3	443.1E-6
470.0E-9	2.136E-3	489.1E-6
480.0E-9	2.343E-3	536.5E-6
490.0E-9	2.555E-3	585.1E-6
500.0E-9	2.771E-3	634.6E-6
510.0E-9	2.991E-3	684.9E-6
520.0E-9	3.212E-3	735.5E-6
530.0E-9	3.435E-3	786.6E-6
540.0E-9	3.657E-3	837.5E-6
550.0E-9	3.879E-3	888.3E-6
560.0E-9	4.100E-3	938.9E-6
570.0E-9	4.318E-3	988.8E-6
580.0E-9	4.533E-3	1.038E-3
590.0E-9	4.744E-3	1.086E-3
600.0E-9	4.950E-3	1.134E-3
610.0E-9	5.152E-3	1.180E-3
620.0E-9	5.348E-3	1.225E-3
630.0E-9	5.538E-3	1.268E-3
640.0E-9	5.721E-3	1.310E-3
650.0E-9	5.898E-3	1.351E-3
660.0E-9	6.068E-3	1.390E-3
670.0E-9	6.230E-3	1.427E-3
680.0E-9	6.385E-3	1.462E-3

690.0E-9	6.533E-3	1.496E-3
700.0E-9	6.673E-3	1.528E-3
	<b>ΣIrr =</b>	<b>ΣIrr =</b>
	<b>122.7E-3</b>	<b>28.09E-3</b>
	<b>[mW/mm<sup>2</sup>]</b>	<b>[mW/mm<sup>2</sup>]</b>

Next two Tables F.6 and F.7 show the spectral irradiance  $I_{SP}$  and total irradiance  $I_{TOT}$  (in red letters) vs  $\lambda$  for red and green LEDs. First column is for a total irradiances of **1 [mW/mm<sup>2</sup>]** and second column for a total irradiance of **0.229 [mW/mm<sup>2</sup>]**. They are the segments from previous Table corresponding to each LED.

**Table D.7: Red LED Spectral Irradiance  $I_{SP}$  vs  $\lambda$  and total irradiance  $I_{TOT}$**

$\lambda$ [m]	$F0\lambda(3175, \lambda)$ [mW/mm <sup>2</sup> ]	<b>x 0.229</b> $F0\lambda(3175, \lambda)$ [mW/mm <sup>2</sup> ]
510.0E-9	2.991E-3	684.9E-6
520.0E-9	3.212E-3	735.5E-6
530.0E-9	3.435E-3	786.6E-6
540.0E-9	3.657E-3	837.5E-6
550.0E-9	3.879E-3	888.3E-6
560.0E-9	4.100E-3	938.9E-6
570.0E-9	4.318E-3	988.8E-6
580.0E-9	4.533E-3	1.038E-3
590.0E-9	4.744E-3	1.086E-3
600.0E-9	4.950E-3	1.134E-3
610.0E-9	5.152E-3	1.180E-3
620.0E-9	5.348E-3	1.225E-3
630.0E-9	5.538E-3	1.268E-3
640.0E-9	5.721E-3	1.310E-3
650.0E-9	5.898E-3	1.351E-3
660.0E-9	6.068E-3	1.390E-3
<b>&lt;λ&gt; =</b>	<b>ΣIrr =</b>	<b>ΣIrr =</b>
<b>594.6E-9</b>	<b>73.54E-3</b>	<b>16.84E-3</b>
<b>[m]</b>	<b>[mW/mm<sup>2</sup>]</b>	<b>[mW/mm<sup>2</sup>]</b>

\* Red Figures are the Spectral Irradiance summation  
 Green Figures is the Mean Wavelength in the sub-band

$$\langle \lambda \rangle = 594.6E-9 \text{ [m]} \quad (D.6)$$

**Table D.8:** Green LED spectral irradiance  $I_{SP}$  vs  $\lambda$  and total irradiance  $I_{TOT}$

$\lambda$ [m]	$F0\lambda(3175, \lambda)$ [mW/mm <sup>2</sup> ]	<b>0.229</b> $F0\lambda(3175, \lambda)$ [mW/mm <sup>2</sup> ]
350.0E-9	364.6E-6	83.49E-6
360.0E-9	450.1E-6	103.1E-6
370.0E-9	547.4E-6	125.4E-6
380.0E-9	656.7E-6	150.4E-6
390.0E-9	778.2E-6	178.2E-6
400.0E-9	911.5E-6	208.7E-6
410.0E-9	1.056E-3	241.8E-6
420.0E-9	1.213E-3	277.8E-6
430.0E-9	1.379E-3	315.8E-6
440.0E-9	1.556E-3	356.3E-6
450.0E-9	1.741E-3	398.7E-6
460.0E-9	1.935E-3	443.1E-6
470.0E-9	2.136E-3	489.1E-6
480.0E-9	2.343E-3	536.5E-6
490.0E-9	2.555E-3	585.1E-6
500.0E-9	2.771E-3	634.6E-6
510.0E-9	2.991E-3	684.9E-6
520.0E-9	3.212E-3	735.5E-6
530.0E-9	3.435E-3	786.6E-6
$\langle \lambda \rangle =$	$\Sigma Irr =$	$\Sigma Irr =$
<b>471.0E-9</b>	<b>32.03E-3</b>	<b>7.335E-3</b>
[m]	[mW/mm <sup>2</sup> ]	[mW/mm <sup>2</sup> ]

\* Red figures are the spectral irradiance summation  
 Green figures is the mean wavelength in the sub-band

$$\langle \lambda \rangle = 471.0E-9 \text{ [m]} \quad (D.7)$$

### Mean Wavelength in a Band

The sub-bands of irradiance corresponding to red and green LEDs let's calculate the wavelength that corresponds to the mean-wavelength  $\langle \lambda \rangle$  of this distribution.

$$\langle \lambda \rangle = \frac{\sum_{SUB\_BAND} (\{Irradiance\_Components\} \times \{Wavelengths\})}{\sum_{SUB\_BAND} \{Irradiance\_Components\}} \quad (D.8)$$

Where the product and quotient are made term by term. (Arrays)

These values are presented – in green letters – for each sub-band after Table F.6 and Table F.7, respectively.

- **LED's active area calculation**

LED's Active Area is a coefficient required to calculate absolute responsivity.

The central idea to calculate **active area** is **photoelectric effect** i.e.: measured photocurrent is due to photon annihilation. Photons are in the sub-band where each LED produces photo-conversion.

This first approach assumption is:

$$\left[ \frac{\sum \text{photoelectrons}}{\text{second}} \right]_{in\_LED\_band} = \left[ \frac{\sum \text{annihilated\_photons}}{\text{second}} \right]_{in\_LED\_band} \quad (D.9)$$

Now, from the first term:

The number of photoelectrons per second is the photocurrent  $I_{phot}$  :

$$I_{phot} = \frac{\Delta Q}{\Delta t} = I_{measured} \quad ; \quad [A] \quad (D.10)$$

Where:

$I_{measured}$  is known

Since the electron's  $q_e$  charge is:



$$q_e = 160.2 \times 10^{-21} \quad [C] \quad (D.11)$$

and:

$$1[A] = 1 \left[ \frac{C}{s} \right] \quad (D.12)$$

then, expressing  $\Delta Q$  in number of electrons; finally it is obtained:

$$I_{phot} = \left| I_{measured \text{ in } [A]} \right| \times 6.242 \times 10^{18} ; \left[ \frac{electrons}{s} \right] \quad (D.13)$$

This equation expresses the measured photocurrent in number of electrons per second.

For  $t = 1 [s]$  the magnitude of  $I_{phot}$  coincides with  $Q_{phot}$  the number of electrons. The fraction  $Q_{phot} / \text{electron} = n_e$ , the number of electrons.

$$n_e = \left| I_{measured \text{ in } [A]} \times 1[s] \right| \times 6.242 \times 10^{18} ; [dimensionless] \quad (D.14)$$

Now, from our assumption, this number of electrons per second corresponds to equal number of annihilated photons.

Since:

- a) LED's are irradiated with a Planck's light source of spectral temperature  $T_{SP}$  known.
- b) The LED's spectral bands are delimited in wavelength.
- c) The LED's spectral bands are narrow bands compared with the whole spectrum.

Then:

A representative wavelength has been calculated for each LED by considering:

- a) Planck's spectral distribution for  $T_{SP}$
- b) The bound-wavelengths for each LED.  
This parameter is the **photon mean wavelength**  $\langle \lambda \rangle$  previously defined and calculated for both LEDs.

So:

The corresponding **photon mean energy**  $\langle E \rangle$  in the LED's band is calculated with equation:

$$E = h \times \left(\frac{c}{\lambda}\right) ; [eV] \quad (D.15)$$

in this case:

$$\langle E \rangle = h \times \left(\frac{c}{\langle \lambda \rangle}\right) ; [eV] \quad (D.16)$$

where:  $h$  is Planck's constant and  $c$  is the speed of light.

Now:

From the measured photocurrent we do know  $n_e$  the number generated of electrons per second. According to the initial assumption, these number of photoelectrons correspond to equal number of photons  $n_{ph}$  with a mean wavelength  $\langle \lambda \rangle$  - or mean energy  $\langle E \rangle$ .

$$n_{ph} = n_e ; [dimensionless] \quad (D.17)$$

These  $n_{ph}$  photons carry an energy  $E$  :

$$E = n_{ph} \times \langle E \rangle = n_{ph} \times h \times \left(\frac{c}{\langle \lambda \rangle}\right) ; [eV] \quad (D.18)$$

Converting this magnitude to Joules using the conversion factor:

$$1 [eV] = 160.2 \times 10^{-21} [J] \quad (D.19)$$

Energy  $E$  has interacted with the LEDs Active Area per second

So:

Interacting Irradiance on Active Area is:

$$Irr_{Active\_Area} = \frac{W}{Active\_Area} = \frac{E}{s \times Active\_Area} ; \left[ \frac{W}{Active\_Area} \right] \quad (D.20)$$

On the other hand, since spectral temperature  $T_{SP}$  is known

$$3175 \text{ [K]} \text{ (in this example)} \quad (D.21)$$

and total irradiance is also known using  $F_{0\lambda}(T, \lambda)$ :

$$(0.229 \text{ [mW / mm}^2\text{] in this example)} \quad (D.22)$$

the corresponding irradiance in the LED's band is calculable from data.

Under these circumstances, it is possible to calculate the area factor  $K_A$  that matches the LEDs active area with the standard area of 1 [mm<sup>2</sup>]

$$K_A = \frac{Irr_{Measured}}{Irradiance_{in 1mm^2}} \quad ; \quad [dimensionless] \quad (D.23)$$

**Comment:**

$$1 \left[ \frac{mW}{mm^2} \right] = 1 \times 10^{-3} \left[ \frac{W}{mm^2} \right] \quad (D.24)$$

Once  $K_A$  is known it is possible to scale measured irradiance to the standard surface [1 mm<sup>2</sup>] for the sub-bands for both LEDs. So the information to estimate spectral temperature is completed.

#### Numerical Example

This is a continuation of procedure using data for red and green LEDs. Table D.9 summarizes the procedure described here.

**Table D.9: Summary of procedure for red LED and green LED**

Physical Parameter	Red LED	Green LED	UNIT
Spectral Temperature T <sub>SP</sub>	3175	3175	[K]
Total Irradiance (measured previously)	0.229	0.229	[mW/mm <sup>2</sup> ]
Minimum Wavelength λ <sub>MIN</sub>	510	350	[nm]
Maximum Wavelength λ <sub>MAX</sub>	660	530	[nm]
<u>Measured Parameters in the LED band</u>			
Photocurrent (measured)	3430	502	[nA]

Number of Photo-electrons $n_e$	$21.41 \times 10^{12}$	$3.133 \times 10^{12}$	[--]
Mean Wavelength in the Band $\langle \lambda \rangle$	$594.6 \times 10^{-9}$	$471.0 \times 10^{-9}$	[m]
Mean Photon Energy in the Band $\langle E \rangle$	2.085	2.632	[eV]
Number of Photons $n_{ph}$	$21.41 \times 10^{12}$	$3.133 \times 10^{12}$	[--]
Total Energy $E = n_{ph} \times \langle E \rangle$	$7.152 \times 10^{-6}$	$1.321 \times 10^{-6}$	[J]
Total Power $P_w = E/s$	$7.152 \times 10^{-6}$	$1.321 \times 10^{-6}$	[W]
Total Power $P_w = E/s$	$7.152 \times 10^{-3}$	$1.321 \times 10^{-3}$	[mW]
Irradiance $Irr = P_w/Active\text{-Area}$	<u><math>7.152 \times 10^{-3}</math></u>	<u><math>1.321 \times 10^{-3}</math></u>	<u>[mW]</u>
	Active-Area	Active-Area	[mm <sup>2</sup> ]
<u>Calculated Parameter in the LED band</u>			
Irradiance $Irr = P_w/Active\text{-Area}$	<u><math>16.84 \times 10^{-3}</math></u>	<u><math>7.335 \times 10^{-3}</math></u>	<u>[mW]</u>
	mm <sup>2</sup>	mm <sup>2</sup>	[mm <sup>2</sup> ]
LED's Active Area*	0.4247	0.1801	[mm <sup>2</sup> ]
(From Measured / Calculated Ratio)			
LED's side = (LED's Act. Area) <sup>1/2</sup>	0.6517	0.4244	[mm]
Scaled Area Factor *to 1 [mm <sup>2</sup> ]	2.356	5.553	[mm] <sup>-1</sup>
Scaled LEDs Current to 1 mm <sup>2</sup>	$8.081 \times 10^{-6}$	$2.788 \times 10^{-6}$	[A]
(Scld Area fact x LEDs Msrd Current)			

\*Note: LED's Active Area and Scaled Area Factor to 1 [mm<sup>2</sup>] are reciprocal values.

## Absolute Responsivity Calculation

At this point of the process, when the scaled area factor to 1 mm<sup>2</sup> it is known, then, it is possible to re-scale measured photocurrents from the third columns in Table F.2 and Table D.3. This time the re-scale factor converts the actual active area of red and green LEDs to an active area of 1 [mm<sup>2</sup>].

Those Tables are reproduced here as Table D.9 and Table D.10, respectively, incrementing a new column with photocurrents scaled to 1 [mm<sup>2</sup>].

**Table D.10: Red LED Absolute Responsivity Calculation**

Scale Intensity Factor = 19.3 Scaled Factor to 1 [mm<sup>2</sup>] = 2.356

$\lambda$ [m]	Current B [A]	Current B [A] **	Irradiance [mW/mm <sup>2</sup> ]	Abs Resp [A/W]
510.0E-9	7.797E-9	18.37E-9	684.9E-6	26.82E-3
520.0E-9	9.766E-9	23.01E-9	735.5E-6	31.28E-3
530.0E-9	19.49E-9	45.92E-9	786.6E-6	58.38E-3
540.0E-9	52.69E-9	124.1E-9	837.5E-6	148.2E-3
550.0E-9	115.2E-9	271.4E-9	888.3E-6	305.5E-3
560.0E-9	283.7E-9	668.4E-9	938.9E-6	711.9E-3
570.0E-9	389.9E-9	918.6E-9	988.8E-6	929.0E-3
580.0E-9	411.1E-9	968.6E-9	1.038E-3	933.1E-3
590.0E-9	440.0E-9	1.037E-6	1.086E-3	954.9E-3
600.0E-9	442.0E-9	1.041E-6	1.134E-3	918.0E-3
610.0E-9	409.2E-9	964.1E-9	1.180E-3	817.0E-3
620.0E-9	393.7E-9	927.6E-9	1.225E-3	757.2E-3
630.0E-9	332.0E-9	782.2E-9	1.268E-3	616.9E-3
640.0E-9	101.5E-9	239.1E-9	1.310E-3	182.5E-3
650.0E-9	19.49E-9	45.92E-9	1.351E-3	33.99E-3
660.0E-9	5.848E-9	13.78E-9	1.390E-3	9.914E-3
	<b><math>\Sigma I =</math> 3.43E-6 [A]</b>	<b><math>\Sigma I =</math> 8.089E-6 [A]</b>	<b><math>\Sigma Irr =</math> 16.84E-3 [mW/mm<sup>2</sup>]</b>	

\* Red Figures are the current summation

\*\* For dimensional consistency, current is multiplied by a factor  $1 \times 10^3$  to express it in [mA]; then the quotient to calculate Responsivity will be in [A/W] units.

**Table D.11: Green LED Absolute Responsivity Calculation**

\*Scale Intensity Factor 19.3 \*\*Scaled Factor to 1 [mm<sup>2</sup>] = 5.553

$\lambda$ [m]	Current B [A] *	Current B [A/mm <sup>2</sup> ] **	Irradiance [mW/mm <sup>2</sup> ]	Abs Resp [A/W]
350.0E-9	5.85E-9	32.49E-9	83.49E-6	389.1E-3
360.0E-9	7.80E-9	43.31E-9	103.1E-6	420.1E-3
370.0E-9	9.76E-9	54.20E-9	125.4E-6	432.2E-3
380.0E-9	17.6E-9	97.73E-9	150.4E-6	649.8E-3
390.0E-9	25.4E-9	141.0E-9	178.2E-6	791.2E-3
400.0E-9	31.2E-9	173.3E-9	208.7E-6	830.4E-3
410.0E-9	37.1E-9	206.0E-9	241.8E-6	851.9E-3
420.0E-9	46.8E-9	259.9E-9	277.8E-6	935.6E-3
430.0E-9	48.8E-9	271.0E-9	315.8E-6	858.1E-3
440.0E-9	46.8E-9	259.9E-9	356.3E-6	729.4E-3
450.0E-9	48.8E-9	271.0E-9	398.7E-6	679.7E-3
460.0E-9	41.0E-9	227.7E-9	443.1E-6	513.9E-3
470.0E-9	33.2E-9	184.4E-9	489.1E-6	377.0E-3
480.0E-9	27.3E-9	151.6E-9	536.5E-6	282.6E-3
490.0E-9	21.5E-9	119.4E-9	585.1E-6	204.1E-3
500.0E-9	17.6E-9	97.73E-9	634.6E-6	154.0E-3
510.0E-9	15.6E-9	86.63E-9	684.9E-6	126.5E-3
520.0E-9	11.7E-9	64.97E-9	735.5E-6	88.33E-3
530.0E-9	7.80E-9	43.31E-9	786.6E-6	55.06E-3
	<b><math>\Sigma I =</math></b>	<b><math>\Sigma I =</math></b>	<b><math>\Sigma Irr =</math></b>	
	<b>502.E-9</b>	<b>2.785E-6</b>	<b>7.335E-3</b>	
	<b>[A]</b>	<b>[A]</b>	<b>[mW/mm<sup>2</sup>]</b>	

\* Red Figures are the current summation

\*\* For dimensional consistency, current is multiplied by a factor  $1 \times 10^3$  to express it in [mA]; then the quotient to calculate Responsivity will be in [A/W] units.

Now:

Absolute Responsivity is defined as:

$$R_p = \frac{I_p}{W_p} \quad \left[ \frac{A}{W} \right]$$

(F.25)

Since Spectral Current has been calculated for an active area of 1 [mm<sup>2</sup>] and Spectral Irradiance is also known for 1 [mm<sup>2</sup>]; then it is feasible to calculate absolute responsivity for each LED. In the previous two Tables, two columns have been included: One is the Spectral Irradiance for each LED in green letters. The Last Column is Absolute Responsivity (in blue letters).

Tables F.11 and F.12 summarize the main parameters:  $\lambda$  [nm], photocurrent [mA/mm<sup>2</sup>], Irradiance [mW/mm<sup>2</sup>] and Irradiance [A/W] for red LED and green LED.

Figs F.6 and F.7 present graphically these parameters for both LEDs.

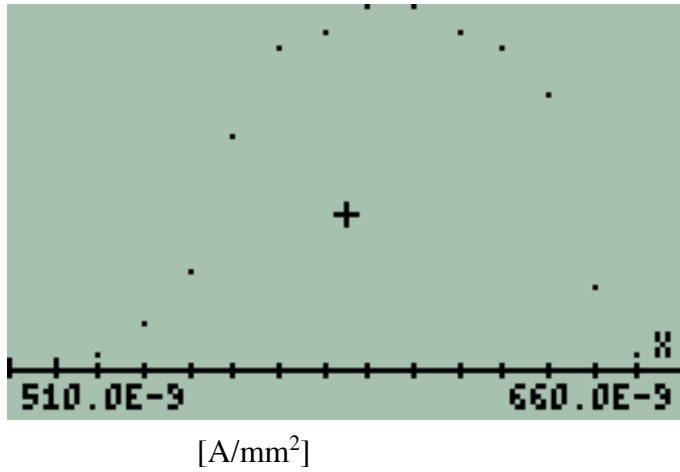
Finally Fig. F.8 is a Plot showing absolute responsivity for both LEDs together is presented.

**Table D.12: Red LED Photocurrent, Irradiance and Absolute Responsivity vs wavelength**

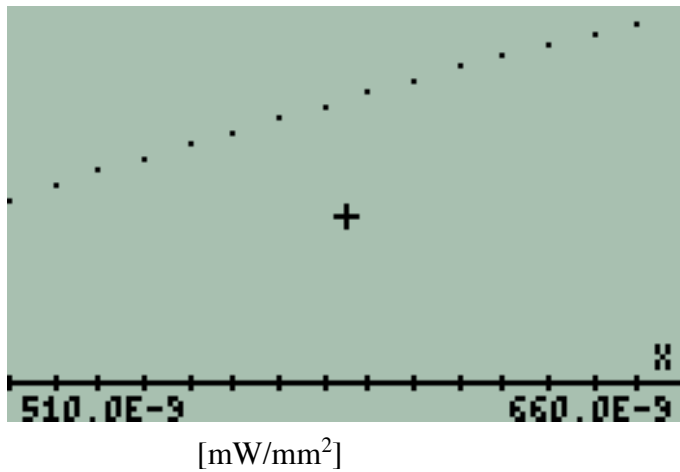
$\lambda$ [m]	Current B [A] **	Irradiance [mW/mm <sup>2</sup> ]	Abs Resp [A/W]
510.0E-9	18.37E-6	684.9E-6	26.82E-3
520.0E-9	23.01E-6	735.5E-6	31.28E-3
530.0E-9	45.92E-6	786.6E-6	58.38E-3
540.0E-9	124.1E-6	837.5E-6	148.2E-3
550.0E-9	271.4E-6	888.3E-6	305.5E-3
560.0E-9	668.4E-6	938.9E-6	711.9E-3
570.0E-9	918.6E-6	988.8E-6	929.0E-3
580.0E-9	968.6E-6	1.038E-3	933.1E-3
590.0E-9	1.037E-3	1.086E-3	954.9E-3
600.0E-9	1.041E-3	1.134E-3	918.0E-3
610.0E-9	964.1E-6	1.180E-3	817.0E-3
620.0E-9	927.6E-6	1.225E-3	757.2E-3
630.0E-9	782.2E-6	1.268E-3	616.9E-3
640.0E-9	239.1E-6	1.310E-3	182.5E-3
650.0E-9	45.92E-6	1.351E-3	33.99E-3
660.0E-9	13.78E-6	1.390E-3	9.914E-3
	<b><math>\Sigma I =</math></b>	<b><math>\Sigma Irr =</math></b>	
	<b>8.089E-3</b>	<b>16.84E-3</b>	
	<b>[A]</b>	<b>[mW/mm<sup>2</sup>]</b>	



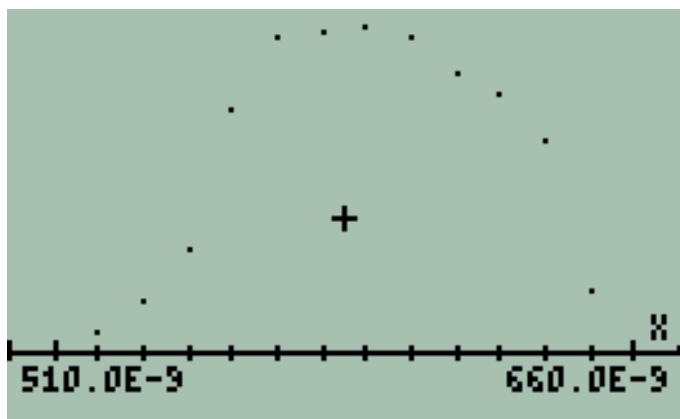
**Red LED:**



Photocurrent



Irradiance



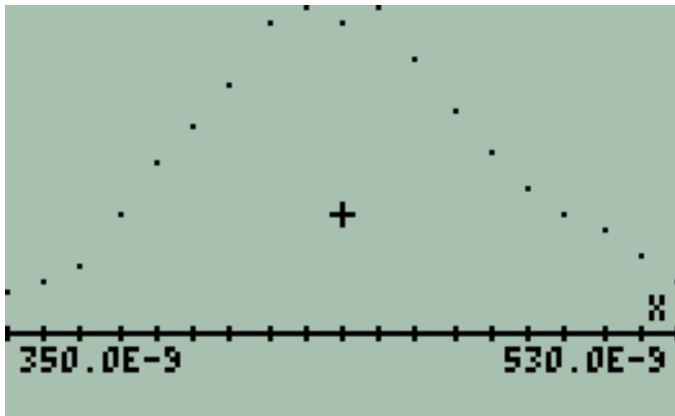
Abs. Responsivity [A/W]

**Figure D.7:** Plots of photocurrent, irradiance and absolute responsivity vs  $\lambda$  for Red LED.

**Table D.13: Green LED Photocurrent, Irradiance and Absolute Responsivity vs wavelength**

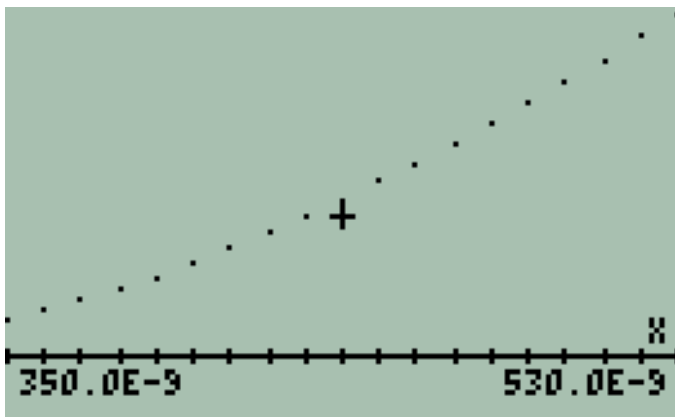
$\lambda$ [m]	Current B [A/mm <sup>2</sup> ] **	Irradiance [mW/mm <sup>2</sup> ]	Abs Resp [A/W]
350.0E-9	32.49E-6	83.49E-6	389.1E-3
360.0E-9	43.31E-6	103.1E-6	420.1E-3
370.0E-9	54.20E-6	125.4E-6	432.2E-3
380.0E-9	97.73E-6	150.4E-6	649.8E-3
390.0E-9	141.0E-6	178.2E-6	791.2E-3
400.0E-9	173.3E-6	208.7E-6	830.4E-3
410.0E-9	206.0E-6	241.8E-6	851.9E-3
420.0E-9	259.9E-6	277.8E-6	935.6E-3
430.0E-9	271.0E-6	315.8E-6	858.1E-3
440.0E-9	259.9E-6	356.3E-6	729.4E-3
450.0E-9	271.0E-6	398.7E-6	679.7E-3
460.0E-9	227.7E-6	443.1E-6	513.9E-3
470.0E-9	184.4E-6	489.1E-6	377.0E-3
480.0E-9	151.6E-6	536.5E-6	282.6E-3
490.0E-9	119.4E-6	585.1E-6	204.1E-3
500.0E-9	97.73E-6	634.6E-6	154.0E-3
510.0E-9	86.63E-6	684.9E-6	126.5E-3
520.0E-9	64.97E-6	735.5E-6	88.33E-3
530.0E-9	43.31E-6	786.6E-6	55.06E-3
	<b><math>\Sigma I =</math></b>	<b><math>\Sigma Irr =</math></b>	
	<b>2.785E-3</b>	<b>7.335E-3</b>	
	<b>[A]</b>	<b>[mW/mm<sup>2</sup>]</b>	

**Green LED:**



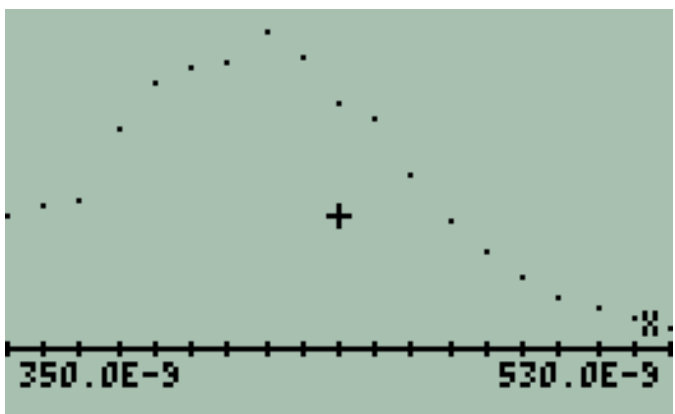
[mA/mm<sup>2</sup>]

Photocurrent



[mW/mm<sup>2</sup>]

Irradiance



[A/W]

Abs. Responsivity

**Figure D.8:** *Plots of photocurrent, irradiance and absolute responsivity vs  $\lambda$  for Green LED.*

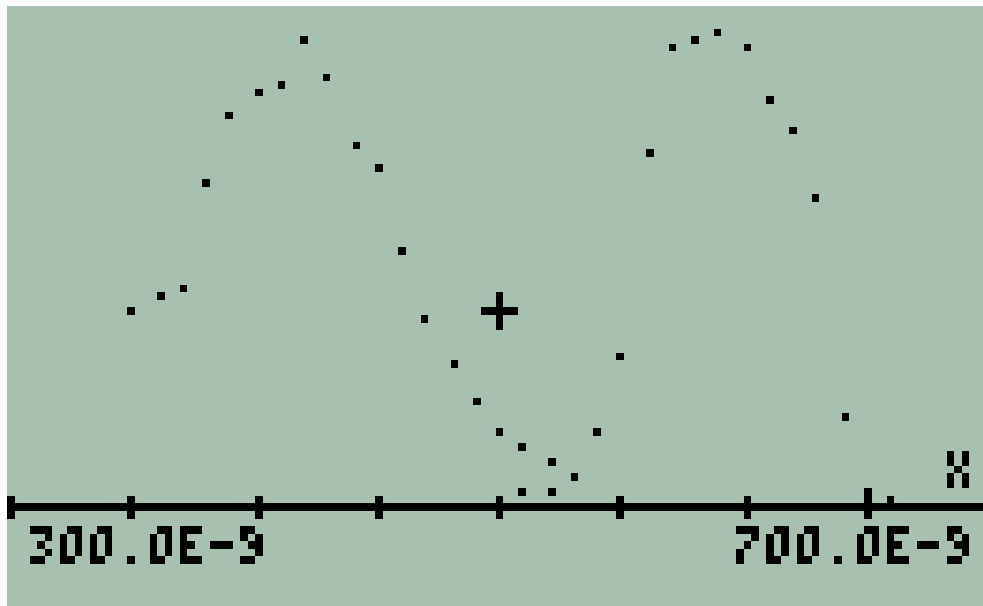


**Figure D.9:** *Absolute responsivity for Red and Green LEDs*

Note that both responsivities have its maximum peak close to 1.00. This implies that at the maximum wavelengths photons interacting with the LEDs active areas practically are converted in photoelectrons.

## SPECTRAL TEMPERATURE CALCULATION

### Virtual Pyrometer Algorithm

The algorithm to obtain spectral temperature from two spectral bands of a Planck's distribution light source constitutes a virtual pyrometer. This idea is explained here. This algorithm combined with data obtained from measurements provides the spectral temperature  $T_{SP}$ .

As prerequisite it is recommended a revision of Chapter 1, particularly the topics "Normalization of Planck's Distribution" and "The function  $F0\lambda$ ".

Starting with the function  $F0\lambda$  as shown in Fig. D.9, a particular Numerical Value for  $F0\lambda$  is obtained for specific values of Temperature  $T$  and wavelength  $\lambda$ , i.e.:

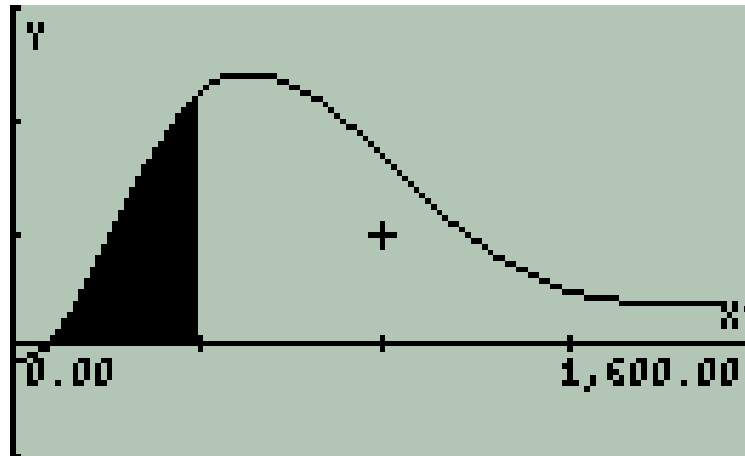


**Figure D.10:** The function  $F0\lambda$  for  $\lambda = \lambda_i$  is the marked area from  $\lambda = 0$  to  $\lambda = \lambda_i$  in the normalized Planck's Equation. Its maximum value when  $\lambda \rightarrow \infty$  is 1.00

$$F0\lambda = F0\lambda(T, \lambda) \quad (D.26)$$

Similarly, the function  $\Delta F0\lambda$  provides a numerical value corresponding to the spectral band defined by two wavelengths  $\lambda_1$  and  $\lambda_2$  for specific T.  $\Delta F0\lambda$  simply is the difference of two values  $F0\lambda$  for a spectral band  $[\lambda_1, \lambda_2]$  for temperature T:

$$\Delta F0\lambda = |F0\lambda(T, \lambda_2) - F0\lambda(T, \lambda_1)| \quad (D.27)$$

Fig. F.10 shows two spectral bands  $[\lambda_1, \lambda_2]$  and  $[\lambda_3, \lambda_4]$  for a temperature T. This means that both bands belong to the same Planck's spectrum for a given temperature T.

Since there is a unique numerical value corresponds to each band, its quotient also is a unique value. This allows to claim the following statement:

#### STATEMENT

*For a Planck's source:*

*The quotient of the irradiance corresponding to two known spectral bands is unique and belongs to the spectrum defined by the Planck's equation for a specific temperature T [K].*

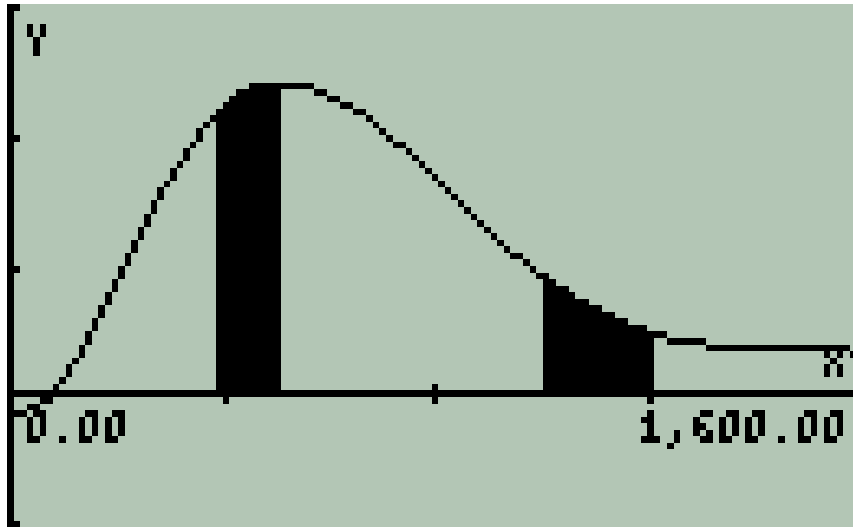


**Figure D.11:** *Two known spectral bands for a Planck's source.*

### Equation

The corresponding Equation is:

$$\frac{F_{0\lambda}[T, \lambda_2] - F_{0\lambda}[T, \lambda_1]}{F_{0\lambda}[T, \lambda_4] - F_{0\lambda}[T, \lambda_3]} = \frac{I_{\lambda_1\lambda_2}}{I_{\lambda_3\lambda_4}} \quad (\text{D.28})$$

### Algorithm

An algorithm to solve this equation has been written and tested. **The algorithm allows calculate iteratively the particular value of temperature T that “fits” Eq. (26).** So, the algorithm is, in principle, a **virtual pyrometer**.

Spectral temperature is calculated using Virtual Pyrometer routine.

The parameters that were used are in Table F.13:

**Table D.14: Virtual pyrometer parameters for LEDs**

---

Green LED:	$\lambda_1 = 350\text{E-9 [m]}$	$\lambda_2 = 530\text{E-9 [m]}$
Red LED:	$\lambda_3 = 510\text{E-9 [m]}$	$\lambda_4 = 660\text{E-9 [m]}$
Band Quotient	$\text{bndqo} = 7.335\text{E-3} / 16.84\text{E-3} = 435.6\text{E-3}$	

---

Results show the consistency of calculations:

```

RAD XYZ HEX R~ 'X'
CHOME PYROMETER3
7:
6:
5:
4:
3:
2:
1:
    
```

```

RAD XYZ HEX R~ 'X'
CHOME PYROMETER3
7:
6:
5:
4:
3:
2:
1: Tspec :(3.215E3_K)
    
```

Once the Parameters are established consistently, the circuit is characterized as a useful instrument to measure Spectral Temperature.

**PROCEDURE**

**Reasoned Procedure**

- 1) LEDs are exposed to a Planck's radiation
- 2) Photocurrents are measured for each LED
- 3) Since Active Area for each LED is known, photocurrents are scaled to an active area = 1 [mm<sup>2</sup>]
- 4) Since spectral distribution of photocurrent is known. Note that photocurrent are split accordingly with a resolution of 10 [nm]
- 5) Since absolute responsivity is known, spectral irradiance is calculated using equation:

$$W_p = \frac{I_p}{R_p} \quad (D.29)$$

- 6) Then Total Irradiance is obtained as a summation for each LED's band.
- 7) Since the wavelengths that delimit the band of each LED are known and total irradiance for each LED are known it is possible to calculate the band quotient. These are the required parameters for the virtual pyrometer algorithm where spectral temperature is finally calculated.

### Practical Procedure

The previous procedure demonstrates consistency of results, however, in the process, spectral temperature is implicitly included but; the purpose of a pyrometer is, precisely, to measure spectral temperature.

However during the procedure insight has been gained and new parameters have been obtained as the wavelength spectra of LEDs, their absolute responsivity, and their active area. Mean wavelengths have been calculated and energies also have been calculated from measured photoelectrons. All these results are summarized in Table F.8.

These new resources allow to overcome the prerequisite to know spectral temperature and validates the possibility to have a virtual pyrometer. Explanation follows.

The fact that the LEDs spectral response is wavelength delimited provides the  $\lambda_1$ ,  $\lambda_2$ ,  $\lambda_3$  and  $\lambda_4$  parameters required for the left hand side of the virtual pyrometer Eq. (F.28). Note that the bandwidth for LEDs is constant.

The fact that LEDs photocurrents are directly measurable and convertible to Irradiance / Active Area through Eq. F.20.

The fact that LEDs Active Areas are calculable by Eq. F.23 allows to have the quotient of irradiances required in the right hand side of Eq. F.28 completing the requirements to solve it and finally calculate the Spectral Temperature as it was claimed.

As example, from Table F.8: the quotient of irradiances is obtained multiplying the (Pw/Active-Area) factor by the (scaled area factor \*to 1 [mm<sup>2</sup>]) for each LED and obtaining its quotient. Explicitly:

$$\begin{aligned} & [(1.321 \times 10^{-3} / \text{Active Area}) \times (5.553 \text{ mm}^2)] / [(7.152 \times 10^{-3} / \text{Active-Area}) \times (2.356 \text{ mm}^2)] = \\ & = 435.3 \times 10^{-3} \quad \text{that is the sought quotient of irradiances.} \end{aligned}$$



## 5. Algorithm Sequence

- Read LED's Photocurrents
- Convert these readings to Irradiance / Active Area
- Calculate LEDs Active Areas
- Scale Irradiances to 1 mm<sup>2</sup>
- Calculate Irradiances Quotient
- Apply data to Virtual Pyrometer equation
- Obtain Spectral Temperature.
- Calculate also LEDs Absolute Responsivity if Required.

## E. SOLAR CELL I – V CURVE GENERATOR

In this Section a simple circuit to measure the current – voltage curve of a single solar cell is developed. The circuit is intended to be a tool to obtain data from single solar cells prototypes developed in a Laboratory.

### 1. Statement of the Problem

Laboratory solar cells are small prototypes made with different materials or structured with different technologies. These cells are small area cells ( $\approx 1 \text{ cm}^2$ ) and are able to generate current densities in the range of few mA/cm<sup>2</sup>.

The procedures to measure accurately current density  $J$  delimits active area to even smaller areas in the order of 0.02 [cm<sup>2</sup>].

This means that their maximum currents ISC are in the order of 1- 10 mA. On the other hand, a single solar cell voltage at open circuit VOC is in the order of 1 Volt.

**So, in principle, a solar cell I-V curve generator is a circuit able to handle and measure few mA and small voltages around 1 volt.**

### 2. Sensors

The sensor for this circuit is the tested solar cell itself. Recall chapter 2, section C.2.

### 3. Front End Circuits

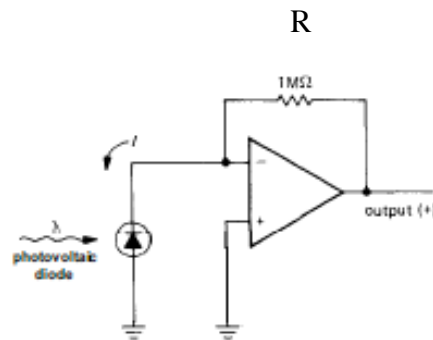
The circuit designed for this purpose has three Front End Circuits. Recall Chpt. 3 Fig. D.2.

**a. VOC Meter**

The first stage is a simple **voltmeter** to measure VOC. This measurement is made to define the (**V = VOC ; I = 0**) coordinate for the cell's I-V Curve. See Chpt. 2 Fig. D.3 (b). Notice that the cell's power consumption is null for VOC since  $I_{CELL} = 0$ .

**b. Photocurrent to Voltage Converter**

The second stage is a **photocurrent to voltage converter** is used to measure the short circuit current, or maximum current obtained when the anode and cathode extremes of the cell have a voltage difference equal to zero. This measurement is made to define the (**V = 0 ; I = Imax**) coordinate for the solar cell I – V curve. Recall Chapter 2, Section D.4. See Fig. D.1



$$I = - V_{OUT} / R$$

**Figure E.1:** Photocurrent to Voltage Converter using Op Amps.  
[Figure adapted from reference shown in ANNEX F]

The tested solar cell positioned in a defined geometry and facing perpendicularly the light source is connected to the **photocurrent to voltage converter**. Then only a single measurement for  $I_{SC}$  is required and the maximum available current in the measurement array is measured. This is the most important parameter to define the I-V curve. Its coordinates are:

$$I_{SC} = I_{MAX} \quad [A] \quad ; \quad V_{SC} \approx 0 [V] \quad (E.1)$$

**c. Cell's Voltage – Current response circuit**

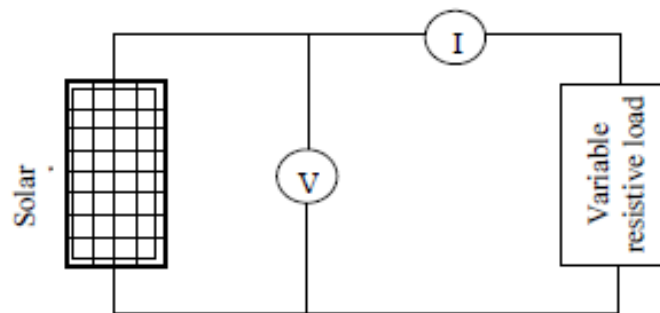
The Third Stage is the tested in this stage the tested **solar cell is biasing a JFET N-Ch transistor operating in its linear region**. The Voltage – Current relationship to generate the curve in the JFET transistor is controlled by a negative Gate – Source voltage. Recall Chapter 2, Section E.5. The central part of this circuit is shown in Fig. E.3

A more detailed explanation of the Third Stage follows.

#### d. The Solar Cell and N-Channel JFET Transistor Front End Circuit

As a preliminary reference Fig. E.2. shows the Experimental Setup and Materials required to measure the I – V curve from a solar cell using the **conventional method** [12].

##### Experimental Setup



##### Material

- A photovoltaic panel (BP Solar 10W, 12V)
- A solar panel rack (support and change positions of a PV panel)
- 2 multimeters (or an ammeter and a voltmeter) or a AVO meter
- Insulated wires with alligator clips or other cables
- A resistor panel (1 $\Omega$ , 4.7 $\Omega$ , 10 $\Omega$ , 22 $\Omega$ , 32 $\Omega$ , 47 $\Omega$ , 51 $\Omega$ , 82 $\Omega$ , 100 $\Omega$ , 220 $\Omega$ , 10W)

**Figure E.2:** *Experimental setup and parts to obtain I – V curve for a solar cell in the conventional way.*

*[Figure adapted from reference shown in ANNEX F]*

An alternative to this **conventional method** is using a **N-JFET Field Effect Transistor operating in its Linear Region as a Variable Resistor**. See Fig. E.3

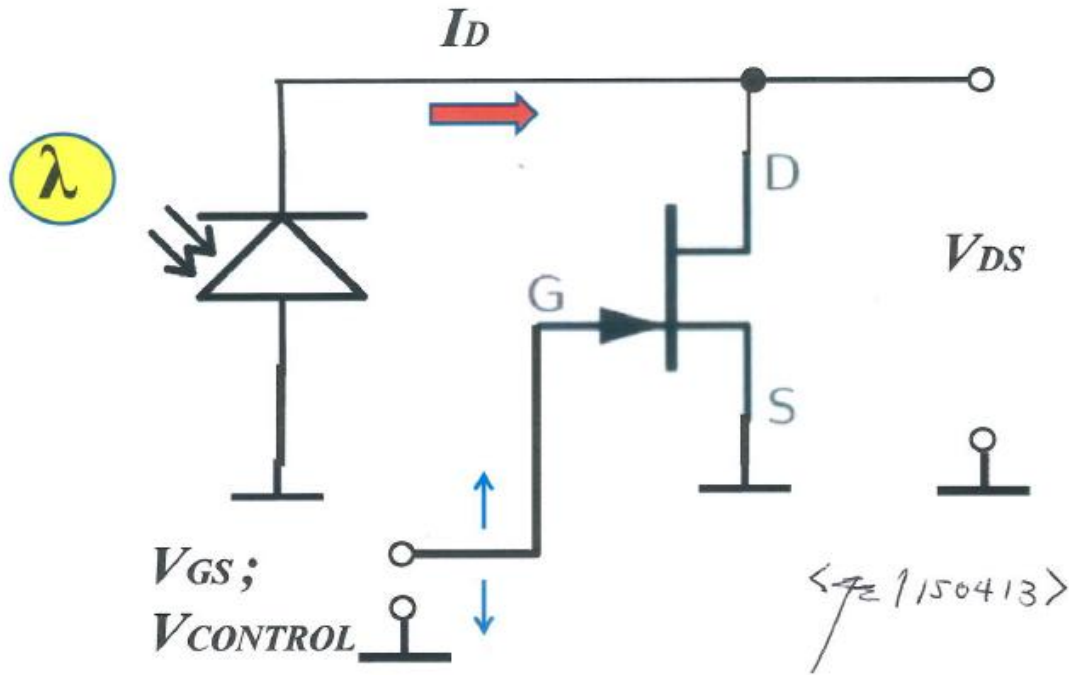


**Figure. E.3:** Basic circuit diagram showing a solar cell connection with a JFET transistor as a variable resistor.

This “**variable resistor**” in Fig. E.3 is a N-Channel JFET transistor controlled by the Gate – Source Voltage  $V_{GS}$ .

When  $V_{GS}$  is lower or more negative than the threshold voltage  $V_T$  – also known as pinchoff voltage  $V_P$  – this “Variable Resistor” is very high – i.e.: in the order of  $10^{10} \Omega$  or even higher – then the cell is practically opened and the cell’s Open Voltage Circuit  $V_{OC}$  is measured. This is the second most important parameter to define the I-V curve its coordinates are:

$$V_{OC} = V_{MAX} \quad [V] \quad ; \quad I_{OC} \approx 0 \quad [A] \quad (E.2)$$

Eq. (E.1) and Eq. (E.2) define the extreme coordinates for the cell’s I-V curve.

Notice that in a specific circuit has been implemented to measure VOC. see Subsection **a**.

When  $V_{GS}$  equal the Threshold Voltage  $V_T$  the JFET transistor starts conducting. At this condition  $V_{CELL}$  is not VOC anymore.

While  $V_{GS}$  is negative but smaller than  $V_T$  , the current  $I_D$  increases, but the voltage  $V_{DS}$  decreases since the photocurrent provided by the cell is limited.

Since the current  $I_D$  is the photocurrent generated by the cell and the voltage  $V_{DS}$  is also provided by the cell to bias the JFET, the current  $I_D$  and the voltage  $V_{GS}$  are the parameters that define the I – V curve for the solar cell.

Now, the control voltage  $V_{GS}$  and the bias voltage  $V_{DS}$  are directly measurable – as example, using a voltmeter. However the current  $I_D$  is not.

However, the above – mentioned parameters are related through **the universal FET drain current formulas** either for the linear region or the saturation region. Recall Chapter 2, Section B.3.

For the Linear Region used here, Eq. E.3 is the relationship that rules these parameters.

$$I_D = 2 \times K \left[ (V_{GS} - V_T) \times V_{DS} - \frac{V_{DS}^2}{2} \right] \quad (E.3)$$

Where:

ID	Drain Current	[A]
K	Calibration Constant	[A/V <sup>2</sup> ]
VGS	Voltage Gate – Source	[V]
VT	Threshold Voltage or Pinchoff Voltage	[V]

A prerequisite to apply Eq. E.3 is to measure the fundamental parameters  $I_{DSS}$  and  $V_T$  for the JFET transistor. See Chapter 2, Section B.2.

Next step is to calculate the calibration constant K in Eq. (E.3) through an experimental procedure detailed here.

Once K has been established it is possible to use Eq. (E.3) to calculate  $I_D$  for different  $V_{GS}$  and, respectively,  $V_{DS}$  voltages and generate the required I – V curve.

It is important to mention that though the current through the JFET is equal to the photocurrent generated by the cell, a voltage shift has to be added to  $V_{DS}$  to obtain  $V_{CELL}$ .

$$I_{CELL} = I_{DS} \quad (E.4)$$

$$\Delta V = V_{OC} - V_{DS0} \quad (E.5)$$

where  $V_{DS0}$  in [V] is the particular value of  $V_{DS}$  for which  $I_{DS} \rightarrow 0$ .

The control voltage  $V_{GS}$  is provided by the microcontroller through a D/A conversion pin. See in this Chapter Section B.6. See also Chapter 3, Section B.5.

To interface the circuit shown in Fig. E.3 with the microcontroller, some additional “gluing circuits” are required. See Chpt. 3 Fig. D.2. However, the basic ideas for this front end circuit are around Fig. E.3.

## 5. Algorithm Explanation

The algorithm is explained through an example. Several steps in the process are illustrated with plots or data from copied from the virtual instrument display-

Comment: Graphics in this numeral are considered as part of the description of the process and are not numbered as figures.

### a. Measurement of VOC

VOC and its Standard deviation are measured from a set of 100 individual measurements acquired through the microcontroller and stored in the internal memory of the Android Device or PC.

```
*VOC and Std Dev for
Tested CELL in [V]
7:
6:
5:
4:
3:
2:          VOC:422.0E-3
1:          StndDev:6.279E-3
|B@VI|EX@X@|@LST@|@LST@|STEP1|STEP2
```

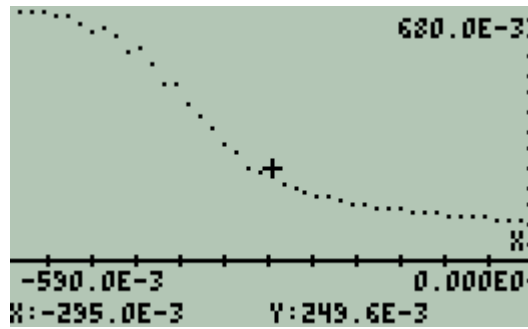
### b. Measurement of ISC

Similarly, ISC and its Standard deviation are measured from a set of .100 individual measurements.

```
*ISC and Std Dev for
Tested CELL in [A]
7:
6:
5:
4:
3:
2:          ISC:(-119.9E-6)
1:          StndDev:2.815E-6
|B@VI|EX@X@|@LST@|@LST@|STEP1|STEP2
```

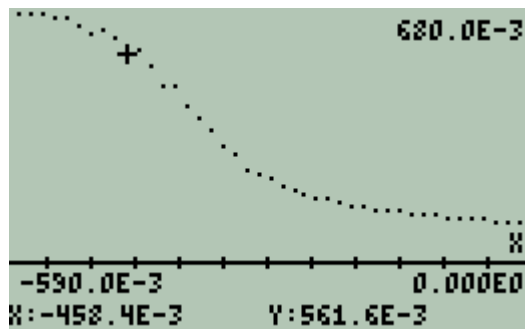
### c. Measurement of VGS and VDS

A set of 45 voltages linearly incremented are generated by the D/A converter and applied to the JFET gate. The Voltage VDS is measured. Then a plot VDS vs VGS (negative voltages) is plotted.

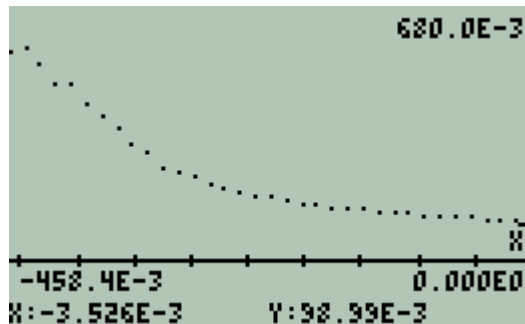


**d. Calibration Constant K calculation**

The plot VDS vs VGS is interactive with user. The coordinates for the threshold voltage VT and ISC current are obtained interactively. These data is applied to the FET's universal equation for the known Conditions for ISC then K is calculated. Next plots illustrate the process. The cursor (+) position and its coordinates shown on the bottom part of the screen are interrelated.



Cursor positioned for VGS = VT



Cursor positioned for VGS → 0 (Lower Right Coordinate)

$$I_D = 2 \cdot K \cdot \left( (V_{GS} - V_T) \cdot V_{DS} - \frac{V_{DS}^2}{2} \right)$$

EDIT CURS BIG EVAL FACTO SIMP

```

SOLVE EQUATION
Eq: 'ID=2.*K*((VGS-VT)...
ID: .00011... K: 1.31780...
VGS: -.003... VT: -.4584
VDS: .09899

Enter function to solve
EDIT CHOOS VARS EXPR=

```

Acquired coordinates allow K calculation using FET's Equation

```

SOLVE EQUATION
Eq: 'ID=2.*K*((VGS-VT)...
ID: .00011... K: 1.49395...
VGS: -.003... VT: -.4584
VDS: .09899

1.49395190418E-3
CANCL OK

RAD XYZ HEX B~ 'X' HLT PRG
CHOME SOLAR23

:K: 1.49395190418E-3
+SKIP SKIP+ +DEL DEL+ DEL L INS

```

$$K = 1.49395190418E-3$$

Note that calibration constant K is calculated for every tested solar cell

**e. IDS Currents Calculation**

Once the calibration constant is known, it is possible to calculate the IDS currents for every pair (VGS, VDS) using the calibrated FET equation. Then, a set of coordinates (VDS, IDS) are generated.

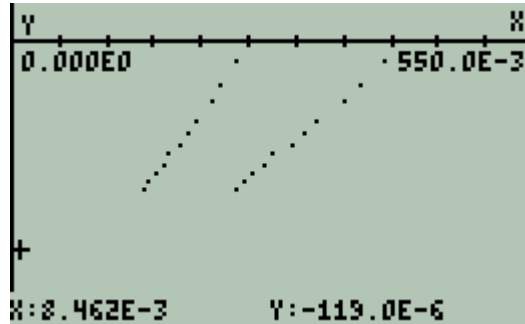
**f. VCELL calculation**

From the set of coordinates (VDS, IDS) the intersection (VDS<sub>0</sub>, 0.0) is calculable. Then the voltage shift ΔV is calculated and added to VDS in every pair of coordinates (VDS, IDS). Review Section E.3 and Eq. E.4.

Adding the coordinates (VOC, 0) and (0, ISC) to the previous set of coordinates (VDS, IDS), a preliminary set of points that belong to the solar cell I-V curve is obtained. See Section E.3.a and E.3.b.



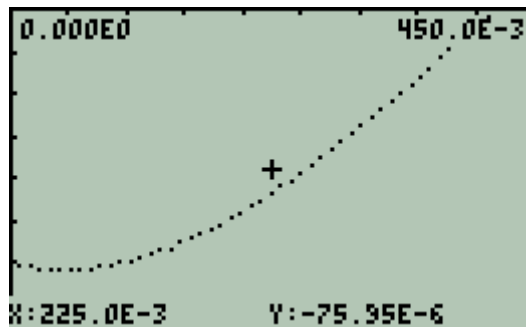
These is the preliminary set of I-V curve for the tested solar cell follows.



VDS and VCell vs ICell  
Cursor is positioned close to ISC

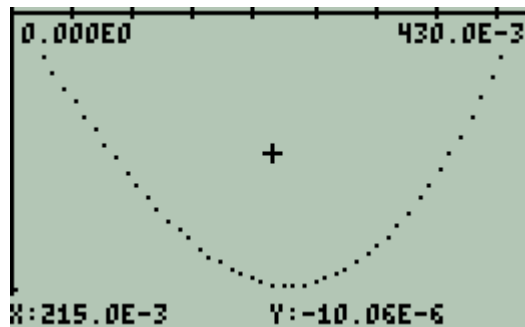
**g. Obtaining the cell's I-V Curve**

A third order polynomial interpolation obtains an explicit function that closely fits the calculated preliminary I-V curve. Then this function is scattered to 50 equidistant abscissas to display the cell's I-V Curve [13].



**h. The cell's V-W curve**

By definition power is the product current x voltage and in directly obtained from previous data. The ordinate scale now is in [W].



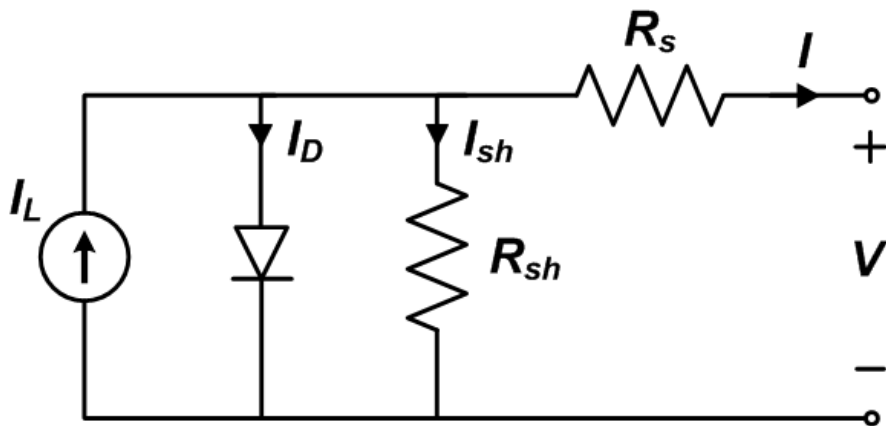
Notice that displayed plots are interactive with user.

### i. Solar Cell Parameters

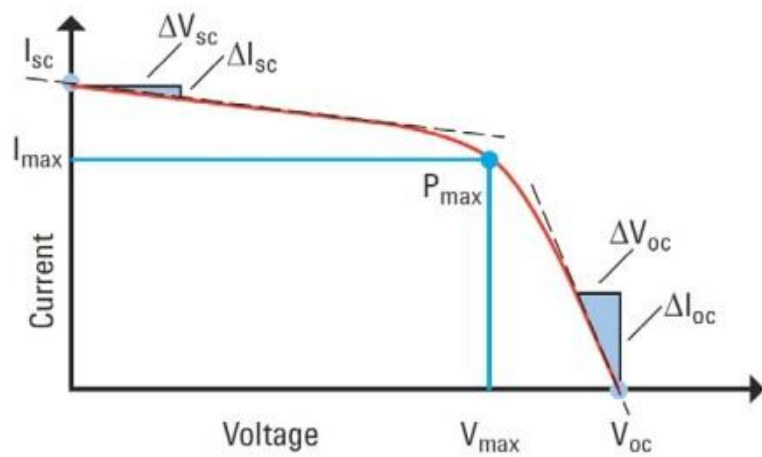
The main parameters for a solar cell are directly calculable from definitions using the fitted polynomials and scattered data now available [14] [15] [16] [17].

#### Cell's Series Resistance $R_S$ and Shunt Resistance $R_{SH}$

Series and shunt resistances are circuit parameters to characterize a solar cell. Fig. E.4 defines these parameters.



(a)



(b)

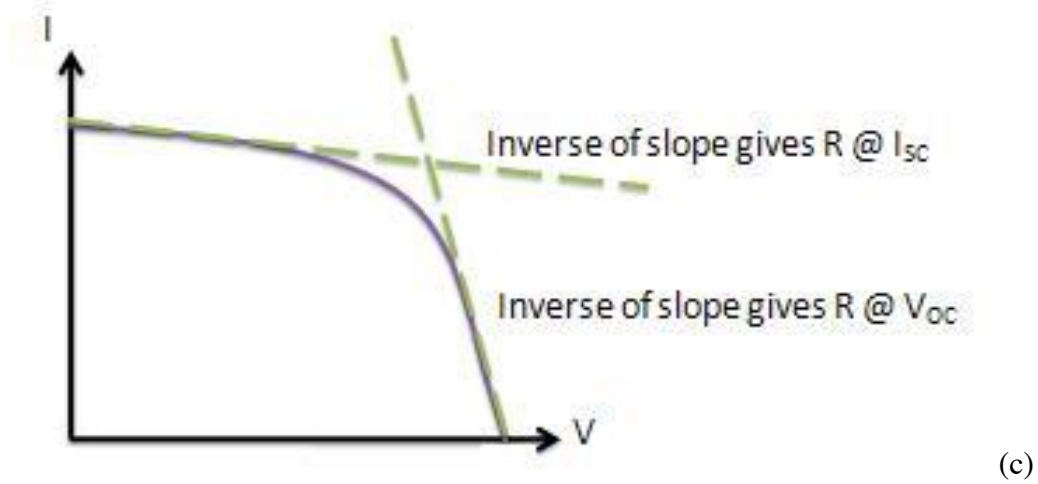


**Figure E.4:** The equivalent circuit diagram for a solar cell and the resistances  $R_S$  and  $R_{SH}$ .

[Figure adapted from reference shown in ANNEX F]

Fig. E.4 (a) shows the equivalent circuit diagram for a solar cell.

Fig. E.4 (b) shows the slope for a  $I - V$  solar cell curve for  $I_{SC}$  and  $V_{OC}$ .

Fig. E.4 (c) defines graphically  $R_S$  and  $R_{SH}$ .

Eq. (E.6.a) and Eq. (E.6.b) are the definitions for these resistances.

$$\frac{1}{R_s} = \left. \frac{dI(V)}{dV} \right|_{for V=V_{OC}} \quad (E.6.a)$$

$$\frac{1}{R_{SH}} = \left. \frac{dI(V)}{dV} \right|_{for V=0} \quad (E.6.b)$$

### Fill Factor FF

Fill Factor **FF** is defined as the quotient:

$$FF_{CELL} = \frac{P_{MAX}}{I_{SC} V_{OC}} \times 100 \ ; \ [%] \quad (E.7)$$

Fig. E.5 shows the corresponding areas to the numerator and denominator in Eq. (E.7) for a solar cell  $I - V$  curve.

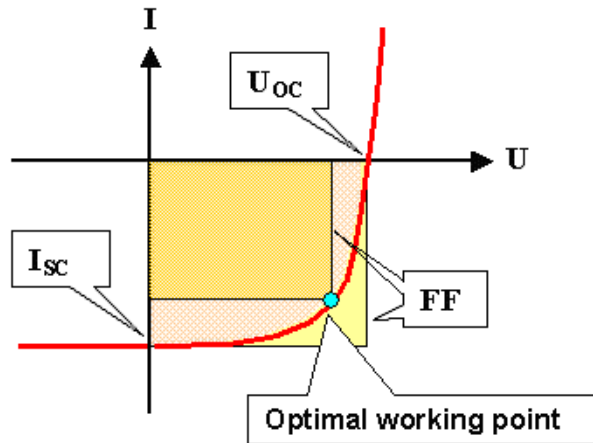


**Figure E.5:** The fill factor  $FF$  for a solar cell and the related parameter.  
 [Figure adapted from reference shown in ANNEX F]

Fill Factor parameter is readily calculated from previous data by- implementing simple additional subroutines.

#### j. Summarizing Solar Cell Parameters

Finally, the virtual instrument summarizes and displays the obtained results as it is illustrated in the following example.

```

Measured Parameters
for Tested Cell
7:      Rs:(8.379E3_Ω)
6:      Rsh:(2.165E3_Ω)
5:      ff:"37.53E0_%"
4:      pmax:(19.54E-6_W)
3:      wtot:(52.05E-6_W)
2:      Isc:(-119.9E-6_A)
1:      Voc:(422.0E-3_V)
EDAT LB0VI EX0X0 QLSTE QLSTU STEP1
  
```

#### k. Algorithm Sequence

- Measure Short Circuit current
- Measure Open Circuit voltage
- Measure and plot VGS vs VDS
- Calculate K
- Characterize Universal Eq.
- Measure IDS – VVDS preliminary points of the curve

- Calculate Shift Voltage, Calculate, Calculate VCELL voltage
- Obtain function through polynomial fitting
- Assemble final I – V curve
- Assemble W – V curve
- Calculate Maximum Power
- Calculate Series Resistance
- Calculate Shunt Resistance
- Calculate Fill Factor
- Display Results

## **F. SUMMARY OF VIRTUAL INSTRUMENTS MEASUREMENTS AND EVALUATION**

Virtual Instruments are an alternative to develop measurement or control instrumentation reducing the distance between the theoretical support and the instrument implementation, making easier the transfer of knowledge and the options of development, freeing instrumentation requirements at a cost without competence. Its price is educate people to be able to develop and use it.

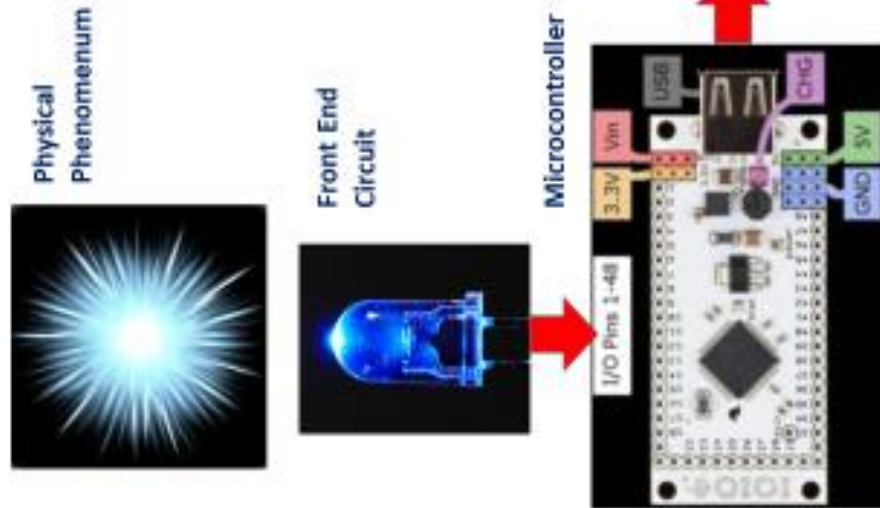
There are many fields to develop and apply virtual instrumentation. It is a new alternative that is starting.

One important field where virtual instrumentation has fascinating alternatives for application is Nanoscience and Nanotechnology.

There is one more advantage: Virtual Instruments easily can be in hands of almost anyone nowadays.

Fig. E.1 suggests one possible approach to virtual instruments.

# VIRTUAL INSTRUMENT

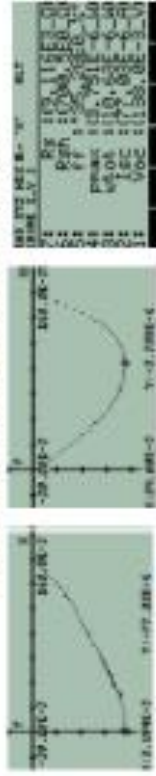


Android Device Programmer



<FE / 160708>

Numerical and Graphical Results



Advanced Programmed Graphic Calculator Emulator inside Tablet

## Bibliography

- [1] HP 48gx Calculator - Product Specifications  
<http://support.hp.com/us-en/document/bpia5074>
- [2] HP 50g Graphing Calculator  
<http://commerce.hpcalc.org/50g.php>
- [3] Wikipedia Word: Emulator  
<https://en.wikipedia.org/wiki/Emulator>
- [4] Wikipedia Word: HP 49/50 Series  
[https://en.wikipedia.org/wiki/HP\\_49/50\\_series](https://en.wikipedia.org/wiki/HP_49/50_series)
- [5] Droid48 for Android  
[http://download.cnet.com/Droid48/3000-2124\\_4-75618896.html](http://download.cnet.com/Droid48/3000-2124_4-75618896.html)
- [6] Droid48 Reader  
[https://play.google.com/store/apps/details?id=com.drehersoft.droid48reader&hl=es\\_419](https://play.google.com/store/apps/details?id=com.drehersoft.droid48reader&hl=es_419)
- [7] Christoph Giesselink  
  
HP All-in-1 Graphing Calculator Emulator  
  
<https://www.educalc.net/881486.page>
- [8] Wikipedia Word: Successive Approximation ADC  
[https://en.wikipedia.org/wiki/Successive\\_approximation\\_ADC](https://en.wikipedia.org/wiki/Successive_approximation_ADC)
- [9] Microchip.com Manual PIC24F Microcontrollers Family  
Section 17. 10-Bit A/D Converter  
<http://ww1.microchip.com/downloads/en/DeviceDoc/39705b.pdf>
- [10] Wikipedia Word Nyquist Criterion  
[https://en.wikipedia.org/wiki/Nyquist\\_rate](https://en.wikipedia.org/wiki/Nyquist_rate)
- [11] SERIC Solar Simulator  
<http://www.seric.co.jp/english/solarsimulator/ss-for-module.html>
- [12] sidney.edu.au Lab 1 – Electrical Characteristics of Photovoltaic Cells  
  
<http://sydney.edu.au/engineering/electrical/people/ruihong.chu/UserFiles/File/PV%20labnotes-lab1%281%29.pdf>

- [13] Hewlett Packard      HP 50G CALCULADORA GRAFICA  
Guía de Usuario  
Capítulo 18 Aplicaciones Estadísticas  
Ajuste Polinómico págs. 18-66 a 18-73  
Edición 1 Número de parte de HP F2229AA-90007  
2003 - 2006
- [14] 8.1.2 Solar Cell Current-Voltage Characteristics and Equivalent Circuit Diagram  
[https://www.tf.uni-kiel.de/matwis/amat/semitech\\_en/kap\\_8/backbone/r8\\_1\\_2.html](https://www.tf.uni-kiel.de/matwis/amat/semitech_en/kap_8/backbone/r8_1_2.html)
- [15] Use of Monochromatic Light for Localized Characterization of Photovoltaic Cells  
<https://www.azom.com/article.aspx?ArticleID=10184>
- [16] Single Diode Equivalent Circuit Models  
<https://pvpmc.sandia.gov/modeling-steps/2-dc-module-iv/diode-equivalent-circuit-models/>
- [17] Comparisons of IV Curves between Xenon Lamp-Based and LED-Based Solar Simulators  
<https://www.azooptics.com/Article.aspx?ArticleID=1116>



## Basic References

### | 1 | **HP 48G Series User's Guide**

By Hewlett-Packard and Eric Rechlin

Complete copy of the eighth edition of the 48G series instruction manual. This PDF document has 612 pages and was scanned by the Author at 300 dpi monochrome. Fully bookmarked in order to easily jump between sections. Included on this site with the permission of HP tech support.

<http://www.hpcalc.org/search.php?query=HP48G+Advanced+User%27s+Reference+Manual>

### | 2 | **HP 48G Series Advanced User's Reference Manual**

Complete copy of the fourth edition of the HP 48G Series Advanced User's Reference Manual. This PDF document has 764 pages and was scanned at 300 dpi color by an unknown individual.

By Hewlett-Packard

<http://www.hpcalc.org/search.php?query=HP48G+Advanced+User%27s+Reference+Manual>

### | 3 | **HP 50g User's Guide**

Complete English-language 887-page user's guide for the HP 50g.

By Hewlett-Packard

<http://www.hpcalc.org/search.php?query=HP+50g+user%27s+guide>

### | 4 | **HP 50g / 49g+ / 48gII graphing calculator advanced user's reference manual**

Edition 2 HP part number F2228-90010 Printed Date: 2009/7/14

<http://h10032.www1.hp.com/ctg/Manual/c02836298>

| 5 | **hpcalc.org**

<http://www.hpcalc.org>

This site is the main repository of programs and information about hp programmable graphic calculators. It is the premier source of software for and information about the HP Prime, HP 50, HP 49, HP 48, and HP 28 RPN programmable graphic calculators and the HP 38G, HP 39, and HP 40 programmable graphic calculators, with 7625 files by 2307 authors and 3204 screenshots totaling 961.81MB.

---

*CHAPTER 5*  
*METHODS*  
*AND*  
*MATERIALS*



## OUTLINE OF THE CHAPTER

- A. CALIBRATION PROCEDURES AND EXPERIMENTAL RESULTS
  - 1. ENVIRONMENTAL THERMOMETER
  - 2. SPECTRAL TEMPERATURE METER
  - 3. IRRADIANCE METER
  - 4. LABORATORY MEASUREMENTS ON THERMAL RADIATION
  - 5. SOLAR I-V CURVE GENERATOR
  
- B. MATERIALS USED IN THE PROJECT
  - 1. ELECTRONIC COMPONENTS
  - 2. MICROCONTROLLER BOARD
  - 3. FREeware



## CHAPTER 5: METHODS AND MATERIALS

This chapter contains the Calibration Methods and Experimental Results for the developed virtual instruments and the materials and freeware used in the project.

This chapter is divided in two sections.

In Section A:

Refers to Instruments Calibration and Experimental Results. It follows identical sequence than previous chapter.

Calibrations were made at the **ICN2** in two laboratories:

**Laboratory for General Services**

and, mainly in the

**Laboratory of Nanostructured Materials for Photovoltaic Energy.**

In Section B:

The materials used in the project: electronic components, microcontroller board and software are summarized.





## A. CALIBRATION PROCEDURES AND EXPERIMENTAL RESULTS

### 1. ENVIRONMENTAL THERMOMETER

#### Calibration Procedure

Thermometer calibration procedure is described based on previous subsections on this matter. Recall Chapter 2, Section B.1; Equations (B.1) to (B.4). Recall Chapter 4 Section C.

For temperature calibration constant temperature references are required.

Table A. shows useful temperature references for calibration.

**Table A1. Useful temperature references for calibration.**

Substance	Temperature [K]
Liquid Nitrogen*	77.36
Solid Nitrogen**	63.15
Solid CO <sub>2</sub>	194.65
H <sub>2</sub> O boiling T	373.16
H <sub>2</sub> O melting T	273.16

\* At a pressure of 1 atmosphere, room temperature

\*\* In equilibrium with surrounding liquid Nitrogen

A Si PN junction biased with constant current  $\sim 10 \mu\text{A}$  is immersed in the constant temperature substance. The voltage drop in the junction is measured after equilibrium is observed. The PN

junction shows a very fast response to changes in temperature and few seconds are enough to obtain equilibrium.

Two reference constant temperature sources are required for the calibration procedure.

Low temperature reference produces the highest voltage  $U_0$  in the junction and high temperature source produces the lowest voltage in the junction.

Applying these values to the calibration algorithm, the thermal voltage drop  $V_{th}$  due only to temperature and the calibration constant  $K_2$  are obtained from Ebers – Moll equation. Recal Chp.4 Subsection C.3.

Then the calibrated range of temperatures is confined by these two temperature references.

The resultant expression is a function of  $I$  (the known constant current through the junction in [A]),  $V$  (the voltage drop along the junction in [V]) and  $T$  (the Absolute Temperature in [K]).

This expression allows calculate any temperature in the calibrated range as a function of the thermal voltage drop in the junction. An algorithm implemented makes this calculation and displays results.

### **Experimental results**

Experimentally, it was found that it is not appropriate to have a single scale for room temperature and cryogenic temperature ranges. It is more convenient to have two temperature scales. For Instance:

$$373.15 \geq T \geq 273.15 \text{ [K]} \quad \text{Room Temperature Range}$$

$$273.15 \geq T \geq 77.36 \text{ [K]} \quad \text{Cryogenic Temp Range}$$

The option to use CO<sub>2</sub> (solid) allows a temperature reference to overlap 273.16 [K] in both previous scales.

Under these conditions accurate and repeatable temperature measurements were obtained in both ranges.

Table A.2 shows the voltage drop in the silicon junction when it is submerged in liquid nitrogen and boiling water as temperature references. Measures were made three using small Si diodes.

**Table A.2: Junction Voltage for liquid nitrogen  
Temperature and boiling water temperature.**

<b>Junction Code</b>	<b>Vlow (77.26[K])</b>	<b>Vhigh (373.16[K])</b>
A	0.990	0.174
B	0.992	0.176
C	0.983	0.175

Note: For 10  $\mu$ A current source

**Example**

For a forward biased Si junction using a constant current source of 9.5  $\mu$ A immersed in an environment at 273.16 K a voltage drop through the junction of 0.722 V was measured. So, the calculated constant is  $k_2 = 3.45047488397 \times 10^{-5}$ . When the junction was exposed to environment and thermal equilibrium was obtained, the voltage drop across the junction was 0.716 V that is equivalent to 294.791 K or 21.63 Celsius.

Calibration was made at:

**Laboratory for General Services – ICN2**

## 2. SPECTRAL TEMPERATURE METER

### Calibration Procedure

Spectral Temperature calibration procedure is described based on previous subsections on this matter. Recall Chp. 4 Section B, particularly Subsections B.2 to B.5.

Spectral Temperature from a thermal radiation source is measured using two narrow bands of the spectrum. These narrow bands are detected using LEDs of two different spectral bands as sensors – as example green and red LEDs. Each LED has a constant narrow band where it is sensitive for radiation.

Once spectral irradiance is obtained for both windows, the algorithm using Eq. (D-28) Chp. 4 calculates the correspondent spectral temperature in [K] .

Section D.2 in Chp. 4 describes in detail this procedure.

### Experimental Results

Table A.3 shows the bands where green and red LEDs are active. Irradiance quotient bndqo measured for both bands is also shown.

**Table A.3: Virtual Pyrometer Parameters for LEDs**

---

Green LED:	$\lambda_1 = 350\text{E-}9$ [m]	$\lambda_2 = 530\text{E-}9$ [m]
Red LED:	$\lambda_3 = 510\text{E-}9$ [m]	$\lambda_4 = 660\text{E-}9$ [m]
Band Quotient	bndqo = $7.335\text{E-}3 / 16.84\text{E-}3 = 435.6\text{E-}3$	

---

As example, Fig. A.1 shows the results of introducing the wavelengths that define each band and the quotient of irradiances in each band and the calculated spectral temperature using the algorithm based on Ec. (D-28) Chp. 4.

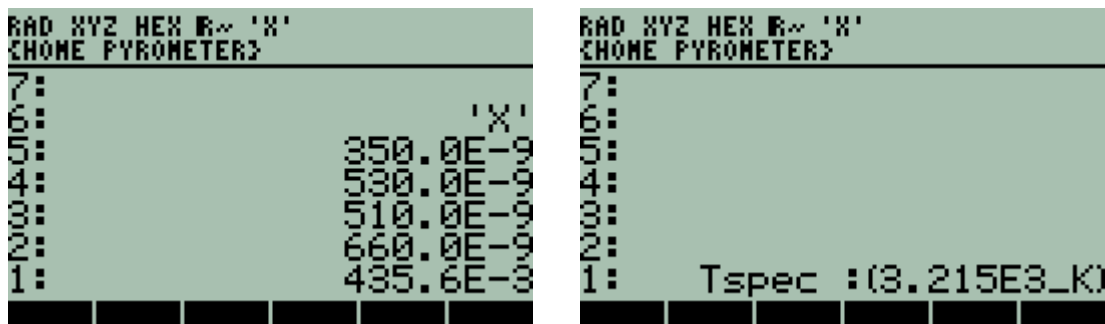


**Figure A.1:** Wavelengths that define each band and the experimental quotient of irradiances for each LED reproduce spectral temperature of the light source using the developed algorithm. It shows consistency of results using this method.

Calibration was made at:

**Laboratory for General Services – ICN2**

### 3. IRRADIANCE METER

#### Calibration Procedure

Spectral Temperature calibration procedure is described based on previous subsections on this matter. Recall Chpt. 4 Section B, particularly Subsections B.2 to B.5.

Spectral Temperature and Irradiance are concomitant parameters that define Thermal Radiation.

Irradiance is measured using a Si photodiode. The Si photodiode is masked with an opaque sheet with a circular hole of known diameter. If spectral temperature is known then thermal spectrum is also known. Measured photocurrents from the Si photodiode and responsivity of Si photodiodes allow that spectral irradiance calculation and total irradiance calculation.

The process is explained in detail in Chapter 4Section D.1.

## Experimental Results

Table A.4 shows the measurement of irradiance using this method.

**Table A.4: Experimental Results for total Irradiance using Si Photodiode**  
 **$T_{SP} = 3175$  [K]**

---

Sensor Component:	Si Photodiode (Masked)	
Si Photodiode Spectral Bandwidth:	$400.0E-9 \leq \lambda \leq 1100.0E-9$ [m]	
Masked Si Photodiode Active Area:	4.144 [mm <sup>2</sup> ]	
Measured Photocurrent:	185.32E-6 [A]	
Photocurrent / mm <sup>2</sup> *	44.817E-6 [A/mm <sup>2</sup> ]	
Normalized Photocurrent **	195.54E-3 [mA/mm <sup>2</sup> ] = 195.54E-6 [A/mm <sup>2</sup> ]	
Fraction coef ***	229.20E-3 $\approx 0.229 \approx 23$ %	
Calculated Irradiance from Irradiance	97.429E-3 [mW/mm <sup>2</sup> ]	Measured
Normalized Irradiance	425.07E-3 [mW/mm <sup>2</sup> ]	
Fraction coef	229.20E-3 $\approx 0.229 \approx 23$ %	

Comment: Identical to current fraction coef.

**Calculated Total Irradiance**                      **0.229 [mW/ mm<sup>2</sup>]**

---

Notes:

\* Measured Photocurrent / Active Area

\*\* Photocurrent Summation. See Numeral (5)

\*\*\* (Photocurrent / mm<sup>2</sup> / Normalized Photocurrent)

Calibration was made at:

**Laboratory for General Services – ICN2**

#### 4. LABORATORY MEASUREMENTS OF THERMAL RADIATION

##### **Irradiance Meter Calibration by Intercomparison with a Standard Pyranometer**

Calibration procedure for irradiance meter described in Subsection A.3 in this chapter requires an additional calibration factor **K<sub>irr</sub>** obtained from Intercomparison with a Calibrated Pyranometer (Secondary Standard). The default calibration factor is 1. However, experimentally was observed that every Si photodiode has different yield due to fabrication processes and, necessarily an intercompared calibration is required.

The virtual irradiance meter was intercompared with the standard laboratory pyrometer. The standard pyrometer is in a fixed position Light intensity from the Xenon arc lamp is regulated to fit a reading of 1000 [W/m<sup>2</sup>]. Both instruments were placed at identical geometry and exposed to the Xenon Arc Lamp of the Solar Cell Simulator in the Laboratory.

##### **Experimental Results**

Since Irradiance and Spectral Temperature are concomitant parameters, experimental results of both parameters are presented at the end of this numeral.

Calibration was made at:

**Laboratory of Nanostructured Materials for Photovoltaic Energy – ICN2**

##### **Spectral Temperature measurement**

Once the spectral windows for red and green LEDs are defined experimentally and the active areas for each LED are calculated from its photocurrents, spectral temperature from another thermal source is measurable. Recall LED's active area calculation pages 4-37 to 4-41. Recall spectral temperature calculation pages 4-50 to 4-53.

Spectral Temperature calibration is not required since the algorithm is based on the standardized Planck's Equation  $F_0\lambda(T, \lambda)$ .

Laboratory where preliminary measurements were made:

**Laboratory of Nanostructured Materials for Photovoltaic Energy – ICN2**

## **EXPERIMENTAL RESULTS FOR THERMAL RADIATION MEASUREMENTS**

In this numeral Thermal Radiation intercomparison and experimental results are reported.

### **Objectives**

- Document Spectral Temperature Measurements from two light sources (Xenon Arc Lamp and commercial 220 Vac Tungsten filament lamp) made with the Virtual Instrument – VI prototype.
- Measure Irradiance from the Laboratory Solar Simulator using the Virtual Instrument – VI prototype and intercompare results with those obtained with the Laboratory equipment.
- Evaluate obtained results.

## **MEASUREMENTS OF SPECTRAL TEMPERATURE**

### **Method**

Spectral Temperature from a thermal radiation light source is measured using the VI prototype. The VI prototype has as sensors two Light Emitting Diodes of different colour (as example green and red LEDs) that are exposed to the light source.

Measured photocurrents from these LEDs are converted to equivalent irradiances scaled to identical active area for both LEDs. A developed algorithm searches for the thermal radiation spectra that matches with the measured data and displays calculated spectral temperature in [K].

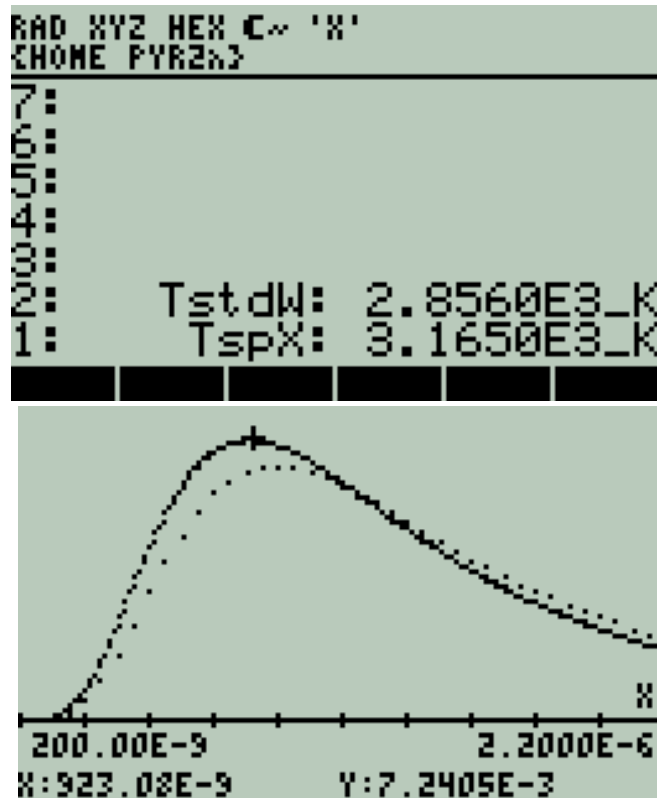
The CIE (International Commission on Illumination) recommended colour temperature was selected as standard reference [1].

**CIE Standard Colour Reference Temperature = 2855.54 [K]**



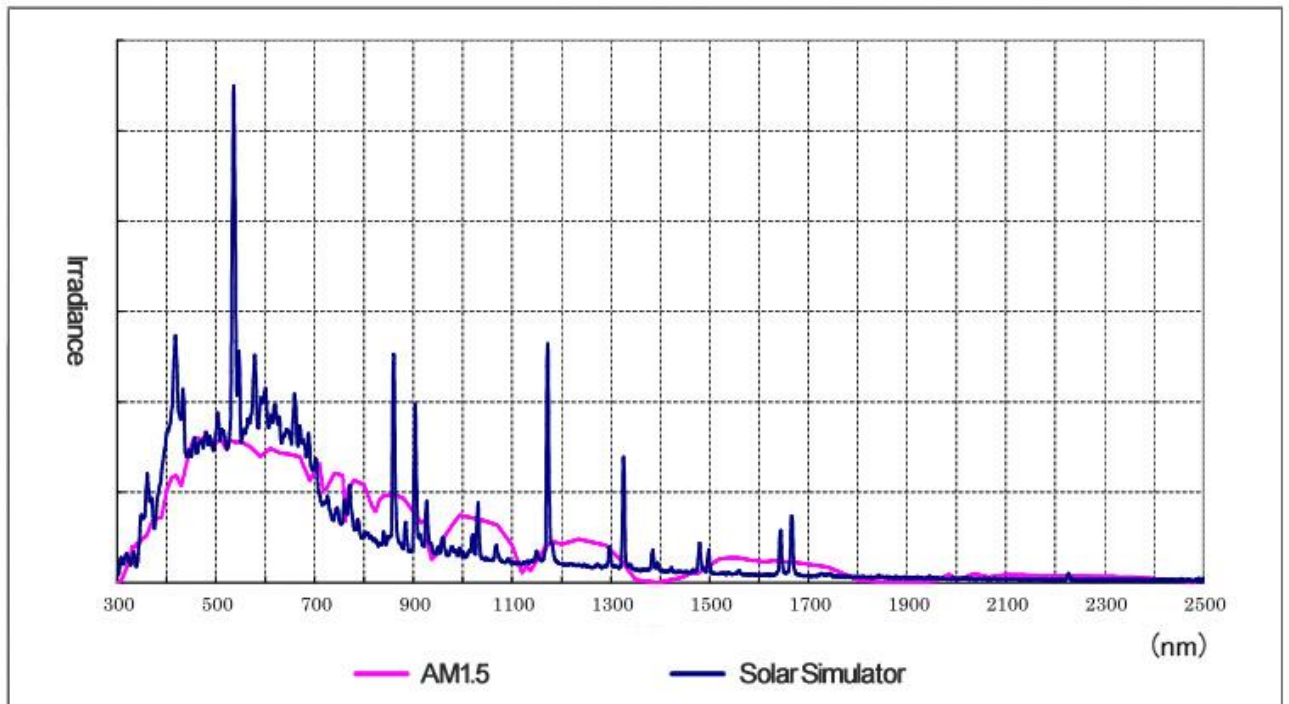
## Results

Fig. A-2 Shows the Thermal Radiation Spectrum for 2856 [K] as standard reference and the spectral temperature measured for a commercial 220 Vac tungsten filament lamp.



**Figure A-2:** Thermal Irradiance spectrum vs. wavelength.  
Lower Curve for  $T\text{-std} = 2856$  [K].  
Higher curve for 3165 [K] measured from a 220 Vac tungsten filament lamp.

Fig. A.3 shows the spectral irradiance for a Xenon Arc Lamp used as light source for solar simulators [2].



**Figure A3:** *Spectral Irradiance of a Xenon Lamp for Solar Simulator.*  
*[Figure adapted from reference shown in ANNEX F]*

Although a Xenon arc lamp is not strictly a thermal radiation light source or Planck's source, its spectral temperature was measured with the VI prototype. Fig.D.14 shows the measured temperature and the corresponding thermal radiation spectrum. As reference, the CIE standard is also presented in the plot.

It is reasonable to think that Irradiance measurements made for a Xenon Lamp spectrum, though representative, should be considered only as referential.

```

Tungsten Std TRef
and Measured TX
7:
6:
5:
4:
3:
2:      TstdW:(2.856E3_K)
1:      TspX:(4.255E3_K)

```

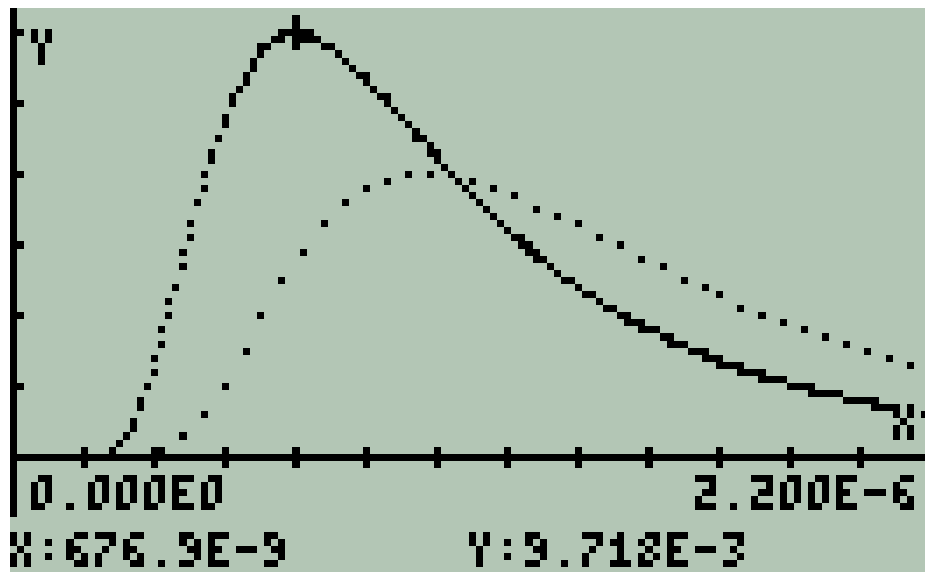


**Figure A.4:** *Thermal Irradiance vs. wavelength.*  
 Lower Curve for  $T_{stdW} = 2856 \text{ [K]}$ .  
 Higher curve  $T_{spX}$  for  $4225 \text{ [K]}$  measured for the solar simulator Xenon Arc Lamp

## **MEASUREMENT OF IRRADIANCE AND INTERCOMPARISON**

### **Method**

Irradiance is measured by the VI prototype using a Si photodiode as sensor. The Si photodiode is masked and only a circular orifice of known area allows incident light to generate a photocurrent. Measured photocurrent is converted into irradiance through an algorithm using the Si photodiode responsivity and the exposed active area.

The Laboratory Pyranometer was calibrated for an Irradiance of 1000 [W/m<sup>2</sup>] using the Lab's solar simulator software. The VI instrument sensor was positioned close to the laboratory pyranometer at the same level of the lab pyranometer sensor (thermopiles) then irradiance was measured. A calibration constant  $K_{irr}$  was obtained to match both readings.

Once the VI prototype was calibrated taking as reference the Lab's pyranometer, a second measurement was made positioning the VI sensor at the level and place where solar cells are normally placed for tests. The purpose is to have a ratio between the irradiance measured by the Lab's pyranometer and the actual irradiance on the tested cell centred on the measuring workbench.

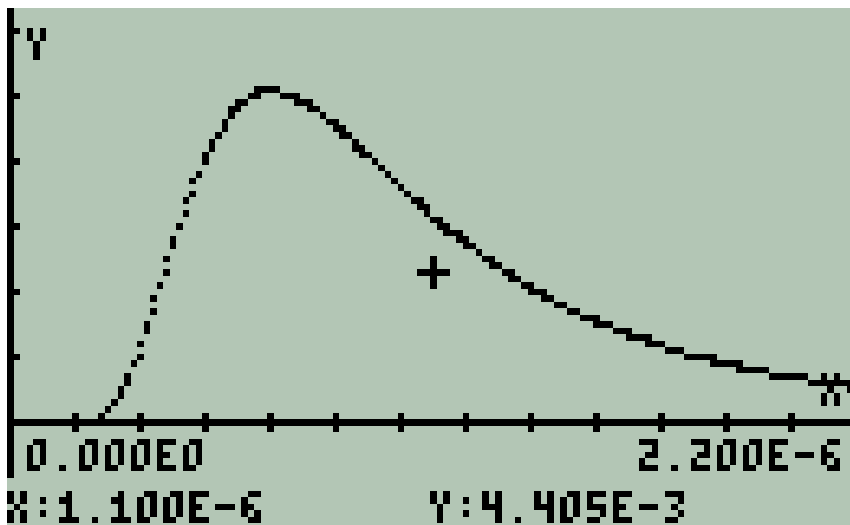
### **Results**

Fig. A.5 shows measured Irradiance after calibration taking as reference the Lab's Pyranometer.

```

One-Tech Sun IRRAD
and Measured IRRAD-X
0:      Tsp:(4.255E3_K)
2:      Irr-std:(1_  $\frac{mW}{m^2}$ )
1:      IrrX:(1.001E0_  $\frac{mW}{m^2}$ )

```



**Figure A.5:** Results after calibration of VI prototype taking as reference the Lab's pyranometer. Sensors from both devices are positioned at equal distance from light source. Standard Irradiance Irr-std and measured irradiance IrrX overlap each other.

Comments:

- This IrrX reading, once calibrated, coincides with the Laboratory reading.
- Irradiance for Laboratory equipment was carefully calibrated before Intercomparison.
- This implies that VI prototype is calibrated with Laboratory Pyranometer at the position where the Lab's Pyranometer is placed.

Observation:

- Lab's Reference Pyranometer sensor and VI prototype sensor are not positioned facing perpendicularly to light source under actual circumstances.

This time, the VI prototype sensor was placed at the same position and distance to light source where solar cells are normally placed to be tested. VI sensor was placed facing perpendicularly to light source. Fig. A.6 shows results.

```

One-Tech Sun IRRAD
and Measured IRRAD-X
3:      Tsp:(4.255E3_K)
2:      Irr-std: [ 1 -  $\frac{mw}{2}$  ]
              [ mm ]
1:      IrrX: [ 1.159E0 -  $\frac{mw}{2}$  ]
              [ mm ]
  
```

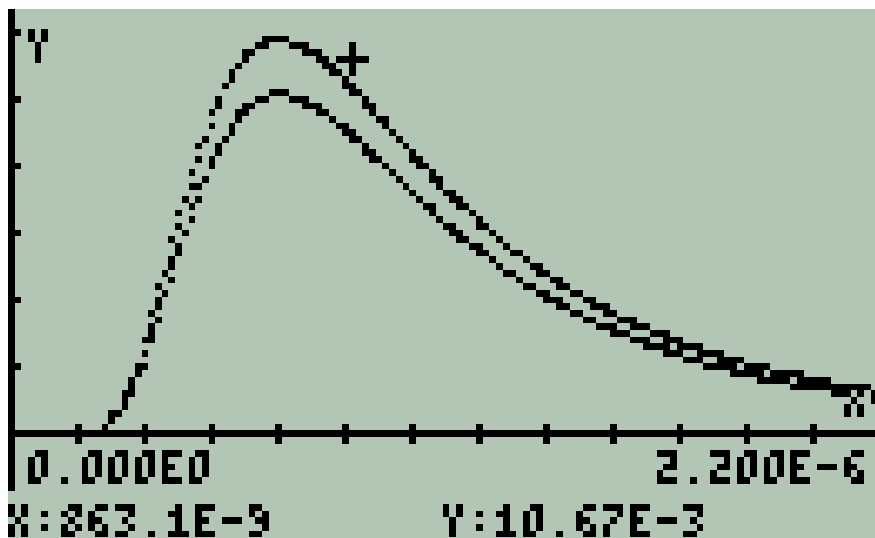


**Figure A.6:** Results measured with VI prototype after being calibrated. The VI sensor this time is positioned where solar cells are normally placed to be tested. Standard Irradiance Irr-std and measured irradiance IrrX differ. Marked (+) function corresponds to IrrX.

## EVALUATION

- Spectral temperature meter from the VI prototype shows consistent measurements when it is exposed to a thermal radiation light sources. It also could be a tool to have approximate measurements where it is exposed to radiation light sources that are not strictly thermal radiation sources as are the Xenon arc lamps used in solar simulator devices.
- Calibrated irradiance meter from the VI prototype is a useful tool to characterize irradiance conditions to test solar cells.
- Besides stable and calibrated light sources, geometry is essential for reproducibility of results when solar cells are being developed or tested.

Laboratory where preliminary Measurements were made:

**Laboratory of Nanostructured Materials for Photovoltaic Energy – ICN2**

### References

- |     |                  |  |
|-----|------------------|--|
| [1] | <b>Wikipedia</b> | <b>CIE Standard illuminant</b><br><a href="https://en.wikipedia.org/wiki/Standard_illuminant">https://en.wikipedia.org/wiki/Standard_illuminant</a>                            |
| [2] | <b>SERIC</b>     | Solar Simulator for Modules<br><a href="http://www.seric.co.jp/english/solarsimulator/ss-for-module.html">http://www.seric.co.jp/english/solarsimulator/ss-for-module.html</a> |

## **5. SOLAR I-V CURVE GENERATOR**

Experimental results of the I-V curve generator and related parameters are presented in Chapter. 4 Section E. Also recall Chapter 3 Fig. D.2.

### **Intercomparison and Experimental Results**

Two experiments are presented: The first one is an Intercomparison of three solar cells I-V curves measured with the virtual instrument. The second one is the temporal response of a solar cell that is degraded by incident light.

#### **a. I-V Curve Intercomparison**

I-V curves for three solar cells prototypes developed in the ICN2 Laboratory for Nanostructured Materials for Photovoltaic were measured using the Laboratory Equipment and the developed Virtual Instrument prototype as well.

A subroutine to transfer data measured in the Laboratory Equipment to the Virtual Instrument prototype was developed and results were intercompared.

Only plots are presented and numerical data and details of procedure are omitted.

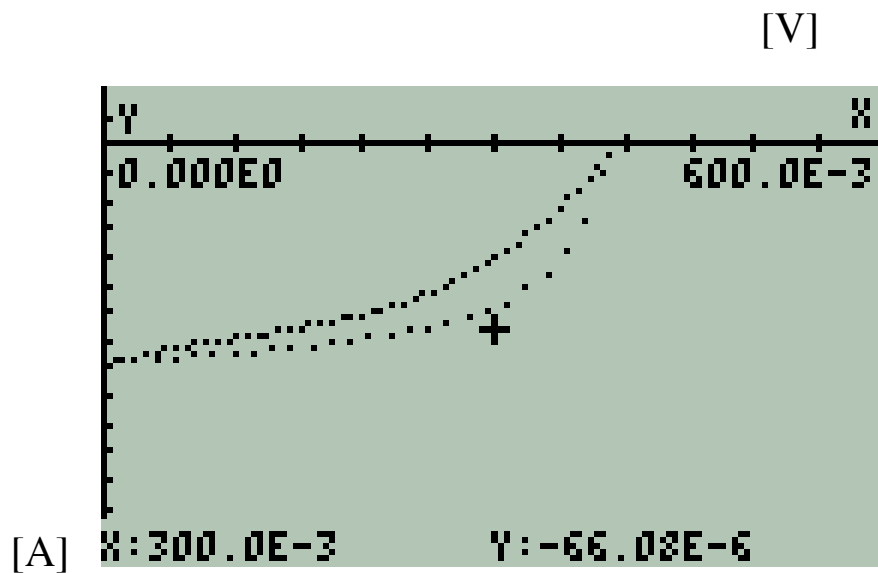
Intercomparison of results follow.



Abscissa: Solar Cell Voltage. Scale in [V]

Ordinate: Solar Cell Current. Scale in [A]

CELL'S CODE: **VR-1**



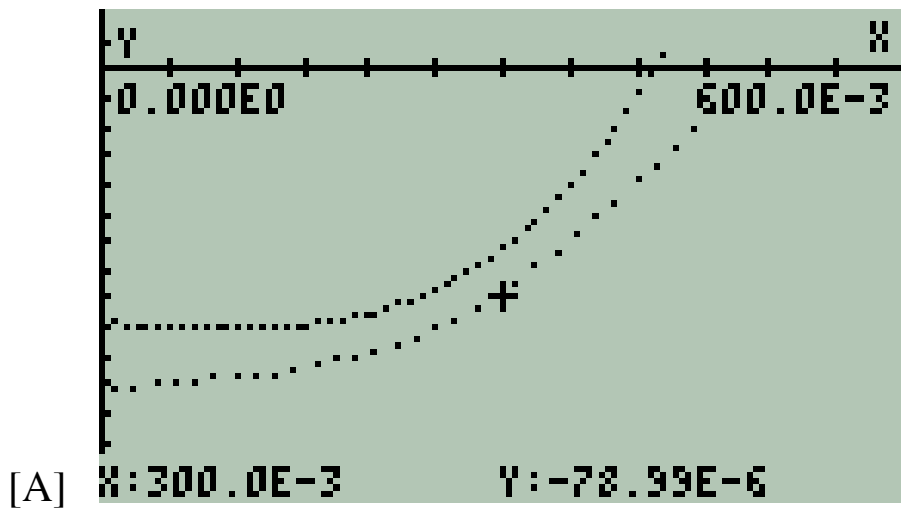
Intercomparison I-V cell plot

(+) Marked curve corresponds to Laboratory equipment

**Figure A.7 :** *Intercomparison for Cell VR-1*

CELL'S CODE: **ALB-1**

[V]



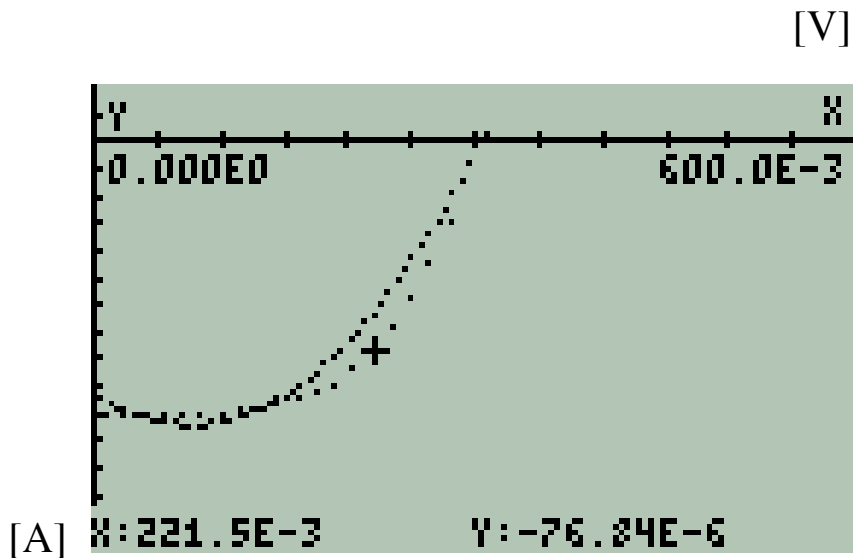
Intercomparison I-V cell plot

(+) Marked curve corresponds to Laboratory equipment

**Figure A.8:** *Intercomparison for Cell ALB-1*

Comment: There is a time difference between both measurements meanwhile the cell's yield has decreased.

CELL'S CODE: **Si-e**



Intercomparison I-V cell plot  
(+) Marked curve corresponds to Laboratory equipment

Figure. A.9 : *Intercomparison for Cell Si-e*

**EVALUATION:**

**A close agreement in obtained results for both instruments is observed.**

**b. Temporal response of a HTL-free perovskite solar cell using a virtual instrument prototype**

**Objective**

Measure and evaluate the temporal response of a HTL-free perovskite solar cell using the developed Virtual Instrument prototype.

**METHOD**

A HTL-free perovskite solar cell provided by the Laboratory were masked with an opaque film with a 0.02 cm<sup>2</sup> circular orifice positioned on the front face of the cell favourable placed to obtain the highest current yield. Copper conductors were built from cell's electrodes and the cell was shielded from external light sources with exception of the 0.02 cm<sup>2</sup> circular orifice.

The tested cell was continuously exposed to 1 technical sun irradiance (1 kw/m<sup>2</sup> = 1 mw/mm<sup>2</sup>) during ten hours under standard laboratory procedure. Irradiance was carefully checked during the process. VOC, ISC and I – V response were measured every 30 minutes. Measurements were compared with those results obtained from Laboratory instruments showing consistent results. Acquired data was fitted to present plotted results.

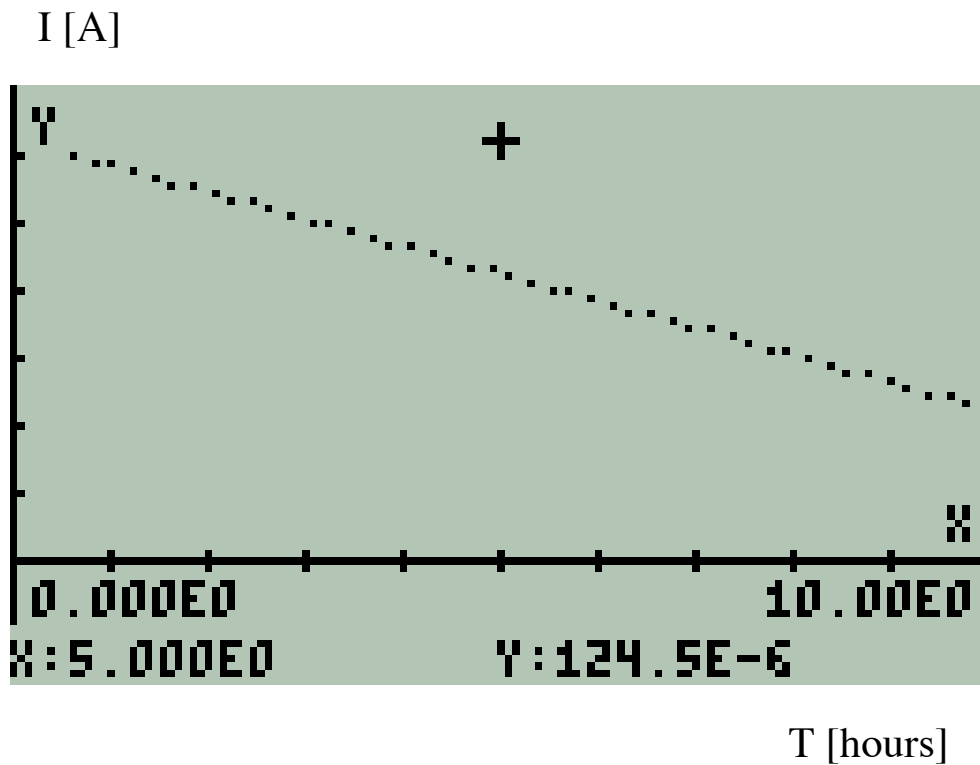
**LABORATORY EQUIPMENT WORK PARAMETERS**

The Laboratory operating parameters were:

Cell's exposed area	0.02	[cm <sup>2</sup> ]
V minimum for scanning	-0.10	[V]
V maximum for scanning	0.80	[V]
V step	15	[mV]
Scan Rate	20	[mV/s]
Irradiance	1000	[W/m <sup>2</sup> ]

## RESULTS

### Short Circuit Current Temporal Response



$$I_{\text{DECREMENT RATE}} = - 8.031 [\mu\text{A}/\text{hour}]$$

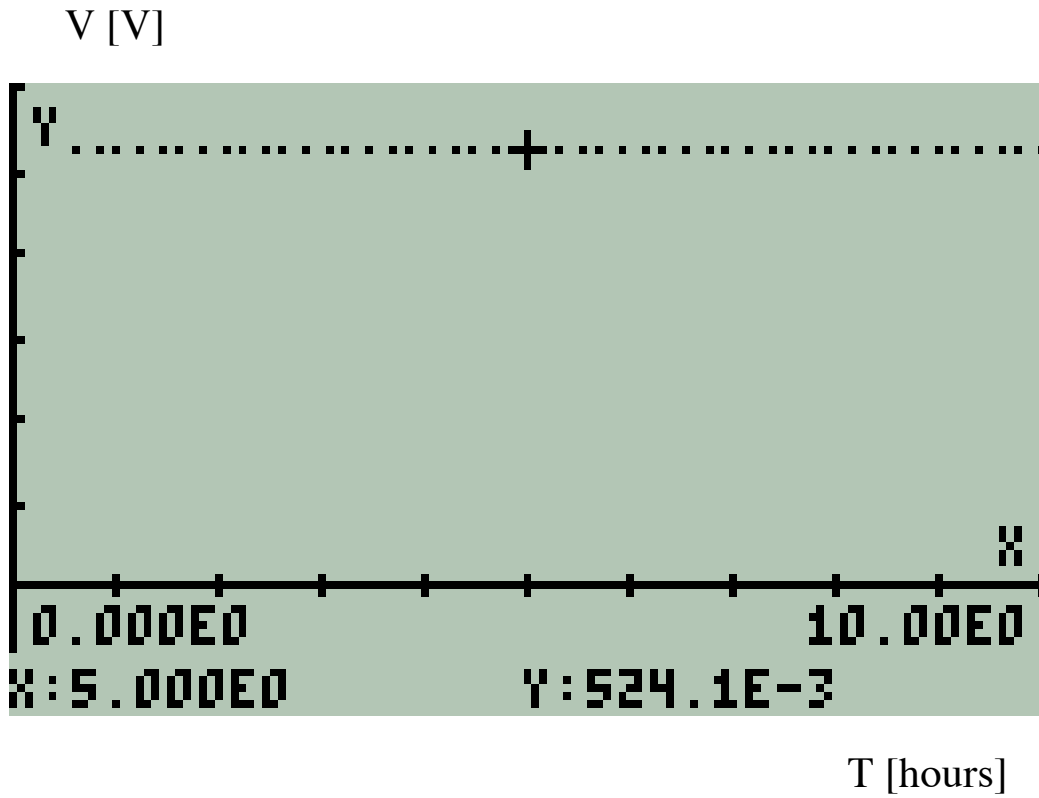
$$J_{\text{DECREMENT RATE}} = -401.6 [\mu\text{A}/\text{cm}^2 \text{ hour}]$$

**Initial Current = 125.4  $\mu\text{A}$  Final Current: 45.09  $\mu\text{A}$**

**Initial J = 6.27 [ $\text{mA}/\text{cm}^2$ ] Final J = 2.255 [ $\text{mA}/\text{cm}^2$ ]**

Figure A.10: Cell's short circuit current temporal response.

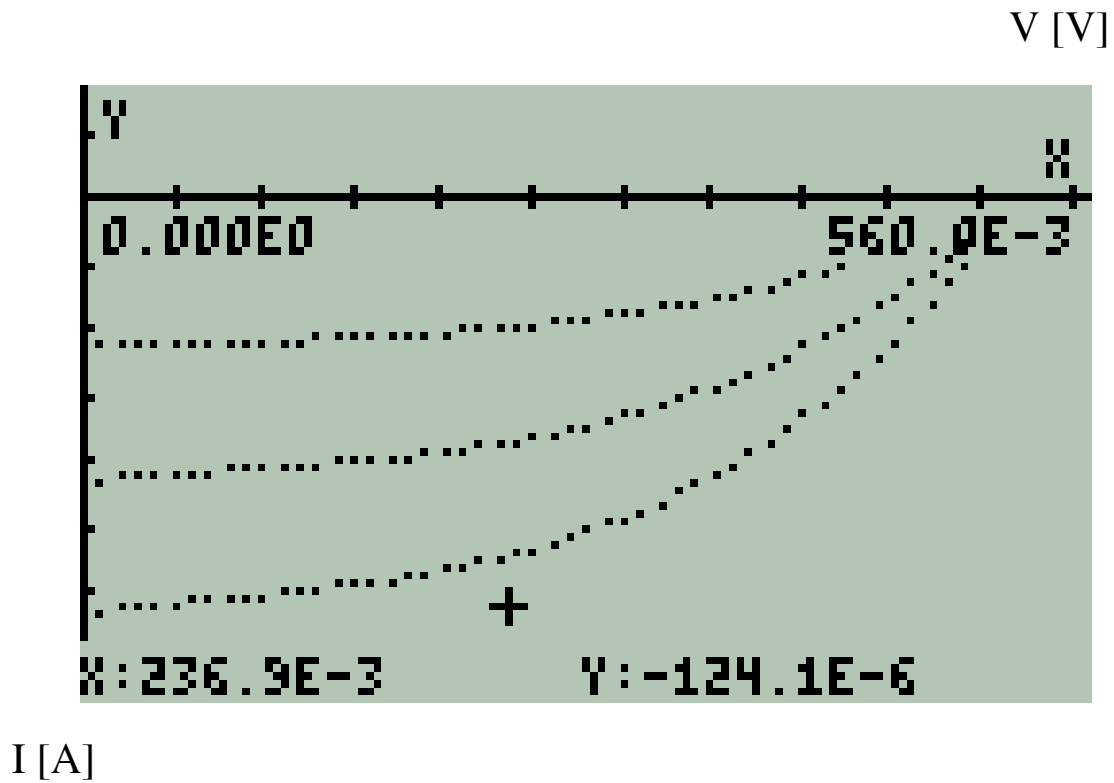
## Open Circuit Voltage Temporal Response



$$\text{VOC} = 0.5204 \pm 0.0167 \text{ [V]}$$

Figure A.11: Cell's open voltage temporal response.

## I-V Curve Response



**Lower curve:** Cell's I-V curve for  $t = 0$

**Middle curve:** Cell's I-V curve for  $t = 5$  hours

**Upper Curve:** Cell's I-V curve for  $t = 10$  hours

**Figure A.12:** *I-V Curves measured for intervals of five hours.*

## EVALUATION

- For an active area  $a = 0.02 \text{ cm}^2$  exposed continuously to an irradiance of  $1 \text{ kW/m}^2$  the yield of the cell decreases linearly with time at a rate of

$$I = -8.03 \text{ } [\mu\text{A}/\text{hour}]$$

or, equivalently, its current density  $J$  decreases at a rate of

$$J = -401.6 \text{ } [\mu\text{A}/\text{cm}^2 \text{ hour}].$$

- This current yield decrement of the cell is irreversible.
- VOC remained constant during the experiment i.e.: bias was not affected during the experiment.
- In ten hours of exposure the short circuit current ISC decreased from  $125.4 \mu\text{A}$  to  $46.1 \mu\text{A}$ . i.e.: the cell's yield decreased in 63.24%.

Laboratory where preliminary Measurements were made:

**Laboratory of Nanostructured Materials for Photovoltaic Energy – ICN2**



## B. MATERIALS USED IN THE PROJECT

In this section the materials used in this work are summarized.

Electronic components, microcontroller board and freeware are presented in the following numerals.

### 1. ELECTRONIC COMPONENTS

Table B.1 Shows the electronic component used to assemble the hardware for this prototype.

**Table B.1. Electronic components for the prototype.**

Electronic Components	Code
Signal Si Diode	1N4148
Signal Ge Diode	1N270
Si Photodiode	BPW34
JFET N Channel Transistor	2N5484
Color LEDs	---
Infrared LEDs	COM-09349
FET input OPAMP	TL 081A
¼ Watt resistances	---
Protoboard	---
DC power supply ± 9 V , 900 mA	---

These components are available in any electronics components shop

## 2. MICROCONTROLLER BOARD

### IOIO OTG

These device is available in SparkFun Electronics, others

## 3. FREEWARE

### Android Studio

<https://developer.android.com/studio/index.html?hl=es-419>

### EMU 50G

<https://www.hpcalc.org/>

others

## 4. HARDWARE

Tablet      **ASUS K011**

Dongle      **CSR 4.0**

PC          ---

+++++

+++++

+++++

+

---

*CHAPTER 5*  
*METHODS*  
*AND*  
*MATERIALS*



## OUTLINE OF THE CHAPTER

- A. CALIBRATION PROCEDURES AND EXPERIMENTAL RESULTS
  - 1. ENVIRONMENTAL THERMOMETER
  - 2. SPECTRAL TEMPERATURE METER
  - 3. IRRADIANCE METER
  - 4. LABORATORY MEASUREMENTS ON THERMAL RADIATION
  - 5. SOLAR I-V CURVE GENERATOR
  
- B. MATERIALS USED IN THE PROJECT
  - 1. ELECTRONIC COMPONENTS
  - 2. MICROCONTROLLER BOARD
  - 3. FREeware



## CHAPTER 5: METHODS AND MATERIALS

This chapter contains the Calibration Methods and Experimental Results for the developed virtual instruments and the materials and freeware used in the project.

This chapter is divided in two sections.

In Section A:

Refers to Instruments Calibration and Experimental Results. It follows identical sequence than previous chapter.

Calibrations were made at the **ICN2** in two laboratories:

**Laboratory for General Services**

and, mainly in the

**Laboratory of Nanostructured Materials for Photovoltaic Energy.**

In Section B:

The materials used in the project: electronic components, microcontroller board and software are summarized.





## A. CALIBRATION PROCEDURES AND EXPERIMENTAL RESULTS

### 1. ENVIRONMENTAL THERMOMETER

#### Calibration Procedure

Thermometer calibration procedure is described based on previous subsections on this matter. Recall Chapter 2, Section B.1; Equations (B.1) to (B.4). Recall Chapter 4 Section C.

For temperature calibration constant temperature references are required.

Table A. shows useful temperature references for calibration.

**Table A1. Useful temperature references for calibration.**

Substance	Temperature [K]
Liquid Nitrogen*	77.36
Solid Nitrogen**	63.15
Solid CO <sub>2</sub>	194.65
H <sub>2</sub> O boiling T	373.16
H <sub>2</sub> O melting T	273.16

\* At a pressure of 1 atmosphere, room temperature

\*\* In equilibrium with surrounding liquid Nitrogen

A Si PN junction biased with constant current  $\sim 10 \mu\text{A}$  is immersed in the constant temperature substance. The voltage drop in the junction is measured after equilibrium is observed. The PN

junction shows a very fast response to changes in temperature and few seconds are enough to obtain equilibrium.

Two reference constant temperature sources are required for the calibration procedure.

Low temperature reference produces the highest voltage  $U_0$  in the junction and high temperature source produces the lowest voltage in the junction.

Applying these values to the calibration algorithm, the thermal voltage drop  $V_{th}$  due only to temperature and the calibration constant  $K_2$  are obtained from Ebers – Moll equation. Recal Chp.4 Subsection C.3.

Then the calibrated range of temperatures is confined by these two temperature references.

The resultant expression is a function of  $I$  (the known constant current through the junction in [A]),  $V$  (the voltage drop along the junction in [V]) and  $T$  (the Absolute Temperature in [K]).

This expression allows calculate any temperature in the calibrated range as a function of the thermal voltage drop in the junction. An algorithm implemented makes this calculation and displays results.

### **Experimental results**

Experimentally, it was found that it is not appropriate to have a single scale for room temperature and cryogenic temperature ranges. It is more convenient to have two temperature scales. For Instance:

$$373.15 \geq T \geq 273.15 \text{ [K]} \quad \text{Room Temperature Range}$$

$$273.15 \geq T \geq 77.36 \text{ [K]} \quad \text{Cryogenic Temp Range}$$

The option to use CO<sub>2</sub> (solid) allows a temperature reference to overlap 273.16 [K] in both previous scales.

Under these conditions accurate and repeatable temperature measurements were obtained in both ranges.

Table A.2 shows the voltage drop in the silicon junction when it is submerged in liquid nitrogen and boiling water as temperature references. Measures were made three using small Si diodes.

**Table A.2: Junction Voltage for liquid nitrogen  
Temperature and boiling water temperature.**

<b>Junction Code</b>	<b>V<sub>low</sub></b> <b>(77.26[K])</b>	<b>V<sub>high</sub></b> <b>(373.16[K])</b>
A	0.990	0.174
B	0.992	0.176
C	0.983	0.175

Note: For 10  $\mu$ A current source

**Example**

For a forward biased Si junction using a constant current source of 9.5  $\mu$ A immersed in an environment at 273.16 K a voltage drop through the junction of 0.722 V was measured. So, the calculated constant is  $k_2 = 3.45047488397 \times 10^{-5}$ . When the junction was exposed to environment and thermal equilibrium was obtained, the voltage drop across the junction was 0.716 V that is equivalent to 294.791 K or 21.63 Celsius.

Calibration was made at:

**Laboratory for General Services – ICN2**

## 2. SPECTRAL TEMPERATURE METER

### Calibration Procedure

Spectral Temperature calibration procedure is described based on previous subsections on this matter. Recall Chp. 4 Section B, particularly Subsections B.2 to B.5.

Spectral Temperature from a thermal radiation source is measured using two narrow bands of the spectrum. These narrow bands are detected using LEDs of two different spectral bands as sensors – as example green and red LEDs. Each LED has a constant narrow band where it is sensitive for radiation.

Once spectral irradiance is obtained for both windows, the algorithm using Eq. (D-28) Chp. 4 calculates the correspondent spectral temperature in [K] .

Section D.2 in Chp. 4 describes in detail this procedure.

### Experimental Results

Table A.3 shows the bands where green and red LEDs are active. Irradiance quotient  $bndqo$  measured for both bands is also shown.

**Table A.3: Virtual Pyrometer Parameters for LEDs**

---

Green LED:	$\lambda_1 = 350E-9$ [m]	$\lambda_2 = 530E-9$ [m]
Red LED:	$\lambda_3 = 510E-9$ [m]	$\lambda_4 = 660E-9$ [m]
Band Quotient	$bndqo = 7.335E-3 / 16.84E-3 = 435.6E-3$	

---

As example, Fig. A.1 shows the results of introducing the wavelengths that define each band and the quotient of irradiances in each band and the calculated spectral temperature using the algorithm based on Ec. (D-28) Chp. 4.

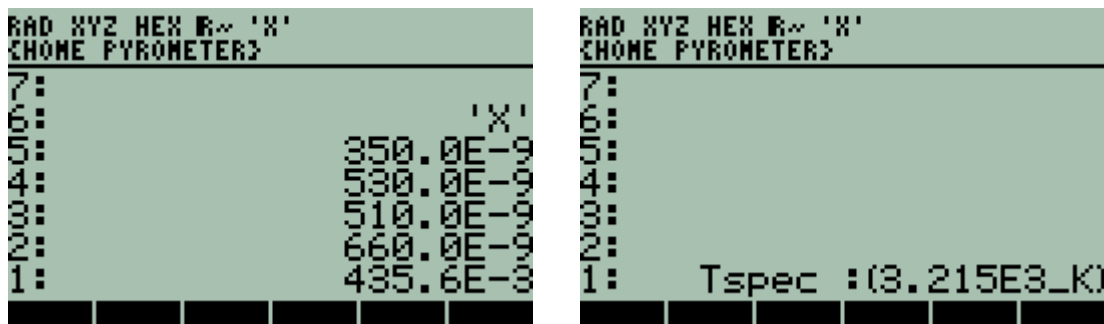


**Figure A.1:** Wavelengths that define each band and the experimental quotient of irradiances for each LED reproduce spectral temperature of the light source using the developed algorithm. It shows consistency of results using this method.

Calibration was made at:

**Laboratory for General Services – ICN2**

### 3. IRRADIANCE METER

#### Calibration Procedure

Spectral Temperature calibration procedure is described based on previous subsections on this matter. Recall Chpt. 4 Section B, particularly Subsections B.2 to B.5.

Spectral Temperature and Irradiance are concomitant parameters that define Thermal Radiation.

Irradiance is measured using a Si photodiode. The Si photodiode is masked with an opaque sheet with a circular hole of known diameter. If spectral temperature is known then thermal spectrum is also known. Measured photocurrents from the Si photodiode and responsivity of Si photodiodes allow that spectral irradiance calculation and total irradiance calculation.

The process is explained in detail in Chapter 4Section D.1.

## Experimental Results

Table A.4 shows the measurement of irradiance using this method.

**Table A.4: Experimental Results for total Irradiance using Si Photodiode**  
 **$T_{SP} = 3175$  [K]**

---

Sensor Component:	Si Photodiode (Masked)	
Si Photodiode Spectral Bandwidth:	$400.0E-9 \leq \lambda \leq 1100.0E-9$ [m]	
Masked Si Photodiode Active Area:	4.144 [mm <sup>2</sup> ]	
Measured Photocurrent:	185.32E-6 [A]	
Photocurrent / mm <sup>2</sup> *	44.817E-6 [A/mm <sup>2</sup> ]	
Normalized Photocurrent **	195.54E-3 [mA/mm <sup>2</sup> ] = 195.54E-6 [A/mm <sup>2</sup> ]	
Fraction coef ***	229.20E-3 $\approx$ 0.229 $\approx$ 23 %	
Calculated Irradiance from Irradiance	97.429E-3 [mW/mm <sup>2</sup> ]	Measured
Normalized Irradiance	425.07E-3 [mW/mm <sup>2</sup> ]	
Fraction coef	229.20E-3 $\approx$ 0.229 $\approx$ 23 %	
Comment: Identical to current fraction coef.		
<b>Calculated Total Irradiance</b>	<b>0.229 [mW/ mm<sup>2</sup>]</b>	

---

Notes:

- \* Measured Photocurrent / Active Area
- \*\* Photocurrent Summation. See Numeral (5)
- \*\*\* (Photocurrent / mm<sup>2</sup> / Normalized Photocurrent)

Calibration was made at:

**Laboratory for General Services – ICN2**

#### 4. LABORATORY MEASUREMENTS OF THERMAL RADIATION

##### **Irradiance Meter Calibration by Intercomparison with a Standard Pyranometer**

Calibration procedure for irradiance meter described in Subsection A.3 in this chapter requires an additional calibration factor **K<sub>irr</sub>** obtained from Intercomparison with a Calibrated Pyranometer (Secondary Standard). The default calibration factor is 1. However, experimentally was observed that every Si photodiode has different yield due to fabrication processes and, necessarily an intercompared calibration is required.

The virtual irradiance meter was intercompared with the standard laboratory pyrometer. The standard pyrometer is in a fixed position Light intensity from the Xenon arc lamp is regulated to fit a reading of 1000 [W/m<sup>2</sup>]. Both instruments were placed at identical geometry and exposed to the Xenon Arc Lamp of the Solar Cell Simulator in the Laboratory.

##### **Experimental Results**

Since Irradiance and Spectral Temperature are concomitant parameters, experimental results of both parameters are presented at the end of this numeral.

Calibration was made at:

**Laboratory of Nanostructured Materials for Photovoltaic Energy – ICN2**

##### **Spectral Temperature measurement**

Once the spectral windows for red and green LEDs are defined experimentally and the active areas for each LED are calculated from its photocurrents, spectral temperature from another thermal source is measurable. Recall LED's active area calculation pages 4-37 to 4-41. Recall spectral temperature calculation pages 4-50 to 4-53.

Spectral Temperature calibration is not required since the algorithm is based on the standardized Planck's Equation  $F_0\lambda(T, \lambda)$ .

Laboratory where preliminary measurements were made:

**Laboratory of Nanostructured Materials for Photovoltaic Energy – ICN2**

## **EXPERIMENTAL RESULTS FOR THERMAL RADIATION MEASUREMENTS**

In this numeral Thermal Radiation intercomparison and experimental results are reported.

### **Objectives**

- Document Spectral Temperature Measurements from two light sources (Xenon Arc Lamp and commercial 220 Vac Tungsten filament lamp) made with the Virtual Instrument – VI prototype.
- Measure Irradiance from the Laboratory Solar Simulator using the Virtual Instrument – VI prototype and intercompare results with those obtained with the Laboratory equipment.
- Evaluate obtained results.

## **MEASUREMENTS OF SPECTRAL TEMPERATURE**

### **Method**

Spectral Temperature from a thermal radiation light source is measured using the VI prototype. The VI prototype has as sensors two Light Emitting Diodes of different colour (as example green and red LEDs) that are exposed to the light source.

Measured photocurrents from these LEDs are converted to equivalent irradiances scaled to identical active area for both LEDs. A developed algorithm searches for the thermal radiation spectra that matches with the measured data and displays calculated spectral temperature in [K].

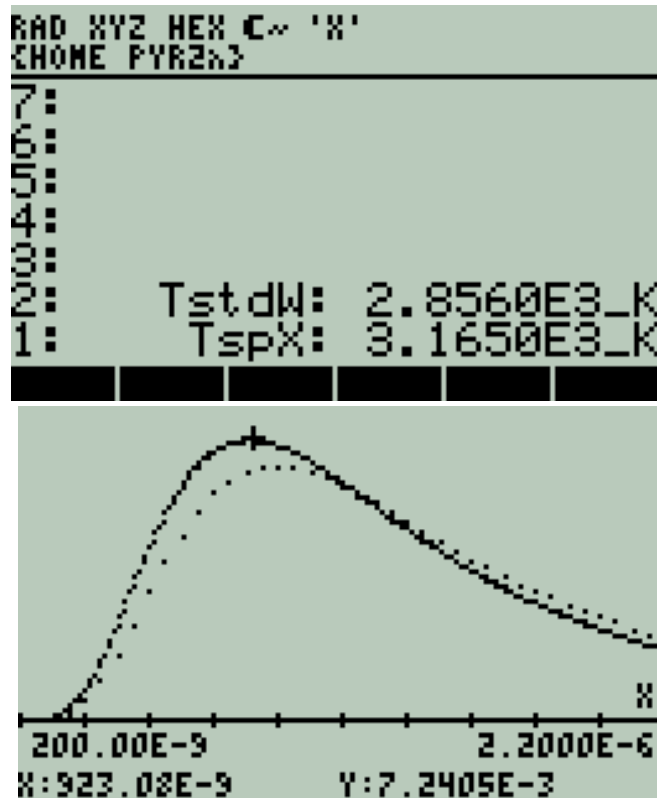
The CIE (International Commission on Illumination) recommended colour temperature was selected as standard reference [1].

**CIE Standard Colour Reference Temperature = 2855.54 [K]**



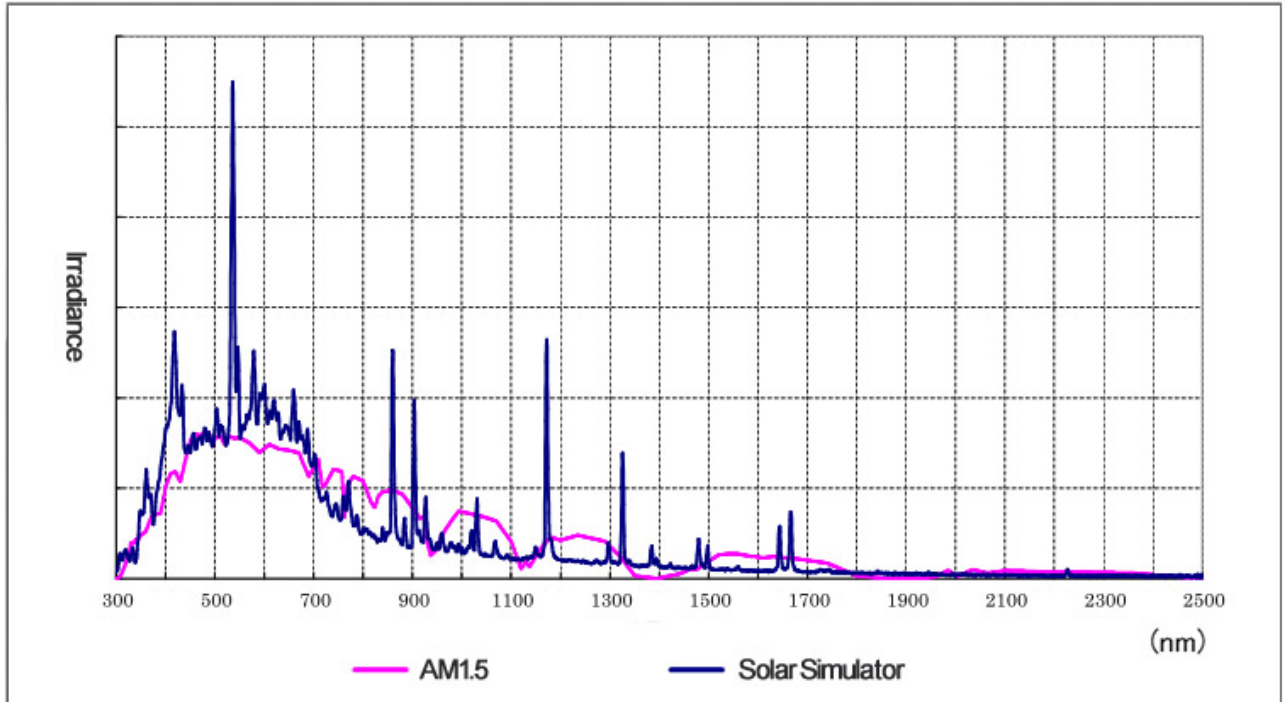
## Results

Fig. A-2 Shows the Thermal Radiation Spectrum for 2856 [K] as standard reference and the spectral temperature measured for a commercial 220 Vac tungsten filament lamp.



**Figure A-2:** Thermal Irradiance spectrum vs. wavelength.  
Lower Curve for  $T_{\text{std}} = 2856$  [K].  
Higher curve for 3165 [K] measured from a 220 Vac tungsten filament lamp.

Fig. A.3 shows the spectral irradiance for a Xenon Arc Lamp used as light source for solar simulators [2].



**Figure A3:** *Spectral Irradiance of a Xenon Lamp for Solar Simulator.*  
*[Figure adapted from reference shown in ANNEX F]*

Although a Xenon arc lamp is not strictly a thermal radiation light source or Planck's source, its spectral temperature was measured with the VI prototype. Fig.D.14 shows the measured temperature and the corresponding thermal radiation spectrum. As reference, the CIE standard is also presented in the plot.

It is reasonable to think that Irradiance measurements made for a Xenon Lamp spectrum, though representative, should be considered only as referential.

```

Tungsten Std TRef
and Measured TX
7:
6:
5:
4:
3:
2:      TstdW:(2.856E3_K)
1:      TspX:(4.255E3_K)

```

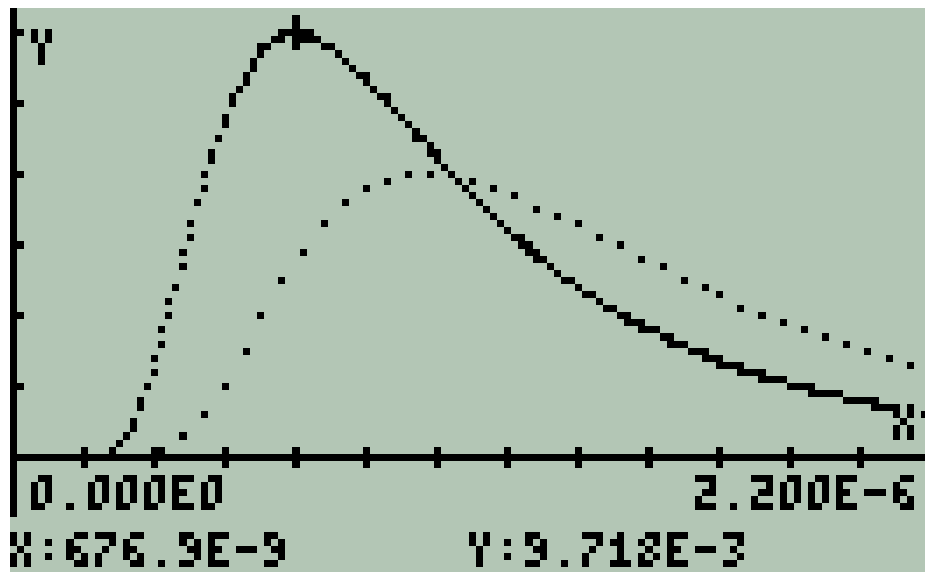


**Figure A.4:** *Thermal Irradiance vs. wavelength.*  
 Lower Curve for  $T\text{-stdW} = 2856$  [K].  
 Higher curve  $T\text{spX}$  for 4225 [K] measured for the solar simulator Xenon Arc Lamp

## **MEASUREMENT OF IRRADIANCE AND INTERCOMPARISON**

### **Method**

Irradiance is measured by the VI prototype using a Si photodiode as sensor. The Si photodiode is masked and only a circular orifice of known area allows incident light to generate a photocurrent. Measured photocurrent is converted into irradiance through an algorithm using the Si photodiode responsivity and the exposed active area.

The Laboratory Pyranometer was calibrated for an Irradiance of 1000 [W/m<sup>2</sup>] using the Lab's solar simulator software. The VI instrument sensor was positioned close to the laboratory pyranometer at the same level of the lab pyranometer sensor (thermopiles) then irradiance was measured. A calibration constant  $K_{irr}$  was obtained to match both readings.

Once the VI prototype was calibrated taking as reference the Lab's pyranometer, a second measurement was made positioning the VI sensor at the level and place where solar cells are normally placed for tests. The purpose is to have a ratio between the irradiance measured by the Lab's pyranometer and the actual irradiance on the tested cell centred on the measuring workbench.

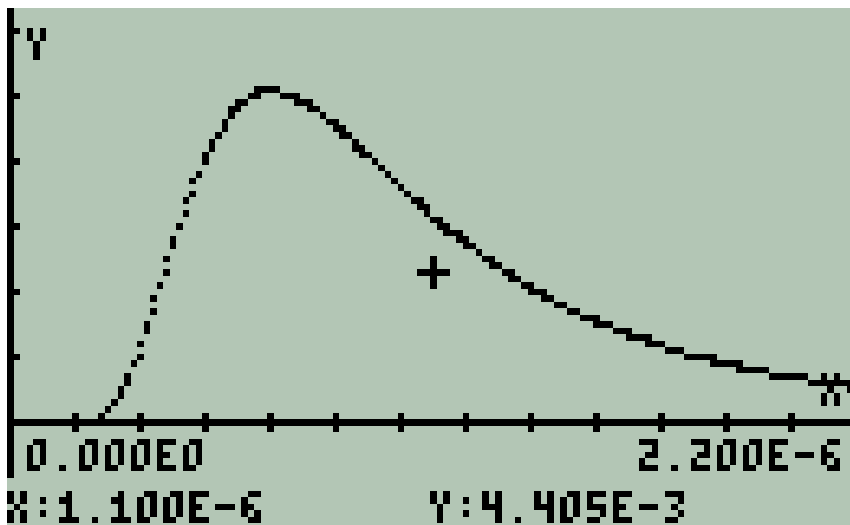
### **Results**

Fig. A.5 shows measured Irradiance after calibration taking as reference the Lab's Pyranometer.

```

One-Tech Sun IRRAD
and Measured IRRAD-X
0:      Tsp:(4.255E3_K)
2:      Irr-std:(1_  $\frac{mW}{m^2}$ )
1:      IrrX:(1.001E0_  $\frac{mW}{m^2}$ )

```



**Figure A.5:** Results after calibration of VI prototype taking as reference the Lab's pyranometer. Sensors from both devices are positioned at equal distance from light source. Standard Irradiance Irr-std and measured irradiance IrrX overlap each other.

Comments:

- This IrrX reading, once calibrated, coincides with the Laboratory reading.
- Irradiance for Laboratory equipment was carefully calibrated before Intercomparison.
- This implies that VI prototype is calibrated with Laboratory Pyranometer at the position where the Lab's Pyranometer is placed.

Observation:

- Lab's Reference Pyranometer sensor and VI prototype sensor are not positioned facing perpendicularly to light source under actual circumstances.

This time, the VI prototype sensor was placed at the same position and distance to light source where solar cells are normally placed to be tested. VI sensor was placed facing perpendicularly to light source. Fig. A.6 shows results.

```

One-Tech Sun IRRAD
and Measured IRRAD-X
3:      Tsp:(4.255E3_K)
2:      Irr-std:  $\left[ 1 - \frac{\text{mw}}{2} \right]$ 
              mm
1:      IrrX:  $\left[ 1.159E0 - \frac{\text{mw}}{2} \right]$ 
              mm
  
```

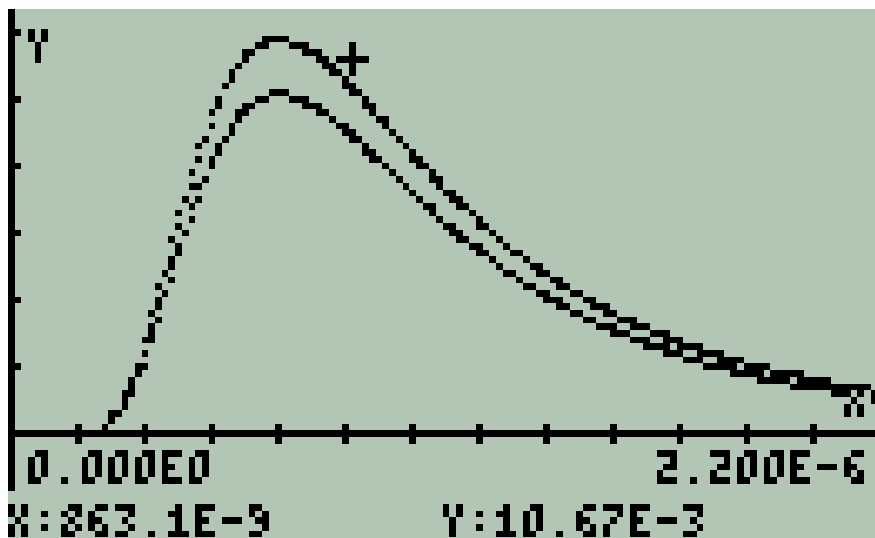


**Figure A.6:** Results measured with VI prototype after being calibrated. The VI sensor this time is positioned where solar cells are normally placed to be tested. Standard Irradiance Irr-std and measured irradiance IrrX differ. Marked (+) function corresponds to IrrX.

## EVALUATION

- Spectral temperature meter from the VI prototype shows consistent measurements when it is exposed to a thermal radiation light sources. It also could be a tool to have approximate measurements where it is exposed to radiation light sources that are not strictly thermal radiation sources as are the Xenon arc lamps used in solar simulator devices.
- Calibrated irradiance meter from the VI prototype is a useful tool to characterize irradiance conditions to test solar cells.
- Besides stable and calibrated light sources, geometry is essential for reproducibility of results when solar cells are being developed or tested.

Laboratory where preliminary Measurements were made:

**Laboratory of Nanostructured Materials for Photovoltaic Energy – ICN2**

### References

- |     |                  |   |
|-----|------------------|---|
| [1] | <b>Wikipedia</b> | <b>CIE Standard illuminant</b>  |
|     |                  | <a href="https://en.wikipedia.org/wiki/Standard_illuminant">https://en.wikipedia.org/wiki/Standard_illuminant</a>                               |
| [2] | <b>SERIC</b>     | Solar Simulator for Modules   |
|     |                  | <a href="http://www.seric.co.jp/english/solarsimulator/ss-for-module.html">http://www.seric.co.jp/english/solarsimulator/ss-for-module.html</a> |

## **5. SOLAR I-V CURVE GENERATOR**

Experimental results of the I-V curve generator and related parameters are presented in Chapter. 4 Section E. Also recall Chapter 3 Fig. D.2.

### **Intercomparison and Experimental Results**

Two experiments are presented: The first one is an Intercomparison of three solar cells I-Vcurves measured with the virtual instrument. The second one is the temporal response of a solar cell that is degraded by incident light.

#### **a. I-V Curve Intercomparison**

I-V curves for three solar cells prototypes developed in the ICN2 Laboratory for Nanostructured Materials for Photovoltaic were measured using the Laboratory Equipment and the developed Virtual Instrument prototype as well.

A subroutine to transfer data measured in the Laboratory Equipment to the Virtual Instrument prototype was developed and results were intercompared.

Only plots are presented and numerical data and details of procedure are omitted.

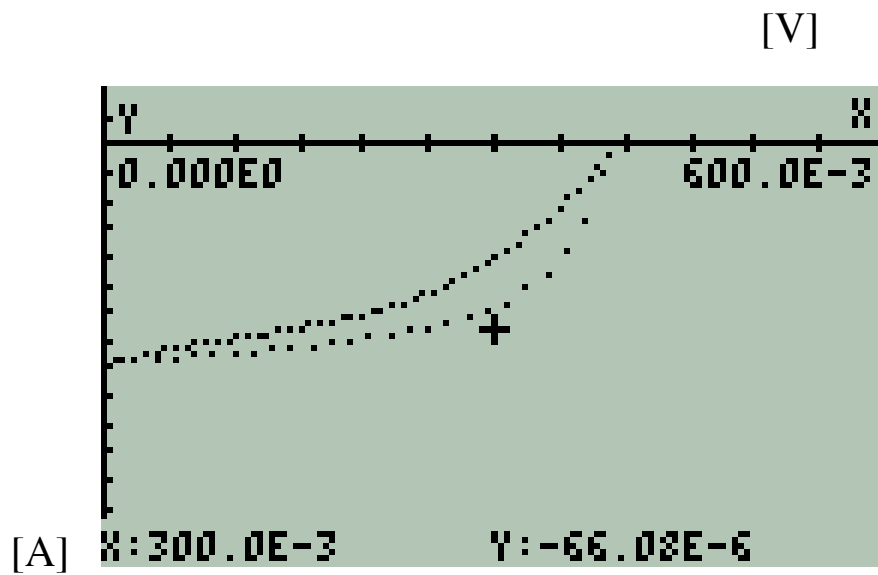
Intercomparison of results follow.



Abscissa: Solar Cell Voltage. Scale in [V]

Ordinate: Solar Cell Current. Scale in [A]

CELL'S CODE: **VR-1**

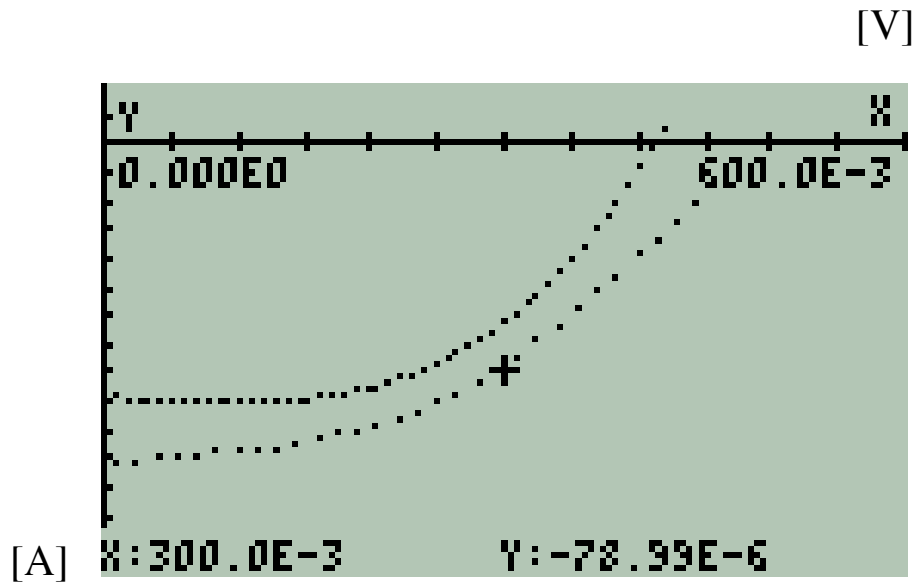


Intercomparison I-V cell plot

(+) Marked curve corresponds to Laboratory equipment

**Figure A.7:** *Intercomparison for Cell VR-1*

CELL'S CODE: **ALB-1**

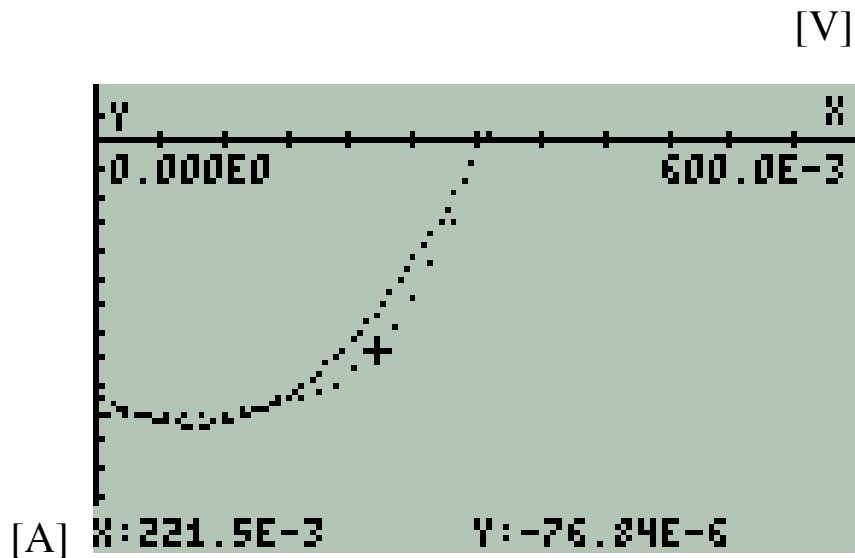


Intercomparison I-V cell plot  
(+) Marked curve corresponds to Laboratory equipment

**Figure A.8:** *Intercomparison for Cell ALB-1*

Comment: There is a time difference between both measurements meanwhile the cell's yield has decreased.

CELL'S CODE: **Si-e**



Intercomparison I-V cell plot  
(+) Marked curve corresponds to Laboratory equipment

Figure. A.9 : *Intercomparison for Cell Si-e*

**EVALUATION:**

**A close agreement in obtained results for both instruments is observed.**

**b. Temporal response of a HTL-free perovskite solar cell using a virtual instrument prototype**

**Objective**

Measure and evaluate the temporal response of a HTL-free perovskite solar cell using the developed Virtual Instrument prototype.

**METHOD**

A HTL-free perovskite solar cell provided by the Laboratory were masked with an opaque film with a 0.02 cm<sup>2</sup> circular orifice positioned on the front face of the cell favourable placed to obtain the highest current yield. Copper conductors were built from cell's electrodes and the cell was shielded from external light sources with exception of the 0.02 cm<sup>2</sup> circular orifice.

The tested cell was continuously exposed to 1 technical sun irradiance (1 kw/m<sup>2</sup> = 1 mw/mm<sup>2</sup>) during ten hours under standard laboratory procedure. Irradiance was carefully checked during the process. VOC, ISC and I – V response were measured every 30 minutes. Measurements were compared with those results obtained from Laboratory instruments showing consistent results. Acquired data was fitted to present plotted results.

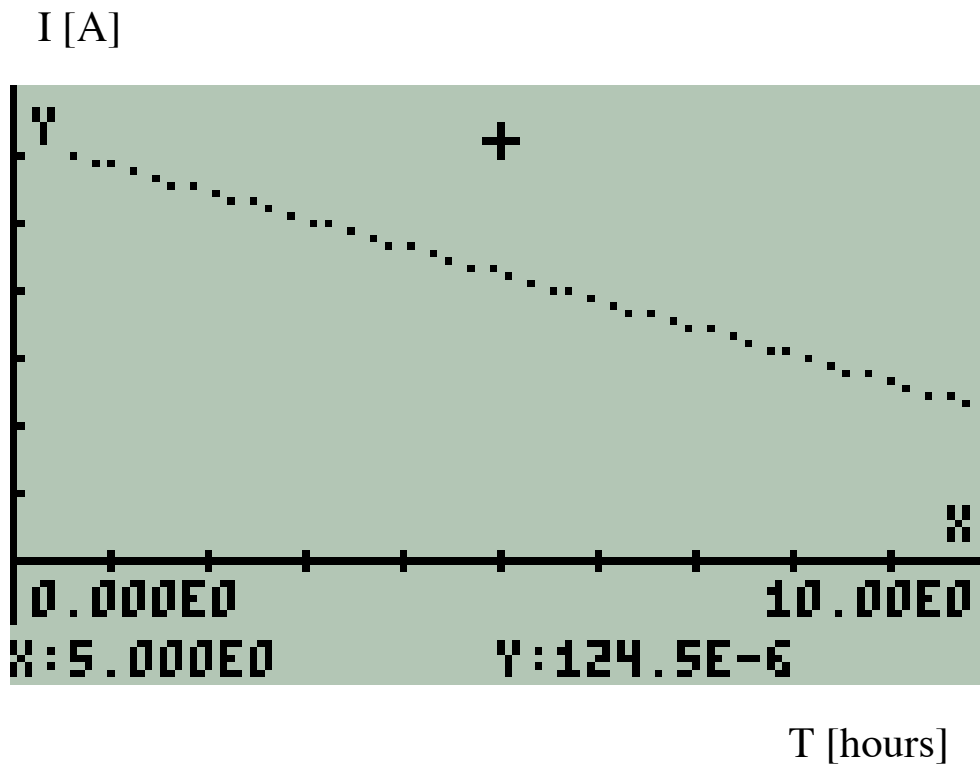
**LABORATORY EQUIPMENT WORK PARAMETERS**

The Laboratory operating parameters were:

Cell's exposed area	0.02	[cm <sup>2</sup> ]
V minimum for scanning	-0.10	[V]
V maximum for scanning	0.80	[V]
V step	15	[mV]
Scan Rate	20	[mV/s]
Irradiance	1000	[W/m <sup>2</sup> ]

## RESULTS

### Short Circuit Current Temporal Response



$$I_{\text{DECREMENT RATE}} = - 8.031 [\mu\text{A}/\text{hour}]$$

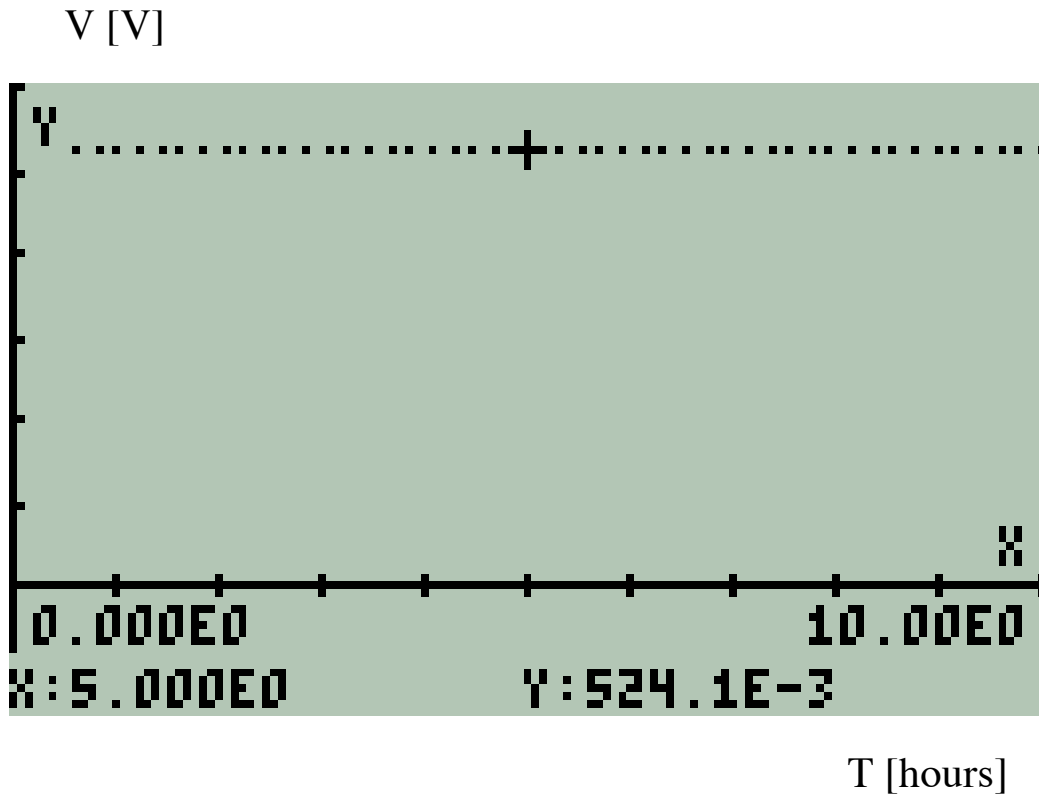
$$J_{\text{DECREMENT RATE}} = -401.6 [\mu\text{A}/\text{cm}^2 \text{ hour}]$$

**Initial Current = 125.4  $\mu\text{A}$  Final Current: 45.09  $\mu\text{A}$**

**Initial J = 6.27 [ $\text{mA}/\text{cm}^2$ ] Final J = 2.255 [ $\text{mA}/\text{cm}^2$ ]**

Figure A.10: Cell's short circuit current temporal response.

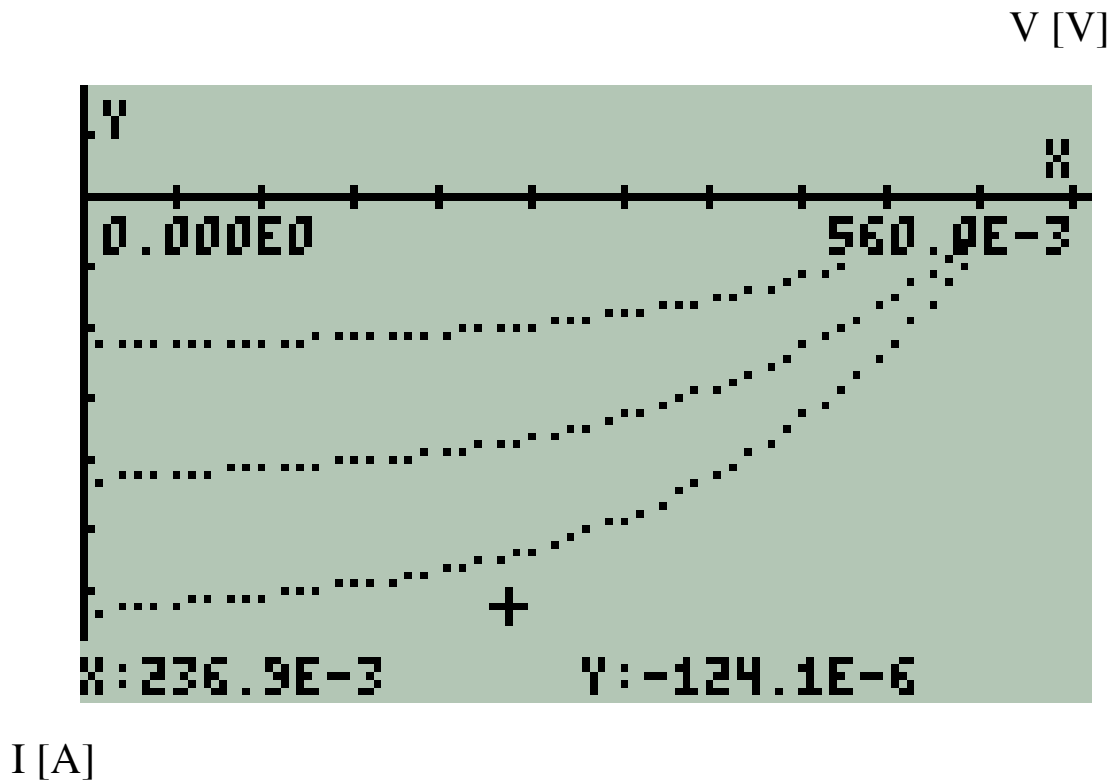
## Open Circuit Voltage Temporal Response



$$\text{VOC} = 0.5204 \pm 0.0167 \text{ [V]}$$

Figure A.11: Cell's open voltage temporal response.

## I-V Curve Response



**Lower curve:** Cell's I-V curve for  $t = 0$

**Middle curve:** Cell's I-V curve for  $t = 5$  hours

**Upper Curve:** Cell's I-V curve for  $t = 10$  hours

**Figure A.12:** *I-V Curves measured for intervals of five hours.*

## EVALUATION

- For an active area  $a = 0.02 \text{ cm}^2$  exposed continuously to an irradiance of  $1 \text{ kW/m}^2$  the yield of the cell decreases linearly with time at a rate of

$$I = -8.03 \text{ } [\mu\text{A}/\text{hour}]$$

or, equivalently, its current density  $J$  decreases at a rate of

$$J = -401.6 \text{ } [\mu\text{A}/\text{cm}^2 \text{ hour}].$$

- This current yield decrement of the cell is irreversible.
- VOC remained constant during the experiment i.e.: bias was not affected during the experiment.
- In ten hours of exposure the short circuit current ISC decreased from  $125.4 \mu\text{A}$  to  $46.1 \mu\text{A}$ . i.e.: the cell's yield decreased in 63.24%.

Laboratory where preliminary Measurements were made:

**Laboratory of Nanostructured Materials for Photovoltaic Energy – ICN2**



## B. MATERIALS USED IN THE PROJECT

In this section the materials used in this work are summarized.

Electronic components, microcontroller board and freeware are presented in the following numerals.

### 1. ELECTRONIC COMPONENTS

Table B.1 Shows the electronic component used to assemble the hardware for this prototype.

**Table B.1. Electronic components for the prototype.**

Electronic Components	Code
Signal Si Diode	1N4148
Signal Ge Diode	1N270
Si Photodiode	BPW34
JFET N Channel Transistor	2N5484
Color LEDs	---
Infrared LEDs	COM-09349
FET input OPAMP	TL 081A
¼ Watt resistances	---
Protoboard	---
DC power supply $\pm 9$ V , 900 mA	---

These components are available in any electronics components shop

## 2. MICROCONTROLLER BOARD

### IOIO OTG

These device is available in SparkFun Electronics, others

## 3. FREEWARE

Android Studio

<https://developer.android.com/studio/index.html?hl=es-419>

EMU 50G

<https://www.hpcalc.org/>

others

## 4. HARDWARE

Tablet      **ASUS K011**

Dongle      **CSR 4.0**

PC          ---

+++++

+++++

+++++

+

---

*ANNEXES*  
*TO*  
*ALL CHAPTERS*

---



## **ANNEXES OUTLINE**

### **CHAPTER 1**

ANNEX 1: ARTICLE: SINGLE PHOTON: its size and internal electromagnetic fields Author: Fernando Echeverría T.	1-1
ANNEX 2: RESPONSIVITY FOR Si AND Ge PHOTODIODES	ANNX 2-1
ANNEX 3: RESPONSIVITY FOR Si AND Ge PHOTODIODES (Resol. 10[nm])	ANNX 3-1
ANNEX 4:	ANNX 4-1
a. STANDARD AND NORMALIZED TUNGSTEN FILAMENT LAMP SPECTRUM (Resol. 10 [nm])	
b. STANDARD AND NORMALIZED TUNGSTEN FILAMENT LAMP SPECTRUM (Spectral Range Bandwidth for Silicon	
c. STANDARD AND NORMALIZED TUNGSTEN FILAMENT LAMP SPECTRUM (Spectral Range Bandwidth for Germanium)	
ANNEX 5: PHOTODIODES TECHNICAL DATA	ANNX 5-1

### **CHAPTER 2**

ANNEX 1: A DISGRESSION ON FOURIER TRANSFORMS	ANNX 1-1
--	----------

### **CHAPTER 3**

ANNEX 1: DESCRIPTION OF ALGORITHM TO MEASURE A PHYSICAL MAGNITUDE	ANNX 1-1
ANNEX 2: ANDROID RELATED COMMAND SEQUENCES	ANNX 2-1
ANNEX 3: REQUIRED COMMANDS FOR THE PROJECT (CANONICAL FORM)	ANNX 3-1

### **ANNEX F:**

#### **REFERENCE ON FIGURES INCLUDING THEIR ORIGIN**

REFERENCE ON FIGURES INCLUDING THEIR ORIGIN	ANNX F- 1
---	-----------



# Single Photon: its size and internal electromagnetic fields

Fernando Echeverría Troya

July 5, 2017

Physics Department  
Graduate School  
Universidad Autonoma de Barcelona UAB  
Instituto Catalan de Nanociencia y Nanotecnologia ICN2  
Nanostructured Materials for Photovoltaic Energy

## ABSTRACT

Light is described by Electromagnetic Theory as a transversal wave and by Quantum Mechanics as a set of photons. There must be consistency between both descriptions of light.

This document summarizes the basic set of equations for light from Electromagnetic Theory and for a photon from Basic Quantum Mechanics and solve them as a set of equations to produce a *simple mathematical model for a single photon*.

The model accounts for: The Electric Field  $\mathbf{E}$  and the Magnetic Field  $\mathbf{B}$  for a single photon in the visible range. Numerical magnitudes of the "cross section" and the spatial extension of a single photon. It accounts for how the spatial extent of a photon counted in wavelengths "shrinks" when its frequency or energy increases. The model also allows to estimate the percentage of volume occupied by photons in a monochromatic light beam.

The basic equations for this article are taken from the "Feynman's Lectures on Physics". The set of equations is solved trying to strictly follow the reasoning set forth in Feynman's Lectures.

As End Note it is included an organized list of those sections within the "Feynman's Lectures on Physics" regarding the subject that is exposed.

*Annex 1* is a graphical representation of physical parameters for a single photon as a function of its energy. Expressed in [eV].

*Annex 2* summarizes the set of equations from Electromagnetic Theory and Basic Quantum Mechanics related with photons.

The whole document is thought as a didactic material for those students and persons interested in the border between Electromagnetic Theory and Basic Quantum Mechanics.

Words: "*Electromagnetic Wave, Photon, Photon Size, Photon Physical Parameters, Electric and Magnetic Fields for a single photon, Volume occupied by photons in a beam, Photons and vacuum*".

## INTRODUCTION

Light has a dual characteristic: it behaves as a wave and as a partible. Light is part of the Electromagnetic Spectrum so, in vacuum, it has an Electric Field  $\mathbf{E}$  and a Magnetic Field  $\mathbf{B}$  perpendicular to each other and both perpendicular to the direction of propagation as a transversal wave. The energy transported by an electromagnetic wave per unit area per unit second is the magnitude of the Poynting Vector  $\mathbf{S}$  this vector is in the propagation direction for the electromagnetic wave.

Photons have a defined energy, proportional to its frequency and  $h$ , the Planck's constant. They propagate in vacuum in a straight line as a light field with the speed of light  $c$ . Photons have a momentum  $p$ .

There must be consistency between the Electromagnetic and Quantum descriptions of light.

In this document the magnitudes of the physical parameters for a single photon including the magnitudes of  $\mathbf{E}$  and  $\mathbf{B}$  are calculated. Then the size of a photon is estimated in the Visible Region.

The sequence of reasoning for this paper takes as a basic reference the Feynman's Lectures of Physics. At the end, detailed list of the consulted sections is presented as an End Note.

*Annex 1*: summarizes the results expressed as a function of Photons Energy in the Visible Region. Energy is expressed in [eV].



*Annex 2:* summarizes the equations that define light as wave and as a set of photons.

## INITIAL ASSUMPTIONS

In order to obtain the physical parameters for a photon, the following assumptions are made:

- A photon in vacuum propagates in a straight line. The propagation direction is defined by the Poynting Vector  $\mathbf{S}$ .
- A photon propagates in vacuum at constant speed  $c$ .
- A photon is monochromatic and the  $\mathbf{E}$  and  $\mathbf{B}$  are considered constant magnitudes in the photon spatial extension.
- It has a definite energy  $\Delta U$  and definite momentum  $\Delta p$
- It is a very short train pulse with a definite duration  $\Delta t$
- It is spatially confined or it has a finite spatial extension
- Its magnitudes  $\Delta U, \Delta t ; \Delta p, \Delta x$  comply with the Heisenberg's Uncertainty Principles

## APPROACH TO THE PROBLEM

Perhaps, the best way to develop the idea is through a numerical example.

In this section, the related equation is followed by the numerical value for a specific example. Numerical values for the specific example are shown in bold.

Let's choose a monochromatic wavelength in the middle of the visible spectrum.

$$\lambda = \mathbf{520E - 9} \quad [m] \quad (1)$$

It is in the green band of the visible spectrum. See Fig. 1

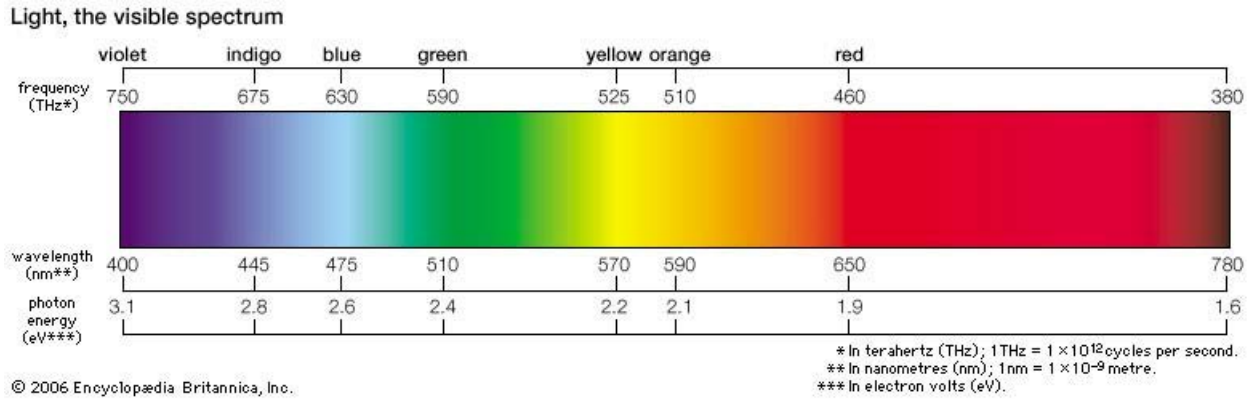


Fig. 1  
The visible spectrum of light

\* Note: The exponential notation  $10^n$  is expressed as E. Example  $10^2 = 1E2$

## PHOTON'S ENERGY, MOMENTUM AND WAVE RELATED PARAMETERS

From the wavelength in (1), the frequency  $f$  is obtained from (2)

$$\lambda = cT = c/f \quad (2)$$

$T$  is the wave period in [s] and  $f$  is the wave frequency in [Hz]

$$f = c/\lambda \quad [Hz] \quad (3)$$

where:

$$c = \mathbf{299792458} \quad [m/s] \quad (4)$$

$$f = \mathbf{580.3E12} \quad [Hz] \quad (5)$$

From frequency in (5), the angular frequency  $\omega$  is obtained from (6).

$$\omega = 2\pi.f \quad [radian/s] \quad (6)$$

$$\omega = \mathbf{3.646E15} \quad [radian/s] \quad (7)$$

From the angular frequency in (7), the photon's energy  $\Delta U$  is obtained from (8).

$$\Delta U = \hbar.\omega = h.f \quad [J] \quad (8)$$

where:

$$\hbar = h/2\pi = \mathbf{1.05457266E-34} \quad [J.s] \quad (9)$$

$$h = \mathbf{6.6260755E-34} \quad [J.s] \quad (10)$$

then:

$$\Delta U = \mathbf{384.5E-21} \quad [J] \quad (11)$$

This magnitude of energy  $\Delta U$  in (11) could also be expressed in electronvolts [eV], a non SI unit, but useful to deal with atomic and nuclear energy magnitudes. The conversion factor between both energy units is:

$$\mathbf{1 J = 6.242E18} \quad eV \quad (12)$$

So,  $\Delta U$  in (11) expressed in eV is

$$U.eV = \mathbf{2.384E0} \quad [eV] \quad (13)$$

equations (11) and (13) are the same photon's energy in different units. The wavenumber  $k$  for this example is obtained replacing (4) and (7) in (14):

$$k = \omega/c \quad [radians/m] \quad (14)$$

$$k = \mathbf{12.16E6} \quad [radians/m] \quad (15)$$

From (11) and (4), the photon's momentum  $\hat{\Gamma}p$  is obtained from (16).

$$\Delta p = \Delta U/c \quad [N.s] \quad (16)$$

$$\Delta p = \mathbf{1.283E-27} \quad [N.s] \quad (17)$$

So, for now, the photon's energy  $\Delta U$ , the momentum  $\Delta p$  and the remaining wave- related parameters have been obtained from the wavelength  $\lambda$  chosen in (1) and the physical constants  $c$ ,  $\hbar$  or  $h$ . The photon's angular momentum is not considered here. Neither circular polarization for light nor the quantum angular momentum for a photon, what it is sought is a simple model to obtain the order of magnitude of the physical parameters involved to characterize a single photon. Now, in order to obtain the photon's Electromagnetic parameters, it is necessary to spatially confine or, in certain way, to establish a spatial boundary for the photon. In this attempt, the photon is considered as a classical electromagnetic wave pulse where the Electric field  $\mathbf{E}$  and the magnetic field  $\mathbf{B}$ , as a first approach, are considered constants in magnitude during the photon's spatial extension. Then, obtaining a photon cross section in order to confine the photon in a volumetric boundary is tried. The explanation follows.

## THE CUTOFF RADIUS AND THE CROSS SECTION

From microwaves theory is well known that electromagnetic waves are able to go through a waveguide up to certain minimum frequency  $\omega c$ .

For frequencies  $< \omega c$  the microwave attenuates meanwhile it travels through the waveguide. So it becomes an evanescent wave. For frequencies  $> \omega c$  the microwave is transmitted

through the waveguide by a continuous reflection on the interior waveguide walls. The microwave travels with a group velocity smaller than  $c$

For the frequency  $= \omega c$  the microwave travels through the waveguide without internal reflections at the speed  $c$  and without suffering any attenuation. This frequency  $\omega c$  is known as the cutoff frequency.[1]

Let's imagine that for the photon selected for this example, the photon's frequency is just the cutoff frequency  $\omega c$  for a microscopic circular waveguide or a conductor nanotube.

Under these circumstances it is possible to calculate the cross section radius for the circular waveguide for a transmission mode [2]. For the dominant mode TE<sub>11</sub>, this expression is:

$$\omega c = \chi'_{11} \cdot c/r \quad [radians/s] \quad (18)$$

where:  $\chi'_{11}$  is the first root of the first derivative from the  $J_{11}$  Bessel function

$$\chi'_{11} = \mathbf{1.84118378134} \quad (19)$$

then, from (18) the radius is:

$$r = \chi'_{11} \cdot c/\omega c \quad [m] \quad (20)$$

so, for our photon:

$$r = \mathbf{151.4E-9} \quad [m] \quad (21)$$

and the cross section area  $\Delta A$  is:

$$\Delta A = r^2 \cdot \pi \quad [m^2] \quad (22)$$

$$\Delta A = \mathbf{72.00E-15} \quad [m^2] \quad (23)$$

finally, the volume  $\Delta Volm$  is:

$$\Delta Volm = \Delta A \cdot \Delta x \quad [m^3] \quad (24)$$

where  $\Delta x$  is the longitudinal extension of the photon, still to be defined.

## THE PHOTON'S ELECTROMAGNETIC FIELD

From **Maxwell's Equations**, an electromagnetic wave in free space is a transversal wave where the Electric field  $\mathbf{E}$  is perpendicular to the magnetic field  $\mathbf{B}$  and both are perpendicular to the propagation direction. In vacuum  $\mathbf{E}$  and  $\mathbf{B}$  are interrelated through the speed of light  $c$ , the speed at which electromagnetic fields propagate. The electromagnetic field has an Energy Density  $u$  and every unit volume in space has an Energy  $\Delta U$ . Energy is transported in an electromagnetic field and it occurs interchanging energy between the  $\mathbf{E}$  and  $\mathbf{B}$  fields in an oscillatory manner. The electromagnetic field has a momentum  $\Delta \mathbf{p}$  and a Momentum Energy Density  $\mathbf{g}$ . The propagation vector or Poynting Vector  $\mathbf{S}$ , perpendicular to  $\mathbf{E}$  and  $\mathbf{B}$  besides defining the propagation direction of the electromagnetic wave, through its magnitude provides the energy flow rate through the unit area in a unit of time. The **magnitudes**  $x$  ,  $\Delta p$  ,  $\mathbf{E}$  ,  $\mathbf{B}$  and  $\mathbf{S}$  are vectors. [3]

### Annex 2

The equations and SI units for these physical parameters follow.

$$\text{ElectricField} \quad E \quad [V/m] \quad (25)$$

$$\text{MagneticField} \quad B \quad [T] \quad (26)$$

$\mathbf{E}$  and  $\mathbf{B}$  relation for electromagnetic waves in free space are interrelated

$$\mathbf{E} = c\mathbf{B} \quad [V/m] \quad (27)$$

Electromagnetic Energy Density,  $u$

$$u = \frac{\epsilon_0}{2}\mathbf{E} \cdot \mathbf{E} + \frac{\epsilon_0 c^2}{2}\mathbf{B} \cdot \mathbf{B} \quad [J/m^3] \quad (28)$$

Electromagnetic Energy,  $U$

$$U = \int \left( \frac{\epsilon_0}{2}\mathbf{E} \cdot \mathbf{E} + \frac{\epsilon_0 c^2}{2}\mathbf{B} \cdot \mathbf{B} \right) dV \quad [J] \quad (29)$$

Poynting Vector,  $\mathbf{S}$

$$\mathbf{S} = \epsilon_0 c^2 \mathbf{E} \times \mathbf{B} \quad [J/m^2 \cdot s] \quad (30)$$

Momentum Density,  $\mathbf{g}$

$$\mathbf{g} = \mathbf{S}/c^2 = \epsilon_0 \mathbf{E} \times \mathbf{B} \quad [Ns/m^3] \quad (31)$$

Momentum,  $p$

$$p = U/c \quad [N.s] \quad (32)$$

where  $\epsilon_0$  is the universal physical constant:

$$\epsilon_0 = \mathbf{8.85418781761E-12} \quad [F/m] \quad (33)$$

Now:

Replacing the magnitude of the magnetic field  $\mathbf{B}$  from (27) in: (28), (29), (30) and (31), these expressions depend only on electric Field  $\mathbf{E}$ :

Electromagnetic Energy Density,  $u$

$$u = \epsilon_0 E^2 \quad [J/m^3] \quad (34)$$

Electromagnetic Energy,  $U$

$$U = \int \epsilon_0 E^2 dV \quad [J] \quad (35)$$

Poynting Vector,  $S$

$$S = \epsilon_0 c E^2 \quad [J/m^2.s] \quad (36)$$

Momentum Density,  $g$

$$g = S/c^2 = \epsilon_0 E^2 / c \quad [Ns/m^3] \quad (37)$$

expressions that show in a simpler manner the relations between the magnitudes of these parameters.

## **E and B FOR A SINGLE PHOTON**

Since  $\mathbf{E}$  and  $\mathbf{B}$  are assumed as constant magnitudes in this approach, a photon is considered as a finite and continuous wave pulse with a longitudinal extension  $\Delta x$  :

$$\Delta x = c\Delta t \quad (38)$$

Fig. 2 shows this idea for the electric field  $\mathbf{E}$ .



Fig. 2 The constant magnitude of an electric field  $\mathbf{E}$  pulse within a spatial extension  $\Delta x$

Now, from (35) since a cross section  $\Delta A$  has been obtained in (23) and since the magnitude of  $E$  is considered constant, the Electromagnetic Energy  $U$  can be expressed as:

$$\Delta U = \epsilon_0 E^2 \Delta A \int dx \quad [J] \quad (39)$$

$$\Delta U = \epsilon_0 E^2 \Delta A \Delta x \quad [J] \quad (40)$$

By definition,  $S$  is the energy that flows through a unit area per unit time, this is:

$$\Delta S = \Delta U / \Delta A \Delta t \quad [J/m^2 s] \quad (41)$$

Now, for  $\Delta t = 1s$ , the magnitude  $S$  represents the energy that would flow through  $\Delta A$  during 1 s. Let's obtain the magnitude it represents for our example taking  $\Delta U$  from (11) and  $\Delta A$  from (23),

$$\begin{aligned} \Delta S_{for1second} &= \Delta S_{1s} = \Delta U / \Delta A 1s \\ &= 384.5E - 21_J / 72.00E - 15_m^2 (1s) \\ \Delta S_{for1second} &= \mathbf{5.341E-6} \quad [J/m^2(1s)] \end{aligned} \quad (42)$$

that numerically is equal to the energy  $\Delta U$  1s that would flow through  $\Delta A$  during 1 s i.e, from (42):

$$\begin{aligned} \Delta U_{1s} &= (\Delta S_{1s})(1s) \\ \Delta U_{1s} &= \mathbf{5.341E-6} \quad [J/m^2] \end{aligned} \quad (43)$$

However, from (11), the photon's energy is only 384.5E 21 J

Since we have assumed that  $\mathbf{E}$  and  $\mathbf{B}$  are constant then the time rate at which energy flows through  $\Delta A$  must be constant.

So, the times it takes the energy  $\Delta U$  to flow through the area  $\Delta A$  compared with the energy  $\Delta U$  1s that flows through  $\Delta A$  must be proportional to  $\Delta t$  and 1 s, this implies that:

$$\frac{\Delta U}{\Delta t} = \frac{\Delta U_{for1second}}{1s} \quad [J/s] \quad (44)$$

So:

$$\Delta t = (\Delta U)(1s)/\Delta U_{1s} \quad [s] \quad (45)$$

$$\Delta t = \mathbf{72.00E-15} \quad [s] \quad (46)$$

In other words  $\Delta t$  is the time it takes the train pulse to go through  $\Delta A$  or the photon's duration.

(46) in (38):

$$\Delta x = c.\Delta t = \mathbf{21.58E-6} \quad [m] \quad (47)$$

is the photon's longitudinal extension.

If  $N\lambda$  is defined as the number of wavelengths than contains  $\Delta x$ , a dimensionless number,

$$N\lambda = \Delta x/\lambda \quad [dimensionless] \quad (48)$$

$$N\lambda = \mathbf{41.78E0} \quad [dimensionless] \quad (49)$$

$N\lambda$  represents the photon's longitudinal extension expressed in wavelengths.

From this stage of the exposition it is possible to calculate all the remaining parameters. The process follows:

(47) in (24):

$$\Delta Volm = \mathbf{1.554E-18} \quad [m^3] \quad (50)$$

(11), (23), (33) and (47) in (40):

$$E = \left(\frac{\Delta U}{\epsilon_0 \Delta Volm}\right)^{1/2} \quad [V/m] \quad (51)$$



$$E = 167.2E3 \quad [V/m] \quad (52)$$

(52) in (27):

$$B = E/c[T] \quad (53)$$

$$B = 557.6E-6 \quad [T] \quad (54)$$

(33) and (52) in (34):

$$u = 247.4E-3 \quad [J/m3] \quad (55)$$

(17) and (50) in (37):

$$g = 825.3E-12 \quad [N.s/m3] \quad (56)$$

From (36):

$$S = 74.18E6 \quad [J/m2s] \quad (57)$$

## INTERPRETATION OF RESULTS

### For the Poynting Vector S

The calculated magnitude for the Pointing Vector is a tremendously enormous magnitude.

$$S = 74.18E6 \quad [J/m2s] \quad (57)$$

However, in agreement with the results here obtained, our chosen photon neither has a temporal duration of 1 second, nor has a cross section of 1 square meter.

Let's put this magnitude in its proper scale: From (23), the cross section through which the Poynting photon flows is

$$\Delta A = 72.00E-15 \quad [m2] \quad (23)$$

And the temporal photon's extension from (46) is:

$$\Delta t = 72.00E-15 \quad [s] \quad (46)$$

When these factors are applied to (57), the energy transported by the photon is:

$$\Delta U = 384.5E-21 \quad [J] \quad (58)$$

This value of energy is exactly the magnitude obtained in (11). So, independently of the enormous magnitude (57) is a consistent result when this magnitude is expressed in the appropriate scale. The point is that the photon neither is a continuous wave as an electromagnetic wave, nor has a temporal duration of 1 second or a longitudinal extension of  $(c \times 1s)[m] = 3 \times 10^8[m]$ . Our photon is a very compact physical entity.

### For the electromagnetic field $\mathbf{E}$

Similarly, from (52), the electric field  $\mathbf{E}$  is very huge:

$$E = \mathbf{167.2E3} \quad [V/m] \quad (52)$$

However, the electric field is a gradient, in other words it is rate between a potential difference  $\Delta\phi$  in Volts and a distance in which the potential difference is measured.

As example, an Electric Field of  $100V/m$  is identical with an electric field  $\mathbf{E}$  of  $1V/cm$ .

So, the electric field should also be reduced to its proper scale; again, there is a proportionality between the potential difference and distance, so:

$$\frac{V}{1m} = \frac{v}{r} \quad [V/m] \quad (59)$$

Where, for our photon,  $r = 151.4E-9[m]$ , from (21).

So:

$$v = \mathbf{25.31E-3} \quad [V] \quad (60)$$

for a length of  $r$ . Anyway is in the order of millivolts for such a small distance  $r$ . However, the SI magnitude for  $\mathbf{E}$  for the photon of our example is expressed by (53).

### COMPATIBILITY WITH UNCERTAINTY PRINCIPLES

Heisenberg's uncertainty principles are:

$$\Delta x \Delta p \geq \hbar/2 \quad [Js] \quad (61)$$

$$\Delta U \Delta t \geq \hbar/2 \quad [Js] \quad (62)$$

$$\hbar/2 = \mathbf{5.2728633E-35} \quad [Js] \quad (63)$$

Replacing the results obtained for these parameters for the selected photon, the following values are obtained:

$$\Delta x \Delta p = \mathbf{4.885E-33} \quad [Js] \quad (64)$$

$$\Delta U \Delta t = \mathbf{4.885E-33} \quad [Js] \quad (65)$$

When one compares these values with (63), they do not contradict the Uncertainty Principles (61) and (62).

## PHOTONS IN A BEAM

Let's imagine a 1mm<sup>2</sup> cross section monochromatic laser beam containing photons of our example.

Let's suppose that the irradiance from the beam is equivalent to the irradiance for one sun (technical).

$$\begin{aligned} 1sunIrradiance_{(technical)} &= 1[kW/m^2] = 1[mW/mm^2] \\ &= 1E - 3[J/smm^2] \end{aligned} \quad (66)$$

How many photons there are in the length  $x = 1$  [m] of the beam?

Converting [J] to [eV] using (12):

$$1sunIrradiance_{(technical)} = 6.242E15[eV/smm^2] \quad (67)$$

Since our test photon has an Energy of 2.384 [eV] from (13), the number of our test photons per second, per  $mm^2$  is:

$$1sunIrradiance_{(technical)} = 2.618E15[testphotons/smm^2] \quad (68)$$

Since  $x = ct$ , for  $x = 1[m]$  the time it takes the wave front is  $t = x/c$  and for  $x = 1[m]$  is  $1/c$  shorter than 1 [s]; i.e.:

$$t_{(for1m)} = 3.336E - 9[s] \quad (69)$$

So the number of photons  $N_{photons}$  in 1 [m] of beam is:

$$\begin{aligned} N_{photons} &= (2.618E15)(3.336E - 9)[testphotons/mmm^2] \\ &= 8.734E6[testphotons/mmm^2] \end{aligned} \quad (70)$$

Now, a cylinder of 1[m] length and 1[mm<sup>2</sup>] cross section has a volume:

$$Volume(1_{mbeam}) = 1E - 6[m^3] \quad (71)$$

And from (50) and (64), the volume occupied by the photons in 1 [m] beam is the calculated volume for each photon multiplied by the number of photons in the volume of (1m)(1mm<sup>2</sup>) of the beam.

$$\begin{aligned} Volume(Photonsin1mbeam) &= \\ &= (1.554E - 18[m^3/testphoton])(8.734E6[testphotons]) \\ &= 13.57E - 12[m^3] \end{aligned} \quad (72)$$

So, the quotient:

$$\begin{aligned} Volume(Photosin1mbeam)/Volume(1mbeam) &= \\ &= 13.57E - 12/1E - 6 = 13.57E - 6[dimensionless] \end{aligned} \quad (73)$$

This implies that the volume occupied by photons in the beam is only about the ten-millionth fraction of the beam volume. The dominant remaining volume is vacuum.

## MODEL AND SUMMARY OF RESULTS

With a set of the above mentioned equations, a program has been implemented and results have been summarized for several representative energies. Table I shows the results for three photons in the visible range and Table II shows the results for a 1 GHz microwave photon and a 13.6 eV the ionization energy for Hydrogen compared with the photon selected as test example.

**Table I Physical Parameters for three representative photon energies**

Physical Parameter	U=1.6 eV (NearIR)	U=2.4 eV (Near UV)	U=3.0 eV (Near UV)	SI UNITS
Frequency, <b>f</b>	386.9E12	5803E12	725.4E12	<b>Hz</b>
Wavelength, $\lambda$	774.9E-9	516.6E-9	413.3E-9	<b>m</b>
Number of cycles, $N\lambda$	62.67E0	41.78E0	33.42E0	<b>adim</b>
Wavenumber, <b>k</b>	8.109E6	12.16E6	15.20E6	<b>radian/m</b>
Angular Frequency, $\omega$	2.431E15	3.646E15	4.558E15	<b>radian/s</b>
$\Delta$ Energy, $\Delta U$	256.4E-21	384.5E-21	480.7E-21	<b>J</b>
$\Delta$ Momentum, $\Delta p$	855.1E-30	1.283E-27	1.603E-27	<b>N.s</b>
$\Delta$ Time, $\Delta t$	162.0E-15	72.00E-15	46.08E-15	<b>s</b>
$\Delta$ Extension, $\Delta x$	48.56E-6	21.58E-6	13.81E-6	<b>m</b>
Electric Field, <b>E</b>	60.68E3	167.2E3	292.1E3	<b>V/m</b>
Magnetic Field, <b>B</b>	202.4E-6	557.6E-6	974.2E-6	<b>T</b>
Energy Density, <b>u</b>	32.60E-3	247.4E-3	755.2E-3	<b>J/ m<sup>3</sup></b>
Momentum Density, <b>g</b>	108.7E-12	825.3E-12	2.519E-E9	<b>N.s/m<sup>3</sup></b>
Cross section radius, <b>r</b>	227.1E-9	151.4E-9	121.1E-9	<b>m</b>
Cross Section Area, $\Delta A$	162.0E-15	72.00E-15	46.08E-15	<b>m<sup>2</sup></b>
Spatial Extens, $\Delta Volm$	7.865E-18	1.554E-18	636.4E-21	<b>m<sup>3</sup></b>
Energy flow in 1s, <b>S1.s</b>	1.583E-6	5.341E-6	10.43E-6	<b>J/m<sup>2</sup>s</b>

**Table II Physical Parameters for two extreme photon energies compared with a test photon in the Visible Region**

Physical Parameter	U=7E-27 eV (1 GHZ)	U=2.4 eV (V-Green)	U=13.2 eV (H ionization)	SI UNITS
Frequency, <b>f</b>	1.0E9	580.3E12	3.288E15	<b>Hz</b>
Wavelength, $\lambda$	299.8E-3	516.6E-9	91.16E-9	<b>m</b>
Number of cycles, $N\lambda$	24.25E6	41.78E0	7.373E0	<b>adim</b>
Wavenumber, <b>k</b>	20.96E0	12.16E6	68.92E6	<b>radian/m</b>
Angular Frequency, $\omega$	6.283E9	3.646E15	20.66E15	<b>radian/s</b>
$\Delta$ Energy, $\Delta U$	662.6E-27	384.5E-21	2.179E-18	<b>J</b>
$\Delta$ Momentum, $\Delta p$	2.210E-33	1.283E-27	7.268E-27	<b>N.s</b>
$\Delta$ Time, $\Delta t$	24.25E-3	72.00E-15	2.242E-15	<b>s</b>
$\Delta$ Extension, $\Delta x$	7.269E6	21.58E-6	672.1E-9	<b>m</b>
Electric Field, <b>E</b>	651.7E-12	167.2E3	12.78E6	<b>V/m</b>
Magnet Field, <b>B</b>	2.174E-18	557.6E-6	42.63E-3	<b>T</b>
Energy Density, <b>u</b>	3.760E-30	247.4E-3	1.446E3	<b>J/m<sup>3</sup></b>
Momentum Density, <b>g</b>	12.54E-39	825.3E-12	4.823E-6	<b>N.s/m<sup>3</sup></b>
Cross section radius, <b>r</b>	87.85E-3	151.4E-9	26.71E-9	<b>m</b>
Cross Section Area, $\Delta A$	24.25E.3	72.00E-15	2.242E-15	<b>m<sup>2</sup></b>
Spatial Extens, $\Delta Volm$	176.2E3	1.554E-18	1.507E-21	<b>m<sup>3</sup></b>
Energy flow in 1s, <b>S1.s</b>	27.33E.24	5.341E-6	971.9E-6	<b>J/m<sup>2</sup>s</b>

## CONCLUSIONS

From the previous equations and the obtained results; taking the photon's energy  $\Delta U$  as the most representative photon's physical parameter, the following conclusions are obtained:

- Frequency  $f$ , Angular Frequency  $\omega$ , Wave Number  $\mathbf{k}$ , Momentum  $\Delta p$  are proportional to the Photon's Energy  $\Delta U$
- Wavelength  $\lambda$  and Photon's Energy  $\Delta U$  are inversely proportional
- The photon Cross Section Radius  $r$  and the Photon's Energy  $\Delta U$  are inversely proportional. When  $\Delta U$  increases  $r$  decreases
- When the Photon's Energy  $\Delta U$  increases: The photon Cross Section Radius  $r$ , the Cross Section  $\Delta A$ ,  $\Delta \text{Volm}$ , and the Photon's Length expressed in wavelengths  $N\lambda$  decrease this implies that the photon becomes more compact diminishing its cross section and its spatial extension; so its energy density  $u$  increases
- $N\lambda$  and  $\lambda$  decrease at the same time while the photon's energy increases. Following the same procedure for this example it is found that for a photon's energy of 100 [eV], the number of wavelengths  $N\lambda$  is reduced to a single  $\lambda$ . In other words  $N\lambda = 1 \lambda$  in this this model.
- $E^2$  is proportional with  $\Delta U$  and inversely proportional with the single photon's volume  $\Delta \text{Volm}$
- $E$  and  $B$  are proportional
- The model is consistent with Classical Electromagnetism and several basic equations from Quantum Mechanics
- The model does not contradict the Heisenberg's uncertainty principles
- The volume occupied by photons in a beam is extremely low when compared with the volume of the beam.
- It is considered that this model may be an useful tool for many experimental applications

From the above mentioned Equations the different physical parameters has been plotted as a function of the photon energy expressed in eV.

**Annex 1** summarizes the graphic results.

## ADDITIONAL TOPICS

### Equivalent mass of a photon

A photon is a massless elementary particle, however, through the relation:

$$E = mc^2 \quad (74)$$

it is possible to obtain the mass equivalent for the photon's energy.

For our sample photon with an Energy

$$U \text{ [eV]} = 2.4 \text{ [eV]} \text{ or } \Delta U = 384.3\text{E-21 [J]} \quad (75)$$

the mass equivalent is

$$m_{equiv} = 4.276\text{E-36} \quad [\text{Kg}] \quad (76)$$

Since the mass of an electron, the lightest elementary particle is:

$$m_{elec} = 9.1093897\text{E-31} \quad [\text{Kg}] \quad (77)$$

The ratio (mass of electron) / (mass equivalent) for our photon is:

$$(m_{elec} / m_{equiv}) = 213.0\text{E3} \quad (78)$$

That is, a very small equivalent mass.

Now, is there a photon with an equivalent mass of an electron?

By replacing (63) in (60), the result is:

$$E_{elec} = 81.87\text{E-15 [J]} = 511.0\text{E3 [eV]} = .511 \text{ [MeV]} \quad (79)$$

This magnitude makes sense, since two photons in opposite direction are generated when an electron and its antiparticle a positron collide and annihilate. [4]

## **Electron- Photon interaction**

Photons interact with electrons.

At higher energies electrons and photons interact producing effects like positron- electron creation and annihilation, X- ray fluorescence, Compton Effect, Ionizing Radiation, among others.

In the Visible and IR regions, photons interact with the external electrons of atoms and molecules, in chemical reactions, molecular excitation, molecular dissociation, Raman Spectroscopy, atomic and molecular vibrations, interaction with crystals, semiconductors and other synthetic materials; interacting with free electrons in conductors, among others other processes.

## **ACKNOWLEDGEMENT**

This document is written as part of a Research Project developed in the Catalán Institute of Nanoscience and Nanotechnology- ICN2 and the Physics Department, Graduate School from the Universidad Autónoma de Barcelona- UAB. The Project is supported by the Secretaría Nacional de Educación Superior Ciencia Tecnología e Innovación- SENESCYT from the Government of Ecuador.

## **END NOTE**

**Bellow follows a list of the sections in the "Feynman's Lectures on Physics" linked to the topic of these document. The list is organized according to the chain of reasoning presented here.**



**The Feynman's Lectures on Physics.**

**Vol. 2: Electromagnetism and Matter.**

Chp. 18: The Maxwell Equations.

Sect. 18.4: A travelling field

Cap. 13: Magnetostatics

13.1 The Magnetic Field

Chp. 15: The potential vector A

Section 15.6: What is true for statics is false for dynamics

Chp. 18: The Maxwell Equations.

Section 18.4: A travelling field

Chp. 18: The Maxwell Equations.

Section 18.5: The speed of light.

Chp. 8: Electrostatic Energy.

Section 8.5 Energy in the electrostatic field.

Chp. 15: The vector potential.

Section 15.3 The energy of steady currents

Chp. 15: The vector potential.

Section 15.6: What is true for statics is false for dynamics

Table 15.1

Chp. 17: The Laws of Induction.

Section 17.8: Inductance and Magnetic Energy.

Chp. 27: Field Energy and Field Momentum.

Section 27.3: Energy Density and Energy Flow in the Electromagnetic Field

**The Feynman's Lectures on Physics.**

**Vol. 1: Electromagnetism and Matter.**

Chp. 34: Relativistic Effects in Radiation  
Section 34.9                      The momentum of light

Chp. 27:  
Section 27.6:                      Field Momentum

**Feynman Richard**

**The Feynman's Lectures on Physics.**

**Vol. 3 Quantum Physics**

Chp. 7: The dependence of Amplitudes on Time

## **BIBLIOGRAPHY**

[1]

Neri Vela Rodolfo  
Líneas de Transmisión.  
Capítulo 4 Teoría de las guías de ondas.  
Págs. 315- 340. Mc. Graw Hill 1999

[2]

Constantine A. Balans  
Circular waveguides  
Arizona State University, Tempe Arizona

*[http : //www.tuks.nl/pdf/ReferenceMaterial/CircularWaveguides.pdf](http://www.tuks.nl/pdf/ReferenceMaterial/CircularWaveguides.pdf)*

[3]

Feynman Richard  
The Feynman's Lectures on Physics.

*[http : //www.feynmanlectures.caltech.edu/I\\_toc.html](http://www.feynmanlectures.caltech.edu/I_toc.html)*

*[http://www.feynmanlectures.caltech.edu/II\\_toc.html](http://www.feynmanlectures.caltech.edu/II_toc.html)*

*[http://www.feynmanlectures.caltech.edu/III\\_toc.html](http://www.feynmanlectures.caltech.edu/III_toc.html)*

[4]

Wikipedia

Word: Electron- Positron Annihilation

[http://en.wikipedia.org/wiki/Electron%E2%80%93positron\\_annihilation](http://en.wikipedia.org/wiki/Electron%E2%80%93positron_annihilation)

Follow in the next page

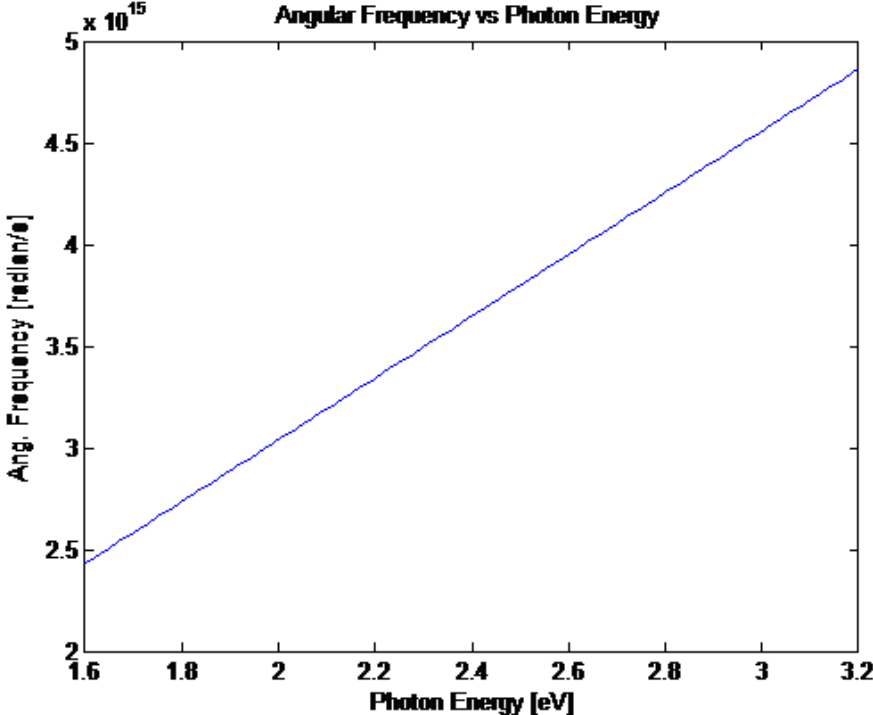
ANNEX 1/

Physical parameters for a Single Photon in the Visible Region

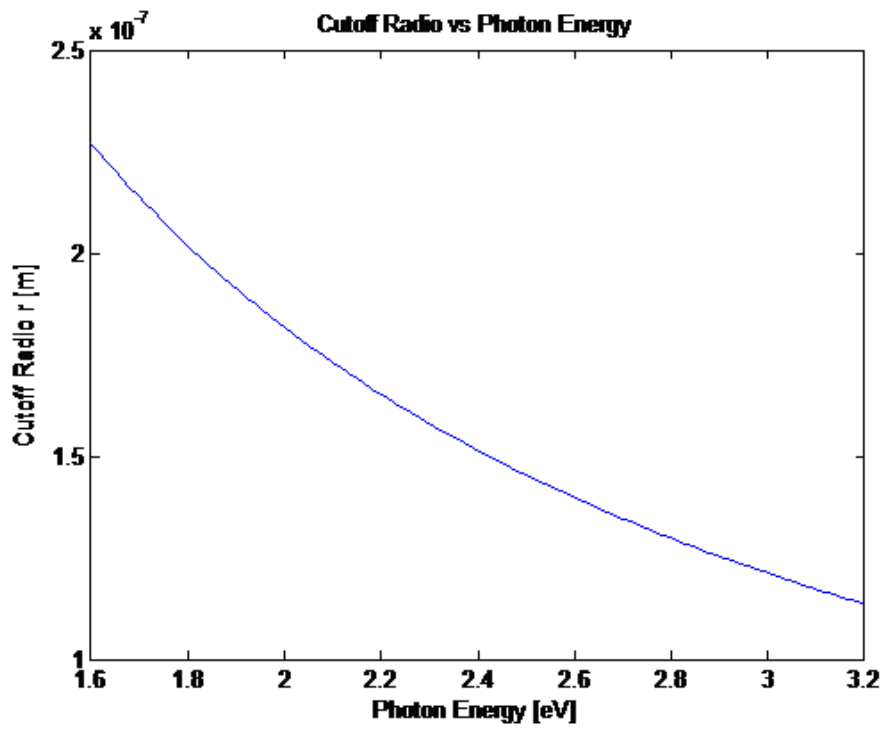
as a function of the Photon's Energy

(Calculated parameters from the model)

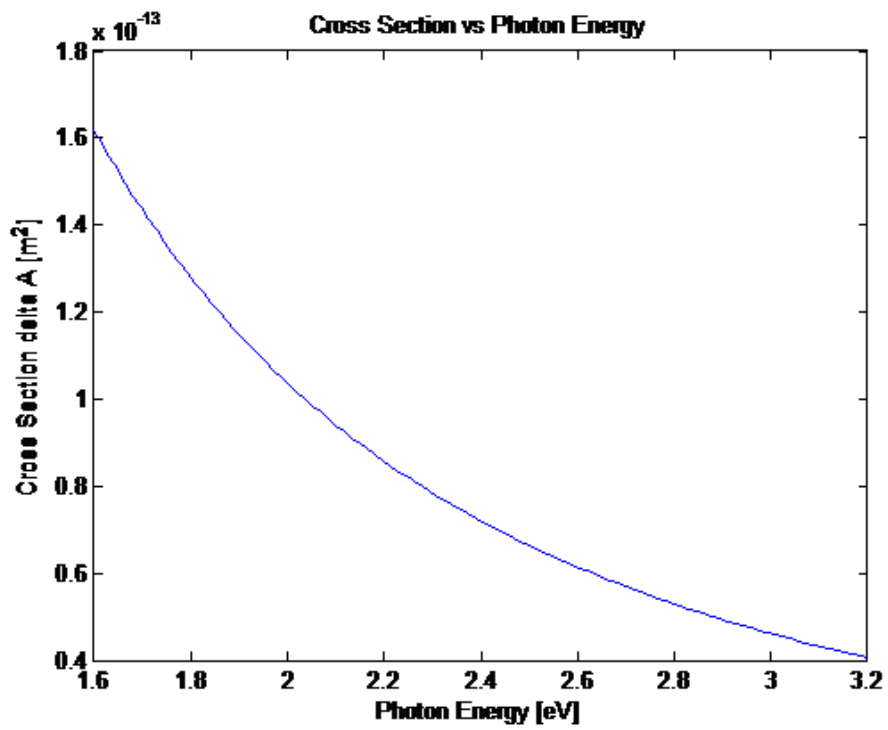
[Angular Frequency vs Photon Energy]



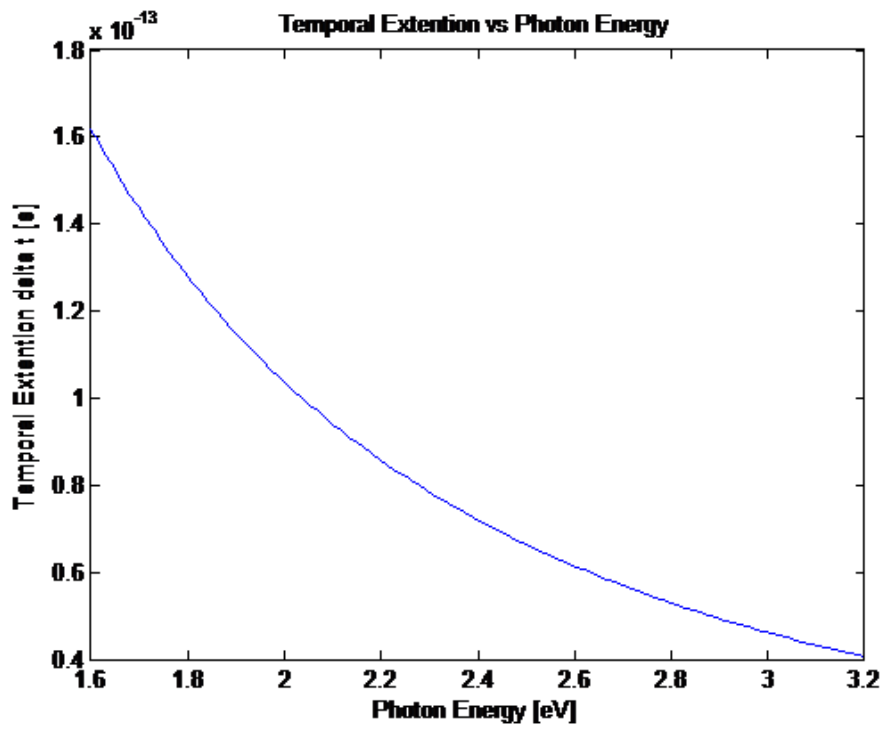
[Cutoff radius vs Photon Energy]



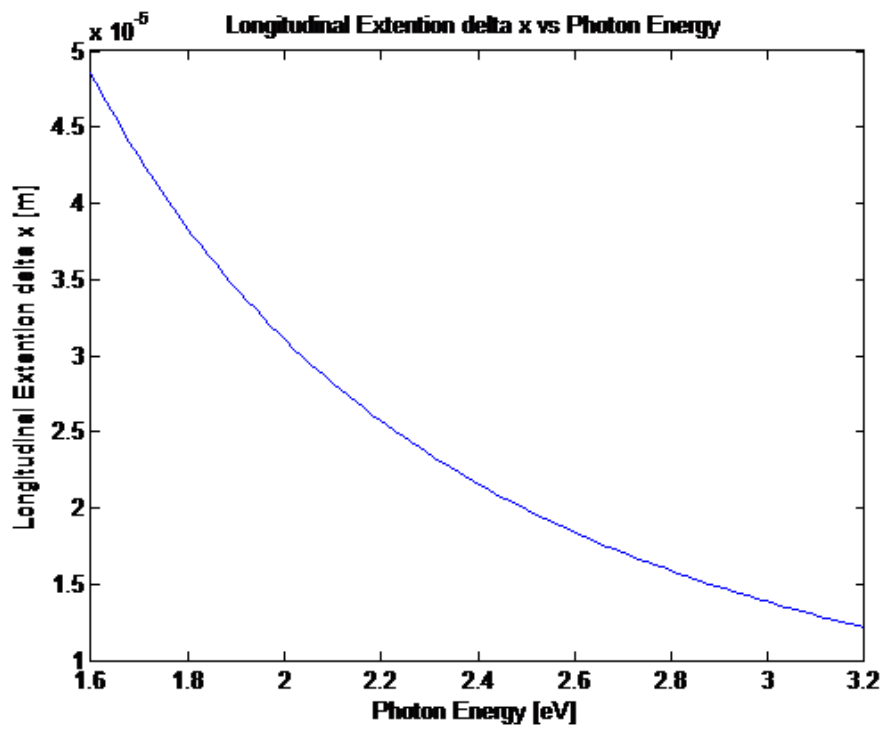
[Cross Section Area vs Photon Energy]



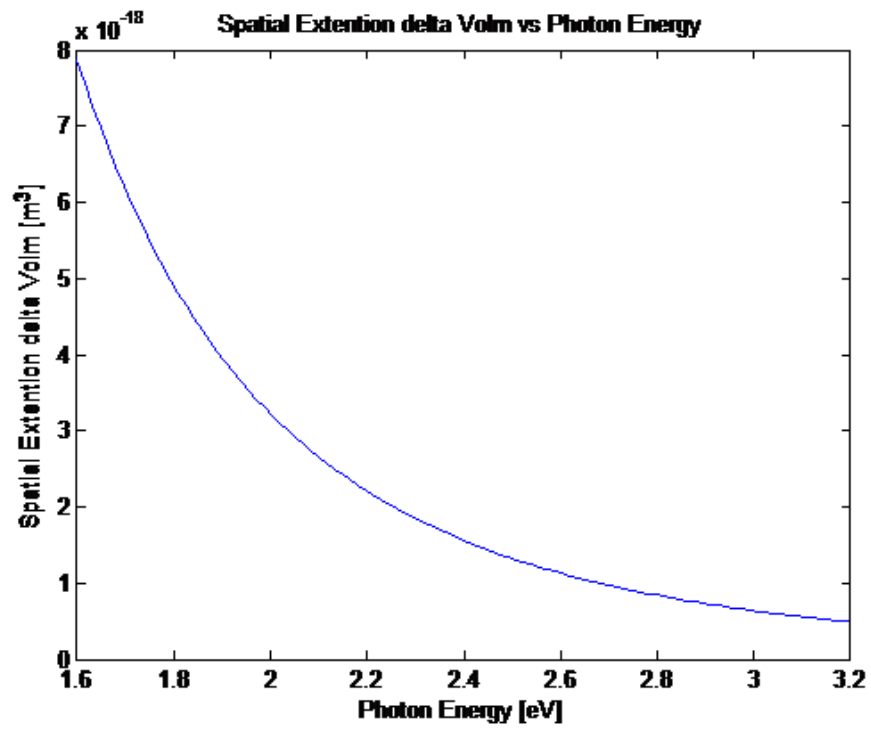
[Temporal Extension vs Photon Energy]



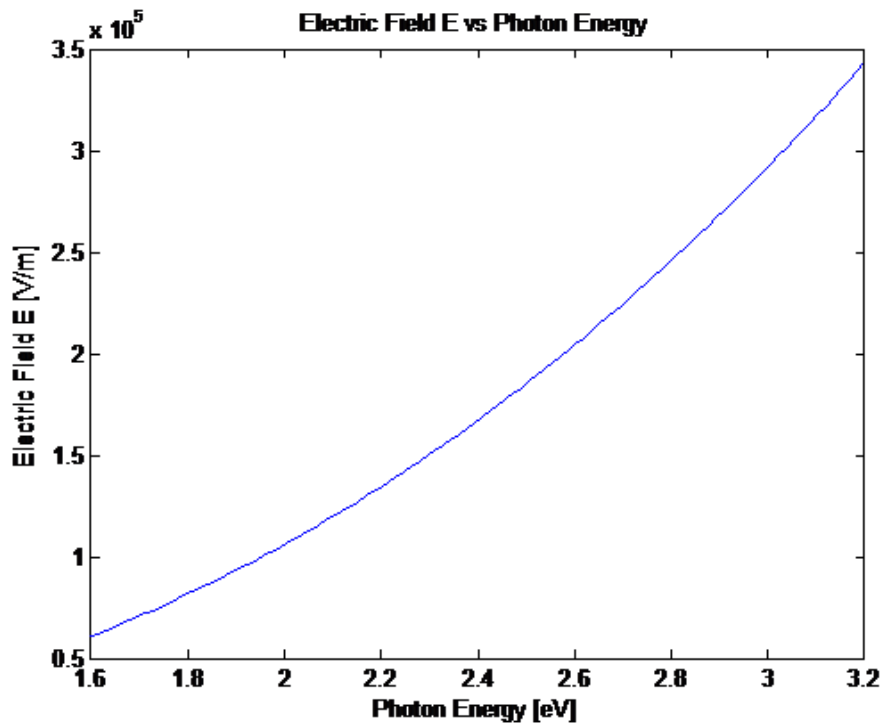
[Longitudinal Extension vs Photon Energy]



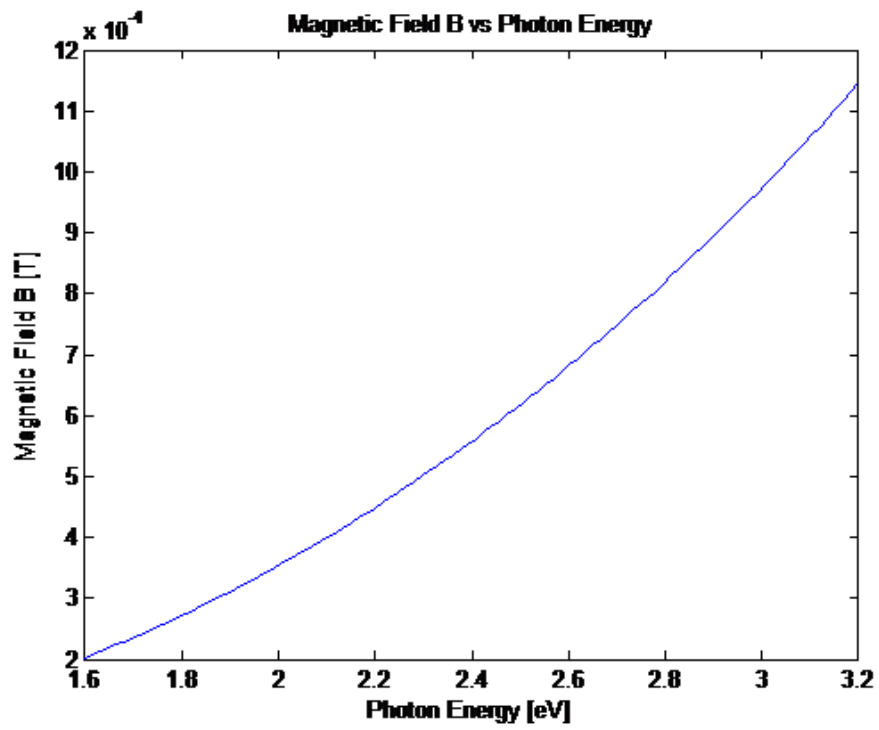
[Volumetric Extension vs Photon Energy]



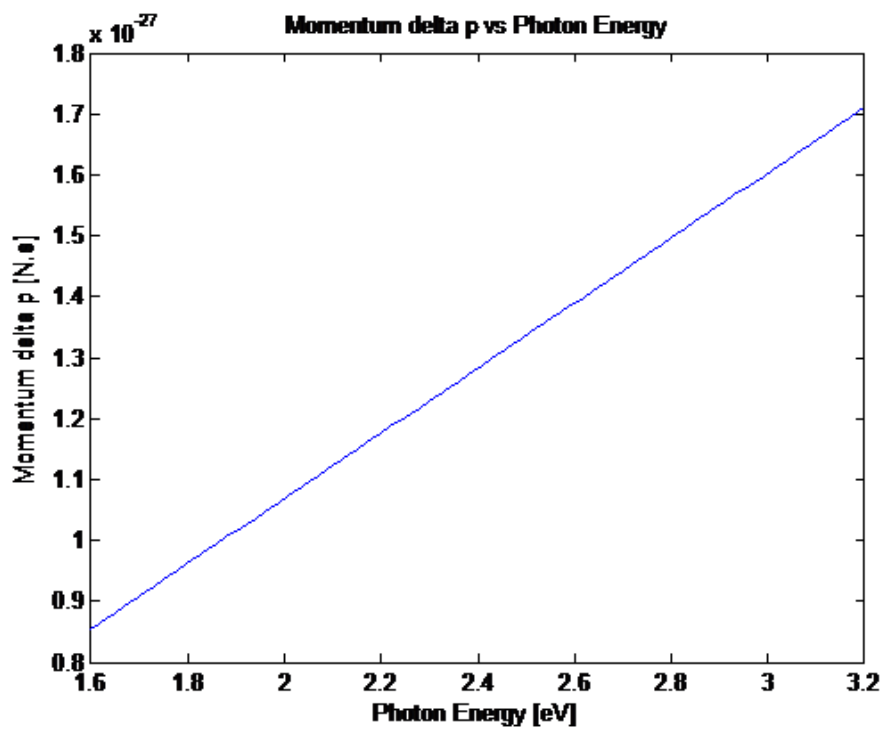
[Electric Field vs Photon Energy]



[Magnetic Field vs Photon Energy]

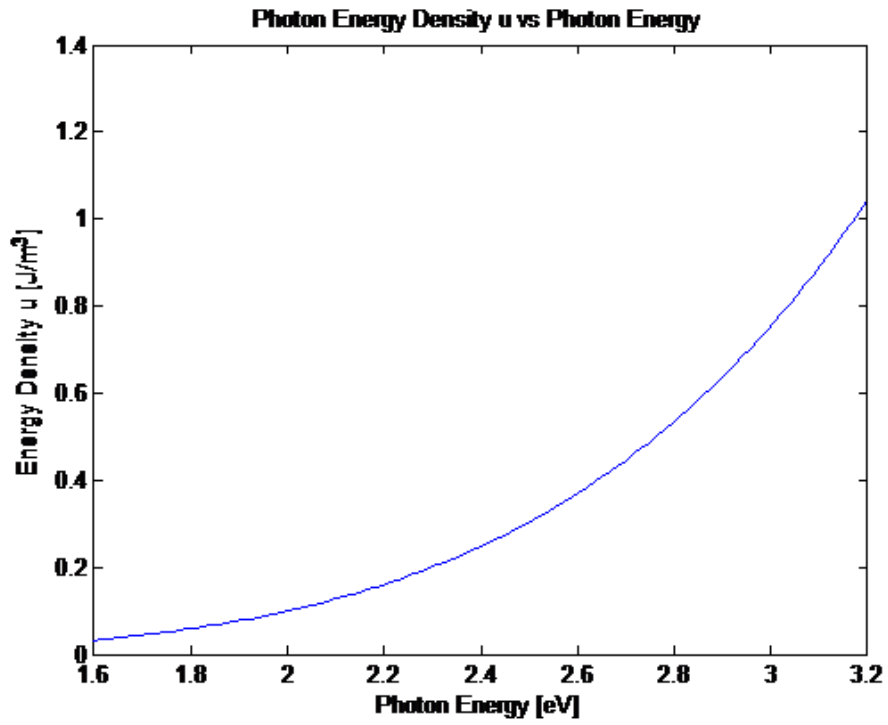


[Momentum vs Photon Energy]

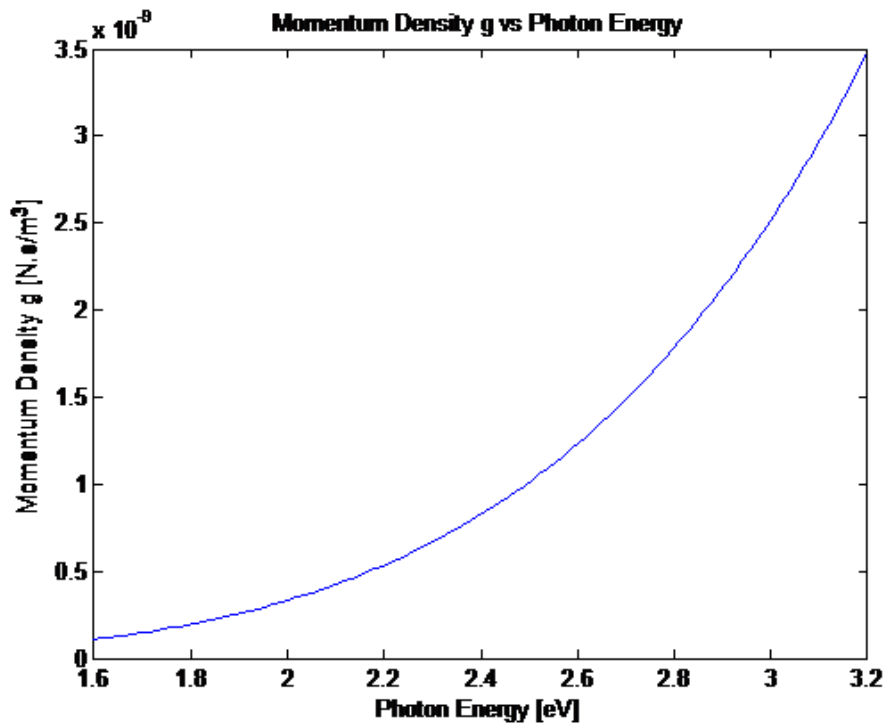




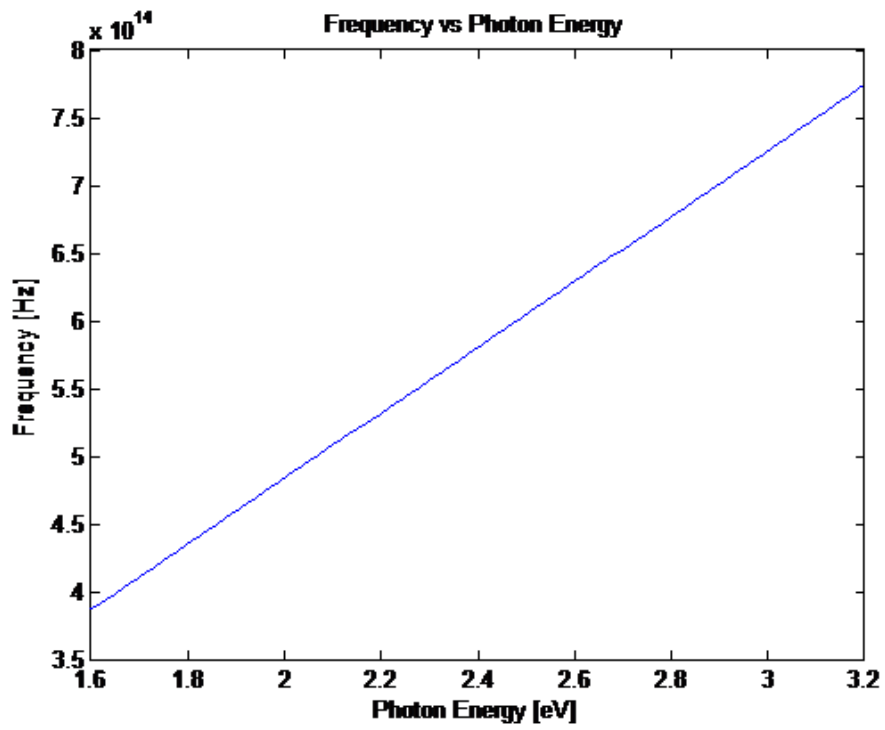
[Energy Density vs Photon Energy]



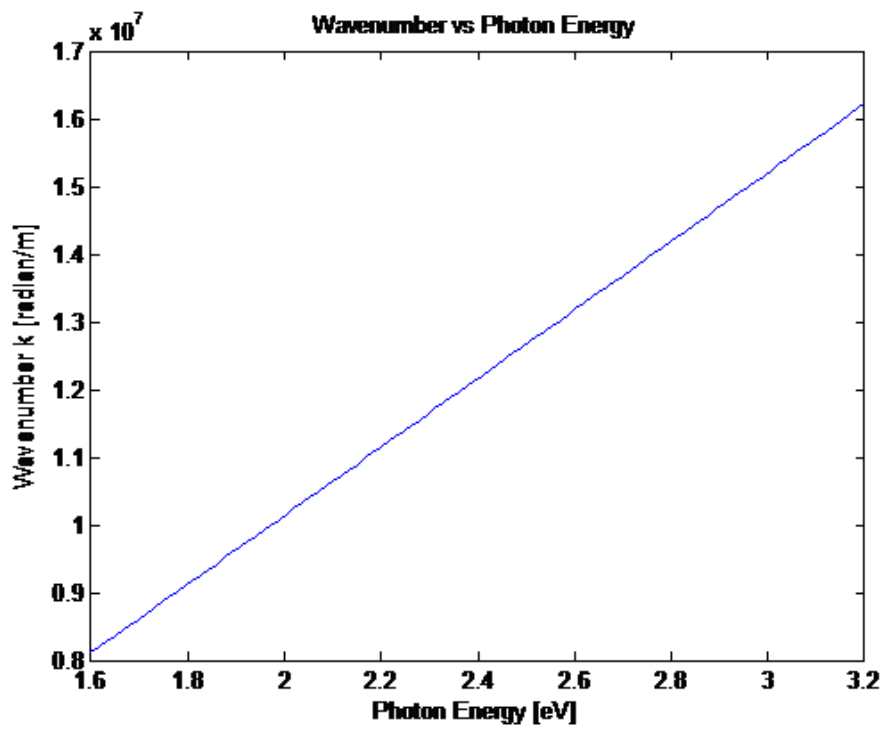
[Momentum Density vs Photon Energy]



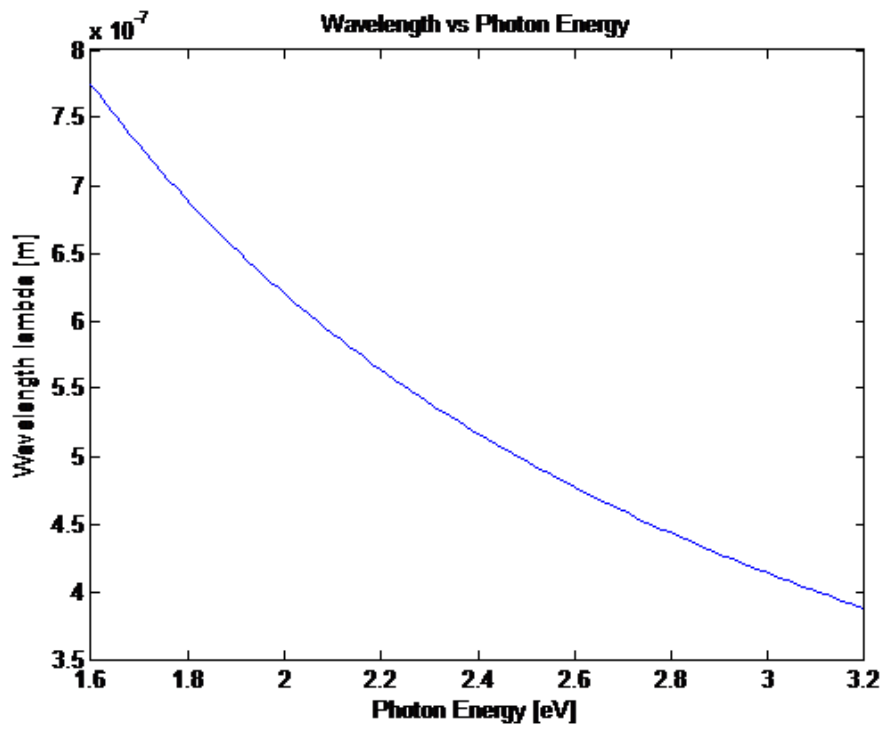
[Frequency vs Photon Energy]



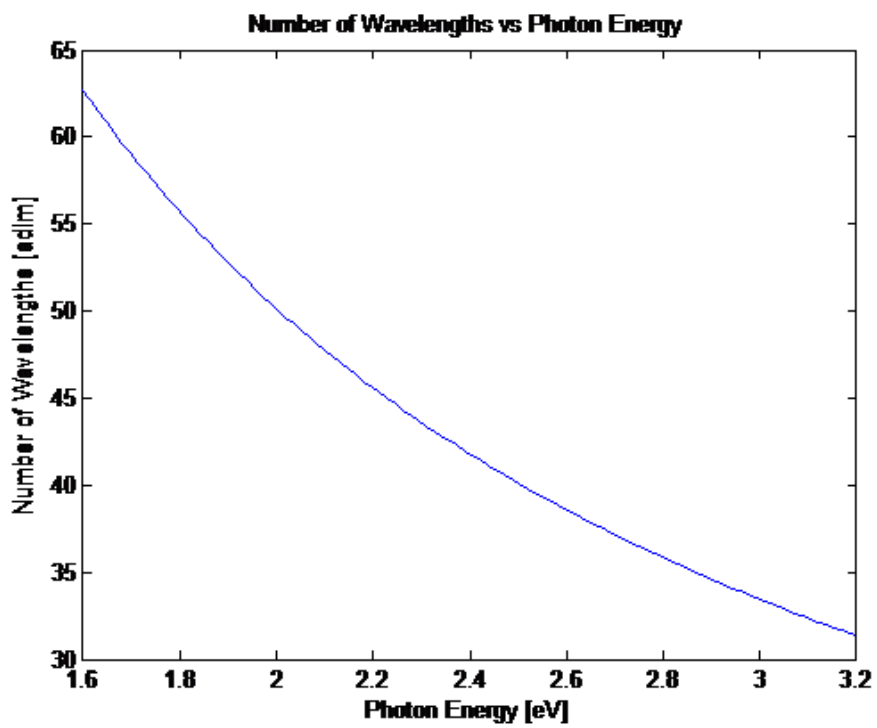
[Wavenumber vs Photon Energy]



[Wavelength vs Photon Energy]



[Number of wavelengths vs Photon Energy]



## ANNEX 2/

### Summary of Equations

related with Photons

- Table 1: Wave related equations
- Table 2: Electromagnetic Theory related equations
- Table 3: Quantum Mechanics related equations

**Table I** Wave related equations

Routine	Application	Equation
$\omega$ o T	Angular frequency $\Leftrightarrow$ Period	$\omega T = 2 \pi$
k o $\lambda$	Wavenumber $\Leftrightarrow$ Wavelength	$k \lambda = 2 \pi$
$\lambda$ o T	Wavelength $\Leftrightarrow$ Period	$\lambda = c T$
$\lambda$ o f	Wavelength $\Leftrightarrow$ Frequency	$\lambda f = c$
$\omega$ o k	Angular frequency $\Leftrightarrow$ Wavenumber	$\omega = c k$
$\omega$ o $\lambda$	Angular frequency $\Leftrightarrow$ Wavelength	$\omega \lambda = 2 \pi c$
$\omega$ o f	Angular frequency $\Leftrightarrow$ Frequency	$\omega = 2 \pi f$

**Table 2** Electromagnetic Theory related equations

Routine	Application	Equation
E o B	Electric Field $\Leftrightarrow$ Magnetic Field	$E = cB$
J o E	Current Density $\Leftrightarrow$ Electric Field	$E = -J/2\epsilon_0 c$
u	Electromagnetic Energy Density	$u = \frac{\epsilon_0}{2} \mathbf{E} \cdot \mathbf{E} + \frac{\epsilon_0 c^2}{2} \mathbf{B} \cdot \mathbf{B}$
U	Electromagnetic Energy	$U = \int (\frac{\epsilon_0}{2} \mathbf{E} \cdot \mathbf{E} + \frac{\epsilon_0 c^2}{2} \mathbf{B} \cdot \mathbf{B}) dV$
S	Poynting Vector	$\mathbf{S} = \epsilon_0 c^2 \mathbf{E} \times \mathbf{B}$ $ \mathbf{S}  = \epsilon_0 c  \mathbf{E} ^2$
<b>g</b>	Momentum Density	$\mathbf{g} = \mathbf{S}/c^2 = \epsilon_0 \mathbf{B} \times \mathbf{B}$
<b>p</b>	Momentum	$p = U/c$
$e^2$	Notation abbreviation	$e^2 = q_e^2/4\pi\epsilon_0$
a	Factor related to $r_e$	$a = (2/3)(e^2/m_e c^2)$
$m_{emg}$	Electromagnetic Mass	$m_{elec} = \frac{2}{3} \frac{e^2}{ac^2}$
$r_e$	Electron Radius = $2.82 \times 10^{-15}$ m	$r_0 = \frac{e^2}{m_e c^2}$

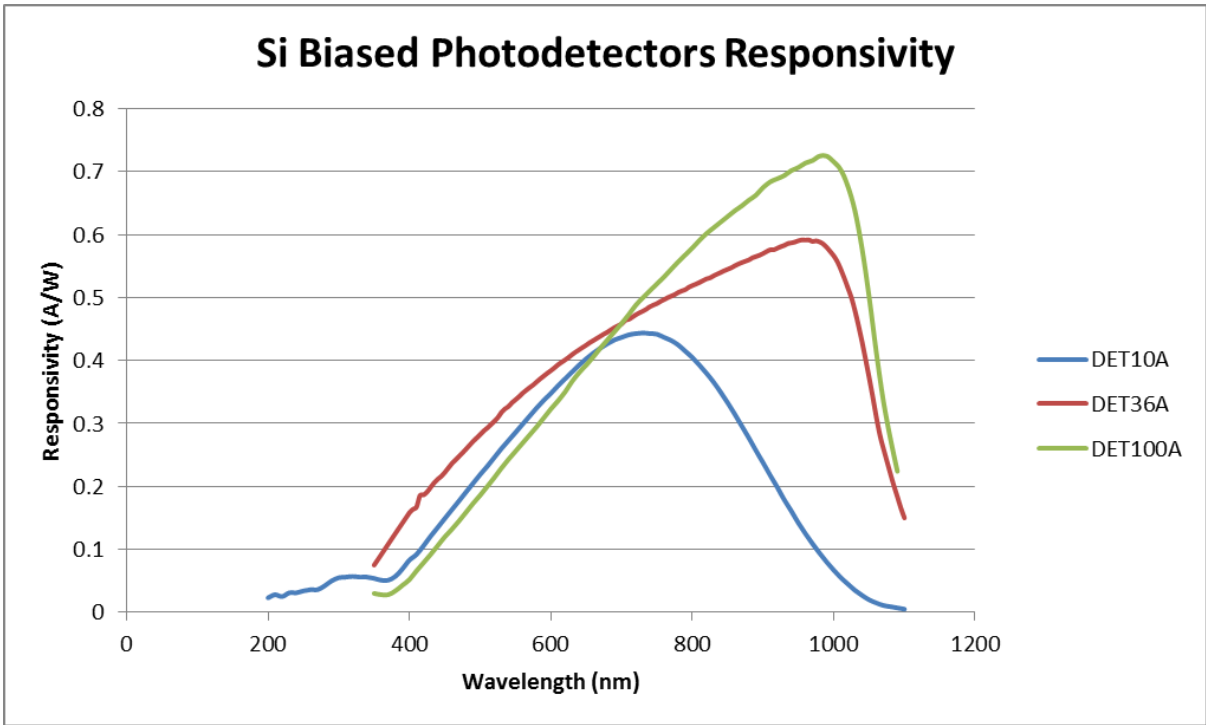
**Table 3**                      **Quantum Mechanics related equations**

<b>Routine</b>	<b>Application</b>	<b>Equation</b>
U o $\omega$	Energy $\Leftrightarrow$ Angular Frequency	$U = \hbar \omega$
<b>p</b> o <b>k</b>	Momentum $\Leftrightarrow$ Wavenumber	$\mathbf{p} = \hbar \mathbf{k}$
$\Delta x$ o $\Delta p$	Position- Momentum uncertainty(minimum)	$\Delta x \Delta p = \hbar/2$
$\Delta U$ o $\Delta t$	Time- Energy uncertainty (minimum)	$\Delta U \Delta t = \hbar/2$
p o U	Momentum $\Leftrightarrow$ Energy	$p = U / c$
p o $\lambda$	Momentum $\Leftrightarrow$ Wavelength*	$\lambda = h/p$
$\omega$ o k	Wavenumber $\Leftrightarrow$ Angular Frequency	$k = \omega/c$
$\omega$ o f	Angular frequency $\Leftrightarrow$ Frequency	$\omega = 2\pi f$

\* Note: For Photons

\*\*\* END \*\*\*





Product Raw Data

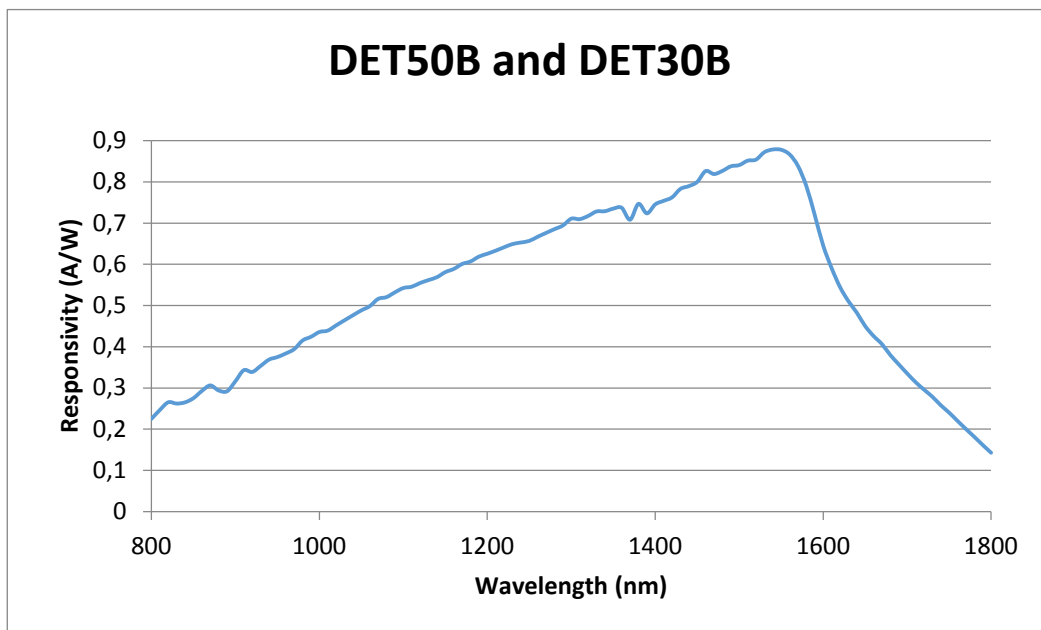
## Ge Biased Photodetectors

Item #

DET30B and DET50B

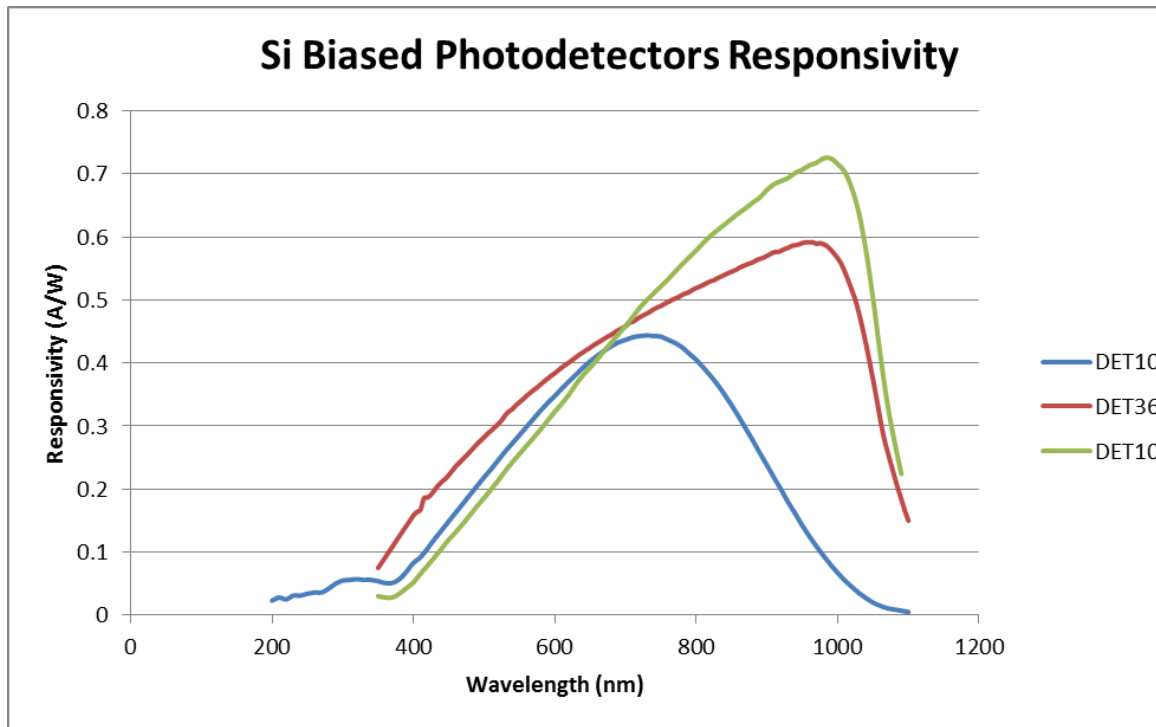
**DISCLAIMER: The data presented here are typical. Slight variations in performance data will occur from lot to lot. Please contact Technical Support with any questions regarding the use or reliability of this data.**

This data may be used in publications. However, please cite Thorlabs as the source.





# Si Biased Photodetectors



## DET10A

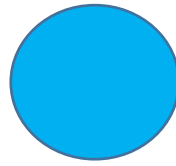
Wavelength (nm)	Responsivity (A/W)
200	0.023
210	0.028
220	0.025
230	0.031
240	0.031
250	0.034
260	0.036
270	0.036
280	0.042
290	0.05
300	0.055
310	0.056
320	0.057
330	0.056
340	0.056
350	0.054
360	0.051
370	0.051
380	0.057

390	0.069
400	0.083
410	0.092
420	0.106
430	0.121
440	0.135
450	0.149
460	0.163
470	0.177
480	0.191
490	0.205
500	0.219
510	0.232
520	0.246
530	0.26
540	0.273
550	0.286
560	0.299
570	0.312
580	0.325
590	0.337
600	0.348
610	0.36
620	0.371
630	0.382
640	0.393
650	0.403
660	0.412
670	0.42
680	0.427
690	0.433
700	0.437
710	0.441
720	0.443
730	0.444
740	0.443
750	0.442
760	0.437
770	0.432
780	0.425
790	0.415
800	0.405
810	0.393
820	0.38
830	0.366
840	0.35

## **Chp 1 ANNEX 2-5**

850	0.333
860	0.315
870	0.296
880	0.277
890	0.257
900	0.238
910	0.218
920	0.199
930	0.179
940	0.161
950	0.142
960	0.125
970	0.109
980	0.094
990	0.08
1000	0.067
1010	0.055
1020	0.045
1030	0.035
1040	0.027
1050	0.02
1060	0.015
1070	0.011
1080	0.009
1090	0.007
1100	0.005

# DET36A



Wavelength (nm)	Responsivity (A/W)
350	0.075
400	0.1583
405	0.1637
410	0.1675
415	0.1858
420	0.1866
425	0.1915
430	0.1987
435	0.2059
440	0.2117
445	0.2162
450	0.2224
455	0.2294
460	0.2365
465	0.242
470	0.2477
475	0.2534
480	0.2594
485	0.2657
490	0.2717
495	0.277
500	0.2824
505	0.2883
510	0.2929
515	0.2983
520	0.3036
525	0.3095
530	0.3176
535	0.3233
540	0.3271
545	0.3332
550	0.3379
555	0.3427
560	0.3483
565	0.3528
570	0.3573
575	0.3614
580	0.3665
585	0.3712

590	0.3756
595	0.3801
600	0.3842
605	0.3886
610	0.3934
615	0.3973
620	0.4011
625	0.4051
630	0.4096
635	0.4137
640	0.4174
645	0.421
650	0.4247
655	0.4286
660	0.4319
665	0.4355
670	0.4389
675	0.4423
680	0.4453
685	0.449
690	0.4526
695	0.4555
700	0.4584
705	0.4638
710	0.4656
715	0.469
720	0.4727
725	0.4759
730	0.4786
735	0.4818
740	0.4857
745	0.4884
750	0.4907
755	0.4941
760	0.4969
765	0.5
770	0.5024
775	0.5049
780	0.5083
785	0.5108
790	0.5128
795	0.5166
800	0.5192
805	0.5216
810	0.5242
815	0.5271

**Chp 1 ANNEX 2-8**

820	0.5299
825	0.5315
830	0.5347
835	0.5374
840	0.54
845	0.5428
850	0.5452
855	0.5475
860	0.5505
865	0.5535
870	0.5558
875	0.558
880	0.5601
885	0.5634
890	0.5655
895	0.5675
900	0.5701
905	0.5733
910	0.576
915	0.5761
920	0.5786
925	0.5811
930	0.5831
935	0.586
940	0.5871
945	0.5885
950	0.5906
955	0.5918
960	0.5915
965	0.5917
970	0.5894
975	0.5903
980	0.5886
985	0.5855
990	0.5802
995	0.5736
1000	0.5665
1005	0.5575
1010	0.5449
1015	0.5311
1020	0.5157
1025	0.5001
1030	0.4795
1035	0.4557
1040	0.4301
1045	0.4026

## **Chp 1 ANNEX 2-9**

1050	0.3737
1055	0.3437
1060	0.3117
1065	0.2831
1070	0.2612
1075	0.2408
1080	0.2209
1085	0.2014
1090	0.1838
1095	0.1655
1100	0.15

# DET100A

Wavelength (nm)	Responsivity (A/W)
350	0.03
360	0.028
370	0.028
380	0.034
390	0.043
400	0.052
410	0.066
420	0.079
430	0.092
440	0.106
450	0.12
460	0.132
470	0.145
480	0.159
490	0.173
500	0.186
510	0.2
520	0.214
530	0.229
540	0.243
550	0.256
560	0.269
570	0.282
580	0.295
590	0.309
600	0.323
610	0.336
620	0.35
630	0.367
640	0.381
650	0.393
660	0.406
670	0.42
680	0.433
690	0.446
700	0.459
710	0.473
720	0.488
730	0.5
740	0.511
750	0.522
760	0.533



770	0.545
780	0.557
790	0.568
800	0.579
810	0.591
820	0.602
830	0.611
840	0.62
850	0.629
860	0.638
870	0.646
880	0.655
890	0.663
900	0.675
910	0.684
920	0.689
930	0.694
940	0.702
950	0.707
960	0.714
970	0.718
980	0.725
990	0.725
1000	0.716
1010	0.703
1020	0.677
1030	0.638
1040	0.578
1050	0.502
1060	0.415
1070	0.337
1080	0.277
1090	0.224



Product Raw Data

## Ge Biased Photodetectors

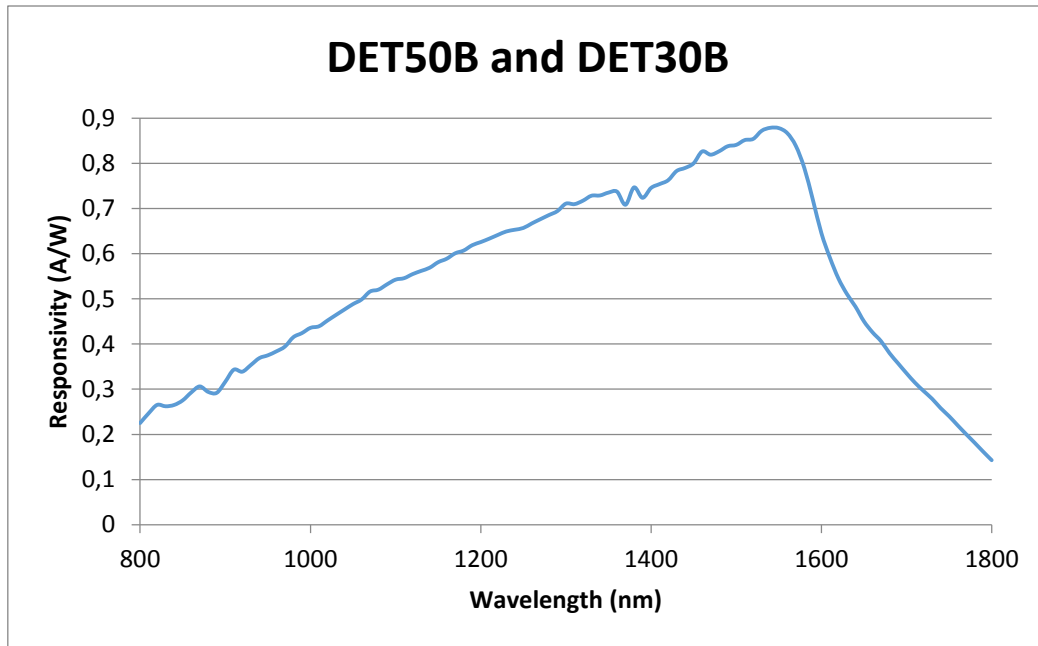
Item #

DET30B and DET50B

**DISCLAIMER: The data presented here are typical. Slight variations in performance data will occur from lot to lot. Please contact Technical Support with any questions regarding the use or reliability of this data.**

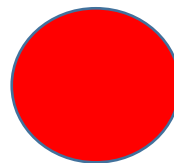
**This data may be used in publications. However, please cite Thorlabs as the source.**

Additional Information:



## Ge Biased Photodetectors

### DET50B and DET30B



Wavelength (nm)	Responsivity (A/W)
800	0.22508
810	0.24665
820	0.26523
830	0.26213
840	0.26513
850	0.27525
860	0.29272
870	0.30612
880	0.29395
890	0.29197
900	0.31639
910	0.34314
920	0.33874
930	0.35345
940	0.36875
950	0.375

960	0.3837
970	0.39427
980	0.41518
990	0.42412
1000	0.43576
1010	0.43922
1020	0.45196
1030	0.46431
1040	0.4764
1050	0.48833
1060	0.49845
1070	0.51611
1080	0.52045
1090	0.5321
1100	0.54247
1110	0.54571
1120	0.55472
1130	0.5618
1140	0.56882
1150	0.5811
1160	0.58872
1170	0.60078
1180	0.60694
1190	0.6187
1200	0.62561
1210	0.63318
1220	0.64138
1230	0.64911
1240	0.65293
1250	0.65686
1260	0.66692
1270	0.67623
1280	0.68537
1290	0.69418
1300	0.71071
1310	0.70957
1320	0.71724
1330	0.72821
1340	0.72881
1350	0.73514
1360	0.73725
1370	0.70826
1380	0.74667
1390	0.72364
1400	0.74545
1410	0.75398

## **Chp 1 ANNEX 2-15**

1420	0.76239
1430	0.78291
1440	0.78974
1450	0.8
1460	0.82617
1470	0.81905
1480	0.82667
1490	0.83774
1500	0.84074
1510	0.85138
1520	0.85405
1530	0.87207
1540	0.87857
1550	0.87788
1560	0.86667
1570	0.8386
1580	0.78947
1590	0.7193
1600	0.64561
1610	0.59115
1620	0.54513
1630	0.51071
1640	0.48288
1650	0.45018
1660	0.42606
1670	0.40636
1680	0.37981
1690	0.35736
1700	0.33524
1710	0.31423
1720	0.29608
1730	0.2788
1740	0.25818
1750	0.24016
1760	0.22004
1770	0.20042
1780	0.18139
1790	0.16173
1800	0.14279